Universidade do Minho
Escola de Engenharia

Rodolfo Bettencourt Pereira Cerqueira

Instrumentation and Validation of a Robotic Cane for Transportation and Fall Prevention in Patients with Affected Mobility

março de 2022

Instrumentation and Validation of a Robotic Cane for Transportation and Fall Prevention in Patients with Affected Mobility

Rodolfo Bettencourt Pereira Cerqueira

UMinho | 2022

Universidade do Minho
Escola de Engenharia

Rodolfo Bettencourt Pereira Cerqueira

Instrumentation and Validation of a Robotic cane for Transportation and Fall prevention in Patients with Affected Mobility

Dissertação de Mestrado

Mestrado Integrado em Engenharia Física

Dispositivos, Microssistemas e Nanotecnologias

Trabalho efetuado sob a orientação de:

Professora Doutora Cristina Manuela Peixoto dos Santos

Nuno Ferrete Ribeiro

março de 2022

DIREITOS DE AUTOR E CONDIÇÕES DE UTILIZAÇÃO DO TRABALHO POR TERCEIROS

ACKNOWLEDGMENTS

First of all, I want to thank my supervisor, professor Cristina Peixoto Santos, for steering the work in the right direction and providing valuable knowledge and experience along the way. I would also like to express my gratitude for allowing me to choose a dissertation project that matches my personal interests, and also for the opportunity it gave me to carry out a curricular internship at the INRIA institute, where I had the pleasure of working with Christine A. Coste and the CAMIN team, for whom I have great affection.

I would also like to thank my laboratory colleagues on the BiRDLab team, for all the camaraderie, positive energy, and for the advice and availability provided throughout the year.

I have a special thanks to the doctoral student Nuno Ferrete Ribeiro for accompanying and guiding me since the first steps in this project, being a great support, always looking for the best of this work. But most importantly, I want to thank him for being a great friend who was always there and willing to help in every situation.

Also, to Mr. Carlos Torres and Mr. Paulo Silva, from the workshop of the industrial electronics department at the University of Minho, thank you for all the demonstrated availability, dedicated time and for being always willing to help me when I needed.

I would like to express my gratitude to my close friends Gabriel and João for making this whole journey a joyful and fun-filled chapter in my life. It was certainly enriching to see us grow and evolve in this mutual learning and face the same challenges throughout these academic years.

Thank you Soraia, for your support, patience, and love, along with all the joy, beautiful and unforgettable moments that mark my life. I also thank you for all the strength you give me, making me always feel capable of facing any challenge, making me seek to be a better version of myself with each passing day.

Finally, I have to thank my parents and brother, for the unconditional support and strength they provided, and for being a foundation through the years of my life. In addition, thank you for always providing the best conditions for my education and personal development, as I owe everything I have to them.

To all of you, my most sincere thank you.

Rodolfo Cerqueira

STATEMENT OF INTEGRITY

I hereby declare having conducted this academic work with integrity. I confirm that I have not used plagiarism or any form of undue use of information or falsification of results along the process leading to its elaboration. I further declare that I have fully acknowledged the Code of Ethical Conduct of the University of Minho.

RESUMO

O ato de andar é conhecido por ser a forma primitiva de locomoção do ser humano, sendo que este traz muitos benefícios que motivam um estilo de vida saudável e ativo. No entanto, há condições de saúde que dificultam a realização da marcha, o que por consequência pode resultar num agravamento da saúde, e adicionalmente, levar a um maior risco de quedas. Nesse sentido, o desenvolvimento de um sistema de deteção e prevenção de quedas, integrado num dispositivo auxiliar de marcha, seria essencial para reduzir estes eventos de quedas e melhorar a qualidade de vida das pessoas. Para ultrapassar estas necessidades e limitações, esta dissertação tem como objetivo validar e instrumentar uma bengala robótica, denominada *Anti-fall Robotic Cane* (ARCane), concebida para incorporar um sistema de deteção de quedas e um mecanismo de atuação que possibilite a prevenção de quedas, ao mesmo tempo que assiste a marcha. Para esse fim, foi realizada uma revisão do estado da arte em bengalas robóticas para adquirir um conhecimento amplo e aprofundado dos componentes, mecanismos e estratégias utilizadas, bem como os protocolos experimentais, principais resultados, limitações e desafios em dispositivos existentes.

Numa primeira fase, foi estipulado o objetivo de: (i) adaptar a missão do produto; (ii) estudar as necessidades do consumidor; e (iii) atualizar as especificações alvo da ARCane, continuação do trabalho de equipa, para obter um produto com design e engenharia compatível com o mercado. Foi depois estabelecida a arquitetura de hardware e discutidos os componentes a ser instrumentados na ARCane. Em seguida foram realizados testes de interoperabilidade a fim de validar o funcionamento singular e coletivo dos componentes.

Relativamente ao controlo de movimento, foi desenvolvido um sistema inovador, de baixo custo e intuitivo, capaz de detetar a intenção do movimento e de reconhecer as fases da marcha do utilizador. Esta implementação foi validada com seis voluntários saudáveis que realizaram testes de marcha com a ARCane para testar sua operabilidade num ambiente de contexto real. Obteve-se uma precisão de 97% e de 90% em relação à deteção da intenção de movimento e ao reconhecimento da fase da marcha do utilizador.

Por fim, foi projetado um método de deteção de quedas e mecanismo de prevenção de quedas para futura implementação na ARCane. Foi ainda proposta uma melhoria do método de deteção de quedas, de modo a superar as limitações associadas, bem como a proposta de dispositivos de deteção a serem implementados na ARCane para obter um sistema completo de deteção de quedas.

Palavras-chave: Bengala robótica anti-queda; Deteção de queda; Prevenção de queda; Controlo de movimento; Instrumentação;

ABSTRACT

The act of walking is known to be the primitive form of the human being, and it brings many benefits that motivate a healthy and active lifestyle. However, there are health conditions that make walking difficult, which, consequently, can result in worse health and, in addition, lead to a greater risk of falls. Thus, the development of a fall detection and prevention system integrated with a walking aid would be essential to reduce these fall events and improve people quality of life. To overcome these needs and limitations, this dissertation aims to validate and instrument a cane-type robot, called Anti-fall Robotic Cane (ARCane), designed to incorporate a fall detection system and an actuation mechanism that allow the prevention of falls, while assisting the gait. Therefore, a State-of-the-Art review concerning robotic canes was carried out to acquire a broad and in-depth knowledge of the used components, mechanisms and strategies, as well as the experimental protocols, main results, limitations and challenges on existing devices.

On a first stage, it was set an objective to (i) enhance the product's mission statement; (ii) study the consumer needs; and (iii) update the target specifications of the ARCane, extending teamwork, to obtain a product with a market-compatible design and engineering that meets the needs and desires of the ARCane users. It was then established the hardware architecture of the ARCane and discussed the electronic components that will instrument the control, sensory, actuator and power units, being afterwards subjected to interoperability tests to validate the singular and collective functioning of cane components altogether.

Regarding the motion control of robotic canes, an innovative, cost-effective and intuitive motion control system was developed, providing user movement intention recognition, and identification of the user's gait phases. This implementation was validated with six healthy volunteers who carried out gait trials with the ARCane, in order to test its operability in a real context environment. An accuracy of 97% was achieved for user motion intention recognition and 90% for user gait phase recognition, using the proposed motion control system.

Finally, it was idealized a fall detection method and fall prevention mechanism for a future implementation in the ARCane, based on methods applied to robotic canes in the literature. It was also proposed an improvement of the fall detection method in order to overcome its associated limitations, as well as detection devices to be implemented into the ARCane to achieve a complete fall detection system.

Keywords: Robotic anti-fall cane; Fall detection; Fall prevention; Motion control; Instrumentation;

CONTENTS

List of Figures

List of Tables

List of Acronyms and Abbreviations

[n]D	[n]-Dimensional
ADC	Analog-to-Digital Converter
ADL	Activities of Daily Living
ARCane	Anti-fall Robotic Cane
BiRD LAB	Biomedical Robotic Devices Laboratory
CAD	Computer-Aided Design
CMEMs	Center of Micro Electro-Mechanical Systems
CNN	Convolutional Neural Networks
COP	Center of Pressure
COP-FD	Center of Pressure Fall Detection
CU	Control Unit
DM	Discriminant Model
DOF	Degree of Freedom
DPS	Degrees Per Second
EMS	Elderly Mobility Scale
FOG	Freezing of Gait
FSR	Force Sensitive Resistor
GUI	Graphic User Interface
HMM	Hidden Markov Model
HRCS	Human-Robot Coordination Stability
HRI	Human-Robot Interaction
I2C	Inter-Integrated Circuit
IADL	Instrumental Activities of Daily Living
IDE	Integrated Development Environment
IMU	Inertial Measurement Unit
IIR	Infinite Impulse Response
IPS	Inverted Pendulum System
ITD	Intended Direction
LAM	Lie Algebra Method

LDR	Light Dependent Resistor
LED	Light Emitting Diode
LIDAR	Light Detection and Ranging
LRF	Laser Range Finder
LSTM	Long Short-Term Memory
MEMS	MicroElectroMechanical Systems
MR	Magneto Rheological
PCA	Principal Component Analysis
PCB	Printed Circuit Board
PLA	Polylactic Acid
PRISMA	Preferred Report Items for Systematic Reviews and Meta-analysis
PWM	Pusle Width Modulation
RBF	Radial Basis Function
RGB	Red Green Blue
RNN	Recurrent Neural Networks
RQ	Research Question
SCI	Spinal Cord Injury
SCL	Serial Clock
SDA	Serial Data
SoA	State-of-the-Art
SVM	Support Vector Machine
TOF	Time-of-Flight
UART	Universal Asynchronous Receiver Transmitter
UN	United Nations
USB	Universal Serial Bus
WHO	World Health Organization
ZMP	Zero Moment Point

1 Introduction

This dissertation presents the work developed in the scope of the fifth year of the Integrated Master's in Physical Engineering during the academic year of 2020/21. All investigation work was developed at BiRD LAB (Biomedical Robotic Devices Laboratory) located at the Center of Micro Electro-Mechanical Systems (CMEMs), University of Minho, Braga, Portugal. The author addresses the instrumentation and subsequent validation of a robotic cane, entitled as Anti-fall Robotic Cane (ARCane), designed to provide support for patients with impaired mobility during human gait, as well as to prevent falls with preventive and cutting-edge technology-based methods.

1.1 Motivation

The world continues to experience a demographic increase, which will further result in a higher incidence of age-related disorders. As the United Nations (UN) referred in "2019 Revision of World Population Prospects", the world's population is expected to increase by two billion people in the next 30 years, from 7.7 billion in 2019 to 9.7 billion in 2050 [1]. Despite the strong evolution of medicine, science and technology, as well as the significant global increase in quality of life and life expectancy in recent decades, there has been a decrease in fertility levels, resulting in a **disproportionality in the age structure of the global population**. Considering these events, the UN recently announced that, for the first time in history, individuals aged 65 and over, have outnumbered children under five years of age globally. Additionally, it can be seen in Figure 1.1 that the number of people aged 65+ in the world is projected to be more than double, reaching more than 1.5 billion (15.9%) in the year 2050, compared to 727 million (9.3%) people in 2020 [2].

As the population ages, the need for health services increases, however, the **nursing profession continues to face shortages** due to a lack of potential educators, high turnover, and unequal distribution of the workforce [3]–[5], presenting in 2018 a shortage of 6 million nursing professionals according to the World Health Organization (WHO) [6]. This decline in nursing professionals results in a more conservative treatment in nursing houses, by keeping the elderly with limited mobility, lying in bed day and night. Although this method can prevent the elderly from getting injured (e.g., from falling over while walking), prolonged bed rest comes with many consequences such as: loss of motor functions, lack of a feeling of independence, monotonous life, many health, mental and physical problems [7]. Therefore, the development of mobility

assistive devices, rehabilitation robots and nursing care robots is strongly needed to close the gap between the large number of elderly people and the limited number of nursing professionals.

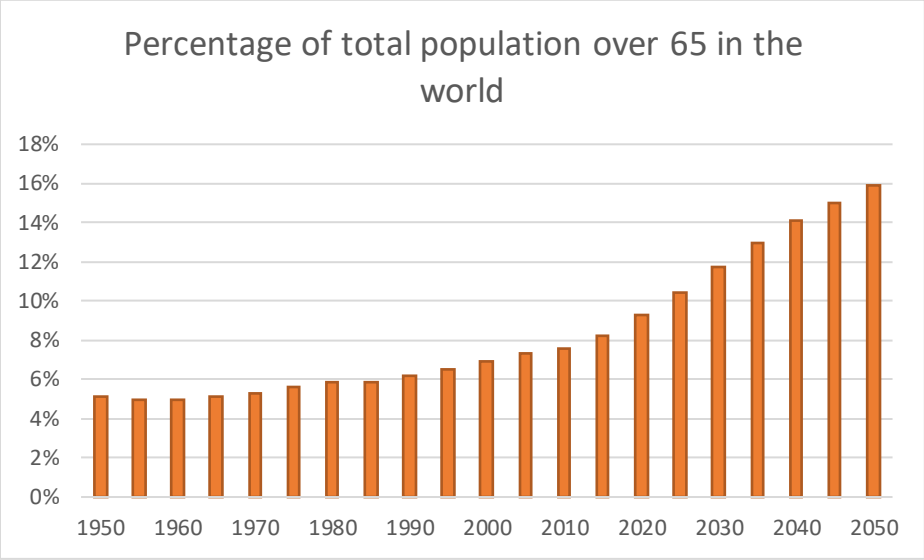

Figure 1.1: Projection and estimation on percentage of ageing population in the world from 1950 to 2050 for people aged 65 and over. Data acquired from [2].

Additionally, **falls are found directly related to age and frailty level** as the elderly are more susceptible to falls with the highest risk of death or serious injury arising from a fall. This level of risk is in part due to physical, sensory, and cognitive changes associated with ageing, such as: (i) muscle weakness in the lower limbs; (ii) slow reaction time; (iii) vision problems; (iv) balance; and (v) poor motor coordination [8], [9]. It is also associated with environments that are not adapted for an ageing population, significantly affecting their ability to move and decreasing the performance of most Activities of Daily Living (ADL) [10].

Regarding the **fall's consequences**, each year an estimated 684 000 individuals die from falls globally, as it is the second leading cause of unintentional injury deaths worldwide. It is also verified that adults over 60 years of age experience the highest number of fatal falls, with a total of 37.3 million falls that are serious enough to require medical attention occurring each year, worldwide [11]. In addition, the fear of falling presents a major problem that results in a high impact on mental and physical health. People who fall, even if they are not injured, become afraid of falling, as the non-fatal injuries associated with falls can range from minor to severe, including: (i) broken bones, particularly hip fractures; (ii) soft tissue injuries; (iii) bruises; and (iv) head trauma. This fear can cause a person to reduce their activities of daily living, which

lead them to become less active, resulting in muscle weakness, and therefore increasing their chances of falling [12]. In terms of financial costs from fall-related injuries, they are substantial, with the average health care cost per fall injury in the Republic of Finland and Australia of US$ 3611 and US$ 1049, respectively, for people aged 65 years or older [11].

Thus, the implementation and use of walking-aid devices finds itself as an essential tool to provide security and stability, by helping in different phases of daily life activities (e.g., getting up, sitting down, providing balance while standing still or while moving, going up or down-stairs) resulting in greater quality of life and autonomy for the elderly.

1.2 Problem statement and scope

The gap between the growth of the elderly population and the decline of nursing professionals finds itself in constant growth, resulting in a greater disproportionality between the number of nursing professionals and the number of elderly people, which leads to more conservative treatments in nursing houses. As a way to solve this problem, **mobility assistive devices** find their application in the field of nursing and therapy, in order to fill this gap, and help people with reduced mobility to regain their independence.

Additionally, with falls being the second leading cause of deaths from unintentional injuries worldwide, with the age group of adults over 60 years of age suffering the highest number of fatal falls, there is a clear path towards the development of a **real-time fall prevention device**. Thus, it is of great importance to design and develop mobility aid devices that are able to assist patients with impaired mobility during gait and rehabilitation training so that their motor function is partially restored, and their quality of life is greatly improved. Currently, most prototypes and designs of mobility assistive devices or walking-aid robots for elderly care do not have an integrated fall detection and prevention system. This is an extremely important parameter, which can prevent possible injuries, deaths, psychological damages that a fall victim may suffer, and reduce the monetary costs associated with falls. Thus, an architecture focused on the hardware of a robotic cane, established with the aim of solving several day-to-day problems of future end-users of this product.

Regarding the **motion control system** of most robotic canes, they often rely on expensive sensors or require major modifications to the cane, which makes them more inaccessible, limiting the number of potential users. Therefore, an innovative, cost-effective and intuitive motion control system was developed, providing user movement intention recognition, and identification of the user's gait phases. In terms of

extrinsic fall risk factors, there are many associated with the surrounding environment, one of which is poor lighting conditions, which results in poor visibility, leading to a direct association with the risk of falling. It was also found that none of the robotic canes present in the State-of-the-Art review contained mechanisms of **detection and actuation related to luminosity**, given that many falls are due to poor visibility conditions. Thus, it is aimed to implement a system capable of detecting low light and subsequently activate a light focus mechanism the ARCane as a context awareness device. In relation to **user-robot interaction**, most devices are based on a one-way communication in which the user interacts with the device but does not receive any feedback from the robot. Thus, a vibrating actuation method was adopted, allowing direct interaction and two-way communication between the robot and the user. The lack of **prevention mechanisms** capable of acting in the event of a fall also appears as a factor for the increase in the statistics of the number of falls. Therefore, a system composed of omnidirectional wheels and motors was then implemented so that the position of the cane can be adjusted in all directions of the displacement plane, providing to be useful for the motion control and future fall prevention strategies. These implementations present an innovative character and allow to improve some problems of the actual robotic canes available in the literature. Lastly, it was possible to identify that currently there are **no commercially available canes with built-in pre-impact fall detection systems**, which opens a window for the insertion of this product in the technological market and in the health industry.

1.3 Goals and research questions

The main objective of this dissertation is to instrument and validate a robotic cane, in order to obtain a prototype of a device with intuitive motion control that can provide gait assistance, and capable of detecting and preventing falls in real-time, in a broad range of environments and situations. It is intended to continue the product design and development, extending teamwork [13], to understand what the users want and need. It is pretended to achieve a better view and understanding of the robotic canes present in the literature, along with the knowledge of sensors, actuators and various electronic components characteristics.

Thereby, with this thesis, it is necessary to achieve the following goals:

- Goal 1: The first goal consists of a **survey and interpretive study** of pertinent information concerning **robotic canes**. In particular, it is intended to understand: (i) what type of sensors and actuators are used and their corresponding placement; (ii) which method of motion control, fall detection and fall prevention was used in the system; and (iii) the experimental

protocol that was carried out. In addition, it is expected to recognize the main results, limitations and challenges on existing devices in order to propose new solutions.

- Goal 2: The second goal is to enhance the **product's mission statement**, by describing the robotic cane and the target market, to study the **consumer needs** in order to have a perspective of the real utility of the device. Then, the **target specifications** of the robotic cane are updated, extending teamwork [13], to obtain a product with a market-compatible design and engineering that meets the needs and desires of the cane users.
- Goal 3: This goal aims to establish the **hardware architecture of the ARCane**, highlighting the main intended features that distinguish it from a conventional cane. It is also intended to describe the control units responsible for processing all the information that encompasses the entire electronic system. Afterwards the **electronic components** required for the sensory and actuation system are identified, as well as their respective electric circuit considering their technical specifications, operating frequencies, and communication protocol, to ensure a robust, universal and adaptable system.
- Goal 4: The fourth goal is the realization of the **interoperability tests** carried out to verify and **validate the singular and collective functioning of all the cane components**. The results of these tests will evaluate if the ARCane can meet the consumer needs and the metrics stipulated by the technical specifications.
- Goal 5: This goal is related to the proposal and implementation of a **motion control method** in the ARCane, simple and intuitive for the user. This methos aims to detect the user's intention, following his movement trajectory, while distinguishing and identifying the different phases of the events of the human gait while using the ARCane.
- Goal 6: The sixth goal aims to test the ARCane motion control in order to validate the methods and components studied throughout this dissertation, that were implemented in the robotic cane. Therefore, there will be an **evaluation of the ARCane performance** in an experimental context to identify further improvements, and research to obtain a future product that is intended for domestic use, but also in the hospital and rehabilitation areas.
- Goal 7: This last goal consists in planning and identifying the best **method of detection and prevention of falls** to be applied in the ARCane, considering the: (i) physical structure of the

cane; (ii) sensory components and actuators that encompass it; and the (iii) intended robot-user interaction.

The following Research Questions (RQ) are expected to be answered in the present work:

- RQ1: How are robotic canes in the scientific literature instrumented to provide motion control?
- RQ2: What are the main fall prevention methods implemented in robotic canes among the scientific literature?
- RQ3: What are the best sensors and the respective location on the ARCane to detect the user's motion intention and gait phase recognition
- RQ4: What is the best fall prevention strategy to be implemented in the ARCane?

1.4 Contribution to knowledge

The main contributions of this work are:

- A systematic literature review of robotic canes as a way to identify and understand the reasons of each implemented component, as well as the implementation of the motion control, fall detection and fall prevention strategies, along with the respective experimental protocol, main results, limitations and challenges.
- The initial development of an instrumented robotic cane system for human gait analysis, fall detection and fall prevention, from a Technology Readiness Level of 1 up to a level 4.
- A hardware architecture capable of responding to various user difficulties based on user information, their gait and the environment context, revealing the main features and functionalities that distinguish a robotic anti-fall cane from a conventional cane.
- The implementation of a cost-effective motion control system that gathers sensory fusion information acquired by the cane, to detect the user movement intention and differentiate the various gait event phases. An evaluation and comparison of the different applied strategies had been fulfilled to attain the best feasible results.
- A sustained analysis of the best fall prevention method for this type of cane.

1.5 Thesis outline

This dissertation is organized as follows. An introduction related to robotics assistive devices and their main distinction in comparison to the conventional assistive devices is available in Chapter 2. Also, it is included a State-of-the-Art review regarding the robotic canes present in literature, encompassing: (i) the different designs and mechanisms; (ii) the used sensors and actuators with the respective functionality and attachment location; (iii) a general overview of the implemented motion control, fall detection and fall prevention methods; as well as (iv) the performed experimental protocols, used as a reference tool for the present work.

In chapter 3, the mission statement of the ARCane is presented, along with the barriers and motivations related to its use, the intended users that correspond to potential consumers, and the gait analysis considering proper handling of the cane. A list of customer needs metrics is identified in order to define the target specifications, and guide the robotic cane overall engineering process. Finally, the structural design of the cane is presented, along with the carried modifications that ensure a robust and stable structure that can support the user's weight during the gait.

Chapter 4 addresses the proposed ARCane architecture, where it describes its present and future capabilities, highlighting the main features that differentiate it from a conventional cane. Afterwards, it is presented the central control units responsible for processing all information, along with the communication protocols and operating frequencies which are associated with the transmission of the data that makes up the electronic system. The electronic components that will instrument the sensory, actuator and power units are also selected and described, considering their technical specifications in singular and their compatibility in a collective.

In Chapter 5, it is proceeded to explain and describe the realization of the interoperability tests carried out to verify and validate the singular and collective functioning of all the ARCane instrumented components. The results of these tests will evaluate if the ARCane can meet the consumer needs and the metrics stipulated by the technical specifications.

Chapter 6 is dedicated to the implementation of motion control, where it is initially defined which method to use in relation to the ones incorporated in the literature review of robotic canes, and which suits best according to the ARCane concept and design. The motion control algorithm was then proposed, encompassing the intended operating mode for the robotic cane, through its interaction with the user, as well as the respective system architecture. Subsequently, the study of strategies that make it possible to

obtain the user's movement intention and gait phase detection was carried out, where analytical static simulations were carried out for the proposed methods. The obtained results led to the final implementation of a haptic sensor system and an axial sensor system based in force sensors. It was also described the method of transforming the forces perceived by the sensors, into movement of the cane. Finally, as a way to validate the proposed motion control method of the ARCane, experimental tests were performed with six healthy participants.

Fall detection and prevention methods are designed and proposed, to be incorporated into the ARCane, in Chapter 7, in order to distinguish the user's gait between normal and abnormal walking, so that actuation mechanisms can operate when a state of emergency is detected. A review of the software and hardware used among all fall detection and prevention systems is carried out, but also focused on robotic cane applications, to obtain the most suitable and compatible detection and prevention system for the robotic cane. The conclusions and future work proposals to continue this work are written in Chapter 8.

2 Robotic Canes: State-of-the-Art

Currently, there are several means of assistance that provide gait assistance, and the displacement of people with mobility impaired. Each device seeks to meet the needs of each subject, in order to facilitate their quality of life, improve their health conditions and offer greater independence to the user. Among the most popular and traditional mobility assistive devices, are the wheelchair, the walker and the cane. However, with technological evolution, there has been a progression towards robotic assistance means, in order to provide greater safety, improve user interaction, enable a controlled handling, and also to provide detection and prevention of falls. Among robotic assistant means, will be discussed the (i) robotic wheelchair; (ii) robotic mobile walker; (iii) robotic exoskeleton; and finally, the (iv) robotic cane.

Inspired by the most traditional means, the new robotic devices, in addition to the advantages already mentioned, present however, several limitations. In the case of electric wheelchairs (Figure 2.1): (i) they present large dimensions, which makes them very inconvenient or even impossible to be used in small spaces; (ii) they are heavy equipment, making transport and storage difficult; and (iii) depending on the person physical condition, it is a means of assistance that does not allow the movement and work of the lower limbs muscles, resulting in a greater decline in the user's bodily functions and a more sedentary mode of movement, leading to a reduction in the user's quality of life and health [14], [15].

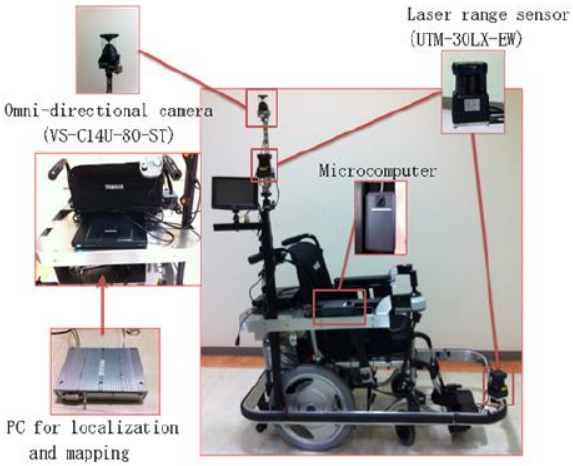

Figure 2.1: Overview of a robotic wheelchair. Image from [16].

Compared to the robotic wheelchair, the robotic walkers (Figure 2.2) assist in gait by forcing the user to move the legs, while supporting much of the user's weight, in order to achieve a more controlled and easier gait [10–12]. For these reasons, this means of assistance is widely used in rehabilitation. However, due to its large dimensions and high weight, its use is often limited to indoor and controlled spaces.

(a) (b)

Figure 2.2: Robotic mobile walkers (a) Image from [18]; (b) Image from [17].

The exoskeleton (i.e., external skeleton) is known from the animal kingdom (e.g., crabs, scorpions, spiders) for being a rigid, resistant, yet thin and malleable external structure, which allows to support the muscles and the body, prevent water loss, and protect the internal organs. Thus, with the evolution of technology, and inspired by this phenomenon, the robotic exoskeleton was developed with the purpose of supporting the body weight and assisting the user's muscles. Over the last 15 years, exoskeletons have shown an evolution in computational power, equipment size and energy requirements needed to function. Some exoskeletons are used for military applications, with the purpose of increasing the strength and speed of the users [15], [16], although most exoskeletons are found in the medical field [20], [22], [23], as represented in Figure 2.3. These are primarily intended for the rehabilitation of people with complete lower limb paralysis or weakness attributable to Spinal Cord Injury (SCI), stroke or other type of neurological impairments, and aim to improve gait or restore lost movement skills in order to achieve a functional gait.

The robotic canes, compared to other means of assistance, stand out for their: (i) low cost, which makes them a more accessible product on the market; (ii) reduced weight, facilitating its use and operation; and for (iii) reduced dimensions, which allows its use in outdoors and uncontrolled environments. With the aim of assisting the gait, the cane offers less body weight support, when compared to the walker, not placing as much support on the upper limbs. Thus, it provides less body support, but promotes greater body activity, and a more extensive and complete muscular use of the lower limbs. By having this moderate support, the user will face a better recovery, greater independence, and a more practical use during walking.

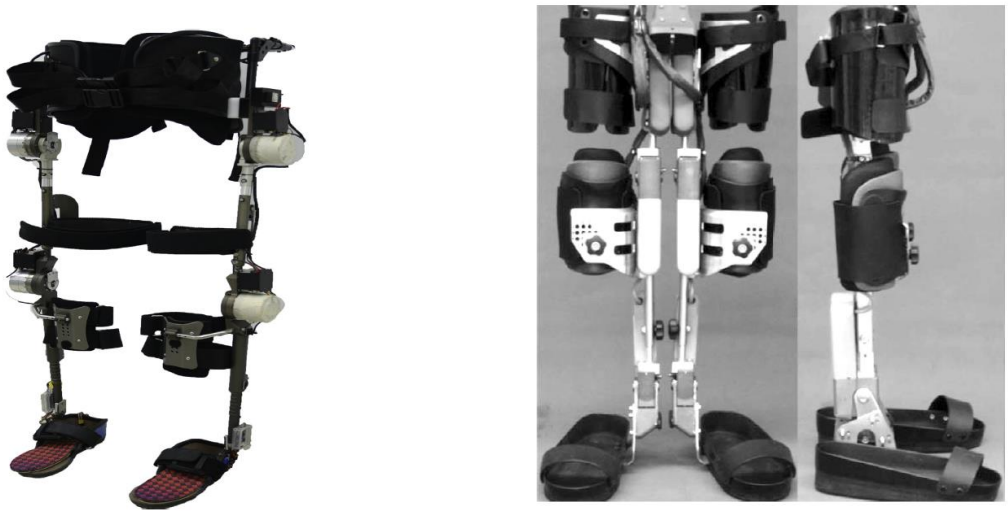

Figure 2.3: Exoskeletons targeted for the medical field. Image from [20].

This discussion and analysis of robotic assistive devices, by proceeding with an evaluation of the benefits and limitations associated with each one, led to the choice of the robotic cane as the robotic assistive device to be implemented and developed. It is intended to obtain possible developments, improvements and adaptations in this area of research, as well as progressive technological advancement.

This chapter seeks to answer some research questions carried out in section 1.3, by analyzing the State-of-the-Art of robotic canes present in the literature, considering a review strategy and eligibility criteria imposed prior to the research. Then, an analysis of all robotic canes found in the literature will be carried out, being evaluated: (i) the different designs and mechanical structures of each robotic cane; (ii) the instrumented components; (iii) the implemented motion control, fall detection and fall prevention strategies; (iv) the performed experimental protocols; and (v) the main results, limitations and challenges obtained.

2.1 Review strategy

To obtain a deeper understanding of robotic canes, an extensive literature review was carried out, based on three databases: Scopus, Web of Science and IEEE. In a primordial phase, an iteration table was created for each database, with a set of keyword combinations in order to obtain the best search terms for a successful review. The chosen keyword combinations were “Robot cane” OR “Robot walking aid” OR “Cane type robot” for Web of Science and IEEE Xplore, and “Robot cane” OR “Robot walking aid” OR “Cane-type robot” OR “Cane-type robot” AND NOT “sugar cane” for Scopus. A total of 1506 results were found using the mentioned keyword combinations. The review of these articles was performed based on the Preferred

Report Items for Systematic Reviews and Meta-analysis (PRISMA) flowchart, as illustrated in Figure 2.4 [24]. After removing 423 duplicates and 1026 articles based on title and abstract, resulted in 57 full-text articles assessed for eligibility. Following a complete reading of the eligible articles, 17 were excluded for not meeting the proposed eligibility criteria, which revealed that they were not relevant to the study in question. This selection concludes with 40 articles included in the final review.

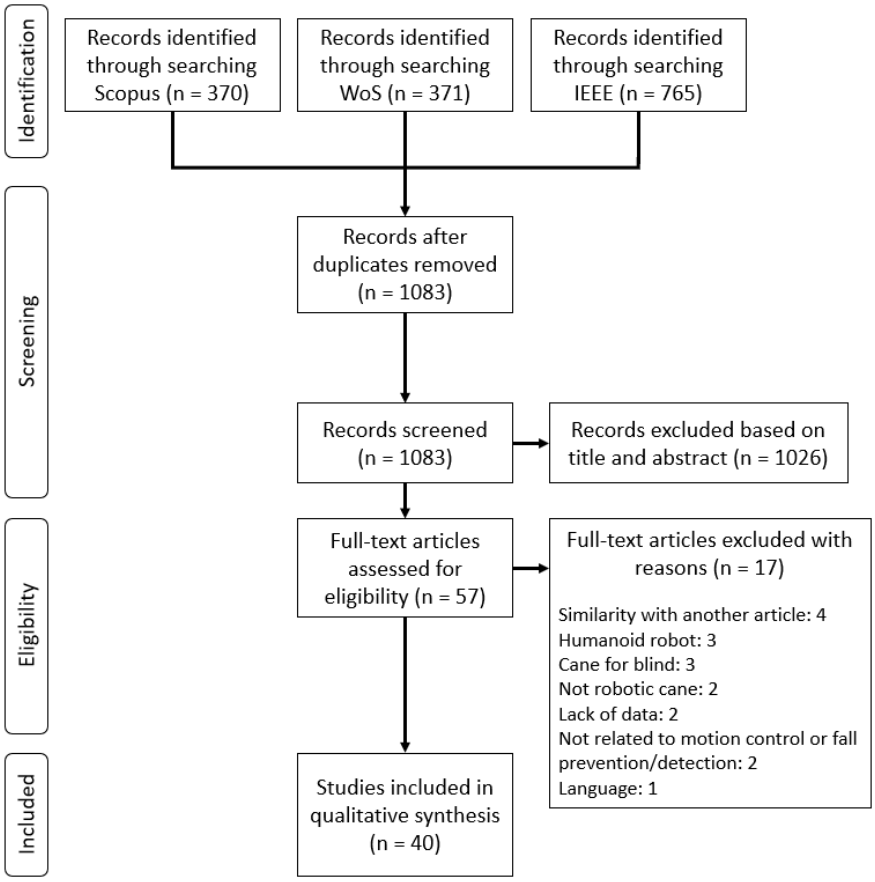

Figure 2.4: Literature review based on PRISMA flow diagram.

2.2 Reviewed robotic canes

After proceeding to read the 40 articles mentioned above, it was found a total of 18 different robotic canes in the literature. Each robotic cane presented a different configuration regarding its: (i) design; (ii) architecture; (iii) sensing systems; (iv) methods of motion control; (v) fall detection systems; and (vi) fall prevention strategies. As most of the canes in the literature are still unnamed prototypes in development, to facilitate and simplify their identification, a respective number was assigned to each robotic cane present in the review articles, as shown below in Table 2.1.

Table 2.1: List of robotic canes present in the selected articles of the State-of-the-Art

Robotic cane number	Author	Referenced articles	Number of referenced articles
1	Pei Di et.al.	[25]–[39]	15
2	Yasutaka Fujimoto et. al.	[40]–[42]	3
3	Shunki Itadera et. al.	[43]–[45]	3
4	Qingyang Yan et. al.	[46], [47]	2
5	Qingyang Yan et. al.	[48], [49]	2
6	Phi Van Lam et. al.	[50], [51]	2
7	Mohamed A. Naeem et. al.	[52], [53]	2
8	Hayang Wang et. al.	[54]	1
9	Muhammad Raheel Afzal et. al.	[55]	1
10	Ragou Ady et. al.	[56]	1
11	Sang-Hun Pyo et. al.	[57]	1
12	Shinki Suzuki et. al.	[58]	1
13	Tomotaka Ito et. al.	[59]	1
14	Yong-Zeng Zhang et. al.	[60]	1
15	Masafumi Kojima et. al.	[61]	1
16	Kento Yamada et. al.	[62]	1
17	Masahiro Kato et. al.	[63]	1
18	Kohei Wakita et. al.	[64]	1

2.2.1 Design and mechanical properties

Throughout the literature review, it was possible to verify that, even though all the robotic canes in question share the same purpose of gait assistance, they presented very **different designs and mechanical characteristics** from each other. Each robotic cane features different weights and dimensions and several types of components. They can also present various modes of handling, which allows the cane to be controlled by one hand, two hands, or even without contact. In addition, there are different robotic cane configurations and models, which can vary between 1 to 5 Degrees of Freedom (DOF), as well as its mobile structure that varies between 1 to 4 wheels. The arrangement of the cane wheels allows a total of three degrees of freedom, i.e., two degrees of translation and one degree of rotation at the base of the cane. With the use of a revolution or universal joint, it allows up to one and two degrees of rotation for the cane rod, respectively, thus obtaining a total of 5 DOF. With a wide variety of DOF, it was found robotic canes with 1

DOF (cane no. 9, 13 and 15), 2 DOF (cane no. 6, 10, 11, 12, 14 and 17), 3 DOF (cane no. 2, 3, 4, 5, 16 and 18), 4 DOF (cane no. 7), and finally with 5 DOF (cane no. 1 and 8).

According to the literature, it was possible to identify that, robotic canes composed of one wheel (cane no.2, 9, 10 and 15) and two wheels (cane no. 6, 11 and 17), as shown in Figure 2.5, are lighter, smaller and more portable than other robotic canes. Although, they present some disadvantages associated with their design, that can compromise the safety of the user. As they have only 1 or 2 points of contact with the ground, these types of canes. (i) provide few degrees of freedom to the cane system, limiting the movement of the user; (ii) cannot stand upright by themselves without the assistance of motors on the wheels, highlighting the system instability if motors are faulty; and (iii) are not robust enough to provide sufficient support to bear the user's body weight transferred to the cane in case of a fall situation.

(a) (b)

Figure 2.5: Robotic canes with (a) one wheel. Image from [63]; and (b) two wheels. Image from [51].

Among the total of 18 robotic canes, there is one robotic cane that stands out for not using wheels to move, namely the cane no. 13, as illustrated in Figure 2.6. Resembling a conventional four-leg cane, this cane features an expansion and contraction mechanism in each leg, using Magneto Rheological (RM) fluid and passive springs. This cane is designed to be able to absorb disturbances from unexpected steps on uneven terrain, as well as to stabilize the balance of the gait in order to match the gait condition of the user, in order to prevent the elderly from falling. As this cane represents a prototype still in development, it does not appear to have physical and mechanical capabilities to maintain stability while supporting body weight during a fall situation. In addition, the fact that this cane requires it to be lifted during the gait, just like a

conventional cane (300g), but with a weight of 1.2 kg, it would be uncomfortable and more difficult to use for an elderly person.

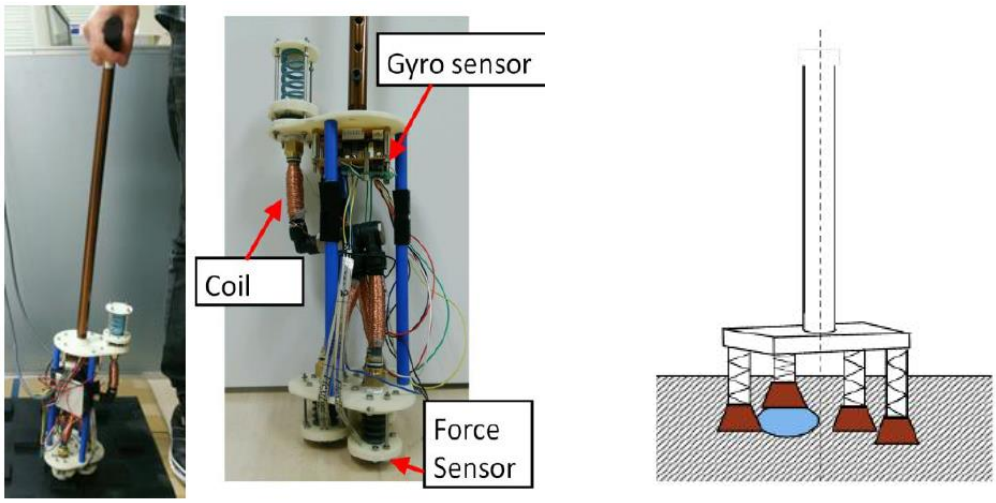

Figure 2.6: Prototype of the MR fuild-based gait assist cane [59].

Developed with the purpose of providing stability to robotic canes, there is the revolution joint, with 1 DOF (Roll), and the universal joint, with 2 DOF (Pitch and Roll) that allows to vary the angle of the cane rod (Figure 2.7). Thus, in fall situations, the angled position of the cane's rod is changed to reduce the moment that is applied to the robotic cane, and consequently help the user from falling [25], [34], [36], [49]. The second objective of this mechatronic component is to prevent the cane from falling, by offering handling and removing the rigidity of the typical fixed rod of conventional canes. Despite being an innovative method to promote robotic cane stability, the joints involve significant mechanical changes for their implementation in a robotic cane. This method implies the insertion of high torque motors, one motor for revolution joint and two motors for universal joint, in order to control the cane's rod and support the user's body weight, resulting in high costs for the design of a robotic cane. A very important point also to be noted about the use of joints, is that for poorly applied forces, when the rod of the cane is at a certain angle to prevent the user from falling, as illustrated in Figure 2.8, it will increase the chances of the cane falling, which would consequently result in the fall of the user. In perspective, these associated high costs and chances of resulting in the fall of the user, can be avoided with a rigid cane rod.

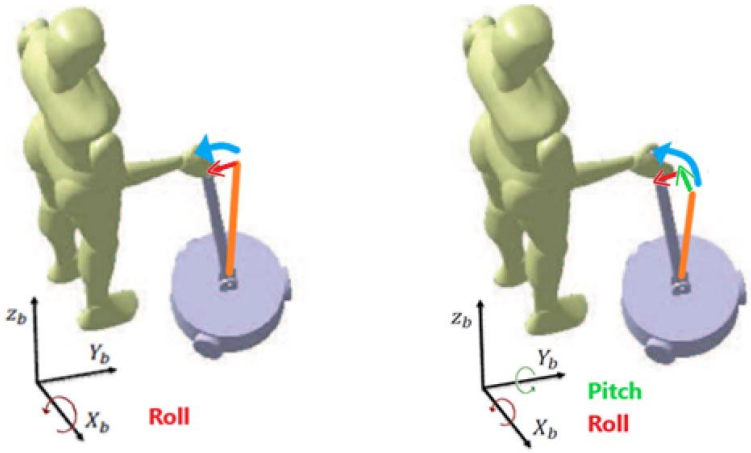

(a) (b)

Figure 2.7: Illustration of a robotic cane with (a) a revolute joint; (b) a universal joint. Image adapted from [53].

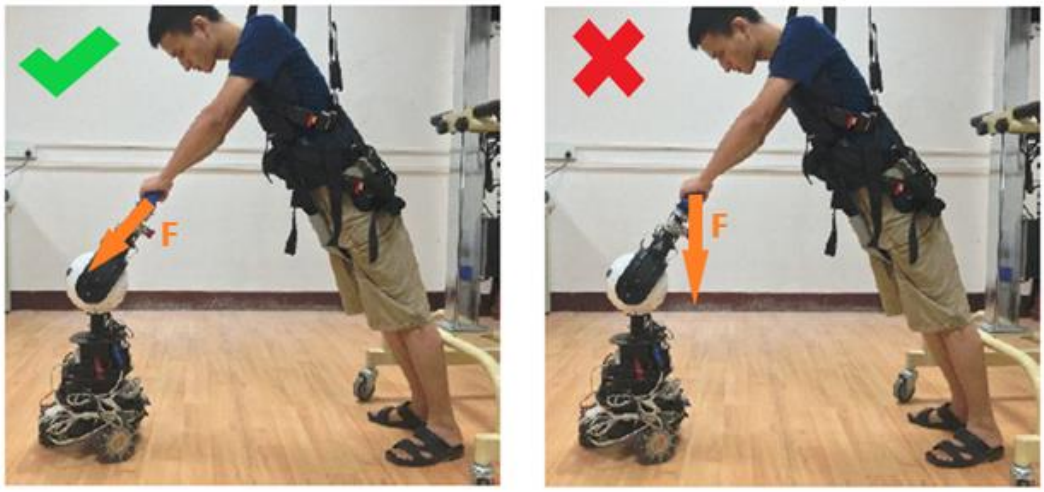

(a) (b)

Figure 2.8: (a) Correct use of the universal joint with forces applied in the direction of the fall; (b) Incorrect use of the universal joint with forces applied in the vertical direction towards the ground, potentiating the fall of the cane. Images adapted from [47].

2.2.2 Cane sensors

Cane sensors are electronic sensor-based devices that are implemented in the cane. These devices have the intent to acquire important information of: (i) the user, such as the user's gait status and gait phase recognition, (ii) the robot-user interaction by detecting the user intention of movement with forces applied on the cane; as well as (iii) important information about the cane itself, such as the cane relative position,

velocity and orientation. Within the scope of this research, it is found to beimplemented in the robotic canes: (i) axial force/torque sensor; (ii) Inertial Measurement Unit (IMU); (iii) Laser Range Finder (LRF); (iv) force sensor; (v) tilt sensor; (vi) camera; (vii) ultrasonic sensor; and (viii) infrared sensor. An overview of the cane sensors with the respective functionalities and location in the robotic canes is given in Table 2.2 and Table 2.3, along with the respective sensor location. It is found that a total of 18 out of 18 (100%) robotic canes use cane sensors. A brief review of each sensor is provided later to contextualize their use in relation to the literature.

Table 2.2: List of sensors present in robotic canes from the review literature, and their respective functionalities

Sensor	Functionality
Axial force/torque sensor	Senses the value of the translational and rotational forces applied to the cane in and around the axial directions (x-, y-, and z-axis).
IMU	It consists of the combination of an accelerometer, a gyroscope and a magnetometer, providing up to 9 degrees of freedom. • Accelerometer: measures the rate of change of velocity (acceleration) of an object along its axis; • Gyroscope: measures rotational changes concerning orientation and calculates the angular velocity along three axes, pitch (x-axis), roll (y-axis), and yaw (z-axis); • Magnetometer: measures the relative change of a magnetic field, its direction, and strength.
Laser Range Finder	Emits electromagnetic pulses in laser beams to determine the distance to an object.
Force sensor	It measures the contact reaction between two objects by calculating the pressure or the force exerted.
Tilt sensor	Used for measuring the tilt of an object in multiple axes with reference to an absolute level plane.
Camera	Obtains visual information from the environment surrounding the robotic cane.
Ultrasonic sensor	Measures the distance of a target object by emitting ultrasonic sound waves.
Infrared sensor	It emits and detects infrared radiation to detect the proximity of an object.

Table 2.3: Overview of the cane sensors with the respective sensor location

	Axial force/torque sensor	IMU	Laser range finder	Force sensor	Tilt sensor	Camera	Ultrasonic sensor	Infrared sensor
1- Pei Di	Rod (x1)		Base (x1)		Rod (1x)			
2- Yasutaka Fujimoto		Base (x1)		Handle (x1)				
3- Shunki Itadera	Rod (x1)	Base (x1)	Base (x1)			Base (x1)		
4- Qingyang Yan (1)	Rod (x1)		Base (x2)					
5- Qingyang Yan (2)	Rod (x1)		Base (x1)	Handle (x4)				
6- Phi Van Lam	Rod (x1)	Base (x1)						
7- Mohamed A Naeem	Rod (x1)		Base (x1)					
8- Haiyang Wang		Rod (x1)		Handle (x1)				
9- Muhammad Raheel Afzal				Handle (x1)				
10- Ragou Ady		Rod (x1)						
11- Sang-Hun Pyo	Rod (x1)				Rod (x1)			
12- Shinji Suzuki			Base (x1)		Base (x1)			
13- Tomotaka Ito		Base (x1)		Cane legs (x1)				

	Axial force/torque sensor	IMU	Laser range finder	Force sensor	Tilt sensor	Camera	Ultrasonic sensor	Infrared sensor
14- Yong-Zeng Zhang	Base (x1)						Base (x1)	Base (x2)
15- Masafumi Kojima		Base (x1)						
16- Kento Yamada	Base (x1)			Handle (x1)				
17- Masahiro Kato		Base (x1)						
18- Kohei Wakita	Rod (x1)		Rod (x1) Base (x1)		Rod (x1)			
Total	10	8	7	6	4	1	1	1

Regarding the **axial force/torque sensor** its main purpose is to detect interaction forces between the user and the robotic cane. Through the force map obtained by such sensors, it is possible to calculate the user's displacement intention, allowing to control the motors in order to move the cane to the desired location. This type of sensing is central to the admittance control of the robotic cane. A total of 55% of the robotic canes used axial force sensors. Throughout the literature, it was possible to identify that most of these canes used 6-axis force/torque sensors [25], or 2-axis (bi-axial) force sensors [60] (Figure 2.9). These sensors can obtain viable measurements with high precision, however, they present high costs, which makes it hard to implement in a consumer-oriented device, such as the robotic cane.

In order to reduce costs, the robotic cane no.5 [48] decided to implement four FSR sensors in the plane perpendicular to the cane's rod, situated just below the handle, as shown in Figure 2.10. With this configuration it is possible to determine the magnitude and direction of the forces exerted in the displacement plane of the robotic cane. As this idea is a good alternative to the axial sensors, due to the reduced cost, this

configuration also requires substantial changes to the cane structure, which can be a disadvantage of implementing this system

(a) (b)

Figure 2.9: Examples of a (a) 6-axis force/torque sensor [65] and (b) Bi-axial force sensors [66], [67].

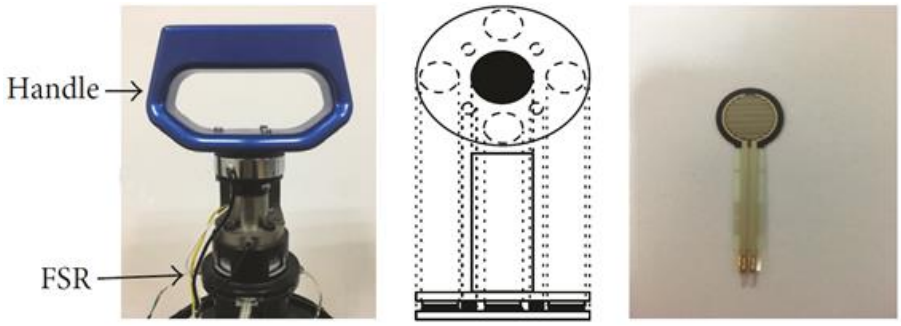

Figure 2.10: Configuration of FSR sensors to obtain an axial force sensor [48][21].

The **IMU** sensor, mostly located on the base and rod of the cane, seek to provide important information about the state of the cane. As it is composed of an accelerometer, gyroscope and magnetometer, it allows knowing the orientation and direction of the movement of the cane, as well as its acceleration values [43], [50], [61]. Consequently, the speed and relative position of the cane can be obtained through integration calculations of the acceleration.

Considering the **Laser Range Finder**, **ultrasonic sensor** and the **infrared sensor**, these are the types of sensors that are used to measure distances, as they work with the same basic principle: (i) a signal is transmitted at the target from the sensor; (ii) the target reflects the signal back to the sensor; (iii) the sensor receives the reflected signal; and finally, (iv) by knowing the velocity of propagation of the signal, and the time delay between the sending of the signal and its reception i.e., time-of-flight, the distance to the target can be calculated. Although there are many ways of measuring distance with light, e.g., by measuring the intensity, the angle or the phase shift of the reflected beam, the most common way is the Time-of-Flight (TOF) reflection time measurement mentioned above, which will be taken as reference. Even though the basic principle of the light sensors is the same, they execute it differently. The LRF, included in the category

of LIDAR (Light Detection and Ranging) sensors, uses laser beams, while the Infrared sensor uses infrared light as the signal that is being transmitted and received. The ultrasonic sensor is a sound sensor, which uses ultrasonic sound as the transmitted and received signal, at frequencies of 40 kHz, which is too high for humans to hear. Since the speed of light is much faster than sound, the light sensor has a faster response time and can be consulted more frequently than ultrasonic sensors, at the cost of requiring advanced electronics. On the other hand, ultrasonic sensors cover a wider field-of-view, being ideal for obstacle detection, and cheaper devices compared to light sensors. In general, each sensor has its inherent limitations, being sensitive to external environments. The light sensors can get inaccurate measurements due to ambient light intensity, although this is less likely in the case of infrared light sensors, and the sound sensors are dependent on the temperature and humidity of the environment in which they operate, as it changes the speed at which sound propagates (equation 2.1).

$$S = 331.4 + (0.606 * T) + (0.0124 * H) \tag{2.1}$$

- S - Speed of Sound (m/s)
- T - Temperature (°C)
- H - Humidity (%)

All canes that intend to detect and measure the distance between the user and the cane, which is a parameter of high importance in the **detection and prevention of falls**, use **LRF sensors**, due to their high accuracy, high resolution and fast response time [31], [33], [47], [49]. On the other hand, **ultrasonic and infrared sensors** are only used to **detect surrounding obstacles** [60]. Laser range finder sensors have become essential for measuring the distance between the user and the cane, however, their major disadvantage is related their high cost. Di et. al. [28] states that an alternative to these LRF sensors would be using ultrasonic sensors which would substantially reduce the cost involved in the robotic cane. However, the practical application of the use of ultrasonic sensors in robotic canes in order to replace LRF sensors is not yet found in the literature, which possibly makes this application unfeasible.

The **force sensors** located on the cane have the purpose of detecting the touch, and the forces exerted on the cane by the user. With the exception of the cane no. 13 [59], which uses force sensors in the legs of the cane to detect the balance and stability of the cane, all robotic canes use their force sensors in the handle. The cane no. 16, through a matrix of low-cost piezoelectric sensors located on the two handles of the cane, enabled the detection of the user's intention through the forces applied in the intended direction of movement, thus obtaining its admittance control (Figure 2.11) [62]. In the case of canes no. 2, 5, 8 and

9, force sensors were used with the purpose of detecting: (i) when the user is manipulating the cane; (ii) the amount of force to be exerted; and (iii) in which phase of the gait the user is, in order to slow down or stop the cane to prevent it from moving while the user is leaning more on it. The force sensors demonstrate overall a multitude of applications, being able to be located in different places of the cane in order to obtain various parameters of the gait and the user.

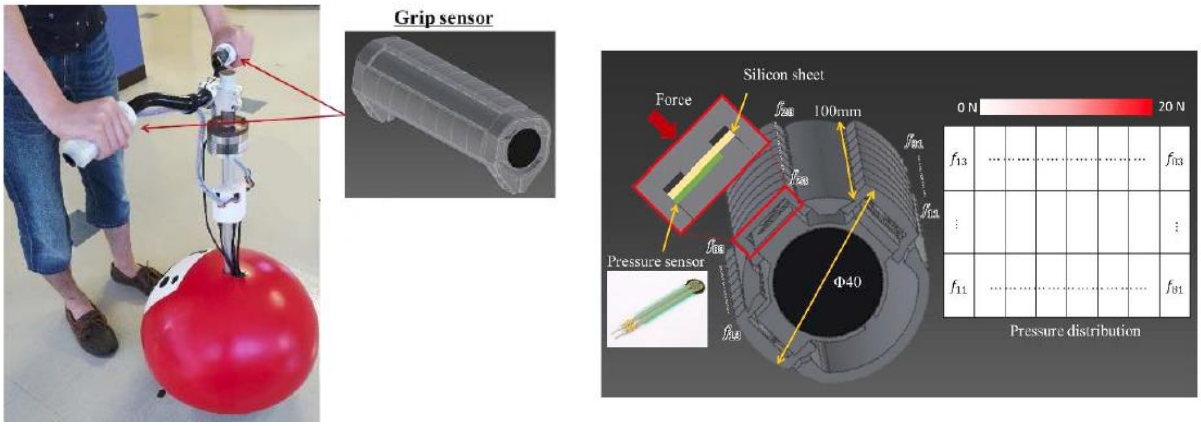

Figure 2.11: Grip force sensors matrix to detect user intention. Image from [62].

A **tilt sensor** is a device used for measuring the slope of an object in multiple axes with reference to an absolute level plane. Mostly used in robotic canes with universal and revolute joint, the tilt sensor allows to keep track of the angle of the rod that is bent, in order to compensate the weight and forces that are applied to the cane when a fall is occurring [57], [58], [64].

A **camera**, comprising RGB cameras and depth cameras, allows for sensing and detecting the surrounding environment in greater detail and collecting peripheral information. More specifically, the cane no. 3 uses an RGB-D camera, which is a specific type of depth sensing device that works in association with an RGB camera [44]. Thus, it is able to increase the conventional image with depth information in a per-pixel basis, used to detect obstacles in front of the robot for collision avoidance. The use of cameras as a sensing mode can have intrinsic disadvantages due to issues of privacy and intrusive characteristics, which may result in lack of acceptance by the users. However, it is to point out that depth cameras may not suffer from the same consequences since they are less intrusive to privacy.

2.2.3 Wearable sensors

Wearable sensors are electronic sensor-based devices that are worn by the user, under, with or on top of clothing in order to obtain relevant and important information related to the user state and position,

enabling a deeper interaction between the user and the cane. Within the scope of this research, the wearable sensors used were: (i) an IMU; (ii) force sensors (iii) a smartphone; and (iv) an oximeter. An overview of the wearable sensors with the respective functionalities and location in the robotic canes is given in Table 2.4 and Table 2.5, showing that a total of 9 in 18 (50%) robotic canes uses wearable sensors.

Table 2.4: List of wearable sensors from the review literature of robotic canes, and their respective functionalities

Sensor	Functionality
IMU	It consists of the combination of an accelerometer, a gyroscope and a magnetometer, providing up to 9 degrees of freedom.
Force sensor	Measure the contact reaction between two objects by calculating the force or the pressure exerted.
Smartphone	Used to measure the user's posture and body sway.
Oximeter	Used to obtain the heart rate, and thus calculate the rate of effort that is being performed by the user when handling the cane.

Table 2.5: Overview of the wearable sensors with the respective sensor location

	IMU	Force sensors	Smartphone	Oximeter
1- Pei Di	Shoes (x1)	Shoes (x1)		
3- Shunki Itadera				Pulse (x1)
5- Qingyang Yan (2)	Waist (x1)			
7- Mohamed A Naeem	Waist (x1)	Shoes (x1)		
9- Muhammad Raheel Afzal			Waist (x1)	
10- Ragou Ady	Weakest leg (x1)			
11- Sang-Hun Pyo			Waist (x1)	
15- Masafumi Kojima	Waist (x1)			
17- Masahiro Kato	Waist (x1)			
Total	6	2	2	1

The **IMU** presents itself as the most used wearable sensor in the review literature, since is capable of sensing multiple parameters of important character, namely due to the accelerometer, magnetometer, and gyroscope. Providing critical information about the relative position of the user, his orientation and the direction of movement. It is mostly used on the waist [63], but also on the wearer's weaker leg and shoes [35], so that the cane can follow their movement and always maintain an appropriate distance to accompany and support while walking. However, the use of an IMU may have little adherence on the part of the users as they have put it on whenever they require to use the cane. Because sometimes people might forget about using the wearable sensor, it may result in low user compliance.

Wearable **force sensors** can obtain information about forces acted upon by the user. These were used in canes no. 1 and 7, being located on the user's shoes in order to obtain information on the position of the body center of mass through the force exerted by the feet on the ground [29], [52]. They can also provide the detection of the user's gait phase, by detecting when the foot is in contact with the ground and when it is in motion. Although, the use of these force sensors may require changes to the users' shoes, which can cause discomfort, and may prove to be impractical if it is necessary to change shoes or change the person using the cane, in case of the cane is being used by various patients.

The use of a **smartphone** on the waist allows the use of software applications to identify body orientation, and to obtain body sway measurements in order to provide sensory feedback for body balance and stability, as well as for the user posture while walking with the cane [55]. Regarding the accessibility, more and more people have a smartphone, which prevents additional costs since users are more likely to carry smartphones rather than extra wearable devices. However, as people may not carry smartphones all the time with them, especially the elder, it can come as a limitation of its use.

Finally, the **oximeter**, present in the cane no. 3, has the purpose of detecting the physical state, the amount of physical effort and energy consumed while walking [44]. Thus, it allows the manipulation of the cane's motion control parameters for a more efficient and facilitated use and manipulation, corresponding to the physical condition of the user. However, the oximeter can present a barrier, as it may to be uncomfortable and unwanted whenever its continuous use is required during the use of the robotic cane.

2.2.4 Motion control

The motion control is responsible for the handling and movement of the cane, which allows a simpler and more intuitive control between the user and the cane, as well as a more controlled and safe movement,

so that the cane can accompany the user throughout progress of the gait. There are a total of four types of motion control strategies used: (i) admittance control; (ii) self-balance cane; (iii) passive control; and (iv) accompanying control mode. An overview of the motion control types is represented in Table 2.6, showing a total of 18 in 18 (100%) robotic canes uses motion control.

I. Admittance control

Admittance control is one of the most common methods to make the connection between humans and robots. This method controls the motion of the cane by using force or/and torque sensors, which consequently interprets the acquired force values to moves the cane in the user Intended Direction (ITD). It is a widely used method, as it is very intuitive, in which the forces applied result in the movement of the cane in the direction and sense of the force [26], [27], [44] . Another property is the possibility to control the speed of the cane depending on the force applied, i.e., the quantity of the user intention can be characterized by the measured resultant force. This proportionality offers a more complete level of the robotic cane control.

II. Cane self-balance control

This method is a mathematical control model of the robotic cane based on the inverted pendulum model. It can be achieved mainly using the Lie Algebra Method (LAM) [40], but also with a control law derived from a differential kinematic model of the active cane [56]. When the cane is pushed forward or backward, it drives the wheels, which consequently generates torque to adjust the cane's angle and maintain its balance (Figure 2.12). This control method is mostly used for robotic canes with one or two wheels (Figure 2.5) that are not able to maintain vertical position without the actuation of external elements. For this reason, this method can compromise the user's safety in walking and falling situations, since they offer little support to the user of the cane and present a certain instability and lack of robustness.

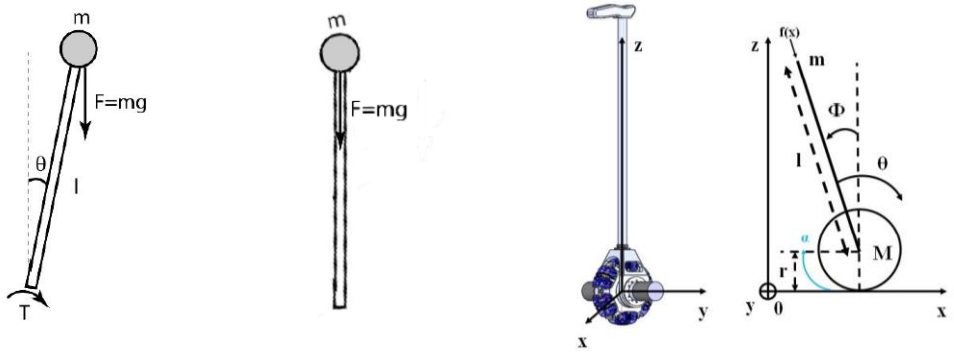

(a) (b)

Figure 2.12: Analogy between (a) inverted pendulum and (b) robotic cane based on the inverted pendulum model. Image from [41].

III. Passive control

With passive control method, the robot cane can be controlled passively without actuation of the motor's wheels. This is the simplest method, as it does not require action from external sources for the movement of the cane, apart from the natural strength of the user, which guarantees total freedom of control, movement and manipulation of the cane. Usually, canes that use this method, such as cane no. 12, usually use wheel brakes as a way to control the speed of the cane and adjust the user's gait, while maintaining the freedom of movement from the user (Figure 2.13).

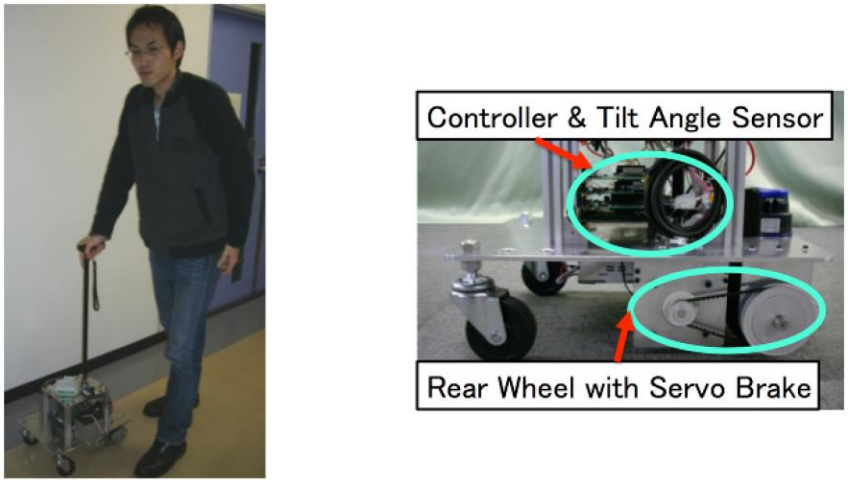

Figure 2.13: A robotic cane prototype using the passive control method as the cane motion control. Image from [58].

IV. Accompanying control mode

The principle of this control method is that the cane robot should follow the human, in the front or side, while achieving a desired distance apart of the user. With a known human relative position and velocity, it is proposed to estimate the desired position and orientation of the cane robot. This movement mode translates into a distant interaction with the user, following the gait without guaranteeing support, except in the case of a fall detection situation. Thus, the cane requires the users to have walking stability themselves, which is not an ideal way for users who need constant support, which is the majority of cases in the elderly and to those who are in rehabilitation.

Table 2.6: Overview of the motion control methods used in the robotic canes

	Admittance control	Cane self-balance control	Passive control	Accompanying control mode (non-contact)
1- Pei Di	x			
2- Yasutaka Fujimoto		x		
3- Shunki Itadera	x			x
4- Qingyang Yan (1)	x			
5- Qingyang Yan (2)	x			
6- Phi Van Lam		x		
7- Mohamed A Naeem	x			x
8- Haiyang Wang	x			
9- Muhammad Raheel Afzal	x			
10- Ragou Ady		x		
11- Sang-Hun Pyo	x			
12- Shinji Suzuki			x	
13- Tomotaka Ito		x	x	
14- Yong-Zeng Zhang	x			
15- Masafumi Kojima		x		
16- Kento Yamada	x			
17- Masahiro Kato		x		
18- Kohei Wakita	x			
Total	11	6	2	2

2.2.5 Fall detection

The gait can be divided into two states: normal walking, in which the user is in a correct posture, in balance and completing the gait cycle without any interruption; and the abnormal walking state, when the parameters present in the normal gait are not verified, and the subject is in a stop or emergency state. In a simplified way, fall detection is the way to distinguish between normal and abnormal walking, and consequently to be able to determine the emergency state. The fall detection methods used in the robotic canes were: (i) Zero Moment Point (ZMP), (ii) leg-motion-based detection, (iii) Human-Robot Coordination Stability (HRCS), and (iv) cane balance-stability. An overview of the fall detection methods is given in Table 2.7, showing that a total of 9 in 18 (50%) robotic canes have fall detection.

I. **Zero Moment Point**

The support polygon plays an important role to determine the ZMP stability. By knowing the positions of the user feet, and the cane, a support polygon can be obtained. In a quasi-static case, the ZMP is proved be equivalent to the projection of Center of Pressure (COP). By estimating and monitoring the COP position between the user and the cane, a fall can be detected, in case the ZMP moves out of the polygon area (Figure 2.14). According to Di et. al. [28], referring to cane no. 1, the Center of Pressure Fall Detection (COP-FD) method was able to detect falls (including slipping, stumbling, crossover of legs) within 350 ms. In addition, Naeem et. al. [52], referring to cane no. 7, indicates that the impedance controller achieves the desired pose of the end of the stick within 0.5s to prevent the falling of the user. However, these results are obtained with simulations and not experimentally (i.e., in a real environment).

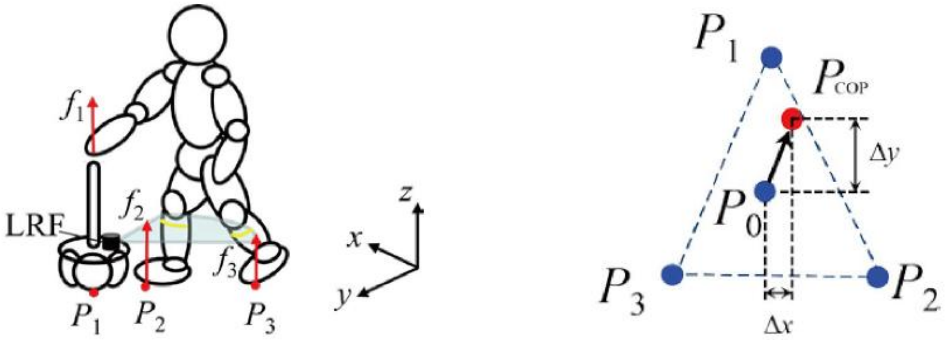

Figure 2.14: Zero moment point as a fall detection method, considering the COP position between the user and the cane. Image from [28].

II. Leg-motion-based Detection

The detection of the user's conditions and parameters of normal walking, in order to gather data, later makes it possible to distinguish and differentiate between normal and abnormal walking, by considering whether the user-cane system is within or outside the parameters, and the previously established and calculated distributions, based on the movement of the user's legs. This detection system has been used by different methods, namely: Duboi's possibility theory and Gaussian distribution.

1. Dubois' Possibility Theory

This method has the learning ability to adapt to different users by building the possibility distributions of the "normal walking" status. By measuring and detecting the distance between the cane robot and the user's legs, and the relative accelerations of the legs, data histograms for each feature are computed from the training set of adequate "normal walking" experimental data (Figure 2.15). The support of a histogram according to a feature is defined by the minimal and maximal values of the feature components of the training points. By using this method, tt was achieved the detection of stumbling within 50ms [28]. Although stumbling does not always lead to people falling down, it represents a high potential risk of falling.

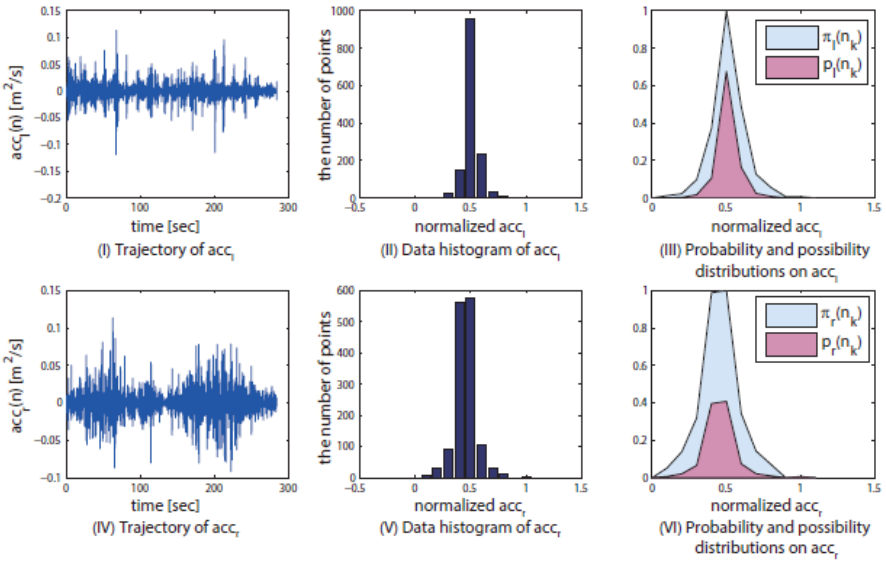

Figure 2.15: Dubois' possibility theory: trajectories, data histograms, probability and possibility distributions of user's leg motion. Image from [28].

2. Gaussian Distribution

In order to distinguish between the walking state and the emergency state, a Gaussian distribution is obtained through data of normal walking, by using the distance between the user's

legs and the robotic cane, and the frequencies of the user's legs position on the x-y plain (longitudinal plane) with respect to the robotic cane, as shown in Figure 2.16. After all the data is acquired, a Gaussian mixture distribution is obtained, and it is decided a high probability to define a range to distinguish between the walking state and the emergency state [58], [68]. Therefore, a fall can be detected by evaluating if the relative position of the user to the cane is within or out of the mixture gaussian distribution, while the user is walking.

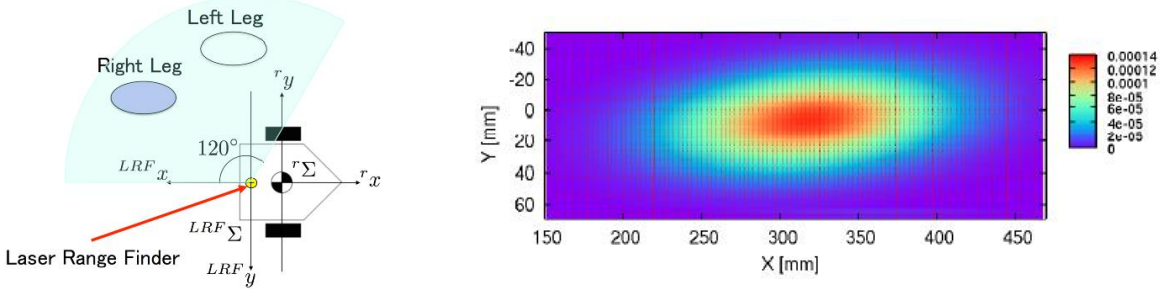

(a) (b)

Figure 2.16: Gaussian distribution as a fall detection method, by using (a) the distance between the user's legs and the robotic cane. Image from [58]. (b) to acquire the distribution of the user's legs position on the x-y plain. Image from [68].

III. Human-Robot Coordination Stability (HRCS)

The HRCS is a fall detection method that relies on a two-object system, i.e., both the stability of the robot and the user are considered during the measuring which makes this method more reliable and convenient for measuring the stability of the human-robot system than current works (Figure 2.17(a)) . Thus, the stability region is also generated by the constraint of stability for the robot and the constraint of the stability for the user [49]. The variables which influence the constraint for the robot are the magnitude of the resultant force and the direction of the resultant force through the center of gravity. The constraints of stability for the user are the posture measurements, such as the angle between the body and the ground, and the distance relevant to the robot and the leg motion speed. The user is considered as a simple two-dimensional linear Inverted Pendulum System (IPS), which makes the model of the user with the function of interactive force and the angle easy to be obtained. If the instantaneous state of the system is on the axis of the stability region, it indicates that the human-robot system is under critical tip-over stability. In case the HRCS runs out of the stability region, it shows that the human-robot system is unstable and therefore, the fall is detected (Figure 2.17(b)). Yan et. al. [46] applied Principal Component Analysis (PCA), a method of calculating optimal

linear combinations through a rotation of the coordinate system, so that the walking state is promptly detected if the sample data deviates from an offline PCA model. Using this method, and abnormal or emergency state could be detected within 55-110 ms.

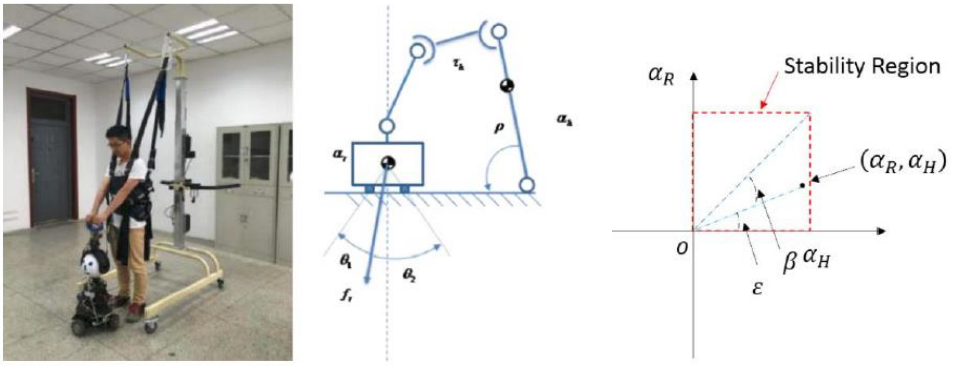

(a) (b)

Figure 2.17: Human-Robot Coordination Stability as a fall detection method, using (a) human-robot system, and the (b) stability region of the human-robot system. Image from [49].

IV. Cane Balance-Stability

This method estimates the direction and the strength of the force applied to the cane grip by the user in order to detect any possible fall [50], [51]. If the user's force can be estimated, it can judge the total balance and the stability of the system by synthesizing the information about the posture of the cane and the contact force of each leg (Figure 2.18). Estimated information about the total balance enables to realize some novel functions such as to predict, prevent and warn the risk of fall to the user.

(a) (b)

Figure 2.18: Cane balance-stability as a fall detection method (a) Image from [50]; (b) Image from [51].

Table 2.7: Overview of the fall detection methods used in the robotic canes

	Zero Moment Point (ZMP)	Leg-motion-based Detection		Human-Robot Coordination Stability (HRCS)	Cane Balance-Stability
		Gaussian Distribution	Dubois' Possibility Theory		
1- Pei Di	x		x		
2- Yasutaka Fujimoto					x
4- Qingyang Yan (1)				x	
5- Qingyang Yan (2)				x	
6- Phi Van Lam					x
7- Mohamed A Naeem	x				
12- Shinji Suzuki		x			
13- Tomotaka Ito					x
18- Kohei Wakita		x			
Total	2	2	1	2	3

2.2.6 Fall prevention

In order to ensure the safety of the robotic cane user, the cane must act to prevent a fall when a state of emergency is detected. This method must consider several parameters to achieve successful fall prevention, which include: (i) analysis of the direction of the fall; (ii) the relative position and orientation of the cane at the beginning and at the end of the fall; and (iii) the interactive forces applied to the cane. With

all these parameters in a small enough window of time to allow the user restore his balance. An overview of the fall prevention methods is given in Table 2.8, showing a total of 8 in 18 (44%) robotic canes have fall prevention.

Table 2.8: Overview of the fall prevention methods used in the robotic canes

	Fall Prevention Method
1- Pei Di	To prevent the user from falling, the cane robot will move to the position which is estimated based on ZMP stability theory and bend its stick toward the opposite direction of falling.
2 - Yasutaka Fujimoto	The cane maintains balance and moves alongside the user in order to assist when falling.
4- Qingyang Yan (1)	The fall prevention control will adjust the movement of the ball-joint and omni-base to change the magnitude and direction of the resultant force through the center of gravity of the robot to adjust its stability.
5- Qingyang Yan (2)	
6- Phi Van Lam	Detects the human force applied to the rod of the cane and consequently changing its position in order to support the user in finding a new standing position
7- Mohamed A Naeem	The fall prevention strategy is to move the cane robot to a desired position and orientation that keep the estimated ZMP inside the triangular support polygon.
12- Shinji Suzuki	To prevent the falling accident of the user, the apparent dynamics of the robot cane is changed by controlling the brake torques of the wheels.
13- Tomotaka Ito	Assists the user to prevent fall by stretching the cane's legs and generating the opposite moment actively with a MR (Magnetorheological) fluid.

Even though the canes no. 1, 4, 5 and 7 use different fall detection methods, their prevention methods are very similar, as they consist of moving the robot cane to a favorable and strategic position, depending on the user's orientation and the direction of the fall. Thus, it will allow the user to support their body weight on the robotic cane so that they can stabilize their balance and avoid falling (Figure 2.19). In the specific case of cane no. 1, 5 and 7 which consist of a universal joint, for the first two, and a revolution joint, for the last one, the angle of the robotic cane rod can be changed and controlled in order to provide extra assistance. With this method, it can increase the stability of the cane during the fall in order to prevent

it from falling over due to forceful thrust. According to Di et. al. [29], the best results to prevent falls using the tiltable rod of the cane, is by placing it with the falling direction and the tilted direction of the cane stick in the same line but in the opposite direction.

The cane no. 2 and 6 present very similar structures and characteristics as they are based on the inverted pendulum model in order to have a robotic cane in self-balance. As a prevention method, when the user applies forces in the cane, as if he is falling, the cane will operate to ensure a favorable position to assist the user during the fall. This method is achieved with the cane moving in the direction of the applied forces, so that the cane can maintain its balance, and be in an upright position. In the case of the cane no. 2, it uses the angle of the cane in relation to the plane of displacement as a main parameter, while cane no. 6 uses as its main parameter the sensing forces applied to the cane's rod (Figure 2.20). As previously mentioned, these types of cane that need to self-balance in order to remain in an upright position, show little robustness, instability and little safety, not being considered ideal for elderly users and those with impaired mobility.

To prevent the falling accident of the user, the apparent dynamics of the robot cane can be changed by controlling the brake torques of the wheels. The braking system used by the cane no.12 allows limiting the speed of the mobile base and consequently helping and preventing the user from falling. This passive system is intrinsically safe because they cannot move unintentionally, however, it may not be ideal for fall prevention due to its lack of active movement when a fall is detected. Since it can only stop the cane from moving, there may be situations where the cane requires to change its position in order to grant a stable and solid support to the user, ensuring balance and stability of the center of mass of the system, and preventing the fall from happening.

Although cane no.13 is a prototype of a robotic cane that has certain disadvantages in terms of its not very robust structure, and the implemented motion control, which requires the user to lift the 1.2 kg cane during walking, it presents an innovative method that ensures the stability of the cane while walking in unstable and irregular circuits. Overall, this walking aid method, which also seeks to help prevent falls, has little ability to provide security and stability to support the user's body weight in the event of a fall.

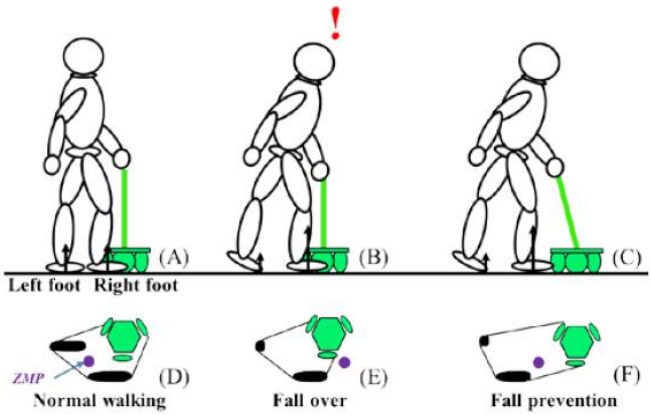

Figure 2.19: Fall prevention method based on the movement of the robotic cane to a favorable and strategic position, with the angle of the robotic cane rod changed and controlled in order to provide extra assistance to the cane during the fall. Image from [29].

Figure 2.20: Fall prevention method based on the cane self-balance and its capability to maintain balance and move alongside the user in order to assist when falling. Image from [51].

2.2.7 Experimental protocol validation

The experimental protocols carried out by the articles in literature are intended to **test and analyze the general functioning of the canes**, namely the: (i) sensory units; (ii) actuation units; their methods of (iii) motion control; (iv) fall detection; and (v) fall prevention. The tests carried out by the literature take into account various parameters, varying between: (i) the environmental conditions of the tests; (ii) test duration; (iii) distance to travel with the robotic cane; (iv) inclination of the travel plan; (v) health conditions; (vi) age groups; and (vii) number of participants. Additionally, there are certain tests in which the participant is instructed to think or act in certain ways in order to carry out the experimental tests. Several features are

then be evaluated, such as the user-cane interaction (adaptation, ease of use, handling, stability and comfort), fall detection (detection time and its accuracy) and the cane's response to fall prevention.

A total of 29 articles performed experimental tests and the number of participants ranged from one to eight people. The study from Pyo et. al. [57] stands out from the other articles, as it performed experimental tests with hemiplegic patients (condition caused by brain damage or spinal cord injury that leads to paralysis on one side of the body), with an average age of 60. The remaining articles performed the tests with healthy subjects, and the mean ages ranged between 23 and 27 years of age. Some of the instructions given to participants before taking the tests included:

I. Walk around freely during five/six minutes to get used to experimental conditions [44], [56];
II. The user of the cane to attach a fixture (leg-brace) to one of his legs under the assumption that it is a weak leg [26], [35];
III. Inform the subjects how to operate the cane robot [38];
IV. The user to practice walking with the cane robot in order to learn how the cane robot behaves [27], [39].

The experimental tests performed which involved using the robotic cane included:

I. Subject walks with cane on flat ground and on a slope [26], [32];
II. Simulate stumbling or falling in different directions [28]–[31], [34];
III. The user tends to fall backward and forward [36], [41];
IV. The subject walks forward 1, 3, 5 or 10 meter straight with the robotic cane [27], [45], [46], [56], [57], [61], [63];
V. Testing upright standing using the cane [55];
VI. Walk in an infinity loop [52];
VII. Walking with the cane for about 12 minutes [28], [30];
VIII. Turn right and left motion with cane [28], [38], [50];
IX. Pretend to walk like an old person [37];

Such procedures allow obtaining results that will later be evaluated to determine and characterize the functioning and behavior of the robotic cane. The parameters in which these experimental tests were carried out, as well as the evaluated features, are procedures to be considered for the experimental protocol of the present study.

2.2.8 Main results obtained

Experimental protocols seek to obtain reliable and complete results that resemble the use of the robotic canes in the real world, and not only for specific environments and users. Several issues were addressed in the results of each literature study. Bearing in mind, that all robotic canes have as their main objective to guarantee the safety of the user, there are several parameters to consider so that stability, comfort, detection and fall prevention are ensured for users.

Regarding **body stabilization**, Itadera et. al. [43] mentioned that touching motion and somatosensory feedback could provide useful restriction for stabilization of body sway, and Afzal et. al. [55] also added that body sway can be reduced with active guidance feedback from a haptic device compared with providing only haptic sensory feedback.

By manipulating the **admittance control parameters,** Itadera et. al. [44] demonstrated that the larger coefficients of admittance control i.e., virtual mass and damping coefficients, the more difficult it is to walk for a long distance. These results of control experiment demonstrate a potential use in gait training for rehabilitation, by varying the admittance control parameters, to adjust to a proper walking load.

In terms of **load exerted**, Nakagawa et. al. [27] refers that by making the cane robot function in a similar in which an ordinary cane functions properly, the average load applied to the affected leg is reduced. Additionally, Wang et. al. [54] mentions that in the supporting phase, the pressure by the palm is the only force applied on the cane, and in the moving phase, the lift force is the main input, and the pressure is the secondary force. In the same scope, Di et. al. [35] developed an optimized motion control of the cane robot based on the characteristics of the gait pattern, achieving an average reduced load of 30% for the affected leg.

The **fall detection** starts by distinguishing normal walking from abnormal walking. Yan et. al. [46] demonstrated that with a small number of built-in sensors, the loss of human-robot coordination could be detected, i.e., a state of emergency has occurred. The emergency state detection time was attained within 55 – 110 ms using the HRCS method along with a PCA algorithm. Using the ZMP method, falls could be detected within 350ms and stumbling detection within 50 ms using Leg-motion-based Detection [28].

There were presented similar methods for **fall prevention** which involved the movement of the cane, by changing its position to support the user's standing motion [40], moving the cane into the direction of the user's fall direction [25], and controlling the position and posture of the cane robot in order to move the COP back into the support polygon [29], [30]. By using impedance control in dynamic simulations, Naeem et. al.

[52] achieved the desired pose of the end of the stick withing the required time to prevent falling of elderly, which equals to about 0.5 s. In a passive way, instead of controlling the movement of the cane, Suzuki et. al. [58] developed a passive cane controlled with a brake system, which can limit the speed of the mobile base. Therefore, when the user state estimated tendency to fall during the walking, high inertia and damping coefficients were derived by the distance between the cane and the user, preventing the user from falling.

In general, these results provide a critical and real knowledge of the products developed by the literature, as well as their respective functionalities and capabilities, being considered in the further development of the present robotic cane prototype.

2.2.9 Limitations and challenges

From the analysis of the experimental results, the obstacles and limitations of the robotic canes in question were defined, as well as future proposals for advances and improvements in order to obtain an optimized and efficient product for its purpose of assisting the gait of people with reduced mobility. It is summarized in Table 2.9 the overall robotic canes limitations gathered from the literature, referring to the respective articles and challenges.

Table 2.9: Robotic canes limitations and challenges, gathered from the literature

Parameters	Limitations	Challenges
Dimensions	-----	- Reduce the size and weight of the system [40], [50], [51], [63].
Costs	-----	- Lower the cost by integrating new motor drivers [40]; - Develop a low-cost sensing system to reduce the cost of the cane robot [64].
Battery life	-----	- Increase the working time of the batteries before recharging is required [40], [50], [51].
System time response	-----	- Address a suitable control scheme to minimize the time delay of operation (using PID and PD controllers) [43]; Direct the study to a finite time fall prevention strategy, by limiting the fall procedure to a shorter time (∼1-2 seconds) [36].

Parameters	Limitations	Challenges
Handling	- The use of both hands is required to operate the cane robot, meaning there is no free hand for external manipulations [38], [50], [61], [62].	-----
Experiments	- Only tested forward falling [48].	- Perform experiments in an extended period to evaluate the long-term effect of gait training with the cane robot [44]; - Conduct a clinical gait trial with elderly or handicapped people to verify the effectiveness and evaluate the proposed methods, mechanism and control algorithms of the assistive cane robot [30], [33], [38], [45], [57], [58], [60], [61].
Motion control	- Cane designed and limited to move in a preplanned walking path [60]; - Cane control only works when the user is walking forward. It is intended, in the future, to deal with situations in which the walking direction changes [56]; - The position of the user is not considered, only the obstacles around [48];	- Estimate the gait and the direction in which the user is walking, as well as the threshold distance between the user legs and the cane, to stop when is too further from the user [27].
Fall detection and prevention	- Requires previous data from the patient gait first, in order to obtain fall detection [46], [58].	- Propose a three-dimensional human dynamics model for simulating fall prevention strategies [28]; - Further investigation into the abnormal walking cases monitoring (e.g., circumduction gait, scissoring gait, tandem stance, slip, legs crossover), and effective fall prevention measures research to avoid injuries of the users based on the walking state monitoring [28], [30], [46].

The predominant parameter, with most articles in common, was related to the experimental trials, more precisely, the **lack of clinical gait trials**, with elderly people or people with impaired mobility. This is seen as a very important mark, as it will allow testing robotic canes in real conditions, with patients who meet the specifications and needs of the cane. Another point, which was not addressed above, but is relevant to consider, is the lack of **robotic canes with fall prevention strategies that do not require the use of wearable sensors** by the users. Out of the total of eight robotic canes with fall prevention, only five do not require wearable sensors. However, of these five, there are two that contain passive fall prevention (canes nº 2 and 6), and there are also another two canes in which the fall prevention does not involve moving the robotic cane, implying that it remains motionless when a fall is detected (cane 12 and 13). This means that out of the 18 reviewed robotic canes, only one robotic cane has an active fall prevention strategy, with a mechanism that involves the movement of the cane, and does not require the use of wearable sensors. Lastly, there is the fact that many robot canes can't **distinguish the user's gait phases**. This is a key factor as it provides enough information for the robotic cane to follow the user during the gait, as well as determining the user's walking state, and detect abnormal walking, which may also be related to a possible fall of the user.

2.3 Discussion

Throughout this chapter, it was possible to obtain a general analysis of robotic canes present in the literature, encompassing their different structures and designs, types of sensory and actuation components, methods of control, detection and prevention of falls. It also helped to get a better idea of the stability, safety, degrees of freedom and the type of maneuverability of each type of the described robotic canes.

Considering the arrangement of the robotic cane wheels, they can have a maximum of three degrees of freedom in terms of mobility. If a revolute or universal joint is added, the cane's degrees of freedom can go up to four and five, respectively. In terms of stability and support, it was discussed that canes that have only one or two wheels may not provide enough stability to support the body weight transferred to the cane during walking and in situations of falling, which can result in an unstable system not recommended for people with reduced mobility.

Of all the robotic canes found, all use sensors included in the cane, while only 50% of robotic canes required the use of wearable sensors in order to complement motion control, fall detection or fall prevention methods. Wearable sensors have shown many advantages but also many associated limitations, either because they are uncomfortable, impractical or because they require the user to remember to wear them

whenever using the cane. These factors can pose usability and acceptability challenges in relation to the users, which in turn can compromise the use of the cane.

It was found that the main limitations that most robotic canes in the review had in common in terms of experimental tests, are the lack of clinical gait trials with the elderly or people with reduced mobility, which demonstrates that the systems developed were not tested in the real environments , but with people who did not match the specifications of the robotic cane's intended user. It was also found that out of the 18 reviewed robotic canes, only one has an active fall prevention strategy, with a mechanism that involves the movement of the cane, that does not require the use of wearable sensors by the user. Another major limitation is the fact that the user's gait phases are not distinguishable by the sensor systems of many robotic canes in the literature, representing an essential factor for gait monitoring and possible detection of falls.

In an also very important note, it was possible to identify that there are no commercially available canes with built-in pre-impact fall detection systems, which opens a window for the insertion of this product in the technological market and in the health industry. Finally, with the combination of all these factors, it enabled to have a more concrete idea of the anti-fall robotic cane to be developed and instrumented.

3 Product Design Enhancement

As previously discussed, an opportunity was identified for the ARCane, opening up the possibility of enhancing a project mission statement in order to understand the relevance of this device. The mission statement is composed by different steps, including: (i) defining a description of the product; (ii) indicating the target market for the product; as well to (iii) determine some premises for the robotic cane, so that the final concept works according to the user.

This chapter also seeks to obtain an in-depth understanding of the main barriers and motivations related to the use of the cane, to whom its use is intended, and a subsequent gait analysis considering the correct use of the cane. The consumer needs for the robotic cane are also identified, as they play an important role in judging the real usefulness of the device. The process of identifying consumer needs is an integral part of future product development phases. Such phases of development are primarily defined by the product specifications, which is a set of individual specifications that describe what the product must do, through precise and measurable terms. They must be defined at an early stage of the development process to achieve a product with market-compatible design and engineering. To close this chapter, the structural design of the cane is presented, along with the main elements that compose it. Some modifications were made to the structure of the cane, so that the capabilities of the robotic cane prototype can be improved, to obtain a device that matches the mission statement.

3.1 Mission statement

It is important to understand the relevance of the ARCane, as well as its possible insertion in the market. The major problem in question lays down to the high rate of falls, which causes great impacts on physical and intellectual health, in addition to high monetary costs worldwide. The main focus lais on people with reduced mobility, which may be due to stroke, Parkinson's disease, or other type of limiting health factors, englobing all age groups. It is aimed to overcome the associated difficulties in the gait process as well as providing assistance in preventing falls.

The data obtained from all the results of the SoA review, demonstrates a potential product and a wide availability in the market opportunities. With this information we can define the product's mission statement, which intends to explain its purpose, intentions and guidelines to be followed for the project in question. The benefit proposition is related to the **real-time fall prevention strategy**, i.e., the ability to prevent the fall and

avoid the related negative consequences. On this matter, the primary market for this device is aimed at **consumers with balance impairments**. Since fall events are caused by many risk factors, it is possible to include every costumer who may need some form of balance assistance.

The secondary market is aimed at **institutionalized elderly and patients undergoing rehabilitation**. Falls are not unique to the elders, however, age has been identified as a prominent major risk factor, and a clear link has been established between aging and higher rates of falls. When opting for a market in institutions and rehabilitations, the objective is to define a starting point for the ARCane as a market product, allowing a study of the product's performance before developing other functionalities for applications in the real world.

The **intentions for the ARCane** are a handheld device with smooth and intuitive motion control, and an integrated real-time fall detection system and fall prevention strategy. The handheld assumption is determined by the nature of the cane as an assistive device, which is a product that is held by one hand. Additionally, according to Afzal et. al. [55], the contact between the user and the cane is of great importance, since the use of haptic light touch improves the balanced posture, assisting the human brain to produce better upright balance and providing lateral stability during walking. Finally, it is desired that the final concept works according to the user, in order to adapt to their type of gait, physical characteristics, health conditions, and needs. The mission statement for the ARCane is summarized in Table 3.1.

Table 3.1: Mission statement for the anti-fall robotic cane

Mission Statement: Anti-fall Robotic Cane	
Product Description	• Cane with built-in real-time fall prevention strategy.
Benefit Proposition	• Prevents falls and avoids injuries related to those events altogether.
Primary Market	• Consumers with balance impairments.
Secondary Markets	• Institutionalized elders. • Rehabilitation patients.
Assumptions	• Handheld. • Built-in fall detection system and fall prevention strategy.

3.2 Usage of the cane

Many adults become less active as they age, which exacerbates the physical effects of aging. In addition to poor balance and coordination, there are some other factors that can make it difficult for an

elderly person to walk, such as: medication side effects, chronic diseases, arthritis, foot discomfort, weakened muscles and bones, dementia, impaired vision, shortness of breath, and poor reaction times. Illness and injuries in general can make an elderly person feel less secure on their feet, which can affect their balance and consequently trigger a fall accident [69]. Due to all these factors, once an elderly person begins to have walking difficulties, it can also cause them to develop a fear of falling that prevents them from performing essential daily activities [70]. Thus, in this chapter the questions "Why use a cane?", "Who should use a cane?" and "How to use a cane?", will be addressed in the respective order.

3.2.1 Barriers and motivations

There is still a high percentage of elderly people with gait limitations who deny the need for a walker or a cane. Some resist to use assistive devices out of pride and vanity because they do not want to look old or fragile. Other reasons for their non-use included believing: (i) it was not needed; (ii) due to forgetfulness; (iii) the device made them feel old; and (iv) inaccessibility [71]. A common issue that is present among the elderly is using the furniture in their homes to stabilize themselves when walking, which provides a false sense of security.

A survey of 262 people aged 60 and over, performed by Luz et.al in [71], showed that the non-use of assistive devices led to a significantly higher proportion of falls resulting in hospitalization than among device users. Of the participants who were hospitalized and required surgery, 100% were non-users of aid devices. Additionally, Resnik et. al. in [69] conducted a survey of 65 participants aged 65 and over, on attitudes and beliefs that strongly affect the decision to use mobility aids. For all participants, the perceived stigma of using mobility aids was due to fear of aging and physical decline. For many, the use of mobility aids was associated with feelings of sadness and depression. Cane users discussed about the discomfort, especially when going from one place to another and requiring finding somewhere to put the cane without it falling over. Participants also expressed concern about the use of unsafe or inappropriate equipment, citing an increased awareness of discrimination against people who use mobility devices. As a way to overcome those limitations, some seniors felt that fashionable aids would make them more likely to use them. Furthermore, sporty looking equipment was preferred over standard medical looking devices and ultimately, they believed that motorized equipment offered not only convenience and ease of use but also in some ways youthful looks.

Although many people are discouraged from using a walking aid device, there are many benefits that come from using it, in addition to those already described in section 1.1. It is to be considered, that many seniors just do not do as well as they did when they were younger because their general senses and reflexes diminish and slow down. Canes and walkers compensate for these senses by helping the brain perceive where the body is and where the feet are going, consequently restoring security and confidence in older adults [69].

In addition to being functional, walking is considered an exercise. The benefits of exercise include maintaining mobility, as well as improving: (i) the ability of weak muscles to utilize energy; (ii) blood flow to the muscles; (iii) endurance; and (iv) improving a sense of well-being [72]. Sedentary injuries and inadequate forms of rehabilitation will lead to a faster decline of body functions if correct walking exercises are not implemented. The muscles of the lower limbs will also atrophy faster, which may bring serious damage to people's health. Thus, appropriate walking exercise is indispensable to improve the quality of life [73]. According to Resnik et. al. [69], the majority of participants indicated that a physician's recommendation to use a device would strongly motivate their decision to adopt one. Clinicians can strongly influence the decision to start using an assistive device and can play an expanded role in discussing and observing mobility, recommending mobility aids, or referring patients to other clinicians (e.g., physical therapists) to prescribe appropriate equipment and gait improvement lessons. They may also suggest that mobility aids would be especially valuable for increasing safety and comfort in crowded places, on dark nights or during slippery weather, emphasizing the device's multiple functions within the user's needs, living environment and lifestyle. Thus, framing mobility aids as a means to enhance patient's independence and autonomy can increase the patient's acceptance. This can be achieved by pointing out that rather than limiting them, walking aids provide more independence and autonomy, as they can help people stay active and engage in all kinds of social events and activities.

3.2.2 Intended users

The use of a walking-aid device is dependent on the health condition in which a certain person is. The subject must first be evaluated by a health professional, and finally, guided to the appropriate type of assistive device that corresponds to the respective needs and limitations of the user. Although many elderly people and patients are not so weak that they can walk, a little support from a cane or stick is needed to

help them maintain balance and walk outdoors, allowing them to carry out high-quality lives or accelerate rehabilitation. In such situations, a robotic cane system can be more useful than a robotic walker because of its flexibility, light weight, and small size.

The ARCane is a device developed to work in the health industry, aiming to improve the health care provided. Being also a device with a multipurpose character, which works in the scope of assistance and body motor assessment. In addition to the context of controlled home use, it can be used in hospitals, rehabilitation centers, nursing homes or other health service delivery units. In the scope of evaluation, with a view to assist and rehabilitate the motor functions of the body, such robotic devices also enable the inclusion of caregivers, allowing them to objectively monitor the motor performance of patients during physiotherapy sessions. In the long term, it is expected that this system can be spread across the broad spectrum of diseases that severely affect the geriatric community. Like the general cane, the intended users can be evaluated based on the assessment of care requirements, such as the "Nursing care level" and the "Elderly Mobility Scale".

3.2.2.1 Nursing care level

Nursing care level is an indicator to judge to what extent the condition is when receiving nursing care service [63]. Typically, the cane users are those who require assistance level 1 and assistance level 2 in nursing care level, as represented in Figure 3.1. The guidelines for assistance level 1 and assistance level 2 are as follows:

I. **Assistance level 1:** Regarding basic actions in everyday life, it is possible to do almost oneself, but in order to prevent progression to care levels, some form of assistance is needed in Instrumental Activities of Daily Living (IADL).

II. **Assistance level 2:** Compared to assistance level 1, the ability to do IADL is slightly reduced, and some kind of support is needed to maintain or improve the function.

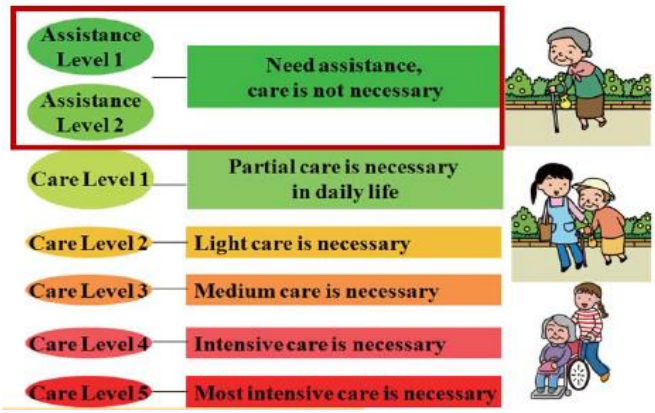

Figure 3.1: Nursing care level degree chart, from [63].

3.2.2.2 Elderly Mobility Scale

The **Elderly Mobility Scale (EMS)** is another indicator of the type of assistance needed, based on a 20-point validated assessment tool for the assessment of frail elderly subjects, mostly used in a hospital setting or daycare facilities. Its purpose is to provide a scale for assessing mobility, considering locomotion, balance and key position changes, being able to predict the risk of falling. The EMS assessment is based on an individual's mobility problems, specifically through seven functional activities, including bed mobility, transfers, and bodily reaction to perturbations.

EMS scores have been found to be useful for allocating people to the most appropriate care environment [74] and have shown a direct correlation between lower EMS scores and higher rates of falls [75], making it a useful tool in determining users who need an auxiliary device. In the EMS, gait is assessed based on the type of assistance needed to walk. The subject achieves maximum points if he walks safely without assistance, and in the case an assistive device, the score decreases. These scores are made up of the following ranges:

- Scores under 10 –These patients are dependent on mobility maneuvers; require help with basic ADL, such as transfers, toileting, and dressing;
- Scores between 10 and 13 – Generally these patients are borderline in terms of safe mobility and independence in ADL i.e., they require some help with some mobility maneuvers;
- Scores over 14 – These patients can perform mobility maneuvers alone and safely and are independent in basic ADL.

From the description obtained in these results, we can conclude that the anti-fall cane is probably in the range scores of 10 to 13. However, these are general interpretations, since for the use of the cane other factors must be considered, such as cognitive impairment, lower limb dysfunction, gait abnormality, and foot problems, being duly evaluated by a health professional from the geriatrics area. The EMS scale can be seen appendix I.

3.2.3 Gait analysis and proper handling

Cane misuse can become a problem for people being introduced to walking aids. Therefore, it is important to understand that education and training in the use of a walking aid is of great importance. If the cane is not being used correctly or is poorly adjusted, it cannot help an unstable individual, and sometimes it can serve as a false sense of security, and even contribute to a fall.

Before examining gait with a walking aid, it is necessary to understand the mechanics of **what is perceived as a "gait cycle"**. The human gait is a complex locomotion with a rhythmic and standardized sequence of movements that end in a forward displacement of the human body center of gravity [76], with the gait cycle defined as the period starting with an initial floor contact (i.e., Initial Contact) to a similar posture [77]. The **cyclical property of the human gait** allows it to be considered as a succession of strides [56]. During a stride, each leg alternates between a stance phase and a swing phase. The stance phase corresponds to the period in which the reference foot is in contact with the ground and the swing phase corresponds to the time when the reference foot is in the air. The transition between the two phases occurs after a double stance, during which both feet touch the ground. The gait cycle is used to describe an entire period of walking. In the past, the gait cycle was described with actions that did not correspond to the gait phases of people in general. For example, initiation of the stance is often called heel strike [69], [78], [79]. However, the heel of a partially paralyzed patient may never be in contact with the ground or may do so significantly later in the gait cycle. Likewise, the initial contact with the ground can be made by the whole foot (i.e., flat foot), instead of having contact with the forefoot, which occurs later, after a period of heel-only support. Therefore, to avoid these difficulties and other areas of confusion, the Rancho Los Amigos gait analysis committee developed a generic terminology for the functional phases of gait [80], being the terminology to be considered when describing the human gait phases.

The **human gait assessment** can be designed as eight discrete subphases with continuous behavior. The stance phase is divided into five subphases: initial contact, loading response, mid stance, terminal stance and pre-swing, while the swing phase is divided into three subphases: early swing, mid swing and terminal swing. The description of the gait phases is listed below, and their representation is portrayed in Figure 3.2.

1. **Initial Contact**: this phase comprises the moment when the foot touches the floor.
2. **Loading Response**: in this phase the shock is absorbed as forward momentum is preserved. The phase begins with initial floor contact and continues until the other foot is lifted for swing. The reference foot goes from heel contact to full foot contact during the loading response phase.
3. **Mid Stance**: it begins when the other foot is lifted and continues until the body weight is aligned over the forefoot. During mid stance the body weight is tolerated by the reference leg while the other leg is in the initial swing and mid swing phases.
4. **Terminal Stance**: it starts with the heel of the reference leg rising and continues until the other foot strikes the ground, completing the single-limb support. Throughout this phase, the body weight progresses past the forefoot.
5. **Pre-Swing**: this final phase of stance begins with the initial contact of the opposite limb and ends with the ipsilateral (i.e., same side of the body) toe-off. The objective of this phase is to position the limb for swing. The pre-swing phase and the terminal stance phase require the largest muscular power to propel the body forward [81].
6. **Initial Swing**: this phase is approximately one-third of the swing period, beginning with a lift of the foot from the floor and ending when the swinging foot is opposite the stance limb.
7. **Mid Swing**: during this phase, it is carried the motion from the initial swing and ends when the swinging limb is forward, and the tibia is vertical.
8. **Terminal Swing**: this final phase of swing begins with a vertical tibia and ends with the leg reaching out to achieve step length and the foot striking the floor. Limb advancement is completed as the leg moves ahead of the thigh, and is completed through knee extension.

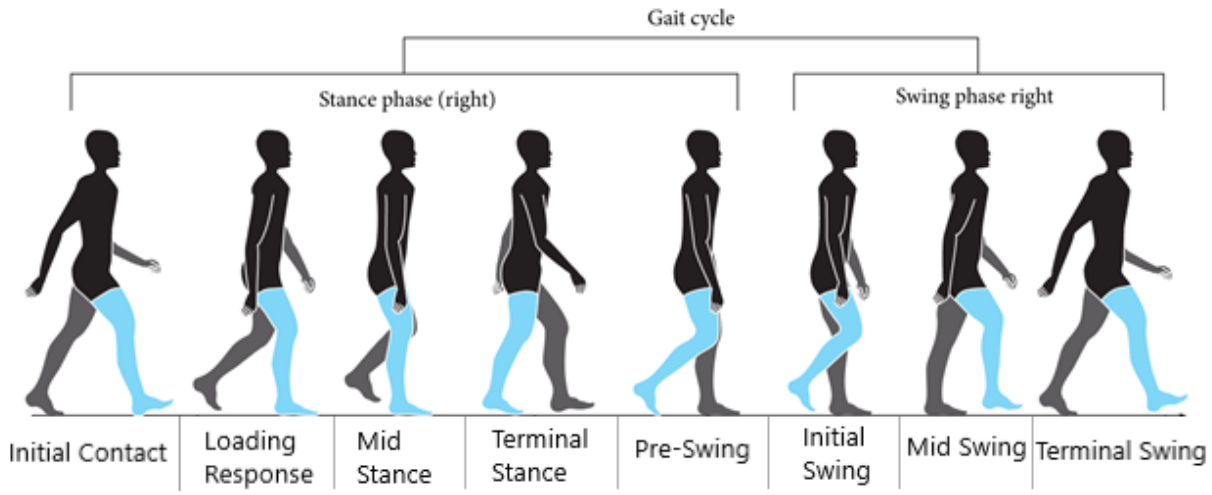

Figure 3.2: Illustration of the human gait phases. Image adapted from [82].

Before starting the human gait assessment with a cane, it is important to emphasize that the **inappropriate use of the cane** can serve as a false sense of security and result in instability of the user gait. Therefore, it is important that the cane and the user have a correct posture, according to physical traits and physical conditions, to ensure safety and provide a reduced load on the lower part of the body when walking with the walking aid device. Statistics from a study realized by Liu et. al. [83] showed that 82% of the cane users were self-taught and only 18% were provided with instructions from medical professionals. These values highlight the importance of education on the appropriate device selection, correct usage and gait pattern, and proper adjustments in the elder community.

Besides the lack of medical professional involvement, there are three major problems from cane assessment. Starting with **handling the cane**, the user needs to decide in a first step which hand will be used to handle the cane. If the goal is to use the cane for general mobility rather due to an injury, it is recommended that the user hold the cane with the dominant hand to support the greater weight. In case the user has a sore, weak or injured leg, the cane should then be handled on the opposite side of the affected leg (i.e., in a contralateral way). The base of support is defined as the area between the cane and the part of the body surface in contact with the ground. When the user handles the cane contralaterally, the base of support is increased, improving balance and reducing the possibility of falling [27], [56]. In addition to improving postural stability by increasing the base of support, a cane provides breaking and propulsion forces to support and reduce the load applied to the subject's weaker leg [84] (Figure 3.3). For general terms on the use of the cane for assisted walking, the second case will be assumed, where the user is holding the cane on the opposite side of an affected or weak leg.

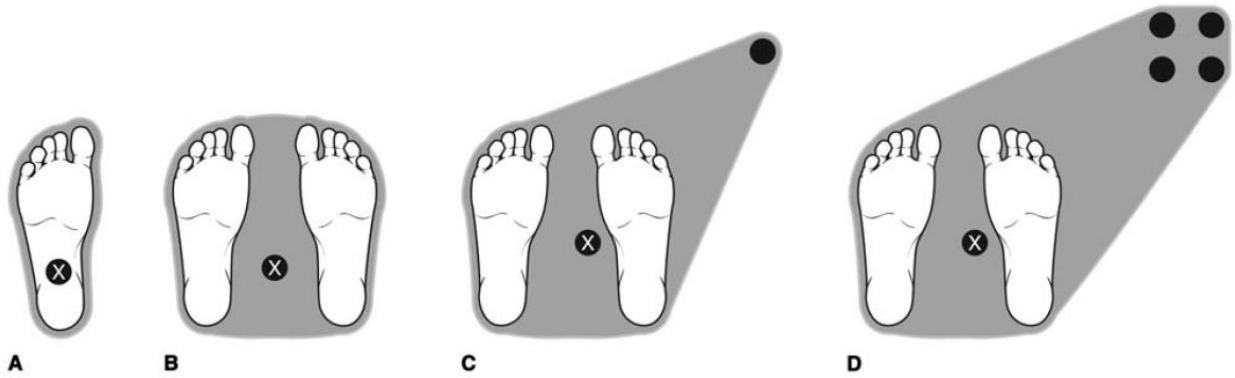

Figure 3.3: The bases of support, shown as shaded areas, and the center-of-mass applied, represented by a cross circle, while standing with and without a cane. (A) One-legged stance, (B) two-legged stance, (C) stance with standard cane, and (D) stance with a four-legged cane. Image from [84]

Inadequate posture during ambulation occurs as the second problem, where cane users with forward leaning posture during ambulation showed a significant association with the rate of falls, while the lateral leaning posture showed no statistically significant association with the rate of falls [83]. The third problem lies in the **incorrect adjustment of the cane**, more specifically, the inadequate height of the cane. Of the 93 subjects recruited into the study carried out by Liu et. al. [83], 50 subjects (54%) had their personal cane at an incorrect height, making incorrect cane height the most common misfit around cane users. These different cane lengths can consequently produce changes in body posture reflecting changes in postural sway [85]. Proper cane height is important due to the biomechanical posture stabilization, and it can be found by measuring the distance from the ground to the wrist joint line while the individual maintains an upright standing position with both upper extremities relaxed at the side of the body [83], [85], [86] (Figure 3.4). The cane should fit so the handle falls comfortably into the palm of the hand when relaxed with the elbow slightly bent.

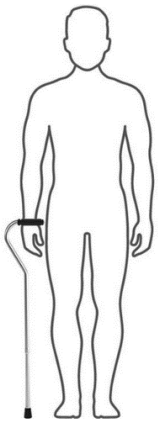

Figure 3.4: Suitable height for a cane, with the handle in line with the wrist joint. Image from [87].

Regarding the **human gait assessment with a cane**, there are two **types of gait with the cane**: two-point gait and three-point gait. The sequential movements of the three-point gait are listed below, and their representation is shown in Figure 3.5 and Figure 3.6.

1. Stand while balancing the body weight on the strong or unaffected limb, with the cane ahead.
2. Move the cane forward by a distance equivalent to one step, assuring the cane is close to the body.
3. Move the affected leg forward one step length.
4. Transfer the weight from the unaffected foot to the affected foot and cane, and then bring the unaffected foot forward to join the affected foot.

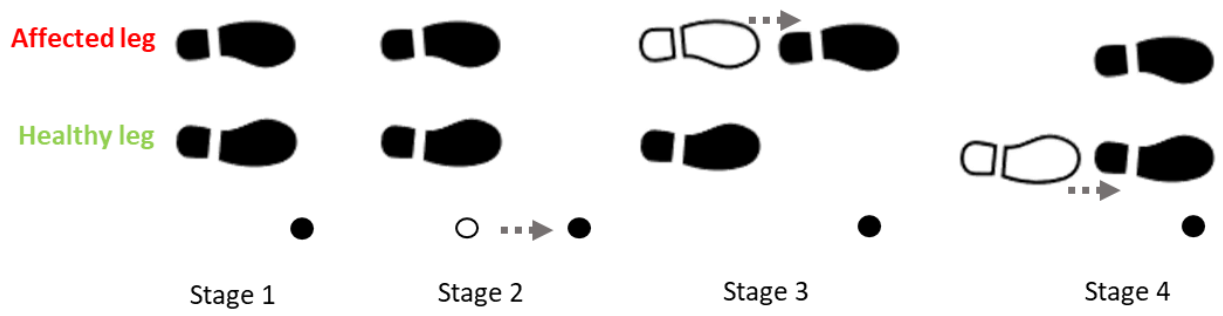

Figure 3.5: Representation of the three-point gait with a cane.

After stage 4 is completed, this series of walking motion will repeat and begin again at stage 1. The two-point gait is similar to three-point gait, except that stage 2 and stage 3 occur at the same time.

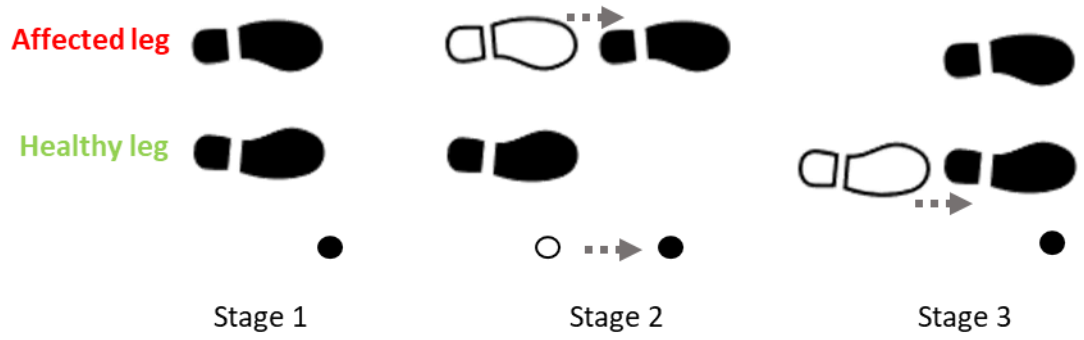

Figure 3.6: Representation of the two-point gait with a cane.

Comparing the two types of gait with cane, the degree of weight bearing carried on the cane is significantly greater in the three-point gait than in the two-point gait. Furthermore, there is significantly greater

muscle activation in the lower limb during the stance phase in the two-point than in the three-point gait [88]. These results demonstrate that a possible and efficient approach to adapt and improve the use of the cane, is the application of the three-point gait in an initial phase of training, to acquire stability and control, and later, the application of the two-point gait for an increased muscle activation of the lower limbs and normal gait pattern training.

3.3 Consumer needs

What a consumer wants usually reflects the desired preferences for specific ways of satisfying a need. It is important to understand and identify the factors that drive people to make purchasing decisions in order to develop something that matches what consumers need to buy. On this matter, this chapter will address two topics that will provide in-depth knowledge of consumer needs. The first, is in relation to human motivation and needs, while the second topic is directed to the needs of a targeted consumer in relation to a service, brand or product, more specifically the robotic cane.

3.3.1 Human needs and motivations

Consumer needs begin with a physical or emotional need, desire or whim, which can be evaluated according to different theories, including Maslow's hierarchy of needs [89]. Abraham Maslow was a psychologist who proposed a theory of needs, stating that some human needs are more important and more common than others. These needs are represented hierarchically, in the following order:

1. **Physiological** – It concerns the biological requirements for human survival, e.g., food, water, rest and shelter.
2. **Safety** - Once the most basic survival needs are met, the needs for security and safety become salient. These needs include emotional and financial security, social stability, health and wellbeing.
3. **Love and Belongingness** - The third level of human needs is social and involves the need to belong and feel loved. It refers to the human emotional need for interpersonal relationships, affiliating, connectedness, and being part of a group.

4. **Esteem** – The fourth level is related to prestige and feeling of accomplishment, being classified into two categories: self-esteem (i.e., feelings of dignity, achievement, mastery, independence) and feeling respected by others (i.e., reputation, status, prestige).
5. **Self-actualization** – The final step of human needs refers to the realization of a person's potential, self-fulfillment, seeking personal growth and peak experiences. Maslow describes this level as the desire to accomplish everything that one can, to become the most that one can be.

Through these important points and factors about what possibly moves and dominates human motivation, it is possible to create a link associated with the product to be developed in the present study, the ARCane. Particularly at the first level, this is intended for the basic necessities of life, for which it is not possible to directly interconnect with the robotic cane. However, as for **safety**, it involves health and feelings of well-being, as well as safety against accidents and injuries, which are factors that the anti-fall cane can prevent. Regarding **love and belongingness**, the independence and autonomy granted to cane users with impaired mobility, can help them stay active and engage in all kinds of social events and activities, allowing for a greater connection and demonstration of affection with other people. Related to the third level, the feeling of freedom acquired by the cane user increases their **self-esteem** and the **feeling of accomplishment**, in a situation in which walking is difficult to perform alone. Finally, referring to **self-actualization**, the desire to improve the quality of life, in terms of social life and personal health, and to go further than one would be able to without any help, is fulfilled by the use of the robotic cane, in accordance with the needs and motivation of the consumer.

3.3.2 Product related needs

It is important to understand why technology users accept or reject a device. This subsection is intended for an analysis of consumer needs, more aimed at a product. A detailed review of consumer needs has been addressed in Rúben Durães study [13] reporting the primary needs for the robotic cane. In terms of **affordability**, it is described that cost (including purchase, maintenance, and/or repair) is the most common reason for unmet needs regarding mobility devices, such as canes [90].

Another parameter to be considered is whether the **cane is easy to set up and use**, i.e., if the user can assemble the product quickly, or if it is already assembled in a suitable package. It is also associated if the user learns to correctly use the device faster, or with less training, and whether the device can be

transported and operated in different locations or only in controlled environments. The **height of the cane** and its proper adjustment are necessary to avoid inadequate postures and even greater risk of falls. To maximize the physical comfort of the user, the **handle should be ergonomic,** and the **cane should be light** to facilitate its use throughout the user's daily routine and avoid possible

Considering the device usage, one consumer need represents the **ease of obtaining the cane** through versatile, yet simple processes, e.g., physical and online stores. In terms of the design process, social stigma can be reduced through the development of more **stylish and fashionable devices**, compatible with the user personality and lifestyle, increasing the overall psychological comfort when using the device in public, or in private [69]. Finally, the **cane needs to be effective, durable, safe and reliable**. The use of the anti-fall cane will improve the living situation of the consumer, through enhanced functional capabilities and independence, by preventing the fall and its related injuries, and meeting the needs of the user for such a device.

A total of 12 primary customer needs for a cane were organized into a hierarchical list, shown in Table 3.2, to understand the relative importance of the different needs. This prioritization is expressed on a numerical scale from 1 to 5, where 5 represents the highest importance and 1 the lowest. This analysis was directed towards a robotic cane prototype, for that reason, needs like the style of the cane and access to the public have been overshadowed, in terms of relative importance, by the more functional needs related to cane height, weight, comfort, and safety, which got the maximum relative importance of 5.

Table 3.2: Relative importance between consumer needs, where 5 represents maximum importance and 1 the least [13]

Number		Need	Importance
1	The cane	is affordable	3
2	The cane	is easy to set up and use	2
3	The cane	has the correct height	5
4	The handle	of the cane is ergonomic	5
5	The cane	is safe to use	5
6	The cane	is light	5
7	The cane	is stylish	1
8	The cane	offers support	4
9	The cane	can be easily obtained	1

10	The cane	is effective	5
11	The cane	is durable	3
12	The cane	is reliable	5

3.4 Robotic cane target specifications

After identifying the consumer's needs, it is necessary to design and characterize the ARCane in order to fulfill these parameters and satisfy the needs identified previously. On this matter, a set of product specifications is defined to guide the design and engineering process, identifying and reporting what the product must do through precise and measurable terms. To establish the target specifications, it is prepared a list of metrics to determine which precise and measurable properties of the cane are associated with the related needs. Competitive benchmarking information is then collected through consultation with ORTHOS XXI, a company manufacturer of orthopedic and hospital products based in Guimarães, Portugal, and by defined international standards. Afterwards, ideal and marginally acceptable target values are defined, while establishing units of measurement and an importance rating for each metric. Considering the work developed by Durães et. al. [13] regarding the target specifications of the prototype of the robotic cane in question, all information regarding the relationship between customer needs and product specification metrics is presented, with the respective relative importance, units, and value range associated with them, summarized in Table 3.3.

Table 3.3: Correlation between customer needs and metrics, with the respective relative importance, units, and value range associated with them, adapted from [13]

Metric no.	Need no.	Metric Description	Value Range	Units	Reference
1	1	Cane manufacturing cost	150-650	€	[91], [92]
2	2	Time necessary to make the cane usable	< 3	s	[93]
3	3	Distance from the user's wrist crease to the floor	350-1100	mm	[94]
4	4	Handle length	65-100	mm	[94]
5	4	Handle width	25-50	mm	[94]

6	4	Handle slope	0-15	°	[94]
7	4	Handgrip surface material biocompatibility test	Pass/Fail	Binary	[95]
8	5	Stability test	Pass/Fail	Binary	[94]
9	5	Separation	Pass/Fail	Binary	[94]
10	5	Friction test	Pass/Fail	Binary	[96]
11	6	Total mass of the cane	≤ 6	Kg	[13]
12	7	The cane is stylish	N/A	Subjective	[69]
13	8	Static load test	Pass/Fail	Binary	[94]
14	9	Possible ways of obtaining the cane	N/A	List	[97], [98]
15	10	Accuracy performance	≥ 84	%	[99]
16	11	Fatigue test	Pass/Fail	Binary	[94]
17	11	Durability of tips	Pass/Fail	Binary	[100]
18	12	Reliability test	≥ 0.8	Pearson's correlation coefficient (r)	[101], [102]

3.5 ARCane design

The ARCane's design is essentially composed of three structures: main body, holonomic base and omnidirectional wheels. The primordial design of the ARCane prototype was directed by Durães et.al. [13], having undergone slight changes and adaptations with the development of the cane during the course of this study. In order to facilitate the visualization of the entire structure of the cane and its various components, a 3-Dimensional (3D) representation of the cane was created in SolidWorks, a Computer-Aided Design (CAD) software. Thus, it will enable an easy visualization of the 3D model of the design in the early stages of the prototype development allowing the detection of unwanted interactions between parts and to perform mechanical simulations on the structure of the cane. With this 3D representation it is also possible to obtain a reference design for future alterations, and productions of the ARCane.

3.5.1 Main body

To ensure a timely and economical solution for the project, it was decided that the best course of action was to adapt a three-legged cane, namely the P1 tripod, inserted in the catalog of walking aids of the company ORTHOS XXI, depicted in Figure 3.7 (a). From the P1 tripod cane, its main structure was removed to be used in the robotic cane (Figure 3.7 (b)). This main structure corresponds to that of an offset cane, which is similar to standard canes except its shape provides a distribution of the patient's weight over the shaft of the cane, as illustrated in Figure 3.8. This allows the cane to be used for occasional weight bearing, being often recommended for patients who have arthritis in the hip or knee and occasionally need to decrease the weight borne on a painful lower extremity [103]. Since the P1 tripod is a cane already on the market, the consumer needs and the respective metrics, are validated for the main body of the cane. In particular, the cane is height adjustable, the handgrip surface material is biocompatible, the length, width and slope of the handle is in the correct value range, and the main structure has been proven to offer support, be effective, durable and reliable.

(a) (b)

Figure 3.7: (a) P1 tripod, a three-legged cane sold by ORTHOS XXI. Image from [104]. (b) Visual model of the ARCane main body constructed in Solidworks.

(a)

(b)

Figure 3.8: Comparison between (a) standard cane and (b) offset cane. Images from [103].

3.5.2 Holonomic base

The base of the ARCane seeks to provide the same stability and support as a multiple-legged cane, while offering enough space to store most of the components responsible for all the cane's functionalities. Multiple-legged canes, depending on the number of legs, are referred to as quadripod or tripod, and provide a larger base of support than standard canes and offset canes, providing more weight bearing by the upper extremity (Figure 3.9). It also can stand freely on its own if the patient needs to use his or her hands, and it can be particularly useful for patients with hemiplegia.

Figure 3.9: Multiple.legged cane. Image from [103].

Based on the way robots move, they can be classified as either holonomic or non-holonomic drive robots. If the controllable degrees of freedom are equal to the total degrees of freedom, then the robot is considered holonomic. Holonomic robots are capable of moving in any direction without changing orientation, being also capable of changing to any desired orientation while in motion [105], [106]. This is especially

important for the ARCane, as the ability to maneuver easily in tight, restricted spaces can dramatically influence the performance of the product. In an initial phase the holonomic base was designed to be compatible with the legs of the P1 Tripod cane. However, with this base, the handle and rod of the ARCane were off-center from the center-of-mass of the holonomic base, being very deviated towards the user's side, and not towards the center of the base. This structure would lead to a decompensation in the distribution of load absorbed by the cane when subjected to large normal forces, namely in situations where greater body support is required by the user while walking, thus making it more unstable and with a high probability of tipping over. To solve this problem, the structure and orientation of the base joints that connect to the main body were configured so that the main rod and the handle of the ARCane coincide with the center of the holonomic base as illustrate in Figure 3.10. This configuration guarantees greater stability and support during all walking phases and possible fall situations, thus preventing the ARCane from tipping over, while being able to prevent the user from falling, as shown in Figure 3.11.

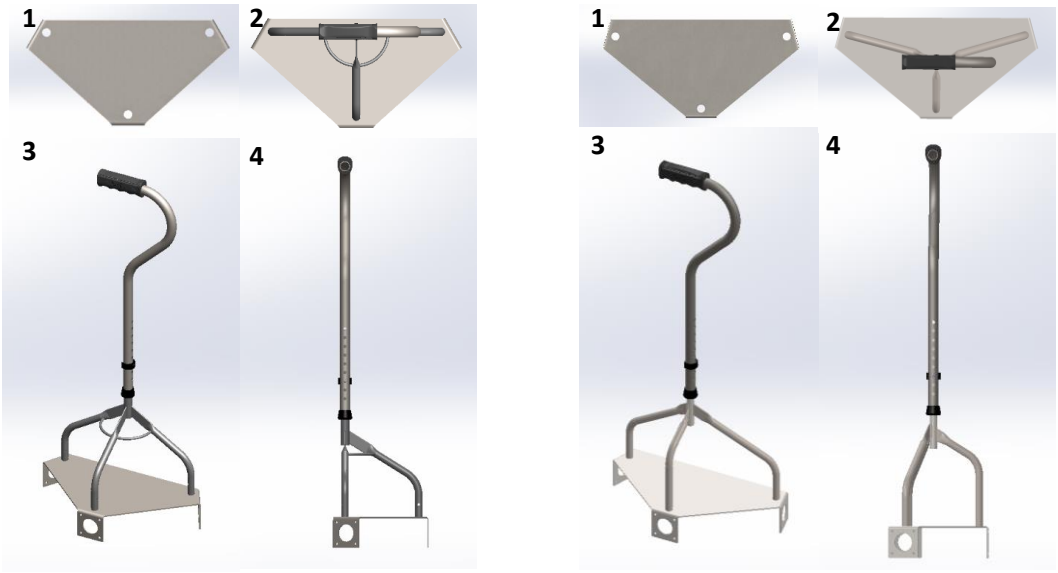

(a) (b)

Figure 3.10: Visual 3D model representation, modeled with Solidworks software, of the holonomic base and ARCane main body. (a) Primary Design (b) Final Design. 1,2- top view; 3- trimetric view; 4- side view.

(a) (b)

Figure 3.11: Example of forces applied vertically in: (a) the primordial design of the ARCcane, resulting in falling over, due to a decompensation between center of mass of the structure and the forces applied by the user on the ARCane handle; (b) the new structural design of the ARCane, where the handle is placed right above the ARCane center of mass, having smaller impact in the stability of the structure.

3.5.3 Omnidirecional wheels

What makes it possible for the ARCane to be a holonomic system are the omnidirectional wheels that incorporate the base of the cane. Being responsible for the mobilization of the ARCane, the omnidirectional wheel, is capable of omnidirectional movement. These wheels with small discs around the circumference make them able to roll with full force, but also slide perpendicular to the rolling direction, providing the ability to easily maneuver around tight and constrained spaces. Its simple structure and design make it relatively cheaper and lighter compared to other types of wheels, e.g., the mecanum wheel.

The chosen wheels were the 100mm double plastic Omni wheels with central bearing, sold by Robot Shop [107] (Figure 3.12). The increased diameter and the 18 rollers give these wheels a greater load capacity, weighing 0.35 kg per unit. To link the axis of movement of the motors and the omnidirectional wheels, a fixing screw hub was designed using both components as a reference, ensuring full compatibility. The 3D model for the set screw hub can be seen in Figure 3.13.

Figure 3.12: Omnidirectional wheel for the ARCane [107][96];

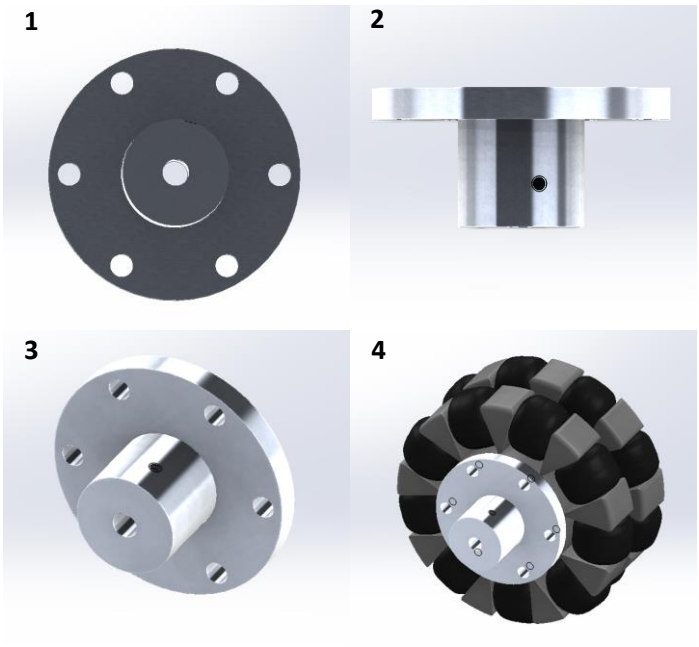

Figure 3.13: The 3D model for the motor-to-wheel coupler and omnidirectional wheel. 1- front view; 2- side view; 3,4- trimetric view.

3.6 Discussion

This chapter covers what the ARCane should have and what it should represent. It is aimed to achieve a robotic cane that matches the defined mission statements, more specifically a robotic cane with a real-time built-in fall detection and prevention system, which is the biggest distinguishing factor between robotic and conventional canes; that makes it possible to avoid injuries caused by fall events, in order to

improve users quality of life and reduce associated health costs; and to be a product intended for people with reduced mobility, that can also be inserted in health institutions, such as hospitals and rehabilitation centers.

In terms of consumer needs, it is important to take into account the accessibility of the product, as well as the height, ergonomics, safety, weight, effectiveness and reliability of the ARCane. As the main purpose of the ARCane is to eliminate the negative consequences of falling events, the product requires to be safe and comfortable to use, to ensure the success of such a device. It was also found that users give a lot of importance on the fashion sense of the product, and that they could potentially reject the product based on its look alone. However, as stated earlier, the style of the product is not a priority at the moment, as this analysis is mainly directed towards functionality needs, due to this being a robotic cane prototype and not a final product. This point also applies to the cost of the cane, as the development of a prototype can be expensive since all components will be experimental and purchased by unit.

To obtain a robotic anti-fall cane that contains the product specifications defined according to the consumer's needs. Although the metrics and their associated range of values represent and classify the ideal model of the robotic cane to be developed, these specifications are preliminary and may change in future phases of product development, once the concept is fully defined and experimental testing begins.

Finally, the ARCane design can be defined by its three main components: main body, holonomic base and omnidirectional wheels. The main body of the ARCane is based on the tripod P1, a three-legged cane marketed by ORTHOS XXI, and since it is already on the market, this structural component meets the needs of the consumer and the respective metrics, being proven to offer support, be effective, durable and reliable. In terms of the cane's mobility, the insertion of an improved model of a holonomic base together with the omnidirectional wheels means that the ARCane can move in any direction without changing its orientation, allowing it to be easily maneuvered in tight and restricted spaces while maintaining its stability. The overall design of the ARCane aims to be lightweight and achieve high maneuverability, while maintaining a robust stability, to ensure its primary objective of ensuring user safety.

4 ARCane Architecture

This chapter seeks to describe the present and future capabilities of the ARCane, highlighting the main features that distinguish it from a conventional cane. In order to process all the information that involves the entire electronic system, involving control strategies, calculations, analyzes and data organization, there are the central control units, which will be explained in more detail later.

Considering the review study of the robotic canes and the components that composed them, as well as after the architecture destined to the robotic cane is well defined, it is time to carry out a benchmark of the best components to be applied in the ARCane. This choice of components must take into account: (i) the parameters to be detected, in order to obtain the desired information about the cane and the user; (ii) the actuation mechanisms, which perform the movement of the cane, provide context awareness and allow the interaction between the cane-user system; and finally, (iii) the different specifications, modes of communication and type of power supply required for each component, in order to transform this set of components into a single system. Once the desired components have been selected, an overview of the hardware is carried out to demonstrate and visualize all the connections and communications established between all the units that make up the ARCane system.

Finally, the types of communication protocols and the operating frequencies of the system are demonstrated, which enables the transfer of information between the ARCane components, control units and external devices, and also the processing and management of all information that make up the ARCane system, ensuring its proper functioning.

4.1 System specifications

The ARCane system is divided into a set of sub-systems that will be responsible for its correct functioning. These subsystems involve: (i) human-robot interaction; (ii) control architecture; (iii) database; and (vi) functionalities.

Human-Robot Interaction (HRI) is a field of study that addresses the design, understanding and evaluation of robotic systems, which involves humans and robots interacting through communication [108]. With the present project, it is intended that the user can manipulate, handle and communicate with the ARCane without any difficulty, intuitively and without any previous training. To this end, this system must

contain prior information about the user (e.g., dominant foot, dominant hand, arm size, physical structure, motor difficulties, and lower or upper limbs affected) in order to facilitate the user's control of the ARCane, corresponding to their abilities and physical characteristics, and still obtain the user's risk of falling based on their activity. Such information is registered into the program prior to using the ARCane, but also obtained during its use through sensory units. Another parameter to consider for the human-robot interaction are the activation features, which correspond to the start of the cane, as well as the actuation systems implemented so that the ARCane can interact with the user. These activation features will be adjusted according to the respective user information previously described.

The **control architecture** is one of the most important systems, as it is the system responsible for all the processing, calculations, data analysis, control and action strategies that involve the ARCane. Being considered the "heart" of the ARCane, this system interconnects all the units and systems, allowing internal communications as well as external device synchronization.

A **database** is an organized collection of structured information so that data can then be easily accessed, managed, modified, updated, controlled and organized. The data sent to the database are related to the human-robot interaction system and some information acquired from the ARCane sensory unit. The database can be either offline, storing the information on a disk or memory card, or online, where the information is sent directly to an online platform, allowing real-time visualization of the data received.

The **functionalities** represent features of the ARCane that are not present in a conventional cane. In addition to the fundamental function of assisting in walking, by improving posture stability, reducing the weight supported by the lower limbs, increasing balance and assisting in the rehabilitation of lower limb movement, the ARCane has, or aims to have, additional characteristics that are clearly distinguished from a conventional cane, namely: gait analysis tools, fall detection, real-time fall prevention, haptic sensing, haptic feedback, omnidirectional movement, and context awareness. This set of features highlights the evolution and great capabilities of the ARCane compared to a conventional cane, as well as its importance and influence as a possible commercial product in hospitals, rehabilitation centers and for home use.

In order to obtain the intended specifications and functionalities for the correct functioning and operation of ARCane, it is therefore necessary to integrate componentes responsible for: (i) the processing and communication of all information; (ii) acquiring sensory information related to the user, the cane and the context of the environment; (iii) action mechanisms so that the cane can interact with the user and the surroundings; and (iv) the supply of energy, compatible with all electronic components, to ensure the correct

functioning of the ARCane's electronic system. Finally, the ARCane hardware architecture can be divided into four distinct units: (i) central control unit; (ii) sensory unit; (iii) actuator unit and (iv) power unit. These units will be addressed separately throughout this chapter, along with an analysis of the respective components to be instrumented in the ARCane. A representation of the ARCane architecture is illustrated below in Figure 4.1.

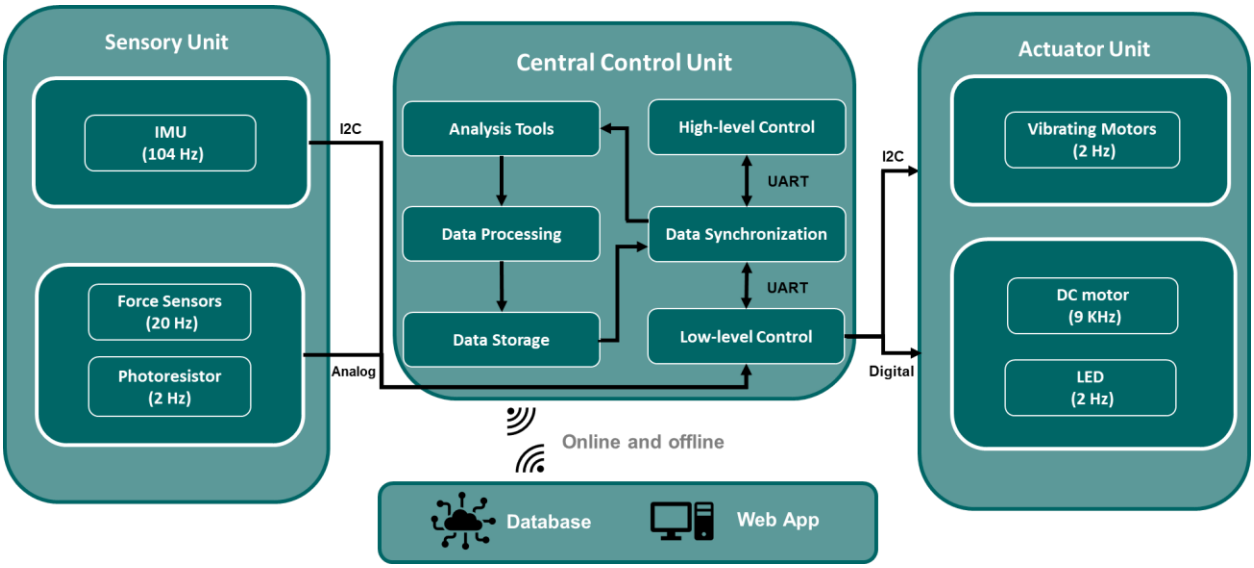

Figure 4.1: ARCane architecture with the respective units, components operating frequencies, communication protocols and data control of the electronic system.

4.2 Control architecture

The Control Unit (CU) is responsible for processing all the information recorded by the sensors, as well as for sending the commands to the actuation units. Subdivided into two parts, there is the low-level and high-level control units. For all processing to be carried out without errors and quickly enough to be able to calculate, receive and transmit all data, it is important that they have a high processing power, as well as various communication modes that allow interconnection to all components of the ARCane. The transfer of information between the two control units will be carried out through Universal Serial Bus (USB) communication.

4.2.1 Low-level control unit

Designed for simpler calculations acquired by data coming from the sensory unit, and transmission of communication with the actuation unit and the high-level CU, the low-level CU stands out for its versatility of connections with different components, being also responsible for the locomotion control of the ARCane, security mechanisms and external device synchronization. A benchmark was performed between Arduino and STM32 control boards, in order to obtain the best quality-price ratio device with respect to their technical specifications. It ended up with the choice of the STM32 F446RE microcontroller (Figure 4.2), demonstrating a high processing power with a maximum clock speed of 180 MHz, as well as a wide range of Pulse Width Modulation (PWM) outputs and 3x 12-bit Analog-to-Digital Converter (ADC) (up to 16 channels) with a selectable resolution of 12/10/8/6 bits. It also supports UART, I2C and SPI communication, which allows to perform the necessary communications with several components and units simultaneously. The technical specifications of the control board responsible for the low-level actions of the ARCane are presented in Appendix II, Table A.2.

Since the STM32 F446RE board, is connected to both the sensory unit and the actuation unit, it needs several connections so that communication between devices is achieved. Also, as the different components communicate using different protocols and electrical signals, the STM32 needs to have a wide range of pins so that communications are possible between the entire system. The final circuit of the actuation and sensing unit has a total of 3 analog connections, 17 digital, 1 PWM and 4 I2C connections. To help visualize and understand the connections of the low-level CU, Figure A.1 displays the board pinout and pin label for the STM32 F446RE and Table A.3 lists the board pins, their respective functions and connections.

The low-level CU is programmed in the Arduino Integrated Development Environment (IDE) with the C++ programming language, as it is an open-source platform with extensible software and an extensive community of use. The computational code of the low-level CU can be divided in two main structures, the setup function, which is intended for defining and initializing variables, pin configurations and include required computer libraries; and the loop function, that runs through the entire program repeatedly, allowing for an active and constant control of the data. Within the loop function, there are secondary functions that correspond to the reading of sensory components, and writing commands intended for the actuators. Figure 4.3 shows the schematic representing the structure of the developed code in the low-level control unit.

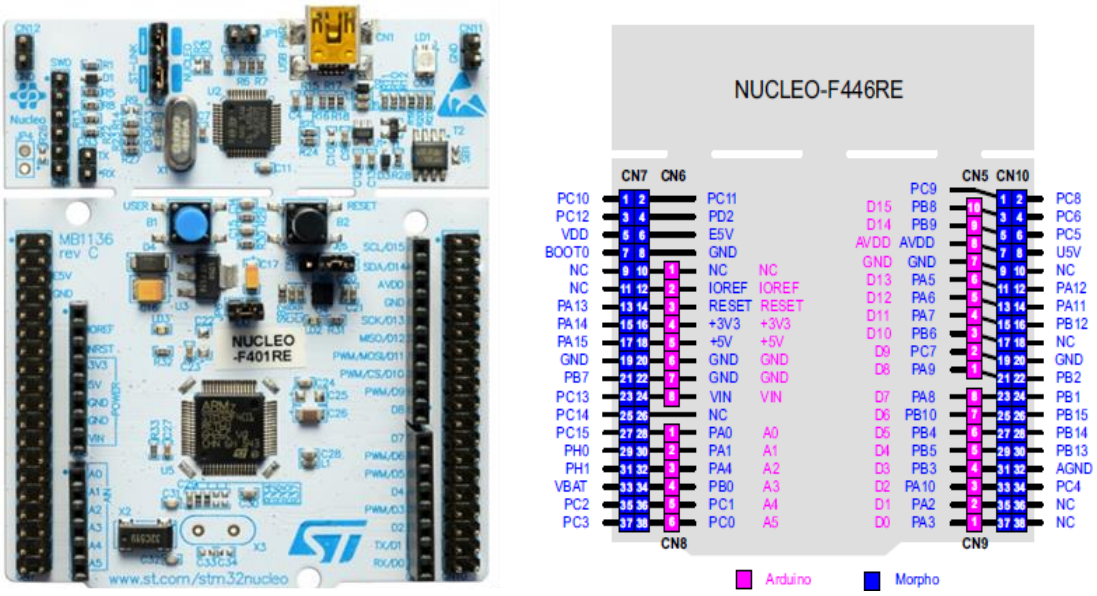

Figure 4.2: STM32 F446RE board and pins legend. Images from [109].

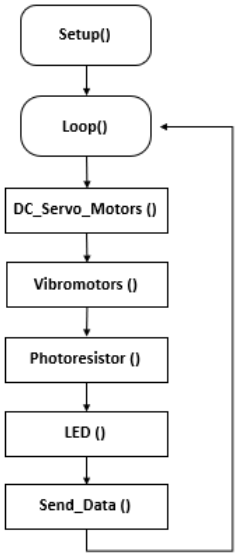

Figure 4.3: Schematic of the programming code inserted in the low-level control unit.

4.2.2 High-level control unit

For high level operations, it is used the NVIDIA® Jetson Nano™ 2GB Developer Kit, a small and powerful computer with high processing power (Figure 4.4). It will be responsible for storing data, communicating with the low-level CU, communicating with the outside via Bluetooth or Wi-fi, as well as all analysis tools, namely: fall risk assessment, processing and calculations for the detection and prevention of

falls, and recognition between normal and abnormal walking state. The high-level CU will also be responsible for supplying power to the low-level control unit via USB. The NVIDIA Jetson Nano technical specifications are listed in Table A.4.

Regarding the high-level CU software, it is used the Linux operating system, which according to Wang et. al. [110] is well known for real-time embedded platforms as it provides several flexible methods of inter-process communication, making it quite suitable for implementing fall detection methods using sensor fusion. The high-level CU was programmed in VisualStudio with C# computational language. Its computacional code is programed to: (i) receive all the information communicated by the low-level CU through the serial port; (ii) storing all the acquired information in the memory storage; and, if necessary, (iii) send commands of actuation mechanisms to the low-level CU.

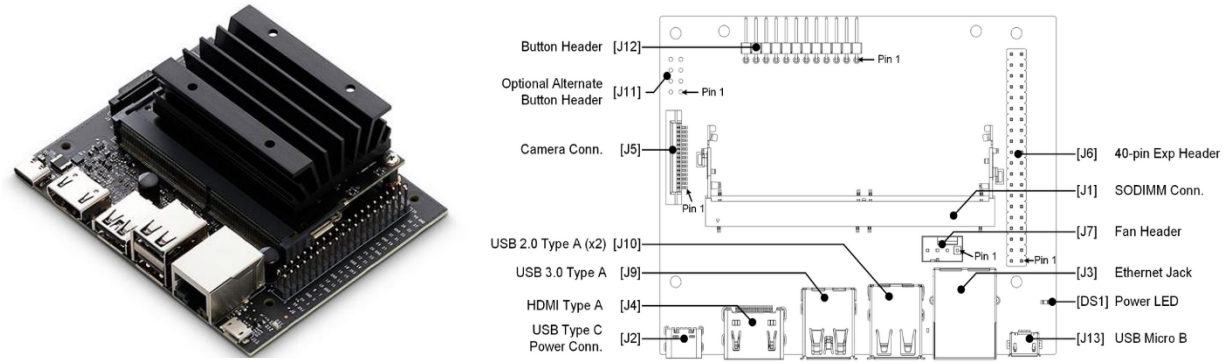

(a) (b)

Figure 4.4: (a) Jetson Nano and (b) Top view board layout. Images from [111]

4.3 Sensory unit

In order to control the ARCane's movement, detect an imminent fall, and ensure the safety of the user, it is necessary to monitor continuously the user's gait. The sensory unit is composed of a set of sensors, which allow the interpretation and analysis of the user's gait and posture, as well as the status and position of the cane in relation to the user and external conditions. As described in section 2.2, the sensory unit is divided into two groups, the cane sensors and the wearable sensors. According to the literature review, 100% of robotic canes used cane sensors, while only 50% of robotic canes used wearable sensors.

Only cane sensors will be used in the ARCane system. This choice is due to the fact that is possible to obtain all the information necessary for the intended operation and functionalities of the ARCane, allowing a simple, fast, viable and intuitive use, without the need for accessories or extra components, such as wearable sensors, which may come as an obstacle in terms of user compliance. The various components that make up the sensory unit are: (i) force sensors; (ii) light sensor; and (iii) inertial sensor. The purpose and context of the sensory unit included in the ARCane is summarized below in Table 4.1. It is indicated that one of the signals acquired in the sensory unit is through context-aware footage, responsible for gait analysis, fall risk assessment and fall detection. However, this sensor will not be discussed in this chapter because it is not implemented in ARCane in the present work. Therefore, its future implementation is discussed further in Chapter 7.

Table 4.1: Contextualization of the ARCane sensory unit

Sensory Unit Purpose	Signals Acquired	Parameters
Gait analysis	• Acceleration • Angular velocity • Cane orientation • Force • Context-aware footage	• Gait phase detection • Stride and support phase duration • Stride length • Support weight • User movement intention • Velocity
Fall risk assessment	• Context-aware footage	• Displacement, velocity and orientation • Fall risk assessment and correlation with the quality of life
Fall detection	• Context-aware footage	• Image processing
Context awareness	• Light intensity	• Environment luminosity

4.3.1 Haptic sensing system

The detection of vertical forces (i.e., on the axis perpendicular to the cane's displacement plane) is very important for monitoring the user's gait status. Such parameters allow detecting when the ARCane is being used, and the amount of support weight of the user being exerted on the cane, to consequently be

able to detect which phase of gait the user is in. Thus, piezoresistive sensors, also known as Force Sensitive Resistor (FSR) will be used for the detection of vertical forces applied on the cane. An FSR is a one-dimensional variable resistance pressure sensor that consists of several thin, flexible layers as illustrated in Figure 4.5. As the pressure increases, the more resistive carbon elements touch the conductive traces, resulting in a decrease in resistance.

The selected sensor is the Interlink FSR® Model 402 Short Tail sensor (Figure 4.6 (a)) as the best choice for detecting human-robot interaction forces to be applied in relatively small systems, due to their small size. The FSR proves to be a durable, thin, flexible, widely available and cost-effective sensor, compared to other previously evaluated force sensors such as capacitive sensors and composite quantum tunnel sensors. Technical specifications for Interlink FSR® sensors are listed in Table A.5. A total of three FSR sensors are used, located on the handle of the ARCane, at an equidistant distance from each other, as shown in Figure 4.6 (b). allowing to obtain a map of the forces applied by the user's palm when manipulating the cane and while supporting its weight during the various gait phases.

To acquire data from force sensors, it is used a current-voltage converter circuit, or also known as a transimpedance amplifier, as represented in Figure A.2. It is used the MIC7300 as the operational amplifier of the circuit. This circuit exhibits a more uniform transfer function than a voltage divider circuit and allows fixed voltage to be applied to a single FSR element regardless of other parallel FSRs. Taking into account that the conductance varies linearly with the applied force in the FSR sensors, therefore the resistance changes hyperbolically as the force increases, as shown in equation 5.1. Since a linear response is desired, the introduction of this circuit will enable to obtain a linear conductance variation when an input DC signal is applied, as shown in Figure 4.7. This method is traditionally used to measure forces on piezoresistive sensors [112], [113].

$$Conductance = \frac{1}{Resistance} \tag{5.1}$$

By using the current–voltage converter circuit to acquire data from the piezoresistive sensors, it results in an output signal which corresponds to the value obtained by the equation 5.2, as shown in Figure 4.7, for certain values of RG.

$$V_{OUT} = -V_{REF} \cdot \left(\frac{RG}{R_{FSR}}\right) \tag{5.2}$$

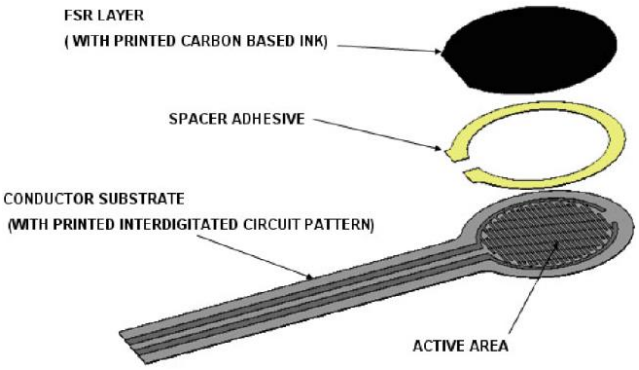

Figure 4.5: FSR sensor construction layers. Image from [114].

(a) (b)

Figure 4.6: (a) Interlink FSR® Model 402 Short Tail sensor. Image from [115]; (b) force sensors disposition in the ARCane's handle.

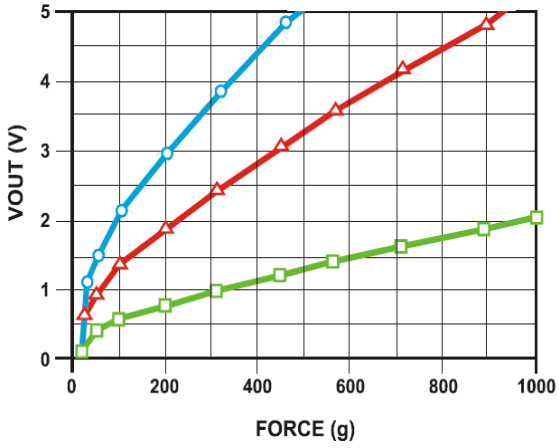

Figure 4.7: Force x Voltage ratio of the piezoresistive sensor, by varying the RG resistance of the voltage-to-current converter circuit. Blue - 7.5KOhm; Red - 4.7KOhm; Green - 1.5KOhm. Image from [116].

As the low-level UC microcontroller, that is used to read the obtained output signal, does not admit negative voltage values, V_{REF} will be used with a negative value, so that V_{OUT} is positive. Considering that the supply voltage of the circuits is positive, namely +3.3V, a voltage converter is needed to obtain V_{REF} with a negative value of -3.3V. For this, the voltage converter to be used is the TL7660 [117] and the conversion circuit is shown in Figure A.3, with V+ equal to +3.3V.

Since multiple piezoelectric force sensors will be used, it would presumably also be necessary to use multiple voltage-to-current converter circuits, each corresponding to each force sensor. One solution that has emerged is to use a multiplexer to get all the readings from the various force sensors interspersed, reducing the amount of current-to-voltage reading circuits into a single and simpler circuit. The multiplexer to be used is the MUX506IPWR, and it allows obtaining a total of 16 analog readings according to the value of the binary address obtained by the digital channels A0, A1, A2 and A3, although the digital channel A3 will not be used, allowing a total of 8 analog readings (Figure A.4).

By joining all the electric components together, as shown by the circuit schematic in Figure A.5, force measurements from the ARCane handle can be obtained. This sensor circuit will be connected to the low-level CU through an analog connection that allows the reading of the values obtained by the reading circuit, and four digital connections that allow controlling the multiplexer to manage which FSR sensor to obtain the reading (Figure 4.8).

Finally, a signal processing is performed in the low-level CU by acquiring data from the force sensors. In an initial phase, it was decided to apply a second-order Butterworth Infinite Impulse Response (IIR) low-pass filter. This was possible with the help of the calculation demonstrations in [118], along with the Filter Designer application of the MATLAB software, and through the visualization of the frequency domains present in the force sensor signal, through the signal amplitude spectrum. However, since the Kalman filter has been used extensively in literature for data acquisition [25], [28], [29], [33]–[36], [44], [45], [47], [54], [64], it was verified that when implementing it, better results were obtained in terms of signal processing, more specifically in the removal of noise from the analog signal of the FSR sensors. This filter represents a mathematical method with the objective of using measurements carried out over time in order to generate results that tend to approach the real values, using an algorithm that provides estimates of some unknown variables given the measurements observed over time. In addition to noise removal, the implementation of this filter is simple to perform and requires little computational power. Appendix III illustrates the low-pass

filter process, as well as a comparison of the original signal processing with the low-pass filter and the Kalman filter.

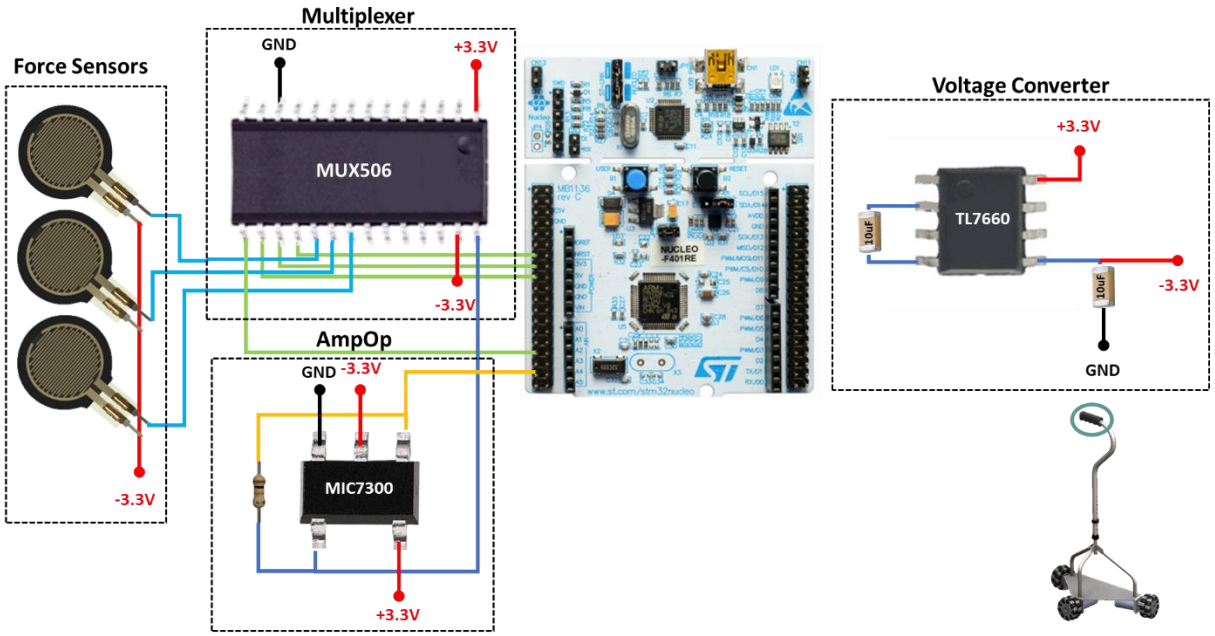

Figure 4.8: Haptic sensing system reading circuit with the low-level CU connection.

4.3.2 Axial force system

To detect the forces of interaction between the user and the ARCane, the use of an axial force sensor is essential. With this sensor it is possible to calculate the intention of movement through the forces applied to the cane and thus obtain admittance control to move the cane to the desired position, and accompany the user while walking. The proposed solution for the ARCane axial force system, is using a combination of four force sensors, located around the cane rod, and perpendicular to the horizontal plane. The force sensors to be used for the detection of axial forces are the Interlink FSR® Model 400 Short Tail, shown in Figure 4.9, presenting the same characteristics (Table A.5) and the same force x voltage linear response (Figure 4.7) as the handle force sensors previously mentioned.

It was taken advantage of the fact that the ARCane's rod is divided into two sub-rods, namely, the handle rod (upper rod) and the base rod (lower rod), which are interconnected to each other, in order to allow the adjustment of the height of the cane handle. Thus, by slightly reducing the diameter of the base rod, it allowed the 4 FSR sensors to be placed between the upper and lower rod of the cane, 90° apart from each other in relation to the center point of the cane's tube, as illustrated in Figure 4.10. With this

configuration there is a small gap between the two rods, and this is what allows to measure the interaction forces, applied in the handle of the cane by the user, at the location that the four force sensors are placed.

(a) (b)

Figure 4.9: (a) One and (b) the combination of four Interlink FSR® Model 400 Short Tail force sensors used as an axial force system.

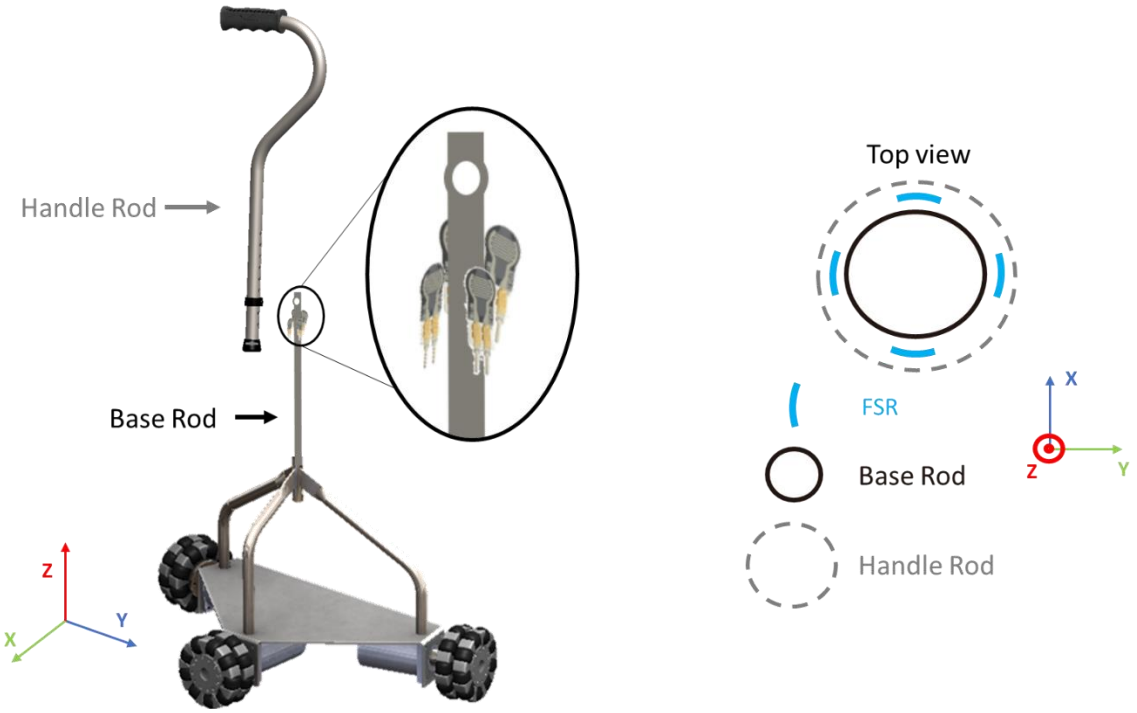

Figure 4.10: Configuration that makes it possible to obtain an axial force system, by placing the force sensors between the base rod and the handle rod of the cane.

By applying this sensor configuration, it is possible to obtain the magnitude and direction of the force applied in the cane's displacement plane, thus indicating the user's intention to move when handling the cane handle. The working principle, data acquisition and signal processing of the axial force sensors are identical to the force sensors located on the cane handle, as previously shown in Figure A.5, with the only difference being in the dimensions and location of the piezoelectric sensors. The final reading circuit of the ARCane axial force system is represented in Figure 4.11.

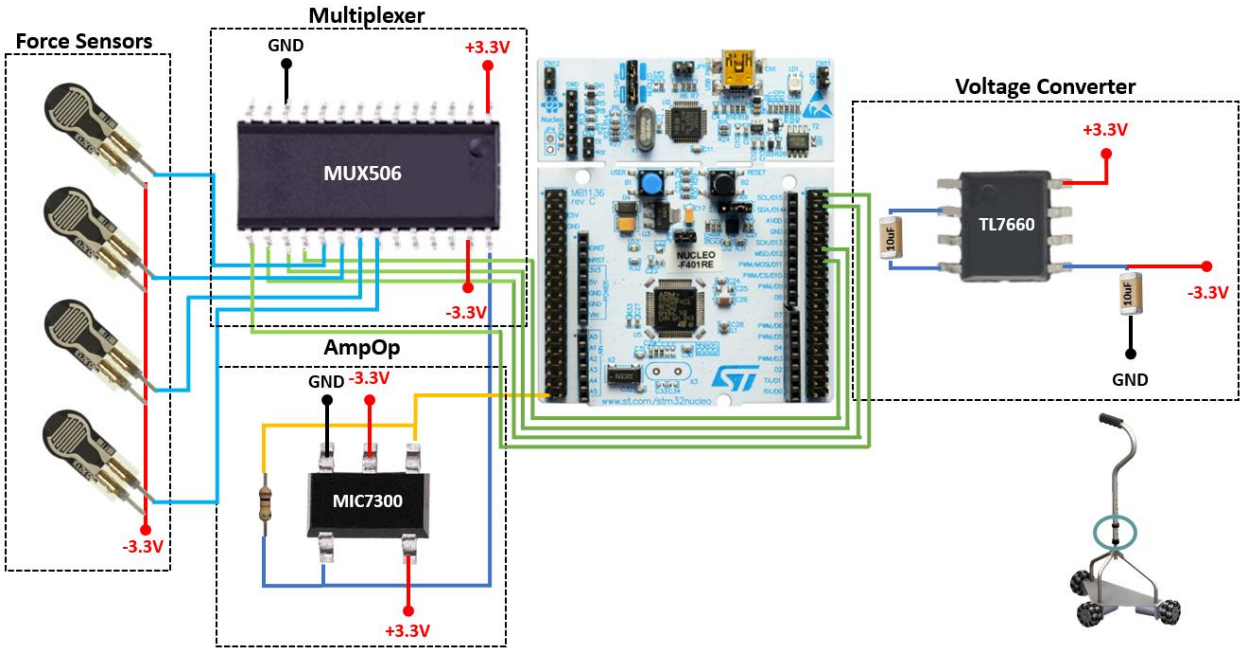

Figure 4.11: Axial force system reading circuit with the low-level CU connection.

4.3.3 Light sensor

There are several extrinsic fall risk factors associated with the surrounding environment, one of which is poor lighting conditions. Inadequate lighting results in poor visibility which leads to a direct association with the risk of falling [119], [120]. On this matter, it was also found that none of the robotic canes present in the SoA study contained mechanisms of detection and action related to luminosity, given that many falls are due to poor visibility conditions. As a way of overcoming this obstacle that increases the risk of the users falling, it was decided to implement a light sensor that aims to detect the environmental conditions, namely the luminosity in the surroundings of the user's circulation, and thus, with the readings obtained, send information to a light triggering mechanism, to provide better visibility to the user of the ARCane. For this

matter, it will be used a photoresistor as a light sensor, also known as Light Dependent Resistor (LDR), located at the base of the ARCane (Figure 4.12).

Figure 4.12: Photoresistor light sensor.

This light sensor is composed of photoconductive materials, i.e., when light falls on a photoresistor, photons with a frequency above a certain value are absorbed (referring to the gap energy of the photo-conducting material), providing enough energy for the electrons that are in the valence band to jump to the conductive band. This phenomenon results in an increase in the conductivity of the material, which equals to a decrease in its resistance. It is used a voltage divider circuit, as the reading circuit used to measure the brightness of the surrounding environment (Figure A.6). Thus, when light hits the sensor, its resistance decreases and consequently the voltage at its terminals also decreases, being later detected by the low-level CU, as shown in Figure 4.13. The photoresistor is connected in series with a resistance of 5.1kΩ, an empirically determined value.

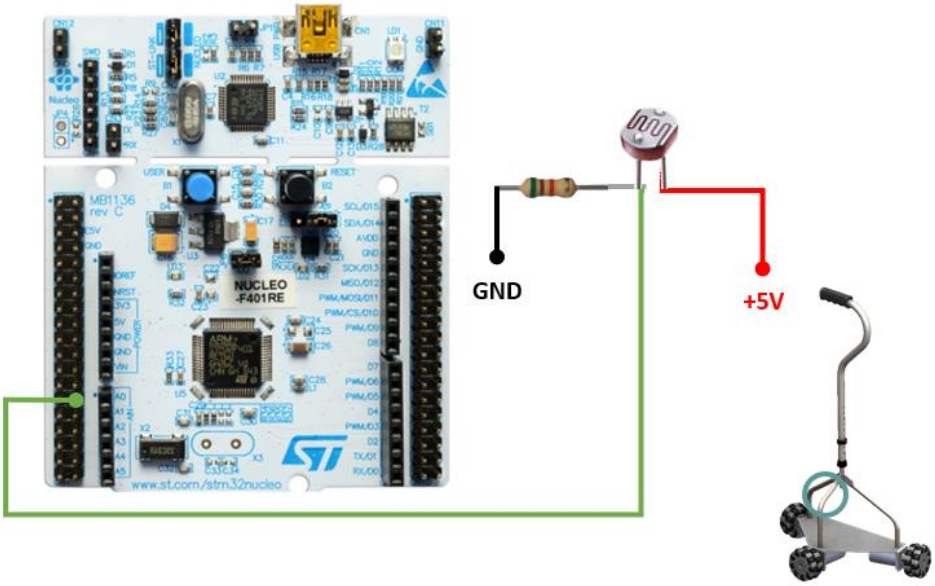

Figure 4.13: Light sensor reading circuit with the low-level CU connection.

4.3.4 Inertial system

The inertial system is composed by an Inertial Measurement Unit (IMU). The IMU consists of an accelerometer, which measures the rate of change of velocity along three axes; a gyroscope, that detects rotational changes with respect to orientation and calculates angular velocity along three axes; and a magnetometer, which measures the relative change of a magnetic field, its direction and intensity. With all these functionalities, important information about the ARCane system will be able to be attained. The IMU to be used is the Adafruit LSM6DSOX + LIS3MD (Figure 4.14), being is located at the base of the cane. This board is composed of the LSM6DSOX component, which is a 3-axis accelerometer and a 3-axis gyroscope, and the LIS3MDL component, which is a 3-axis magnetometer.

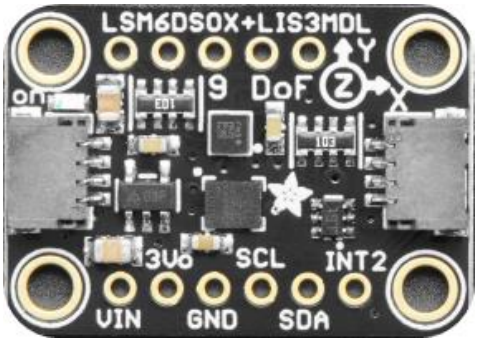

Figure 4.14: IMU Adafruit LSM6DSOX + LIS3MDL [121][110].

This system of three sensors with triple-axis adds up to 9 degrees of freedom, allowing to obtain, through this combination of data, the movement orientation and direction of the cane, as well as its inclination in relation to a predefined reference plane. The accelerometer can measure both static acceleration forces (i.e., gravity) and dynamic acceleration forces (i.e., movements and vibrations), and its typically unit of measurement is in m/s^2, however the measurements can be expressed in G, which refers to the value of the gravitational force (G = 9.8 m/s^2).

The LSM6DSOX + LIS3MDL has flexible data rates and ranges. For the accelerometer it has a data range of ±2/±4/±8/±16 G and from 1.6 Hz to 6.7 KHz of update rate; for the gyroscope, a data range of ±125/±250/±500/±1000/±2000 DPS (Degrees per Second) and from 12.5 Hz to 6.7 kHz of update rate; and for the magnetometer, a data range of /±4/±8/±12/±16 Gauss and from 0.625 to 1 kHz of update rate. For the present work, it is used a data rate and refresh rate of **±2G** and **104 Hz** for the accelerometer, **±250 DPS** and **104Hz** for the gyroscope, and **±4 Gauss** and **104Hz** for the magnetometer.

Through the calculated acceleration from the accelerometer, it is possible to obtain the velocity value and the relative position of the cane. For this, it is necessary to perform integrative mathematical calculations, demonstrated by equations 5.3 and 5.4.

$$v_{i+1} = \int_{t_i}^{t_{i+1}} a\, dt = a\Delta t + v_i \tag{5.3}$$

$$x_{i+1} = \int_{t_i}^{t_{i+1}} v\, dt = a\frac{\Delta t^2}{2} + v_{i+1}\Delta t + x_i \tag{5.4}$$

Where: t_i represents an initial time; t_{i+1} represents an end time; Δt is a time interval between t_{i+1} and t_i ($\Delta t = t_{i+1} - t_i$); v_i e v_{i+1} velocity at initial time t_i and at end time t_{i+1}; and x_i e x_{i+1} represents the position at initial time t_i and at end time t_{i+1}. Thus, obtaining an approximation of the average speed and distance traveled on a specific axis, within a time Δt defined according to the accelerometer data rate. By successively calculating equations 5.3 and 5.4, between successive small-time intervals Δt, it can be obtained a continuous result of the speed and relative position of the cane. Subsequently, a high-pass filter can be used to remove the continuous component of the signals, eliminating cumulative errors resulting from the integration calculations, finally obtaining more cohesive measurements. The IMU will be powered at 5V, coming from a step-down located posterior to the battery. It is connected to two I2C ports, i.e., SCL and SDA, in order to communicate with the low-level CU. The following Figure 4.15 shows the configuration that allows the IMU to communicate with the low-level control unit via the I2C communication protocol.

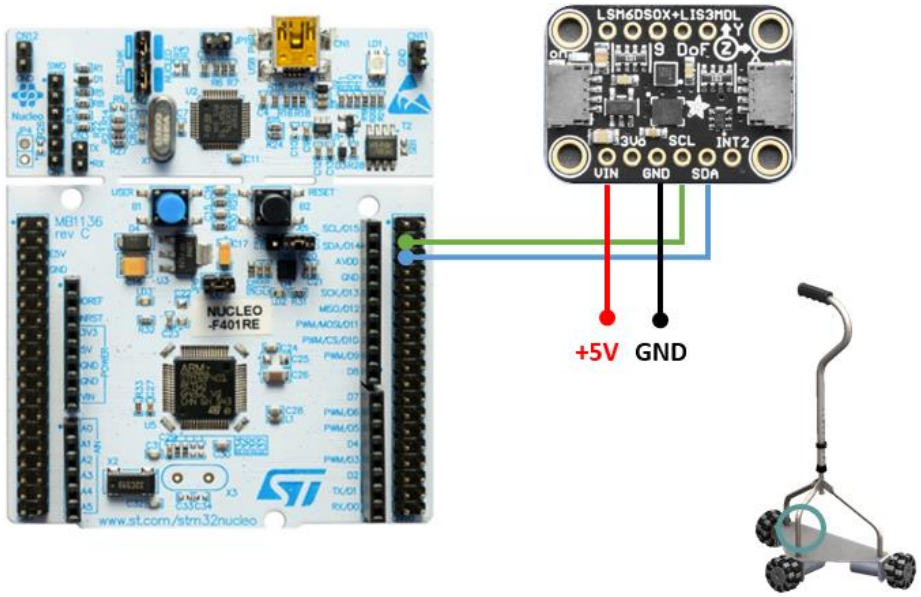

Figure 4.15: IMU reading circuit via I2C communication protocol.

4.4 Actuator unit

After the information and data obtained by the sensors is sent to the control units, and the respective information has been analyzed and processed, the control units will later send commands to the actuator unit. These commands are meant to activate mechanisms of action in order to guarantee the correct functioning of the entire ARCane system, thus guaranteeing the security conditions and corresponding to the intentions and commands transmitted by the user. The actuation unit is composed of a set of systems responsible for the interaction between the cane and the user, also between the user and the surrounding environment, and finally the movement of the ARCane itself. The various components that make up the actuator unit are: (i) vibrating motors; (ii) luminosity device; and (iii) motors to control the wheels. Table 4.2 summarizes the purpose and context of the sensory unit included in the ARCane.

Table 4.2: Contextualization of the ARCane actuation unit

Actuator Unit Purpose	Signals Actuated	Parameters
Gait correction	• Wheels motors • Vibrotactile motors	• Velocity • User alert • Gait rhythm correction
Fall prevention	• Wheels motors	• Cane displacement, velocity and orientation
Context awareness	• Light	• Environment luminosity

4.4.1 Haptic feedback system

To achieve the full spectrum of human-robot interaction, it is essential that the user is able to communicate with the robot, but also that the robot is able to communicate with the human. Goodrich et al. [108] states that these interactions can be divided into two general categories: close interaction, when human and robot are co-located, and remote interaction, when human and robot are spatially or even temporally separated. The ARCane system involves close human-robot interaction and is comprised of applications that require mobility and physical manipulation. In the context of robot-to-human communication, a vibrational actuation method was adopted, allowing direct interaction between the robot and the user.

Typically, assistive devices that incorporate haptic feedback in the form of mechanical vibrations are designed to assist blind users so that they can be guided in some specific direction. In addition, vibrational actuations are used as a resource in people with Parkinson's disease, in order to face symptoms of gait

disorders and Freezing of Gait (FOG) [122]. These symptoms seriously affect the life quality of patients as they can lead to unpredictable loss of movement control and result in falls. Wegen et al. [123] showed that vibrations delivered to the wrist of users at a frequency 10% below the preferred stride frequency resulted in lower stride frequencies and longer stride lengths when walking on a treadmill. Additionally, Miiõ Studio [124] developed a cane that employs haptic feedback through built-in vibrating motors, with the aim of stabilizing the user's walking pace (Figure 4.16).

Inspired by these methods, vibrating motors were integrated into the cane, with the purpose of notifying and adjusting irregular gait through vibratory signals, enabling a controlled march that, consequently, could reduce possible user falls. The vibrating motors are located inside the handle of the cane, as represented in Figure 4.17, with no physical interference of the motors with the user's hold, allowing the propagation of vibration to the user's hands to carry out communication between robot and human. Myles et. al. [125] also report that the hands are the location of the body with the greatest vibrational sensitivity, which motivates the choice of the location and method of the haptic feedback system applied to the ARCane. Taking into consideration that the motors have a flat surface and the tube inside the handle has a circular surface, a 3D printed structure has been developed that allows the motors to establish full surface contact with the handle tube to achieve full transfer of the resulting vibrations, as shown in Figure 4.18.

Figure 4.16: Albert Cane, a cane with haptic feedback designed by Miiõ Studio. Image from [124].

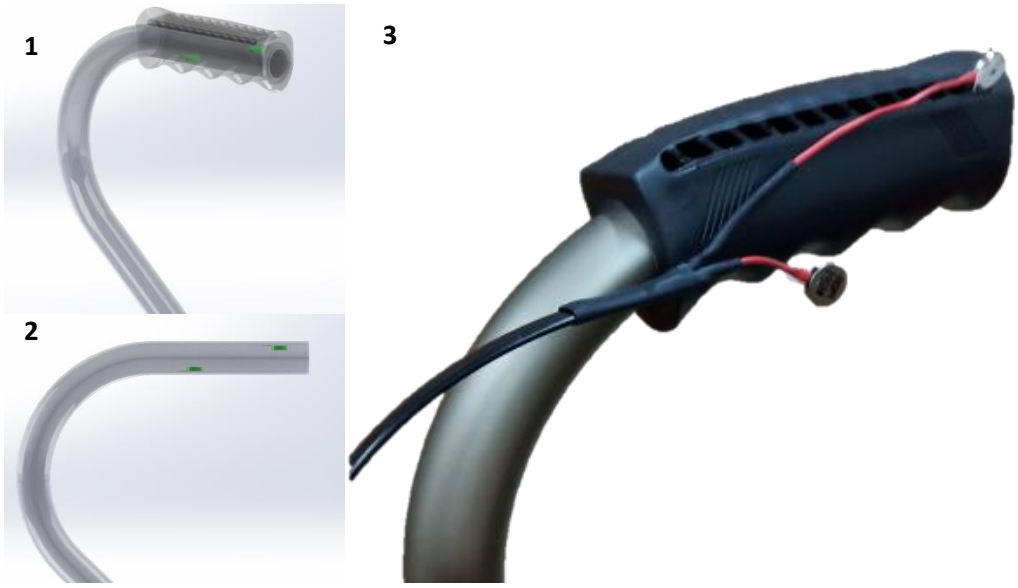

Figure 4.17: Visual representation of the vibrating motors built into the cane handle: 1 – Trimetric view; 2- Side view; 3- External visual representation of how the vibrotactile motors will be arranged inside the handle.

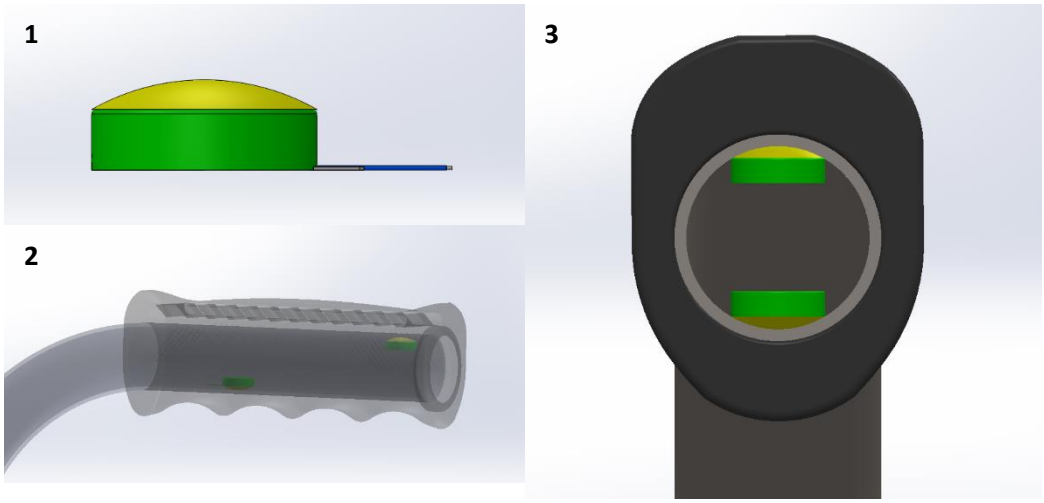

Figure 4.18: 3D model visual representation of the vibrating motors embedded in the cane handle with the 3D printed support; 1.3 - Trimetric View; 2- Side view.

The vibrating units to be used are 10 mm vibrating motors from Precision Microdrivers (Figure 4.19(a)), of the eccentric rotating mass type, which have an off-center load, and when it rotates the centripetal force causes the motor to vibrate [126]. Due to their small size and closed vibration mechanism, it makes them perfectly suited to be placed inside the cane handle, maintaining all their capabilities. For the motor control, the Texas Instruments Haptic Motor Driver DRV2605L is used (Figure 4.19(b)), which requires I2C communication and enables the motors to be controlled by PWM signals, allowing to adjust the vibration

intensity and the motor rotation direction [127], [128]. Table A.6 summarizes the main features of the vibratory motors.

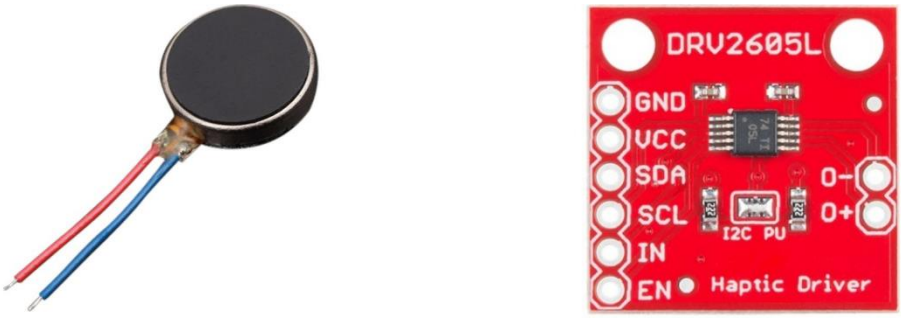

(a) (b)

Figure 4.19: (a) 10 mm vibrating motors from Precision Microdrivers. Image from [126]; (b) Texas Instruments Haptic Motor Driver DRV2605L. Image from [127].

The haptic feedback system, illustrated in Figure 4.20, will be powered at 5V, coming from a step-down located posterior to the battery, and it is connected to a digital port on the low-level CU that allows turning the motors on or off, an analog port to control their modes of vibration, and two ports, SCL and SDA, to perform I2C communication with the haptic drivers.

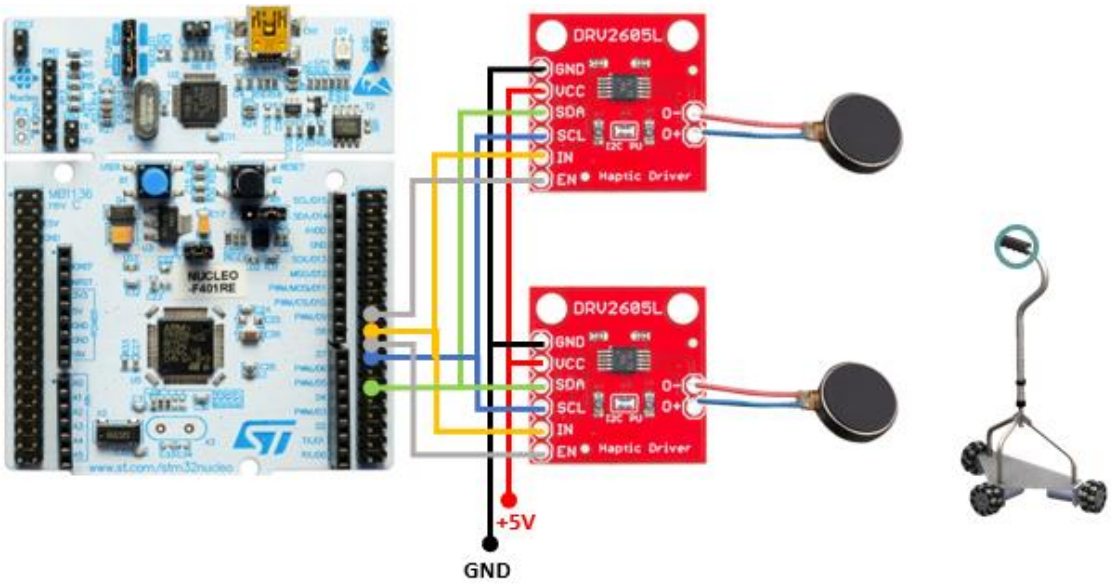

Figure 4.20: Haptic feedback system electrical control circuit.

4.4.2 Luminosity device

The luminosity device is responsible for illuminating the external environment when the user is in poor visibility conditions while using the cane. This actuation system is directly correlated to the light sensor component, i.e., photoresistor. When the control unit detects low light, it activates the respective lighting device to ensure good visibility of the surroundings. The actuator device to be used is a high-brightness Light Emitting Diode (LED) with a large field-of-view capable of illuminating a large area, located on the front of the base of the cane (Figure 4.21). The LED technical specification are presented in Table A.7. This system is powered at 5V, and it is connected to a digital port on the low-level control unit that allows to control when to turn the LED on and off, as shown in Figure 4.22.

Figure 4.21: LED used as the light actuation mechanism for the ARCane. Image from [129]

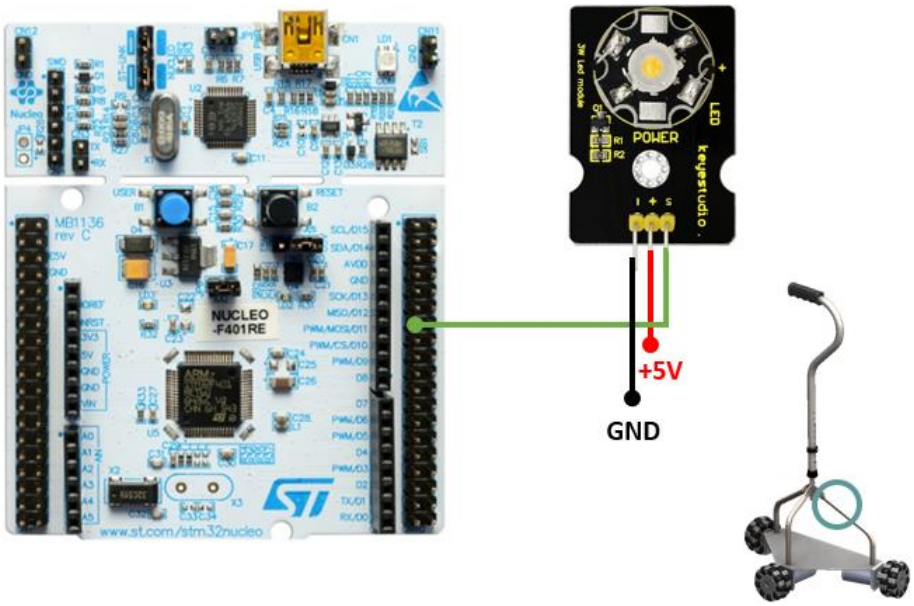

Figure 4.22: LED electric control circuit.

4.4.3 Wheel motors

The actuation system of the omnidirectional wheel motors is what makes possible the locomotion of the ARCane, being responsible for its direction, speed, acceleration and rotation. They are directly correlated with admittance control, which receives sensory information from the user's intention and in turn, it controls the motors to match the intended movement. For that purpose, three NEMA23 motors (RMCS-2255) produced by Rhino Motion Control Solutions [130] are integrated into the holonomic base of the ARCane, as shown in Figure 4.23. These motors have high torque and thrust force, proving to be ideal for admittance control and fall prevention. They use an optical encoder which, compared to magnetic encoder, has improved accuracy and resolution, and can be used in applications where strong magnetic field is generated. The motors technical specifications are shown in Table A.8.

(a) (b)

Figure 4.23: (a) DC Servo motor NEMA23 (RMCS-2255) by Rhino Motion Control Solutions. Image from [130]. (b) Insertion of the motor into the holonomic base of the cane.

Although the technical specifications of the motors indicate that the no-load current is 0.8A and the maximum load current is 7.5A, through experimental tests it was found that the values obtained would actually be on the order of 0.4A for no-load current at maximum motor speed. In addition to these values, it was observed that during walking with the ARCane, the average current consumption is 3.6A of the three motors in total. Such experimental values will be considered for dimensioning the electrical circuits in the power unit, presented in the next section.

Each motor requires a total of six connections for correct operation. Among the six motor terminals, two are intended for motor direction (DIR+ and DIR-), another two for controlling the motor movement (PUL+

and PUL-), one for the circuit ground (GND) and, finally, a terminal for the power supply (V+). The terminals destined for the direction and movement of the motors are connected to digital ports of the low-level control unit, while the GND and V+ terminals are connected to a step-down that regulates the battery voltage to +12V. The electronic circuit for controlling the motors is shown in Figure 4.24.

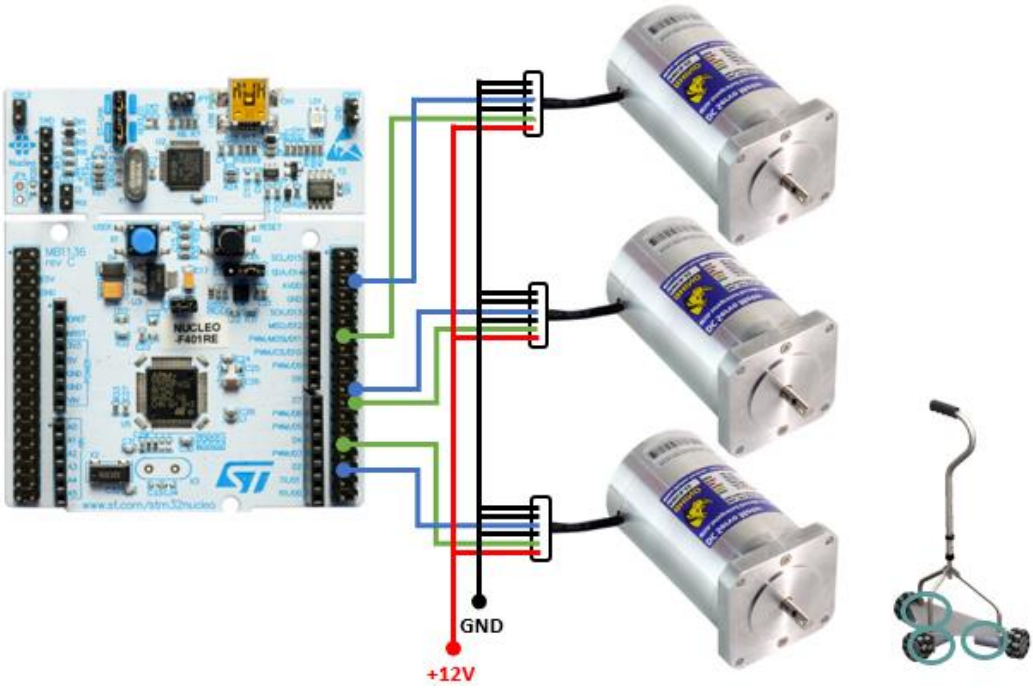

Figure 4.24: DC Servo motors electrical control circuit.

4.5 Power Unit

All units listed in this chapter require energy for their operation, namely voltage and current. This requires an energy source capable of powering the entire ARCane system. However, not all components work with the same amount of energy, which requires the addition of devices capable of delimiting and quantifying the energy to be sent to each component. In addition, since the incorrect administration of current and voltage can lead to malfunction, or even permanent irreversible damage to electrical components, an electrical safety mechanism is necessary to prevent such damage. The power unit circuit is composed of a battery, DC voltage regulators (+5V and +12V), electric fuses, and a power button, being located at the base of the ARCane, as illustrated in Figure 4.25. Such devices will be described in following subsections.

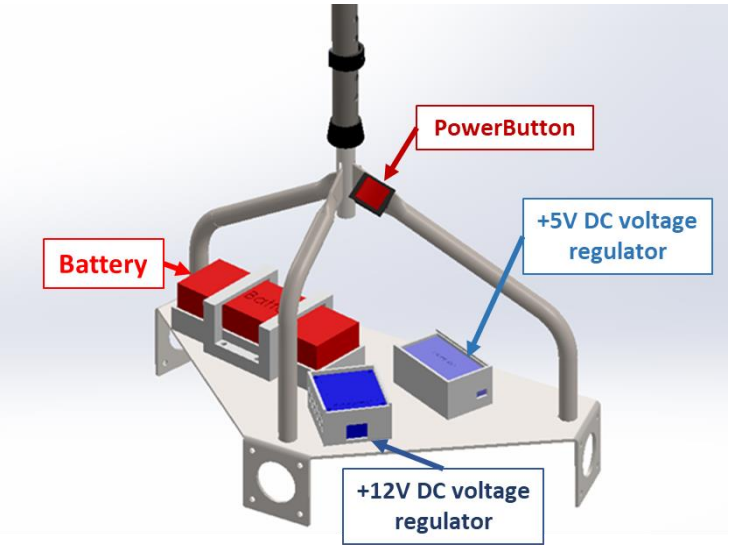

Figure 4.25: Visual 3D model representation of the power unit circuit, including battery, DC voltage regulators (+5V and +12V), and power button.

4.5.1 Battery

The battery works as a power supply and is responsible for providing the energy needed for the entire ARCane system. Dimensions, weight, and price are very important parameters to consider when making the battery choice. Furthermore, it is necessary that the intrinsic characteristics of the battery match the needs of the ARCane and its hardware, i.e., the type of current, voltage and capacity. The battery must then operate with Direct Current (DC), to be compatible with all components present in the cane. As for voltage, among the hardware components, the highest operating voltage is 12V, which becomes the requirement for the battery operating voltage. The battery capacity, usually measured in Ampere-hour (Ah), is given by the following equation 5.5.

$$Battery\ capacity = Current\ drawn\ (A) * Time\ of\ operation\ (h) \qquad (5.5)$$

The total current that is drawn by the prototype can be estimated by the sum of the maximum current drawn from all the parts of the system. Initially, during the design and development of the prototype , extended teamwork [13], the current drawn was estimated to be 23A (without considering the high-level and low-level CU) and the time of operation was set to one hour. However, the batteries that correspond to this capacity were simply too big and heavy. So, a compromise in the operation time was made, reducing it from one hour

to twenty minutes. In addition, it is important to notice that this operation time is continuous and corresponds to the maximum current drawn from the system, and, for this prototype, it is expected that the device only operates at peak performance through small bursts of time. This gives the final battery capacity equal to, approximately, 8Ah, calculated using equation 5.6.

$$Battery\ capacity = 23 * \frac{20}{60} = 7.67\ Ah \quad (5.6)$$

Thus, it was possible to find the Gens Ace lithium-polymer battery [131]. It has a capacity of 8Ah, meeting the previously identified battery capacity, and a voltage of 14.8 V, accounting for any possible voltage drops during operation. As for the battery type, lithium-polymer was the chosen one because of its higher safety, lightweight (0.74 kg), and low profile (157 x 53 x 43 mm), ideal for the ARCane. The technical specifications of the user battery are represented in Table A.9. When considering the control units in the power consumption of the battery system, this rises to 25.2A, resulting in a battery lifetime of approximately 19 minutes, as per equation 5.7.

$$Battery\ life\ (minimum) = \frac{Battery\ capacity\ (mAh)}{Full\ load\ current\ (mA)} = \frac{8000}{25{,}200} = 0.317h = 19min \quad (5.7)$$

This result serves as a reference, and it is assumed that the cane operating time is continuous, and that the system is operating at peak performance, consuming the maximum possible current from each component. However, if we consider the average consumption of the motors mentioned in subsection 4.4.3, as they are the components which consume more energy, we can obtain an average system consumption of 7.8A, enabling a continuous operating time of approximately 61 minutes with a single charge (equation 5.8). This result demonstrates the possibility of the ARCane use in gait rehabilitation sessions.

$$Battery\ life\ (average) = \frac{Battery\ capacity\ (mAh)}{Average\ load\ current\ (mA)} = \frac{8000}{7800} = 1.02h = 61\ min \quad (5.8)$$

4.5.2 DC voltage regulator

The DC Voltage Regulator, also known as step-down, are meant to control the voltage coming from the battery and supply the correct power to the general circuit, keeping the functionality stable. A step-down capable of limiting the input signal to 5V at the output [132], is intended to provide energy to the high-level CU via USB C, which will later provide energy to the low-level CU via USB mini-B. And another step-down with the ability to limit the input signal, coming from the battery, to 12V at the output, is used to power the DC servo motors [133].

4.5.3 Fuses

A current overload, i.e., a sudden increase in the intensity of electrical current flowing through an electrical circuit, can generate overheating, which can damage the integrity of the conductors, with the risk of fire, skin burns or destruction of other circuit elements. To avoid such an event, electric fuses [134] are used as safety and protection mechanisms for the ARCane circuit. A fuse is an electrical safety device that operates to provide overcurrent protection of an electrical circuit. Its essential component is a wire or metal strip with a specific melting point, which when a high current flows through the circuit, it melts due to the Joule effect, thus stopping the flow of current. Thus, the fuses were placed at the output of both step-downs to further prevent damage to the later circuits.

4.5.4 Power Button

Another component that acts as a safety mechanism is the power button [135], with the functionality to cut the connection between the power supply and the high-level and low-level CU. This safety mechanism can be activated by the user when there is a malfunction of one or more components, which can compromise the operability of the ARCane and the safety of the user. The schematic of the final circuit with the power unit configuration is represented in Figure 4.26.

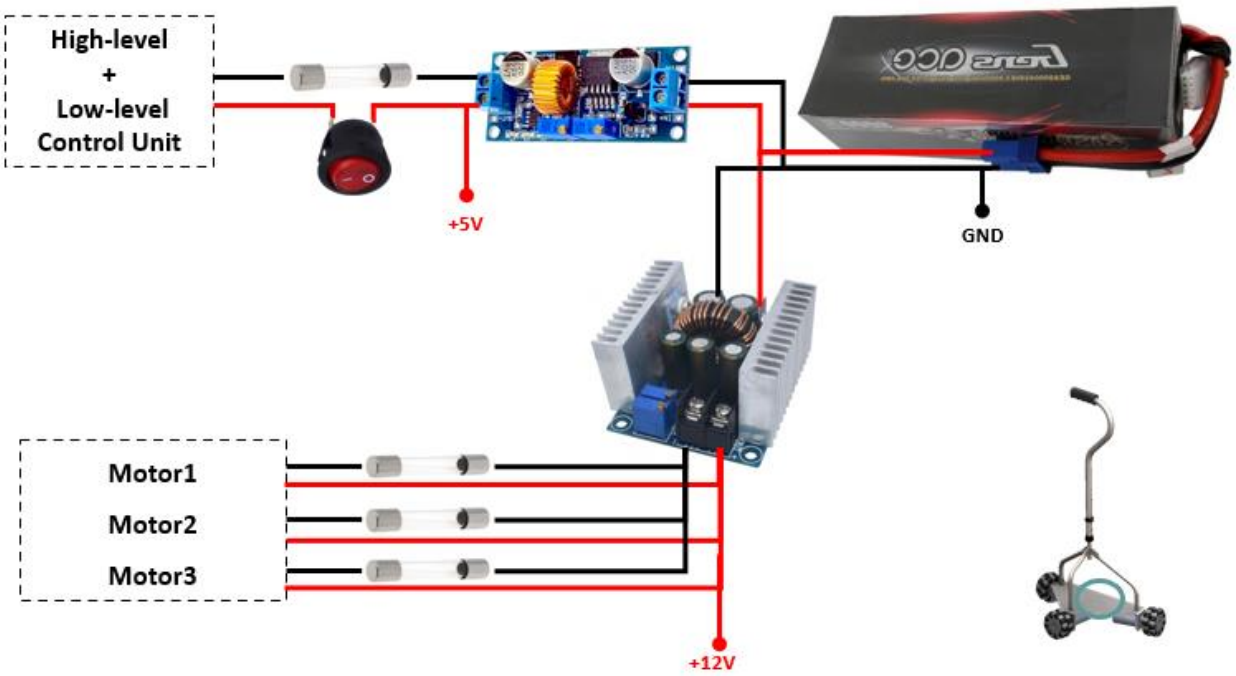

Figure 4.26: Schematic of the ARCane system power circuit, with safety mechanism components included.

4.6 Communication protocols and frequencies

There is constantly data to be acquired by the sensory unit, which after an analysis and mathematical calculations, result in information and commands to be sent out to the actuation unit. The information intermediary is the control architecture, responsible for all its distribution and processing. However, different devices have different communication modes, so it is necessary to match the communication protocol of each one, so that the transmission of information between the ARCane units is successful. The communication modes present in the ARcane system are the Universal Asynchronous Receiver Transmitter (UART) and the Inter-Integrated Circuit (I2C). Their protocol will be briefly discussed and explained in the next subsections.

4.6.1 Inter-Integrated Circuit (I2C)

I2C is a bus interface connection protocol incorporated into devices for serial communication. It only requires the use of two wires to transmit data between devices: (i) SDA (Serial Data), the line for the master and slave to send and receive data; and (ii) SCL (Serial Clock), the line that carries the clock signal. I2C

communication is synchronous, i.e., the output of bits is synchronized to the sampling of bits by the clock signal shared between the master and the slave, with the clock signal always controlled by the master. With I2C, data is transferred in messages, and each one has an address frame that contains the slave's binary address, and one or more data frames that contain the data being transmitted. The message also includes start and stop conditions, read/write bits (which specify whether the master is sending data to or requesting data from the slave), and ACK/NACK bits, whether an address frame or data frame was successfully received, between each data frame (Figure 4.27).

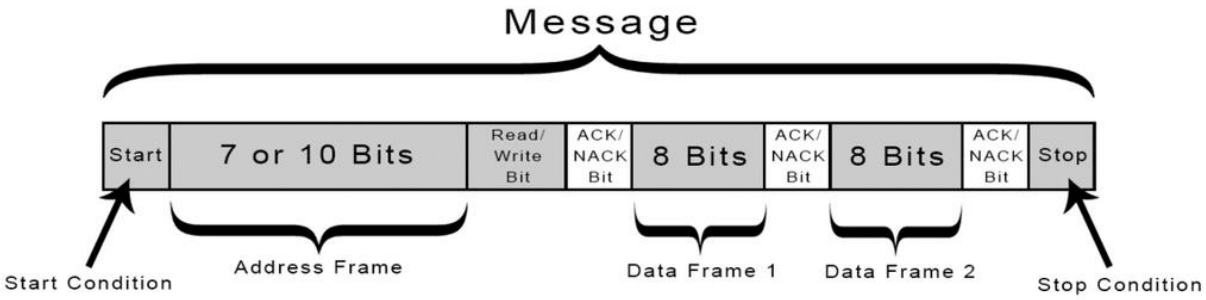

Figure 4.27: I2C communication protocol data frame. Image from [136].

4.6.2 Universal Asynchronous Receiver Transmitter (UART)

The UART is a device-to-device digital communication that uses two data lines, one to transmit (TX) and one to receive (RX) information. As it communicates in asynchronous mode, it does not require a clock, meaning that data is not transmitted at a fixed rate. UART communication happens using a serial frame. The serial frame is defined as a data bit character with sync bits (start and stop bits) and optionally a parity bit for error checking. The UART accepts all 30 combinations of the following as valid frame formats: (i) 1 start bit; (ii) 5, 6, 7, 8 or 9 data bits; (iii) no, even or odd parity bit; and (iv) 1 or 2 stop bits. When a complete frame is transmitted, it can be followed directly by a new frame, or the communication line can be set to an idle state as illustrated in Figure 4.28.

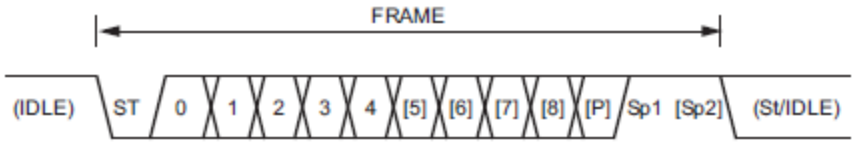

Figure 4.28: UART communication protocol serial frame. [ST]- Start bit, always low; [P] – Parity bit, can be odd or even; [Sp] – Stop bit, always high; [IDLE] - No transfers on the communication line, must be always high. Image from [137].

4.6.3 System frequencies

Another parameter to consider in relation to communication and data processing is the frequency in which information is obtained by the sensory units, processed by the control units and transmitted to the action units. This is a very important variable, as it aims to ensure the cohesion of operation of the ARCane system, enabling the reception and sending of information at pre-defined times, considering the frequency of operation and communication of each component and the processing time of the control units.

Knowing the frequency of each component, it is then possible to obtain a well-structured communication system, ensuring that no information is lost and optimizing the response time of the ARCane processing unit. From the sensory unit, it will be used a sampling frequency of 104 Hz for the IMU, while the sampling frequency of the force sensors and the light sensor is dependent on the ADC sample rate, since their input in the low-level CU is determined by an analog signal. Bearing in mind that the microcontroller of the STM32F446RE low-level control board has an ADC clock speed that varies between 0.6 and 36 MHz, for a 12-bit resolution ADC. This means that with 3 ADC sampling time cycles and assuming the ADC clock frequency at 30 MHz, which is the typical value according to the STM32 F446RE datasheet [138], a sampling rate of 2 million samples per second (MSPS) is obtained. This result is the outcome of the mathematical equations 4.1 - 4.3 presented below:

$$T_{conv} = Sampling\ time + 12\ cycles = 3 + 12 = 15\ cycles \tag{4.1}$$

$$T_{conv} = \frac{15}{30MHz} = 0.5\mu s \tag{4.2}$$

$$f_s = \frac{1}{T_{conv}} = 2MH \tag{4.3}$$

With T_{conv} – Total conversion time; f_s – Sampling frequency.

This value is very high, but it does not demonstrate a real value of the sampling frequency of these components, as it simply represents the reading frequency of the ADC ports of the low-level control unit. In general, the true sampling frequency of the components is defined and limited by how often these data are accessed, and if so, they can also be limited by the frequency that they are transmitted to the high-level control unit or external device, to be later analyzed. Thus, the sampling frequency of the sensory unit components will be defined by the frequency that their data will be accessed by the low-level CU. In the case

of the actuation unit components, the frequency of their status update and the commands to be obeyed will also be defined by the priority given to each component in the low-level CU to interact in the cane-user system. In addition, they may be limited by the reading frequency of certain sensory components in case if the actuation component is dependent on the data received from the sensing component.

The designed mode of operation from the low-level CU developed software code, operates by acquiring the data from the sensors, with different reading frequencies. It first processes the data alternately through each sensor and then performs the necessary calculations and analysis to send commands to the actuation unit components also at different frequencies, each related to the priority of the task. This process of reading data from the sensory unit and then transmitting data to the actuation unit at different frequencies is carried out in order to manage the processing time of the low-level control unit, depending on the relative importance of each component, allowing a correct behavior of the ARCane and its various components to always maintain its proper functioning with a fast enough assigned frequency, ensuring a proper cane operability. In a last step, all the necessary information is gathered to be then sent at the same time to the high-level UC. This synchronized frequency to be transmitted from the low-level UC to the high-level UC may limit the sampling frequency of faster devices and faster communication modes, but it is realized to simplify the communication between the control units, and to simplify the fusion of data from the various components of the ARCane system.

The communication frequency configured for the low-level CU to communicate with the high-level CU was set to 5Hz, using a serial baud rate of 115200 bits per second on the serial port, which proved to be sufficient to perform all necessary levels of communication without any loss of information. In the case that the high-level control unit wants to communicate with the low-level control unit, an interruption occurs in the low-level CU software to immediately process the commands sent by the high-level CU. A representation of the operating frequency of each unit of the cane system, as well as the respective communication protocol is shown in Figure 4.1.

4.7 Final ARCane assembly

With the objective of synthesizing the different units responsible for the entire operation of the cane, this section seeks to demonstrate an overview of the connections that encompass the electronic components present in the ARCane, in order to obtain a better understanding of how the components communicate with

each other, and which connections are necessary for the exchange of information to occur. Beforehand, it is worth mentioning the Printed Circuit Board, which acts as a common reference point between all the electronic components of the cane. It is where the low-level control unit is located, as well as most of the connections that are part of the ARCane electronic system. Printed circuit boards (PCB) are used to mechanically support and connect electrical components using conductive pathways, tracks or signal traces etched from copper sheets laminated into a non-conductive substrate. Some advantages of using a printed circuit board are: (i) it allows an organized circuit with a compact size, with the availability of electronic components of very small size; (ii) saving the use of wires, as the connections are made through conductive paths; (iii) making tight connections and avoiding short circuits as the connections are made automatically; and (iv) considering mass production, they can be manufactured at a reduced cost. All these factors together can bring reliability to the overall circuit performance. The PCB schematic and board layout were made using the EAGLE software, designing a single-sided PCB, where the conductors are placed on only one surface of the dielectric base of the printed circuit board, obtaining the dimensions of 125 x 152 mm. The PCB layout and the final print result with the implemented electronic components is illustrated in are shown in Figure 4.29.

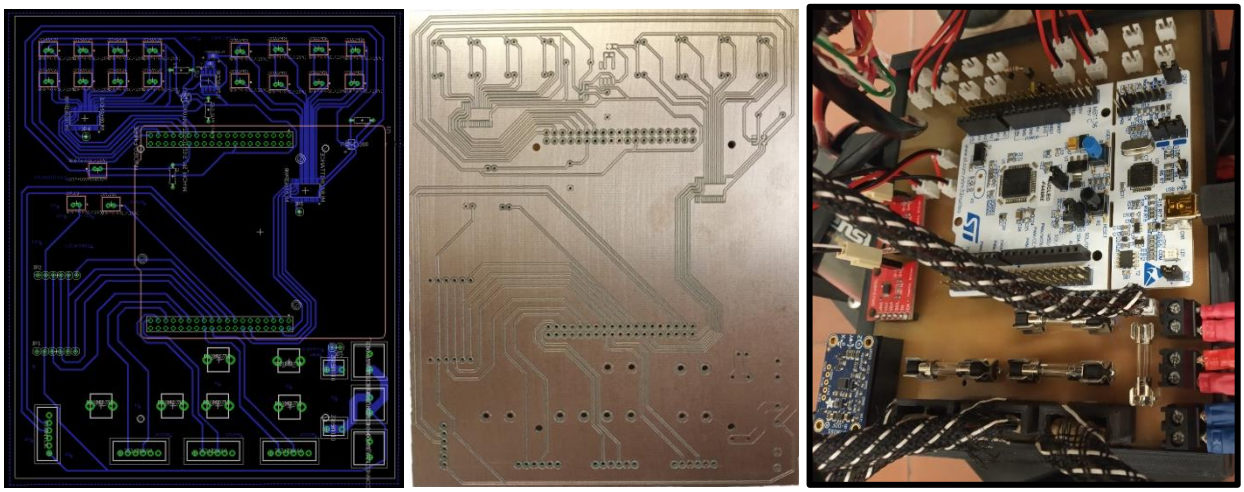

(a) (b) (c)

Figure 4.29: (a) PCB layout with EAGLE software; (b) PCB of the cane (horizontally mirrored); (c) PCB with implemented ARCane components.

Finally, by connecting all the components of the control, sensory, actuation and energy units to each other, we finally obtain the complete electronic system of the ARCane, responsible for all its functioning, comprising all the unique features and functionalities that make it stand out from a conventional cane. For better understanding and visualization of the connections present in the electronic system of the cane, Figure 4.30 presents a diagram of the component's connections, Figure 4.31 has a representation of the final ARCane structure with all components inserted in the structure of the cane, and Figure 4.32 labels all the electric components present in the ARCane. To summarize the components that make up the robotic cane, including the materials of the physical structure and the electronic components of the control, sensory, actuation and energy units, Table A.10 presents the main information of each and the overall components of the ARCane. It is described a total of **71 components** instrumented, a total weight of **5.5Kg**, a total of **7.8A** average current drawn of the electric circuit, and a total price of **688.97€** for the ARCane.

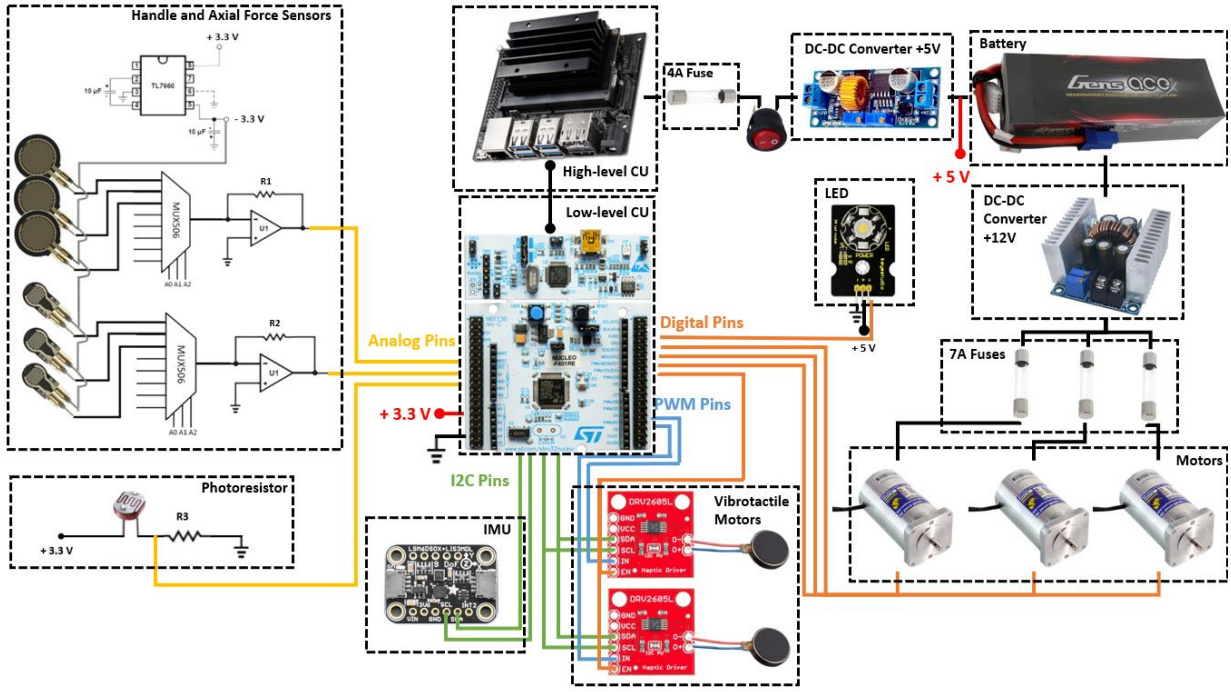

Figure 4.30: Electronic schematic of the component's connections from the different units of the robotic cane.

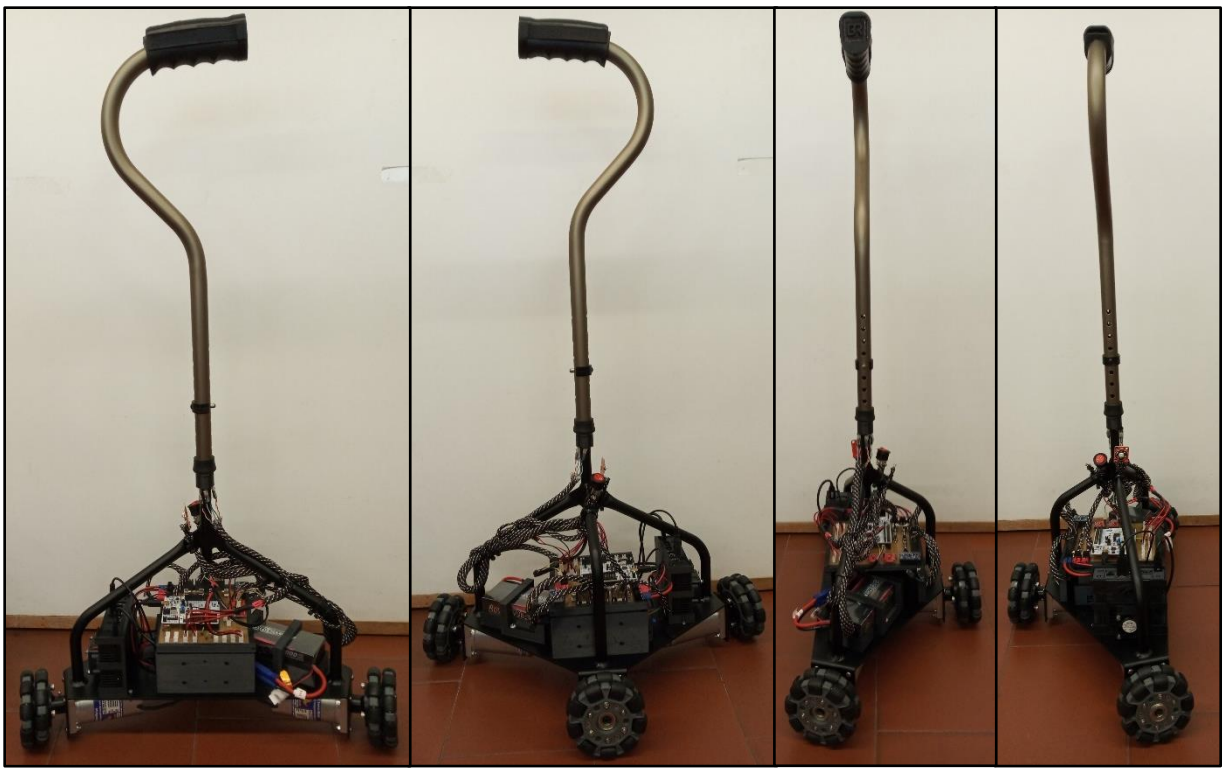

Figure 4.31: Final ARCane structure with all components inserted.

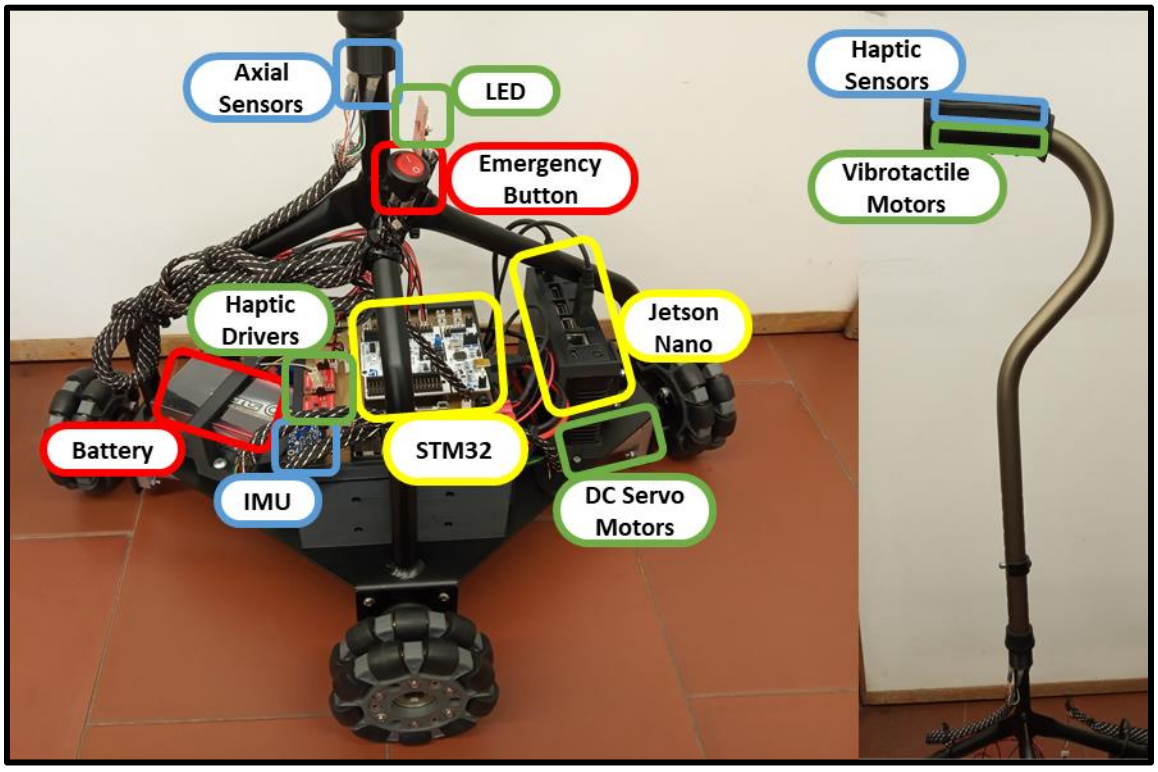

Figure 4.32: Representation of the components inserted in the structure of the cane with the respective label. Red – power unit; Green – actuation unit; Blue – sensory unit; Yellow – control unit.

4.8 Discussion

The set of sub-systems that complement the ARCane system, namely: human-robot interaction, control architecture, database and functionalities, highlight the great evolution and distinction of the conventional cane to the ARCane, as well as its importance and influence as a possible commercial product in various fields of the health industry. For information to be exchanged between the components and control units of the ARCane system in a cooperative and coordinated way, it is necessary to take into account the communication protocols and to have well-defined data transmission frequencies to ensure structured communication, avoid possible packet loss and manage the processing time by the control units for each component. Throughout this chapter, the components were selected to be part of the sensory, actuation and power units of ARCane electronic system, demonstrating their technical specifications, circuits for data acquisition or actuation mechanisms, the respective location in the cane structure, and their role in the cane system.

In the summary of the components that make up the ARCane, including electronic components and structural components, it was possible to verify that a total of 71 components are part of the ARCane system. Subsequently, when evaluating the average energy consumption of each component, it was possible to verify that the average energy consumption of the ARCane electronic system is 7.8A, allowing in theory a continuous use of all the cane functions in a period of approximately 1 hour of use, taking into account the capacity of the battery to be used. In relation to the total weight of the cane, it is 5.5 kg, which corresponds to a weight of less than 6 kg as defined in the target cane specifications (Table 3.3), resulting in better maneuverability of the cane, as well as greater ease for its transportation. Resulting from the acquisition of all the components necessary for the incorporation of ARCane, the total purchase price is 688.97€. Although this value is slightly above the 650€ stipulated in the target cane specification, it is important to bear in mind that this version of the ARCane is not the final product, but a prototype of a potential future commercially available product. Thus, all parts were purchased in single quantities, and all hardware components are considered experimental, which later in the design can be altered or over-engineered, to optimize the performance and also the overall price of the ARCane.

5 Interoperability Tests

Interoperability testing is a type of test that verifies if the various components of the system can interact with each other, in order to guarantee and verify the good functioning of the system in general, assuring that there are no compatibility problems between devices. When performing this type of test, it is verified if the components can work together as a single unit. It also observed if all the system applications perform the expected behavior by themselves, noticing if there is data that during the exchange of information is modified from its original value or state. In this work, the interoperability tests were also adapted to validate the correct functioning of components more related to the hardware, namely the battery and the structure of the cane, as well as some usability tests referring to the interaction between the ARCane and the user.

The structure of the interoperability tests is composed of four phases: the requirements, eligibility criteria, procedures, and finally the results. First, are defined a set of **requirements** that the cane system must meet, considering the established consumer needs and the ARCane target specifications. Subsequently, **eligibility criteria** will be stipulated, which refers to more specific assessment points, according to each selected requirement. Thirdly, the **procedures** are defined, which describe each step of the execution of the tests to be performed. Finally, the procedures will be executed in order to obtain the **results**. Such results will then be analyzed to verify if they are included in the previously established eligibility criteria.

Regarding the ARCane system, interoperability tests were carried out for the: (i) light sensor; (ii) inertial system; (iii) haptic feedback system; (iv) luminosity device; (v) set of motors and wheels; (vi) battery; and the (vii) data processing and storage of the ARCane system. Throughout the chapter, it will be discussed the four phases of the interoperability tests performed for each mentioned component of the ARCane. The set of requirements and eligibility criteria of the performed interoperability tests are presented in appendix IV, along with some details and visual context of how some of the results were obtained. A total of 6 healthy participants, aged between 22 and 27, volunteered to provide a critical and impartial opinion on some of the experimental tests, related to the operability and handling of the ARCane. The interoperability tests and respective results regarding the force sensors, and the motion control will be discussed and described later in chapter 6. This separation is intended, so that the line of thought and actions carried out and discussed related to the ARCane motion control, can be continued with the respective results.

5.1 Light sensor

The requirements defined for the light sensor are related to the detection of luminosity in the environment. This parameter is associated with an extrinsic fall risk factor, poor lighting conditions result in low visibility which leads to a direct association with the risk of falling.

As a way of complementing the requirements, the following eligibility criteria was established: (i) verify if the photoresistor can detect low light conditions in the surroundings.

The test execution steps to be performed, described in the procedures, consisted in placing the ARCane in an enclosed and illuminated space for a few moments. Subsequently, the light was turned off, and the information acquired by the photoresistor was analyzed to verify if it was able to detect the low luminosity of the environment.

As a result of the tests carried out, the validation of the established eligibility criterion was obtained, in which the photoresistor was able to detect poor lighting conditions. The tests performed, and consequently the associated values obtained, were carried out in a laboratory context, i.e., in a closed environment, since it is proposed that ARCane be used in an initial phase in closed environments, such as hospitals, rehabilitation centers and for domestic use, in home.

5.2 Inertial system

The inertial system proposed requirement is related to the performance of inertial measurements, as a way of validating the correct functioning of the acquisition and transmission of information by the IMU sensor.

The following was defined as eligibility criteria for the inertial system: (i) verify that the IMU acquires correct readings with the accelerometer, gyroscope and magnetometer.

The experimental procedures were divided into two situations. The first consisted of keeping the IMU in a resting position, and proceeding with an analysis and comparison of the values obtained in relation to the expected values. The second situation involved placing the IMU on the ARCane, with the latter moving in the x-axis and later in the y-axis, while the acquired values were compared with the expected values. The expected values refer to the value of the gravitational acceleration on the vertical axis for the first situation; as for the second situation, it refers to the zero-acceleration value in the y-axis direction when the ARCane

was programmed to move in the x-axis direction, and the zero acceleration value in the x-axis direction when the ARCane moved in the y-axis direction.

The results of the tests validated the performance of the inertial system, by obtaining reading errors below 5%.

5.3 Haptic feedback system

The requirements defined for the haptic feedback system are related to: the verification of the correct functioning of the vibrating motors; the user's perception of vibration signals applied to the ARCane cable; and with the verification of the vibration of the motors causing interference in the data acquired by other components of the cane, namely by the inertial system, and by the force sensors located in the handle of the ARCane.

As a way of complementing the requirements, the following eligibility criteria were established: (i) verify if the haptic drivers can be successfully calibrated, in order to obtain direct communication with the vibrating motors; (ii) check if the PWM signals were generated according to pre-defined duty cycles; (iii) check if different vibratory stimuli are perceptible and distinguishable by the user; (iv) analyze whether all users were able to perceive the vibrations applied to the ARCane cable; and (v) verify that the IMU and force sensor readings remain unchanged due to vibration propagation from vibrating motors.

The procedures performed began by asking different participants to put their hands on the handle of the cane. Subsequently, different PWM signals were generated so that different types of vibration were applied by the vibrating motors. With the intention to simulate an alert of a detected emergency situation it was proceeded to apply a more accentuated vibration, and aftwerwads was applied a smoother vibration signal a possible gait correction. During these tests, the signals acquired by the inertial sensor and the force sensors were verified.

As final results, it was found that all eligibility criteria were successfully met, noting that the users were able to perceive different vibration amplitudes and frequencies, and that the vibration propagation of the vibrating motors did not influence the readings acquired by the IMU, and by the force sensors.

5.4 Luminosity device.

To validate the functioning of the luminosity device, requirements were proposed based on the average energy consumption of the LED, to consider the theoretical calculations of the battery life; and based on the light provided by the LED to the surrounding environment, in order to guarantee good visibility conditions for the user in low light conditions outdoors.

The following eligibility criteria were defined for the lighting device: (i) verify that the LED consumes up to 1A, this current value was assigned according to the technical specifications presented by the device; and (ii) verify that the LED can illuminate a low-light environment.

The experimental procedures started with placing the ARCane in a bright space for a few moments. As the LED works according to the light sensor working and detecting the external light conditions, it was verified if the LED turned on, when the light went out, and if it managed to illuminate the space around the user.

For the final results, it was found that all eligibility criteria were met, where an average LED power consumption of 0.16A was obtained, which contributes to an extensive period of battery use, taking into account the theoretical calculations performed previously. In addition, it was proven that LED can illuminate a space without light, up to 5 meters away. In the same way as the light sensor, this experimental test was carried out in a laboratory concept, that is, in a closed environment.

5.5 Set of motors and wheels

The proposed requirements for ARCane motors and wheels intend to verify: the average consumption of the engines, by considering the theoretical calculations of battery life; and the maximum speed that the engines can reach.

As a way of complementing the requirements, the following eligibility criteria were established: (i) verify that each motor consumes up to 0.5A without being coupled to the ARCane; (ii) verify that each motor consumes up to 3A when inserted into the ARCane; and (iii) verify that the motor reaches the maximum angular speed of 300 rpm, a value mentioned in the technical specifications of the motors.

To verify that the proposed eligibility criteria are met, it started by placing the power supply to power a single motor with a constant +12V output. Subsequently, commands were sent for the engine to rotate at maximum speed. While the motor was rotating, the values of the drawn current by the motor were measured.

In addition, it was proceeded to record a footage of the wheel while rotation at maximum speed, bearing in mind a reference plane. Then, the cane was set in motion, with all motors at full speed being powered by the power supply, verifying the total current consumption of the motors when inserted into the ARCane. Finally, it was verified through the recording the maximum angular velocity obtained by the motor.

As final results, each motor draws 0.39A at full speed with no torque applied, and up to 1.20A at full speed when inserted into the ARCane. Additionally, it was possible to verify that the engines could reach a maximum of 248 rpm, which demonstrates that the maximum rotation obtained by the motors does not correspond to the maximum rotation stipulated by the technical specifications. To acquire the rotation speed of the engine, it was used the Tracker software, which is a video analysis and modeling tool. Further description and illustration of the process are presented in Appendix IV. The use of these three motors located in the configuration of the holonomic base of the cane was also validated through calculations performed in [13], according to the dynamic and kinetic models of the cane, represented in Figure 5.1. These results proved that the implementation of these motors is suitable for ARCane, being able to withstand the forces and torques necessary to prevent falls and ensure the proper functioning of the ARCane. Considering that the omnidirectional wheels have a radius of 50 mm, and now that is known that the motors can reach a maximum speed of 248 rpm, in theory it is possible to obtain a maximum rotation speed of the wheel of 8.27 rad/s and a maximum translational speed of 1.30 m/s (4.68 km/h). These values are proven to be more than enough in comparison to the gait speed values of 0.89 m/s, for maximal pace, obtained in geriatric assessment [139].

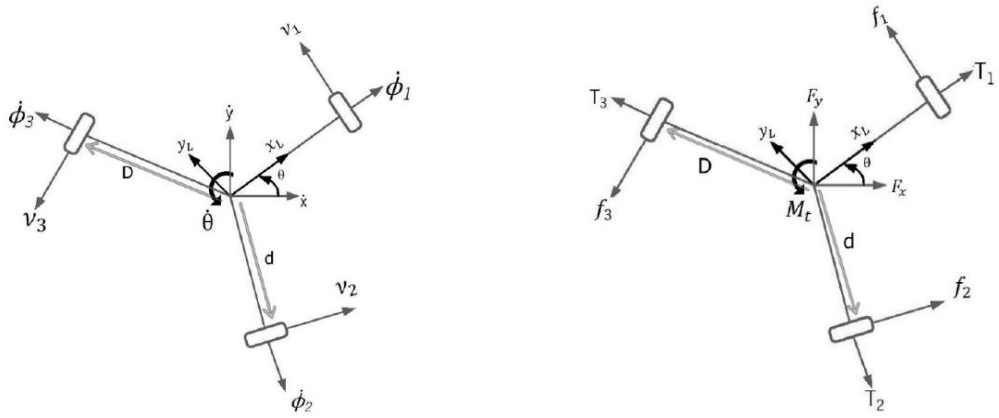

Figure 5.1: (a) Kinetic and (b) dynamic model of the ARCane actuation unit. Image from [13].

5.6 Battery

The requirements set for the battery are based: on the ability to power the entire electronics of the ARCane; in its autonomy, taking into account the time it manages to keep all components in good working order with all their functionalities active; and in the possibility of increasing the autonomy of the system. Safety issues associated with battery interaction are also addressed.

As a way of complementing the aforementioned requirements, the following eligibility criteria were established, by checking if: (i) the power can be turned on and off; (ii) the system can be recharged; (iii) the battery charging connector is easily accessible; (iv) the system displays all functions for 1 continuous hour, this value was obtained as a reference based on the theoretical calculations performed previously in subsection 4.5.1 ; (v) is possible to replace the existing battery with one of greater capacity without hardware and software modifications; and finally (vi) whether it is safe to connect and disconnect the battery from the electrical circuit.

The procedures performed included first to charge the battery until it was fully charged, then measuring the battery voltage value with a multimeter. Afterwards, the electrical system was turned on and left running with monitoring and activation functions active until the battery needed to be recharged. Subsequently, the time that the battery lasted with all the functionalities working was recorded, and the value of the battery voltage was measured with a multimeter. Then, all participants must assess whether the battery charging connector was easily accessible (answer 'yes' or 'no'), and the battery should be replaced with a larger capacity.

Regarding the final results, it was found that the power supply can be turned on and off; the ARCane electrical system has an autonomy of 2 hours and 30 minutes, showing all its functions during this period of time; the initial and final battery voltages were 16.8V and 15.9V; the system can be recharged; participants rated the battery charging connector as easily accessible and safe to connect and disconnect the battery from the circuit; and that it is possible to replace the battery with a larger capacity battery without modifications to the system hardware and software. On a separate note, the time that corresponds to when the cane needed to be recharged, i.e., 2 hours and 30 minutes, refers to when the cane started to lose some speed in the engine rotation. It was not taken until the battery was completely discharged, as this would severely damage the Lipo's battery life. In addition, the initial and final voltage values obtained were above

the 14.8V indicated by the technical batteries of the battery, because for lithium chemistry specifications the maximum charging voltage of a cell is greater than the rated voltage.

5.7 Data processing and storage

The requirements for data processing and storage seek to verify the ability to acquire and store information on the high-level CU memory card, as well as to verify if the acquired data has some direct association with the person who originated. Finally, it is meant to check whether it is possible to increase the overall data storage capacity.

Eligibility criteria for data processing and storage were defined as verifying that: (i) the memory card connector is easily accessible; (ii) all pre-defined data are being monitored; (iii) the pre-defined data organization structure is verified; (iv) the pre-set reading frequency is verified; (v) all pre-set data is being written to the memory card; (vi) there is no logical relationship between the data and the people who originated it; and if (vii) it is possible to change the existing memory card to one with more storage without hardware and software modifications.

The procedures for validating the eligibility criteria started by maintaining the system with monitoring and active data storage for 1h, where the values acquired by the microcontroller were displayed on a computer. It was proceeded to check if all the pre-defined data were being registered in an external file, and if the pre-defined data organization structure was verified. Then, it was checked if the time between samples matches to the pre-defined reading and writing frequency, and if the data volume corresponded to the expected, considering the recording frequency and the monitoring duration. Finally, the memory card was exchanged for one with more storage, and the participants evaluated whether the memory card connector was easily accessible or not ('yes' or 'no' answer).

As final results, it was found that all eligibility criteria were met, demonstrating that as main results it is possible to replace the existing memory card with one with more storage without hardware and system software modifications; the memory card has enough storage for 1h of continuous acquisition; the pre-defined data organization structure is verified; the pre-defined reading and writing frequency can be monitored being verified for 1 continuous hour while not showing packet losses; and finally, the fact that there is no logical relationship between the data and the people who originated it. Regarding the display and monitoring of variables, it was performed through the Arduino IDE, of the low-level UC, which made it possible to use the Serial Monitor and the Serial Plotter, as illustrated in Figure 5.2 and Figure 5.3 respectively for

the purpose of: (i) error detection; (ii) confirmation of the proper functioning of all electrical components; as well as (iii) verification of successful communications in accordance with the respective protocols. Regarding the high-level CU, the variables were displayed through the Graphic User Interface (GUI) programed in Visual Studio, as illustrated below in Figure 5.4. This enables to observe the information that is being received by the high-level CU related to the data acquired from the sensory unit. Thus, it is possible to: (i) confirm the correct functioning of the developed code; (ii) verify the interaction and communication carried out between both control units; (iii) confirm the frequency of the sending data; and (iv) verify if there is exchange or loss of information during the entire process of acquisition, processing and writing of information.

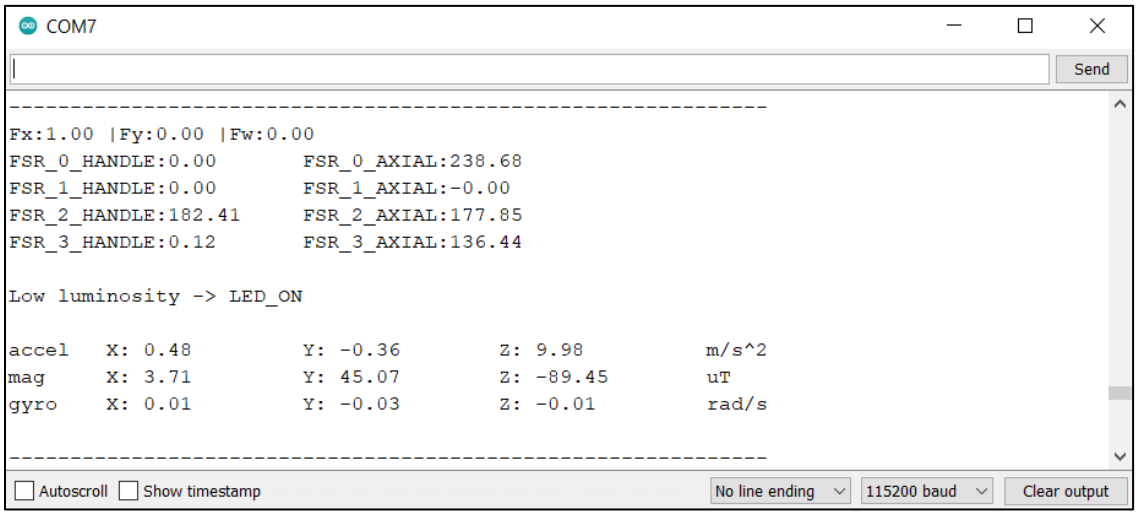

Figure 5.2: Arduino IDE Serial Monitor for system operation check.

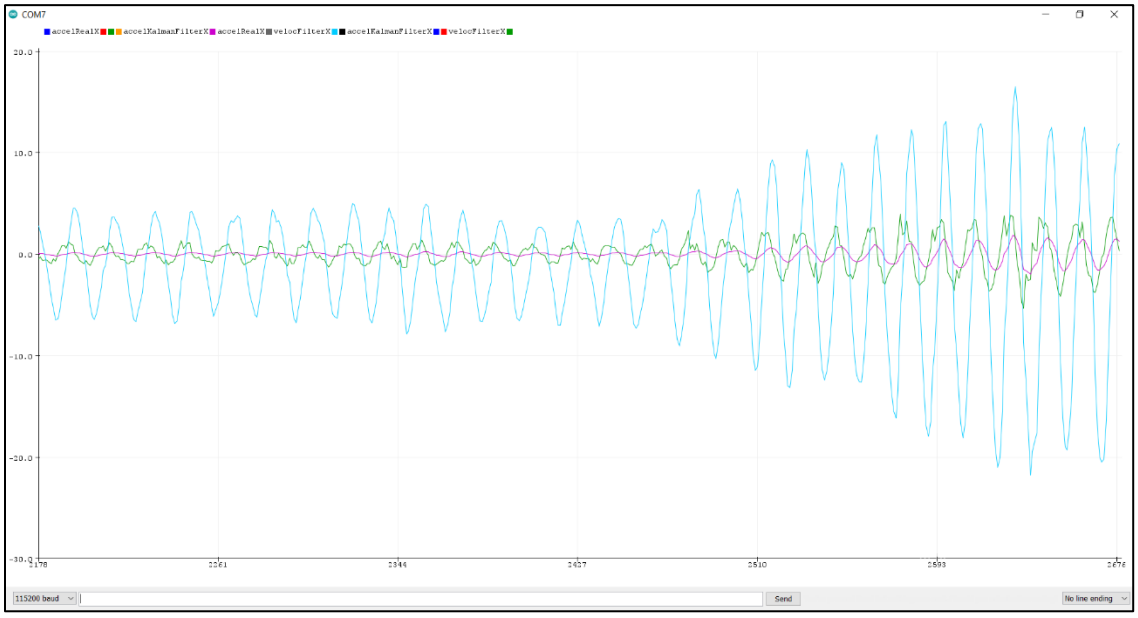

Figure 5.3: Arduino IDE Serial Plotter for system operation check.

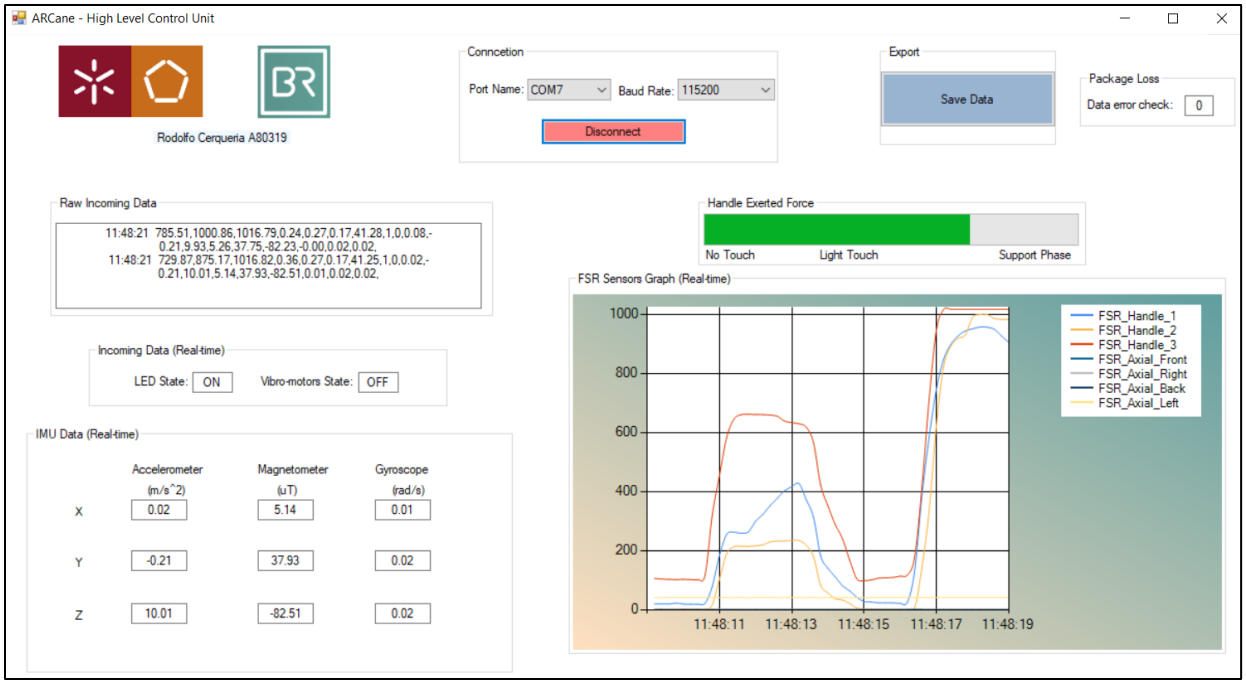

Figure 5.4: Graphic User Interface of the high-level control unit code for system operation check.

5.8 Experimental results

The experimental results related to the interoperability tests are mainly intended to demonstrate whether the eligibility criteria, defined according to the requirements, are verified. This is accomplished by carrying out a sequence of previously stipulated procedures, in order to get the respective results. By executing this sequence of events for the various components implemented, it is possible to verify and validate the functioning of all electronic components and all units, separately and collectively, demonstrating how the ARCane operates as a single unit. A summary of the experimental results obtained when performing the interoperability tests are shown below in Table 5.1.

Table 5.1: Summary of the interoperability tests experimental results

Sensory unit	**Light Sensor** • The photoresistor can detect low visibility conditions in the surrounding environment. **Inertial System** • The IMU can perform correct readings of the accelerometer, gyroscope and magnetometer, with errors of less than 5° in terms of Roll, Pitch and Yaw;

Actuator unit	**Vibrating Motors** • Vibrotactile motor drivers have been successfully calibrated; • It was possible to generate PWM signals according to pre-defined duty cycles; • Users were able to perceive vibration as well as distinguish between different vibration amplitudes and different frequencies; • It was verified that the propagation of vibration from the vibrating motors did not influence the readings performed by the IMU and the ARCane force sensors; **LED** • The LED consumes an average of 0.16A; • The LED can illuminate a path with low luminosity up to 5 meters; **Motors and Wheels** • Each motor consumes 0.39A at maximum speed without any kind of torque; • Each motor consumes up to 1.20A when inserted into the ARCane; • The motor reaches maximum angular speed of 248 rpm;
Power unit	• It is possible to change the battery for one of greater capacity without modifications to the hardware and software of the system; • Power can be turned on and off; • The system has an autonomy of 2 hours and 30 minutes, showing all its functions during this time interval; • The system can be recharged; • The battery charging connector is easily accessible, making it safe to connect and disconnect the battery from the circuit;
Control and Storage unit	• It is possible to replace the existing memory card with one with more storage without hardware and system software modifications; • Memory card has enough storage for 1h of continuous acquisition; • The pre-defined data organization structure is verified; • The memory card connector is considered to be easily accessible; • All pre-defined reading data can be monitored; • All pre-set reading data is written to memory card; • The pre-set reading and writing frequency are verified for 1 continuous hour, with no package losses; • There is no logical relationship between the data and the people who originated it;

5.9 Discussion

These tests represent an evaluation and validation of the singular and collective functioning of the cane components, as well as the verification of the metrics stipulated in the consumer needs and product specifications. All these parameters, including the user-cane interaction and the overall cane system performance were analyzed according to the various obtained results.

The structure of the interoperability tests is composed of four phases: the requirements, eligi bility criteria, procedures, and the results. It was then analyzed the experimental tests performed for all the ARCane electronic components, based on the four stages that characterize the interoperability tests. First, the requirements for each component were addressed, which seeks to define the general characteristics that ARCane must have, according to the consumer needs and target specifications previous established. Then, the eligibility criteria that the experimental tests seek to evaluate are presented, referring to more specific points in relation to the already defined requirements. In order to organize the way in which the experimental tests should be performed, procedures are established to guide the entire process and the sequence of steps to be carried out to obtain the final results. Once the final results are obtained, an evaluation is carried out to compare and verify if they can reach the previously defined eligibility criteria. These final results intend to demonstrate the good functioning of the components individually, but also collectively, revealing their compatibility in terms of communication and technical specifications.

It was obtained as the final main results for the ARCane system:

- The system has an autonomy of 2 hours and 30 minutes, presenting all its functions during this time interval. This result highlights the possibility of using the ARCane in a first stage in rehabilitation sessions.
- The pre-defined data organization structure is verified, in which all read and write data can be monitored; and the reading and writing frequency are verified for 1 continuous hour, with no package losses. Considering this result, it allows to have a perspective of the correct functioning and the validation of all the electrical components that make up the ARCane.
- The light sensor can detect low visibility conditions in the surrounding environment; and the LED can illuminate a path with low luminosity. Thus, it has been proven that the ARCane has a mechanism of detection and actuation related to low luminosity, which is a very important factor, given that many falls are due to poor visibility conditions. It is also important to take into

consideration that none of the robotic canes present in the SoA study contained such a mechanism related to the context-awareness of the environment.

- The participants were able to perceive the vibrations in the cane handle, originating from the haptic feedback system, as well as distinguish between different amplitudes and frequencies of vibration. This result demonstrates the possibility of the cane interacting with the user by varying the vibratory stimuli applied, referring to different indications and alerts for the user to consider.

6 Motion Control

The motion control is responsible for enabling the movement, control and handling of the ARCane through the user interaction. As this control is responsible for locomoting the ARCane, it needs to consider many parameters for a simple, easy, intuitive and comfortable utilization for the end-user. It must provide a controlled gait, always following the user and without any movement limitations, guaranteeing user safety as a priority parameter in all situations. According to Chapter 2, a total of four types of motion control were used: admittance control, self-balance cane, passive control, and accompanying control mode. By evaluating these motion control methods, it was possible to identify the **admittance control** method as the one to be incorporated into ARCane, which later led to the instrumentation of certain sensory components into the cane, previously identified in Chapter 4. This decision resided in the fact that it is the method that best suits the concept of the ARCane. Since it contains a holonomic base, composed of three omnidirectional wheels, providing various DOF to the ARCane. leads to the invalidation of the application of the **self-balancing cane** method intended for canes with only one or two wheels that are based on the inverted pendulum model. In addition, it is desired to obtain a fall prevention mechanism that allows moving the ARCane to a favorable position that guarantees stability and support to the user. With this being only possible through mechanisms that drive the motors, leading to the movement of the cane, it invalidates the implementation of the **passive control** method based on the free control of the cane without any drive mechanism to obtain movement, making the fall prevention mechanism unfeasible; Finally, as the intentions for the ARCane is a handheld device with smooth and intuitive motion control, the **accompanying control mode**, which is based in motion with non-contact, does not suit the ARCane's desired needs.

Having clearly highlighted the reasons for choosing the admittance control, it is necessary to have a better understanding and explore it, so that its incorporation and adaptation in the ARCane is successful, thus, obtaining a complete, viable and effective motion control method. The admittance control method is based on human-robot interaction and translates into the transformation of applied forces into changes in the position and velocity of a system. Its application serves as a way to determine the user's movement intention and, consequently, to obtain a natural and intuitive control of the ARCane's movement, through the force values obtained by the components present in the sensory unit.

This chapter also includes a mechanical study of the ARCane rod structure, carried out through computational simulations, to achieve the method that is able to detect and determine the user's movement

intention, as well as to detect and recognize the user's gait state, while using the ARCane. Finally, the direct kinematics that allow the movement of the ARCane holonomic base, and the experimental results of the interoperability tests with respect to the admittance control and usability of the ARCane will be demonstrated.

6.1 Admittance control strategy

The first implementation phase of the motion control is the proposal of an algorithm that allows controlling the ARCane, by considering the user's gait state and the forces applied by the user. Such a strategy defines the behavior of the cane, by considering the behavior of the user. For decisions to be evaluated and taken by the control units of the cane system, there is a whole process that starts from the acquisition of sensory data to subsequent synthesis of signals through signal processing techniques, thus allowing an analysis and evaluation of how the cane should operate depending on all the information obtained, and thus through direct kinematics, control the motors to originate the movement of the ARCane. In order to establish how the ARCane will work it was done an assessment of the user's movement and the intended movement of the cane when walking with the ARCane, as depicted in Figure 6.1, by considering that Nakagawa et. al. [27] mentioned that it is possible to effectively reduce the load applied to the affected leg when a person walks with the cane robot, by making the ARCane work in a similar way to a proper use of a conventional cane.

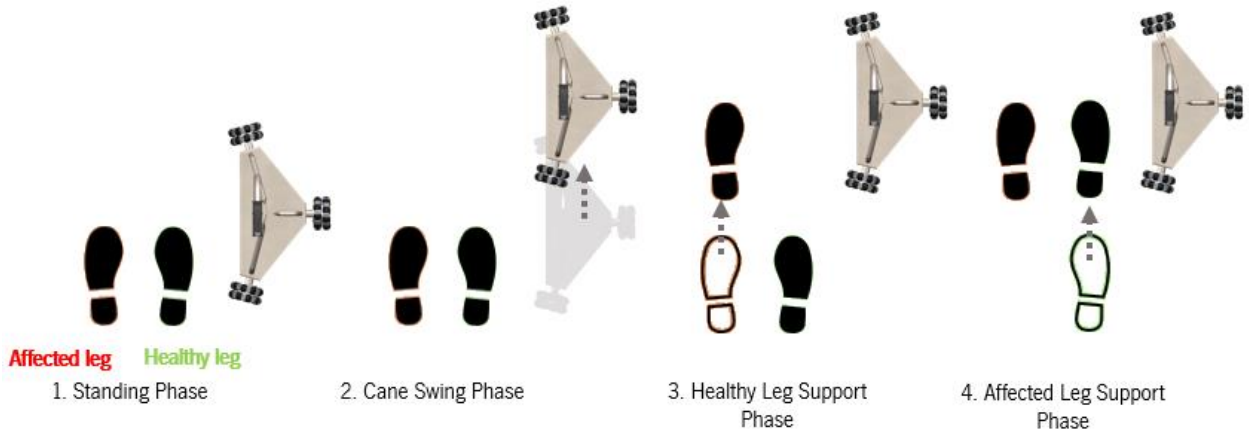

Figure 6.1: Representation of the three-point gait phases with the ARCane.

The start of the gait event occurs with the user's feet aligned with the ARCane, representing the **standing phase**. Subsequently, there is the **cane swing phase**, in which the cane must interpret the user's intention to move it forward, in order to assist the movement of the legs for the following phases of gait. With

the ARCane already placed in a posterior position in relation to the user's feet, the **healthy leg support phase** arises, where the cane must remain stationary to prevent the user from falling during this gait event so that he is able to advance with the affected leg while supporting most of his weight on the healthy leg.

Finally, there is the **affected leg support phase**, representing the most important gait event, in which the healthy leg moves forward. During this phase, the user, rather than supporting the body weight on the leg that remains stationary (i.e., the affected leg), leans on the cane to allow the healthy leg to advance, while the cane remains in a static position throughout this process to ensure a stable support for the user.

For all these sets of consecutive processes to be carried out correctly, the ARCane needs to understand the user's intention of movement in the second phase of the gait. Additionally, it also required to detect when there is a greater application of vertical forces on the cane, symbolizing when the user is supporting his body weight on the cane, namely in the third and fourth gait phases, in order to stop its movement. In the next sections, it will be discussed the proposed methods that enable all data acquisition and actuation mechanisms to obtain the desired ARCane operation, corresponding to the gait event represented in Figure 6.1. A schematic of the intended mode of operation and the proposed admittance control system architecture for ARCane is shown in Figure 6.2 and Figure 6.3, respectively.

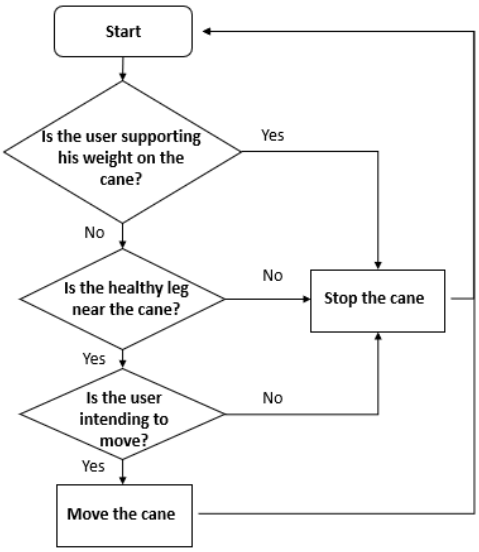

Figure 6.2: Flowchart representing the intended admittance control operating mode of the ARCane.

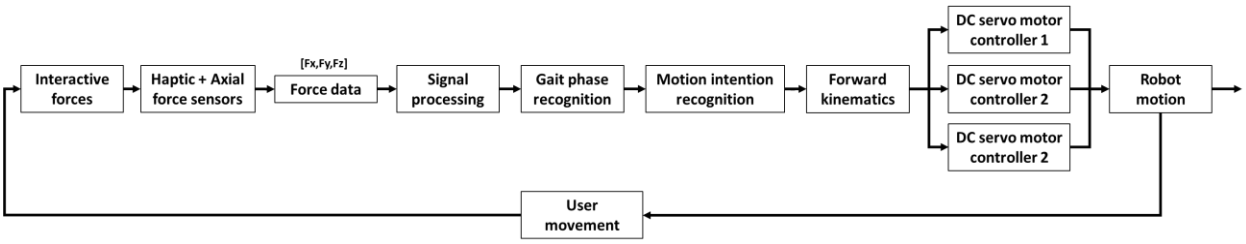

Figure 6.3: Architecture of the admittance control system applied in the ARCane.

6.2 ARCane mechanical study

A total of 55% of the robotic canes included in Chapter 2 used axial sensors, however they do not correspond to an ideal model, due to their high cost associated with the bi-axial and 6-axis force/torque sensors (Figure 2.9), and due to the implication of applying significant changes to the original structure of the cane (Figure 2.10). Therefore, a search for an idea and solution that was equally feasible and more simplistic was carried out, in order to enable the **user's interaction forces** to be obtained in a similar way, so that it can be **detected the user intended direction of movement**.

According to the representation of the three-point gait phases with the ARCane shown in Figure 6.1, it can be seen that there are two support phases, namely the healthy leg and the affected leg support phase. In the case of the healthy leg stance phase, the user may or may not support their weight on the cane to assist in walking, while in the affected leg stance phase, the user should support their body weight on the cane so as not to overload the affected leg as much it would overload without the use of the cane, as shown in Figure 6.4. In both situations it is of great importance that the cane remains stationary during the entire process, in order to provide total stability to the user, and avoid possible falls. Thus, it is important that the detection of the support phase is performed by the ARCane during gait. As the canes partially support the user's weight during the gait cycle, and considering that as the user walks there is a change in the transferred weight to the cane, it is possible to use this parameter to detect which phase of the gait the user is in, by considering the weight transferred to the cane's handle. It is also important to take into account that during a gait cycle, the maximum force applied to the cane is when it is applied fully vertical [177]. Based on this idea, it was then decided to implement a way to **detect the gait phase** from the **user's interaction forces** with the cane. It is then possible to verify that the user's movement intention, as well as the detection of his gait phase, can be detected through the interaction forces applied in the ARCane. On this matter, two sensor proposals will be assigned in this section for the detection of user interaction forces, in which their

implementation will be evaluated based on the results acquired from a mechanical study of the ARCane's rod, given the application of different interaction forces.

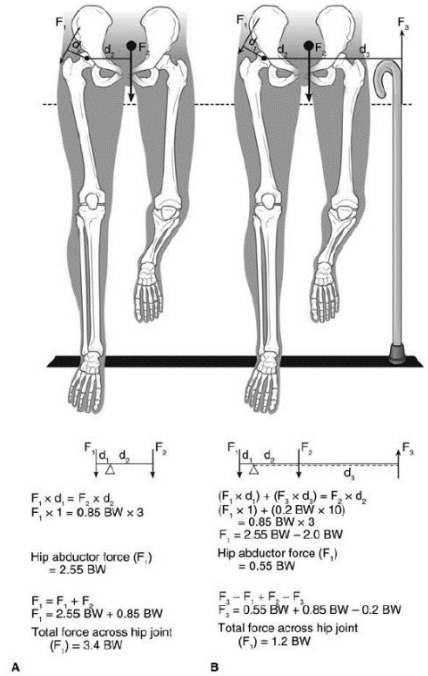

Figure 6.4: Illustration of the total force across the hip joint without a cane (A), and with a cane (B), demonstrating why a cane is used in the hand contralateral to an affected hip or affected leg. F1 represents the force of the hip abductors; F2 is the force of gravity acting on the mass of the body (excluding the stance leg); and F3 the force that can be applied to a standard cane. Image from [76].

6.2.1 Methods

As a way of determining the user's movement intention, one must detect the components of forces applied in the direction of the ARCane displacement plane, defined by the x-axis and y-axis. To identify the user's gait phase, one must detect the component of forces applied in the direction perpendicular to the displacement plane of the ARCane, i.e., the direction in the z-axis. The piezoresistive sensor and the strain gage sensor were defined as the two possible force sensors to detect the user's interaction with the ARCane. The strain gauge is a sensor that can be used to measure force, strain, weight, and pressure, resulting in a difference in its resistance that gives a different electrical output. These sensors are widely used for a variety of electrical transducer devices, primarily due to their high accuracy and excellent reliability, although their performance can be affected by humidity, temperature, and accuracy drops with prolonged use. Thus, it would be possible to measure forces applied to the cane through physical deformations in the ARCane

structure, more specifically, in the rod. It was proposed a method of detecting the user's intention to move, by placing two strain gages at the base of the upper rod of the cane, one directed towards the y-axis (sagittal axis) and the other positioned towards the x-axis (transverse axis), as illustrated in Figure 6.5. Regarding the method of detecting the user's gait phase, it was proposed to place a strain gage on the inner curvature of the upper rod of the ARCane, as illustrated in Figure 6.6, as a prediction of being the point that would suffer the greatest deformation for the forces applied to the cane in the vertical direction.

To prove the feasibility of implementing strain gages sensors in the ARCane, in comparison with FSR sensors, the author proceeded with a study of the deformations in the ARCane rod, resulting from the forces applied by the users. Afterwards, deformation tests were performed with simulations using SolidWorks software. Regarding the user intention of movement, deformation tests were carried out for forces of 100N applied on the cane handle in the direction of the x-axis and y-axis, as illustrated in Figure 6.7 (a) and (b).This applied force is equivalent to a force of approximately 10kg, which is a value that is considered more than enough to move the ARCane, considering its dimensions and weight. For the implementation of the user gait phase detection method, it is important to consider that, according to the literature, the greatest force the values obtained for the transfer of body weight of the user supported on a single tip cane were 29 kg [177] and in percentage terms it was 25% [141]. Considering these values, deformation tests were carried out for forces of 300N (≈30.6 Kg) applied on the cane handle in the vertical direction, i.e., z-axis, as illustrated in Figure 6.7(c). For both simulations, fixings were imposed on the structure geometry of the cane, namely in the plane of the base of the upper rod of the cane, so that there is an action-reaction for the applied forces in order to resemble the real context in which the upper rod of the cane always remains immobile, as it is connected to the lower rod of the cane.

Figure 6.5: Proposed strain gauge sensors configuration to obtain an axial force system, which allows detection of movement intent in both x-axis and y-axis directions.

Figure 6.6: Proposed strain gauge sensor configuration to obtain a gait phase detection sensor, which allows detecting the forces applied to the cane in the z-axis direction.

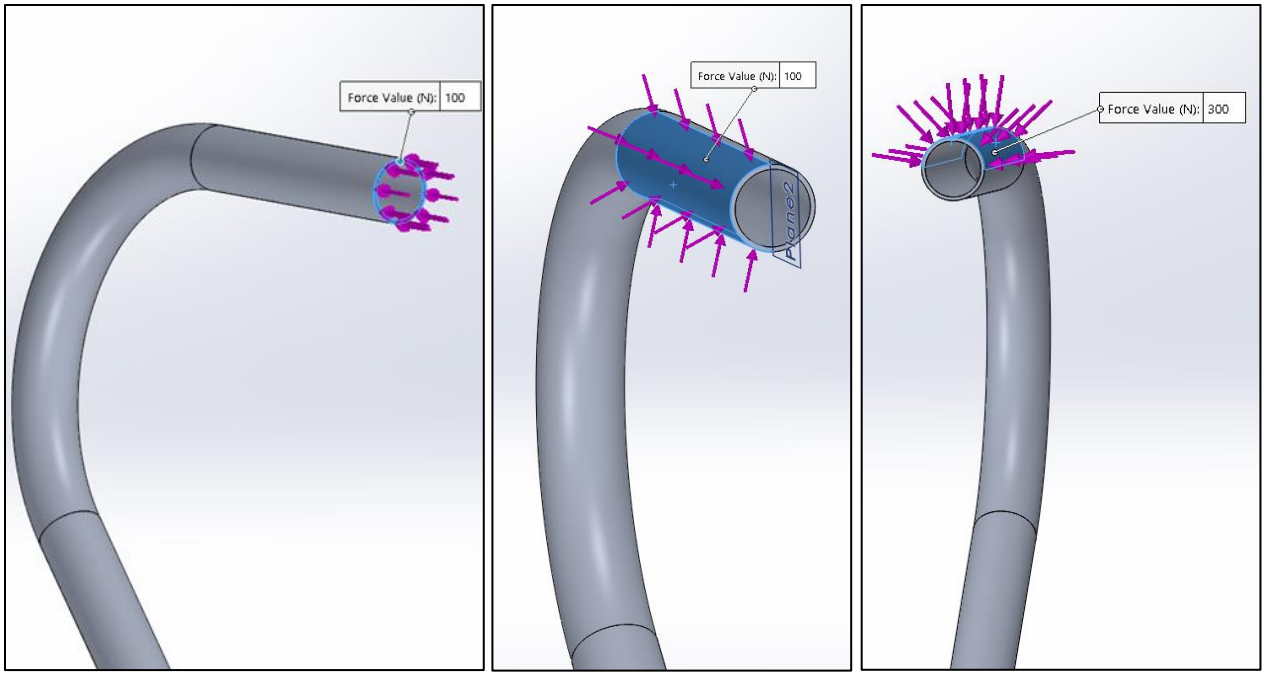

(a) (b) (c)

Figure 6.7: Applied force of (a) 100N on the cane handle in the y-axis direction; (b) 100N on the cane handle in the x-axis direction; (c) 300N on the cane handle in the z-axis direction.

6.2.2 Results

Before proceeding with the results obtained by the simulation, it is important to explain what is known as deformation. Deformation (ε) is a measure to determine the behavior of a material subjected to applied forces, representing in a concrete way the distance that the material stretches or compresses (ΔL), divided by its original distance (L), as presented in equation 6.1.

$$\varepsilon = \frac{\Delta L}{L} \tag{6.1}$$

Based on the performed simulations related to the user motion intention, it was obtained a maximum value of equivalent deformation (ε) of 9.909e-4 and 3.748e-3, at the intended location for the strain gages, for a force of 100N applied to the cane handle in the direction of the y-axis and x-axis, respectively, simulating forward and lateral movement. Regarding the gait phase detection simulations, it was obtained a maximum value of equivalent deformation (ε) of 1,590e-03 for a force of 300N applied to the cane handle in the direction of the z-axis, simulating a support gait phase. The obtained results of the equivalent deformation for both methods are represented in Figure 6.8.

It was found that the material deformation of the of the cane rod is too small to be detected by common strain gauges. The reason these equivalent strain values are not sufficient, is that a common strain gauge has a sensitivity of about ≈2.0mV/V to 1000μm/m (ε = 1*10^(-3)) deformation in a full-wheatstone-bridge configuration [174]–[176], resulting in a value of ≈7.50mV/V for the respective equivalent strain value obtained in the simulations for applied forces on the y-axis, which is the highest value obtained. This sensitivity would result in a signal too small to be feasibly detected considering the specifications of the control unit's analog ports, which have a sensitivity of ≈3.22mV, and also taking into account that the maximum equivalent strain value obtained was at a point location, rather than representing a section of considerable area as comparison to the dimensions of a strain gauge sensor.

Therefore, the use of **strain gages** was considered **unfeasible for the acquisition of interaction forces** to obtain the user's intention of movement and to recognize the user's gait phases. It was then decided to implement **FSR sensors as the sensory device of the motion control system**, as they are durable, thin, flexible, widely available and cost-effective sensors with a wide range of force sensitivity, capable of detecting the user interaction forces applied in the ARCane. All the details about the material, mesh, results, plots for the strain, and resultant displacement, regarding the present section are present in Appendix V.

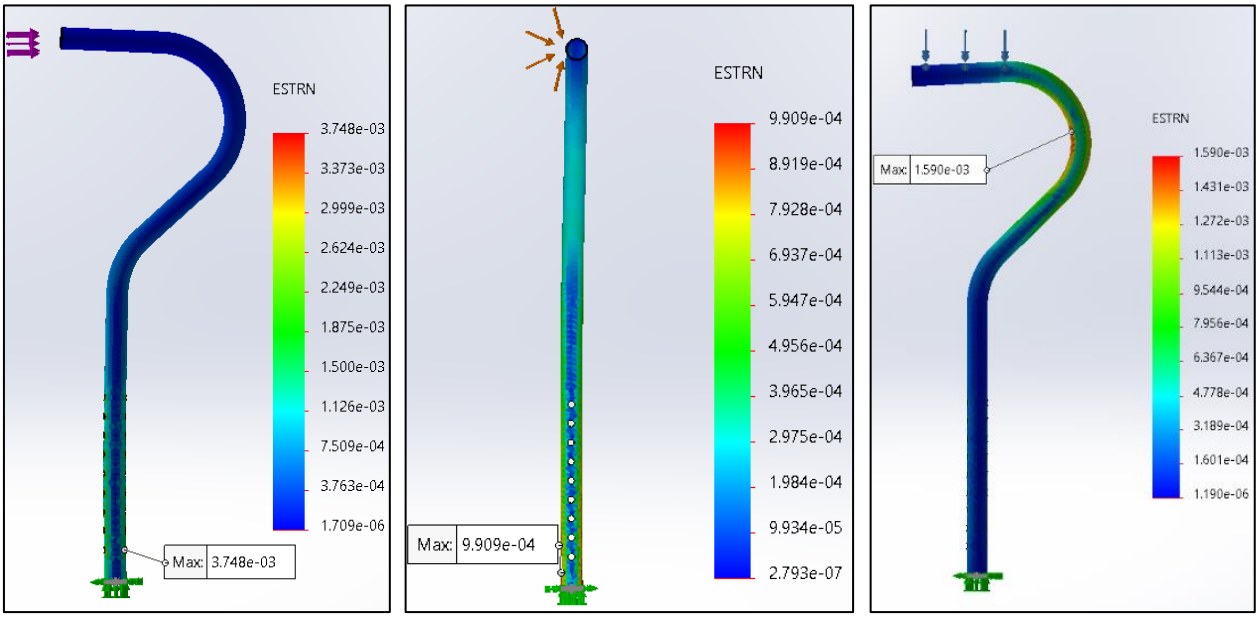

(a) (b) (c)

Figure 6.8: Equivalent deformation values obtained for applied force of (a) 100N in the direction of the y-axis; (b) 100N in the direction of the x-axis; (c) 300N in the direction of the z-axis.

6.3 User motion intention

The final solution for the ARCane axial force system is based on the combination of four force sensors located on the cane rod in a similar way to the idealized configuration for strain gages, perpendicular to the cane displacement plane, in the x-axis and y-axis directions. This solution is already presented in subsection 4.3.2, where the technical specifications and reading circuits of the sensors are described, while in this section it will be discussed ways to obtain a smaller dispersion of forces applied by the user, in order to improve the acquisition of forces by the sensors, as well as to demonstrate and explain the final configuration implemented for the axial force system in the ARCane.

It should be noted that, in a strict technical sense, force sensing resistors sense pressure, which is equal to force divided by area. This means that applying equal amounts of force with a finger, as opposed to applying the same force but with a nail, will result in a completely different resistance response. To address this difference between force and applied pressure, the sensor can be covered with a material to ensure proper force distribution that will result in more accurate readings. For example, a thin elastomer such as silicone rubber placed between the actuator and sensor can be used to absorb some error from inconsistent force distribution [112].

Thus, a 3D printing structure, nominated **axial ring** (Figure 6.9), made out of a polymer known as PLA (Polyactic Acid), is placed on top of the sensors sensitive area to obtain a better distribution of the applied forces, and also to provide stability by preventing them from moving around. In addition to the already purpose of force distribution, this axial ring, together with another 3D printing structure, nominated the **stabilizer ring** (Figure 6.10), placed in a higher position of the base rod, has the secondary function of stabilizing the upper rod of the cane, in order to reduce and mitigate unwanted and accentuated oscillations resulting from the user's interaction with the cane handle, while allowing the detection of forces applied in the direction of the cane's displacement plane.

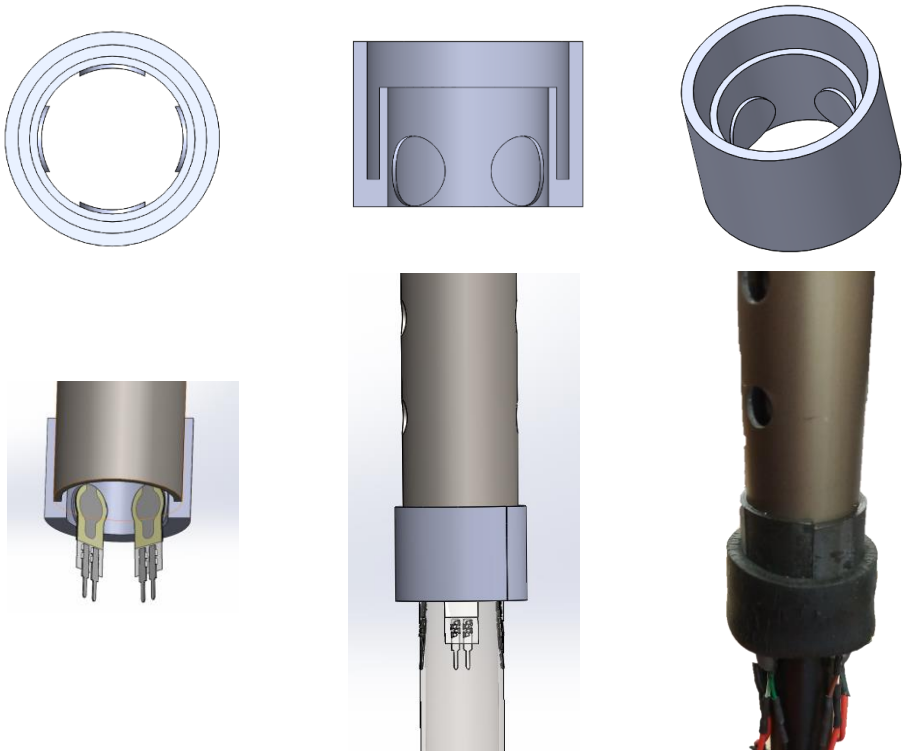

Figure 6.9: Configuration of the axial ring fixed to the upper rod of the cane with the FSR sensors; top view, sectional view and trimetric view of the axial ring in the top row, respectively.

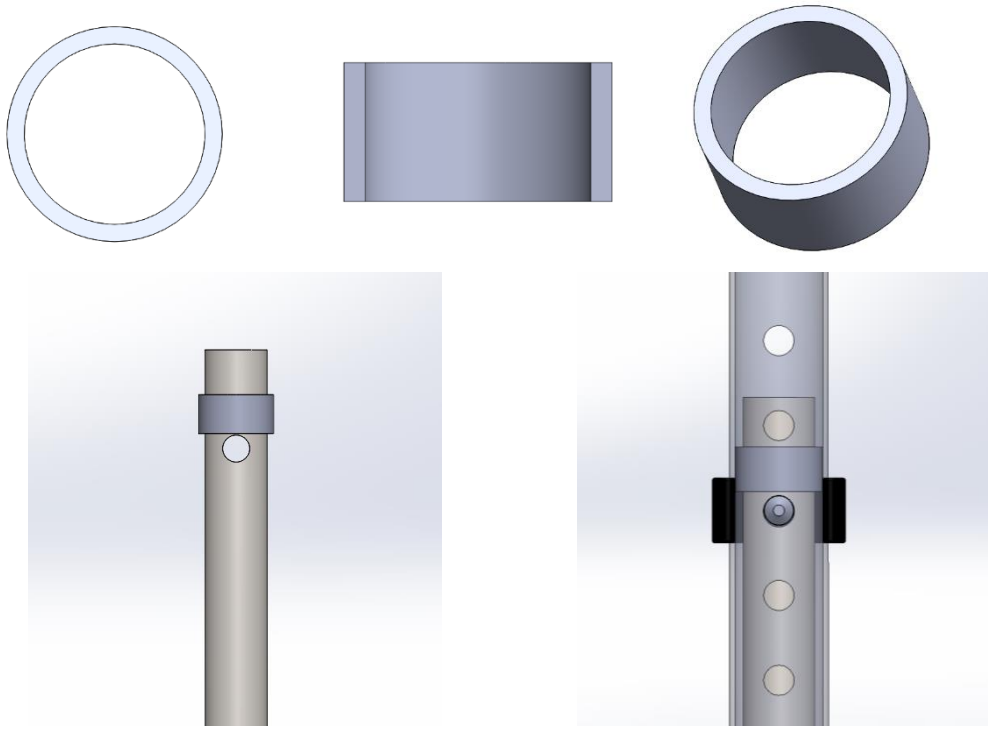

Figure 6.10: Configuration of the stabilizer ring fixed to the lower rod of the cane; top view, sectional view and trimetric view of the stabilizer ring on the top row, respectively.

With the FSR sensors, the stabilizer ring and the axial ring inserted into the cane, as illustrated in Figure 6.11, it is then possible to obtain the user's movement intention. As already mentioned, in addition to the stabilizer ring acting as a stabilizer for the cane rod, it also allows transferring the forces applied by the user to the FSR force sensors, acting as the basis of a first class lever system. A representation of the interaction of forces present in the cane and a demonstration of the analogy of the system with a lever are illustrated in Figure 6.12.

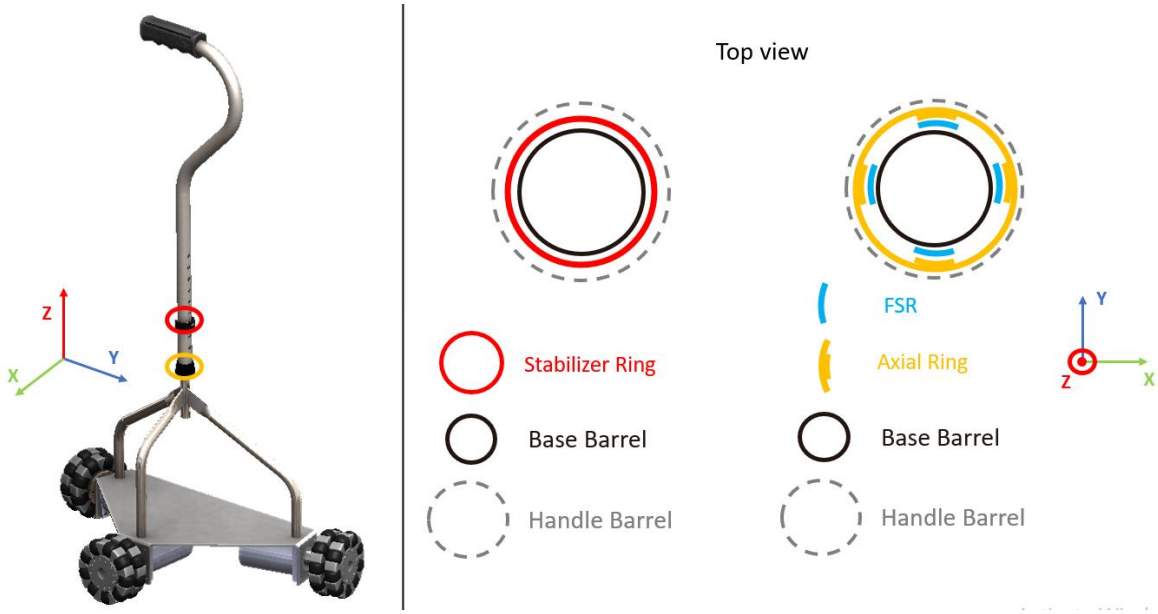

Figure 6.11: Location and top view of the axial and the stabilizer ring inserted into the cane.

This lever model is based on the mathematical equation 6.2, which relates the forces applied by the user to the forces felt by the FSR, through Newton's third law, related to the system conservation of torque and angular momentum, and the fact that for an action force there is reaction force, which can be represented by the rate of change of the angular momentum:

$$F_1 * cos(\theta_1) * D_1 = F_2 * cos(\theta_2) * D_2 \quad (6.2)$$

Considering that θ_1 and θ_2 are zero, and that D=D1+D2=0.55 m, equation 6.2 can be simplified into equation 6.3 and later to equation 6.4:

$$F_1 * D_1 = F_2 * D_2 \quad (6.3)$$

$$F_2 = F_1 * \frac{D_1}{D - D_1} \quad (6.4)$$

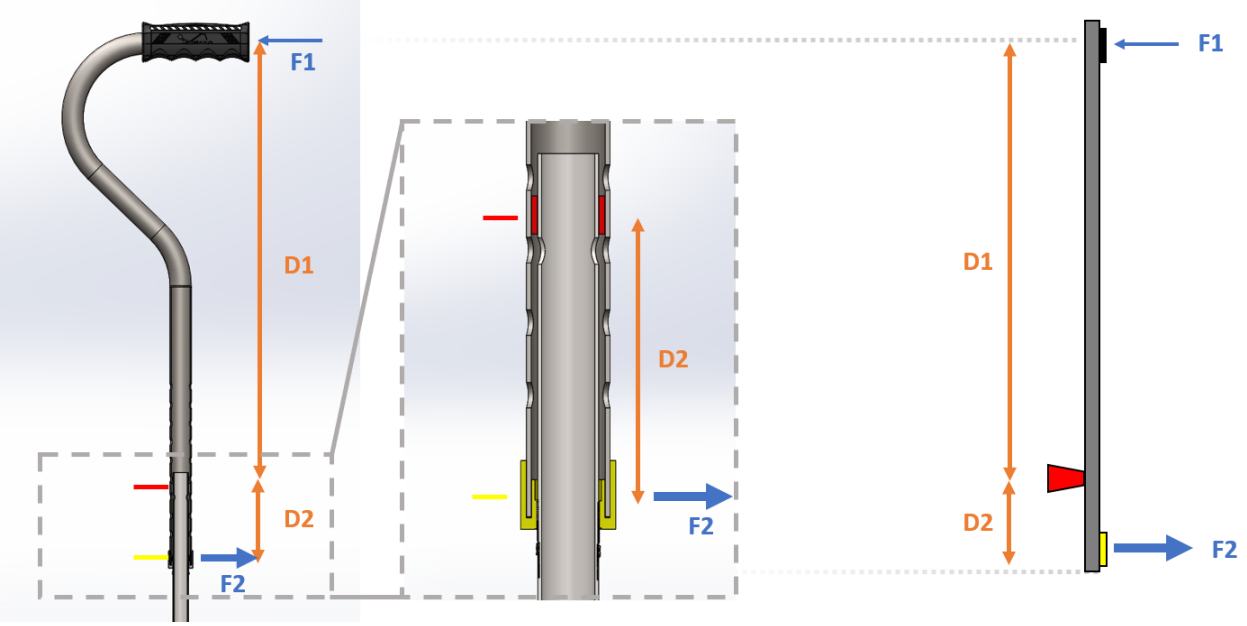

(a) (b)

Figure 6.12: (a) Cross-sectional view of the ARCane main body structure with the axial ring (yellow) and the stabilizer ring (red) implemented, and the interaction of the forces applied in the handle by the user, with the resultant force in the force sensors. (b) Analogy of the force detection system applied to the cane handle to a first-class lever model.

The value D1 can vary, as the height of the cane can be adjusted. By taking as a reference the the average height from the range of heights that the cane can have, the value of D1 becomes 0.43 m, and by taking 10N as the value of F_1, it is obtained the final equation 6.5:

$$F_2 = 3.58 * F_1 \tag{6.5}$$

This relation and the values represented in it are not as linear as they should for the real context, as there are several variables to be taken into account, such as the dissipation of forces along the cane rod, mainly along D1; the contact surface between the cane rod and the stabilizer ring is not punctual, therefore it influences the leverage effect that transfers the user's forces to the force sensors; and the fact that the values of F_1 and D_1 vary from person to person due to their strength and height. These factors are difficult to be determined analytically, however, the result obtained in equation 6.5 provides an idea of the operation of the axial force detection system to acquire movement intention, by relating the force applied by the user to the force actuated on the sensors. It also makes it possible to have an idea of the magnitude of the forces to be applied to the FSR sensors, thus facilitating the choice of the resistance to be placed in the reading circuit of the force sensors, taking into account the linearity of force-tension regression demonstrated

previously in Figure 4.7. The user's movement intention can then be classified in a primary phase as "front", "back", "left" and "right", from the relation of the force components obtained by the FSR sensors, represented by equation 6.6 and as illustrated in Figure 6.13.

$$\begin{cases} F_X = F_B - F_D \\ F_Y = F_A - F_C \end{cases} \tag{6.6}$$

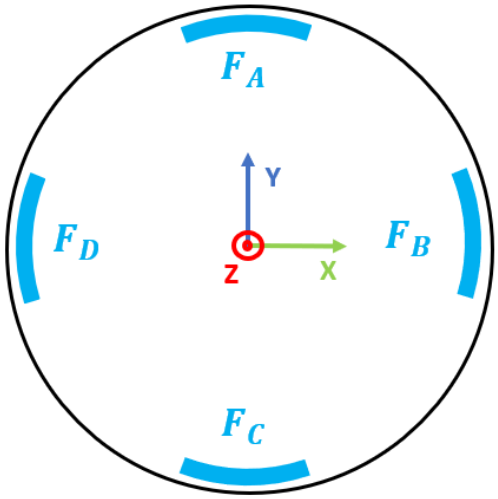

Figure 6.13: Components of forces obtained by FSR sensors on the axial ring.

6.4 Gait phase detection

The proposed solution to obtain the haptic sensing system was then determined, presented superficially in subsection 4.3.1, through the combination of three FSR sensors, equidistant from each other, located on the ARCane handle, as it is the location that is subjected to the user direct forces. This configuration is able to acquire the interaction forces between the user and the ARCane, more specifically the forces applied vertically, in order to detect when the user supports his body weight on the cane and recognize the user gait phase. Taking as a reference the fact that the maximum body support weight to be applied to the cane is approximately 25% of the person's body weight and can reach 30Kg, this value being for forces applied in the vertical direction, it was possible to define the resistance to be used in the reading circuit of FSR sensors, to acquire detectable data between 0-300N.

With the same purpose of the axial force sensors mentioned before, a 3D printed PLA polymer structure, must be placed over the sensors, covering the handle, in order to improve the distribution of the applied forces, as shown in Figure 6.14 and in Figure 6.15. In addition, it is also important to note that the

PLA material is biocompatible, meaning that it is not toxic or harmful to the human skin; the 3D printed structure has the same geometric structure as the handle, maintaining its ergonomics; and that the width and height of the cane handle remains within the range of values shown in Table 3.3 of the cane technical specifications. A visual representation of the force sensors, along with the structure that covers the contact area of the sensors for better distribution of applied force at the cane handle, is portrayed in Figure 6.16.

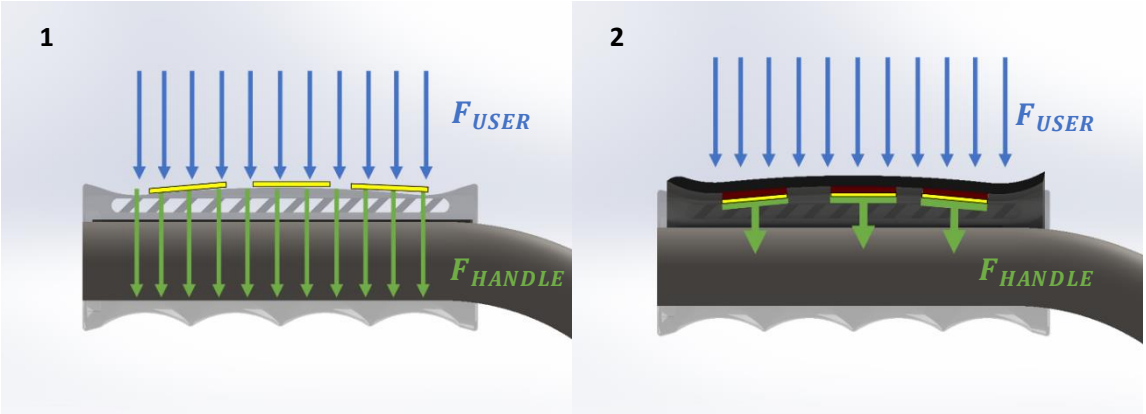

Figure 6.14: Demonstration of the force distribution on the FSR sensors and cane handle, with and without the polymer structure. Blue - force applied by the user; Green - force applied on the handle; Yellow - force sensors FSR; Black and red – 3D printed polymer structure.

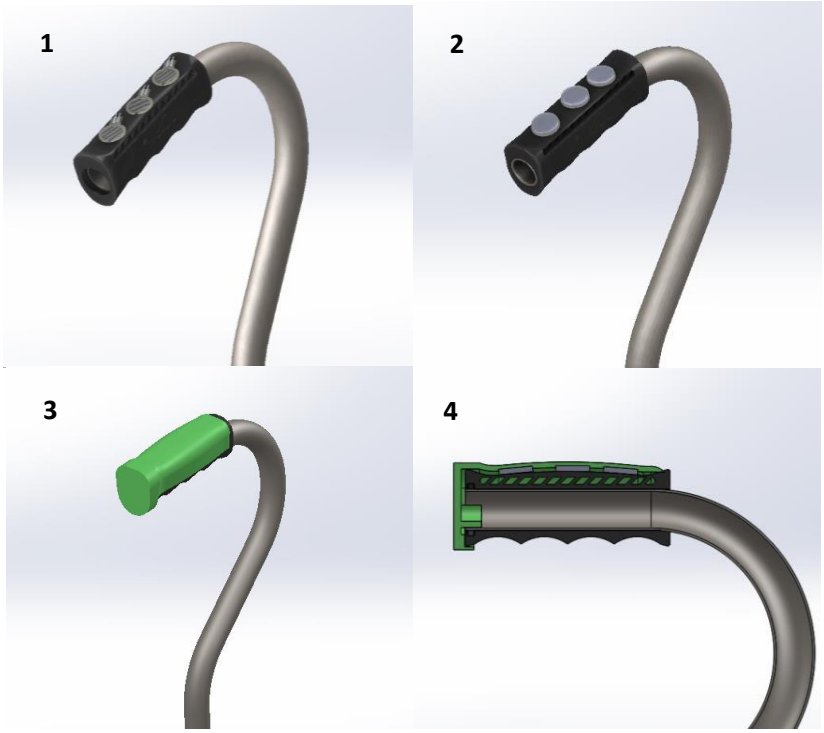

Figure 6.15: Visual 3D model representation of the FSR sensors with the 3D printed structure (represented in green and grey) placed on top of the handle for improved force distribution. 1, 2, 3 – trimetric view; 4 - cross-section view.

Figure 6.16: Visual representation of the 3D structure with the insertion of the three haptic force sensors with its implementation in the ARCane handle.

6.5 Holonomic base movement control

The ARCane base seeks to provide stability and support to the cane-user system. With the insertion of three omnidirectional wheels, it becomes a holonomic base, capable of moving in any direction without changing orientation, and also capable of changing to any desired orientation while in motion. This configuration gives the ARCane the ability to easily maneuver in tight, restricted spaces, achieving high maneuverability while maintaining robust stability.

The same way that with the implementation of the axial force system it is possible to obtain the user's movement intention by detecting the forces applied by the FSR in the x- axis and y-axis directions, obtaining Fx and Fy respectively, it is now necessary to implement a way to **transform these interaction forces into the movement of the cane**. This process is known as direct kinematics, and it is based on the use of kinematic equations that decipher the rotation speed that each motor must have, considering the disposition of each motor and the direction of the applied force, causing the displacement of the cane in the direction intended by the user. As a first step to obtain the cane kinematic equations, it is necessary to have a well-defined reference axis to obtain the locations of each motor in relation to each other through a common point. For reasons of calculation simplification, the origin of the axis of the Cartesian coordinate system was defined at the center of mass of the cane, with the y-axis pointing in the direction of the user's sagittal axis (i.e., in the direction of forward motion), and the x-axis pointing in the direction of the user's transverse axis (i.e., in the direction of motion to the right). This Cartesian referential together with the arrangement of the

base of the cane and the configuration of the wheels plus motors is represented in Figure 6.17(a) with the respective numbering, to help define the kinematic calculations. Thus, it is now possible to define the angles that each motor makes in relation to the x-axis, obtaining α, β and ϒ, for motors 1, 2 and 3 respectively. Having acquired the angles of each motor, it is necessary to take into account that the rotation of the engines will cause translational movement of the wheels in a perpendicular direction. Thus, it can be defined the angle that corresponds to the direction of movement of each wheel as θ_1, θ_2 and θ_3, perpendicular to α, β and ϒ, corresponding to equation 6.7:

$$\begin{cases} \theta_1 = \alpha + 90° \\ \theta_2 = \beta + 90° \\ \theta_3 = \Upsilon + 90° \end{cases} \tag{6.7}$$

As this configuration guarantees a total of 3 DOF, it is possible to **define a force for each degree of freedom**, corresponding to a force acting in the x-axis direction (F_X), in the y-axis direction (F_Y) and the rotation direction of the cane around the vertical axis (F_W), which corresponds to Yall. It is then possible to represent how much the cane will move in each DOF, depending on the contribution that each motor has in the respective direction of movement, through equation 6.8.

$$\begin{cases} F_X = cos(\theta_1) \cdot motor_1 + cos(\theta_2) \cdot motor_2 + cos(\theta_3) \cdot motor_3 \\ F_Y = sen(\theta_1) \cdot motor_1 + sen(\theta_2) \cdot motor_2 + sen(\theta_3) \cdot motor_3 \\ F_W = motor_1 + motor_2 + motor_3 \end{cases} \tag{6.8}$$

We can now transform this system of equations into matrix equations, as represented by equation 6.9, to obtain $F = A * M$, where F represents the components of forces, A represents the contribution that each wheel has in each direction of the 3 DOF, and M represents the contributions that each cane motor has, in order to carry out the movement that corresponds to the respective force components.

$$\begin{bmatrix} F_x \\ F_y \\ F_w \end{bmatrix} = \begin{bmatrix} cos(\theta_1) & cos(\theta_2) & cos(\theta_3) \\ sen(\theta_1) & sen(\theta_2) & sen(\theta_3) \\ 1 & 1 & 1 \end{bmatrix} \begin{bmatrix} motor_1 \\ motor_2 \\ motor_3 \end{bmatrix} \tag{6.9}$$

F A M

With this equation, it allows us to know how much the cane will move in the x, y and w direction for a given speed defined for each motor. However, it is intended to know what is the contribution (ie speed) that each motor must have, with a given direction in which the cane must move. To do this, we must solve the matrix equation as a function of M, and one way to isolate this term in equation 6.9 would be to multiply

on both sides of the equation the inverse matrix of A, which corresponds to A^{-1}, as demonstrated in equations 6.10 and 6.11.

$$A^{-1} * F = A^{-1} * A * M \tag{6.10}$$

$$A^{-1} * F = I_3 * M \tag{6.11}$$

with I_3 representing a 3x3 identity matrix, results in equation 6.12.:

$$M = A^{-1} * F \tag{6.12}$$

With this final equation, we obtain the direct kinematics of the cane system. Therefore, after obtaining the forces detected by the axial force system, and determining the user's intended movement direction, the parameters of the cane movement (F_X, F_Y, F_W) are defined. Then, through the kinematic equation obtained, it is determined the contribution that each motor must have to achieve the desired movement. It is demonstrated in Figure 6.17(b) together with Table 6.1, a force simulation set applied to the ARCane, and the respective results of the contribution of each motor, in order to obtain the displacement of the cane in the direction of the applied force, for values of α =240°, β=0° and Υ=120° for the ARCane wheels.

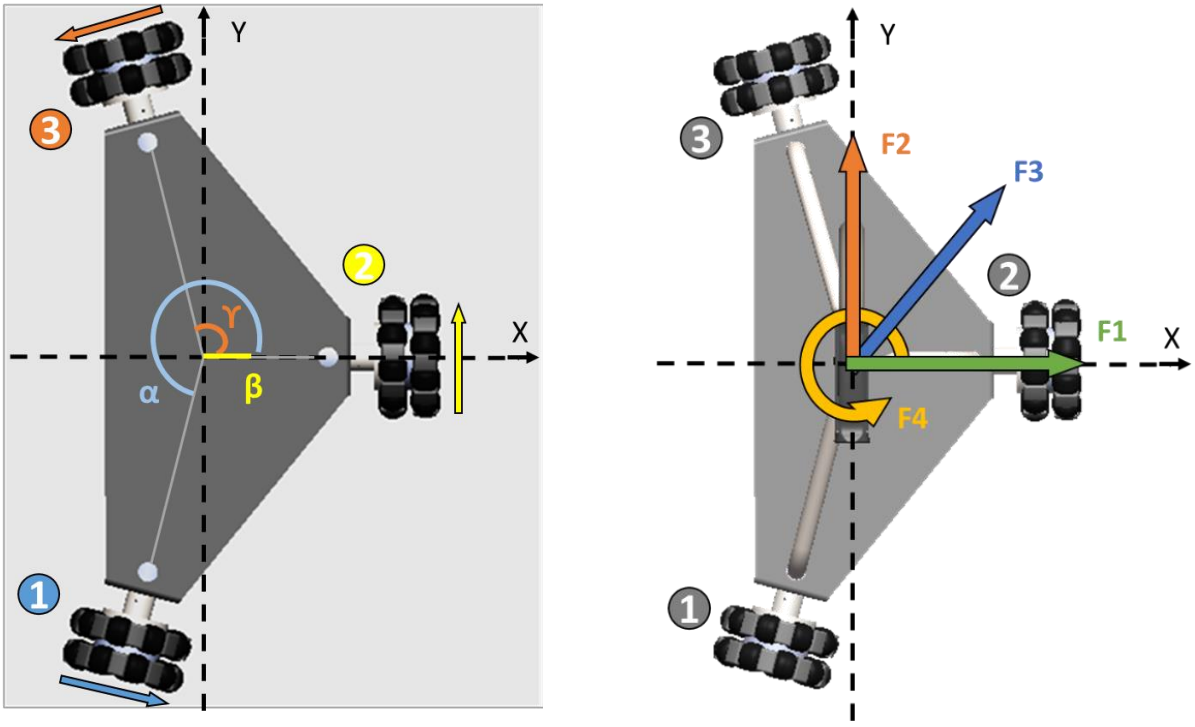

(a) (b)

Figure 6.17: (a) ARCane base with the Cartesian frame of reference located at the cane center-of-mass. (b) Simulation of forces that can be interpreted by the kinematic equations to carry out the movement of the cane in the respective directions.

Table 6.1: Results of the contribution of each engine, in relation to the forces applied to the cane as shown in Figure 6.17(b)

[Fx, Fy, Fw]	M1	M2	M3
F1 (1,0,0)	0.58	0	-0.58
F2 (0,1,0)	-0.33	0.67	-0.33
F3 (1,1,0)	0.24	0.67	-0.91
F4 (0,0,1)	0.33	0.33	0.33

6.6 Experimental validation

Experimental tests were carried out, with the objective of validating the proposed motion control method. A total of six healthy subjects aged between 22 and 27, with body weight between 48kg and 95kg, and with body height between 1.51m and 1.82m, participated in these tests. The tests were performed with the intention of verifying the functioning of the motion control strategy with different users, by analyzing if it can detect the participants' movement intention and recognize the gait phase while using the ARCane. Initially, it will be addressed the methods used during the experimental validation, by mentioning the instructions given to each participant and how to proceed in each phase of the tests. Finally, it will be demonstrated the obtained results related to the sensory data acquisition, along with the participants feedback on the motion control strategy implemented in the ARCane.

6.6.1 Methods

The first stage is dedicated to the user motion intention and aims to verify if the cane could detect the user's intention to move, using the axial force system implemented in the cane, as exemplified in Figure 6.18. Tests were performed only for forward direction as it was the most important in a first phase of testing. Regarding the intention of movement in the lateral directions, data were not acquired, because in this initial phase of the experimental tests with this ARCane prototype, it is intended that the participants focus on the movement in the forward direction, in order to simulate the gait with the gait phases shown in Figure 6.1. Thus, with the cane immobilized, a brief explanation was given on how the cane's axial force system works,

and later the participant was asked to simulate an intention to move forward. Initially, the values acquired by the force sensors were recorded in order to readjust the threshold values to correspond to the person's strength and desired sensitivity. Then, the results acquired by the sensors were recorded in order to verify if they corresponded to the participant intention to move, with this action being repeated 10 times per participant.

The second stage of the experimental tests is related to the detection of the forces applied by the user in the vertical direction with the haptic sensing system. These vertical forces were differentiated into three categories: “no touch”, which represents the absence of forces applied to the cane; “light touch”, which intends to inform when the user has his hand resting on the cane; and “support phase” which represents when the user is supporting their body weight on the cane. A demonstration of the detectable force types by the haptic sensing system is illustrated in Figure 6.19. Again, with the cane immobilized, a brief explanation was given about the types of force detectable by the cane and then the participant was asked to simulate each of the three detectable force categories so that sensory data was collected to define the threshold values for each strength categories, depending on the weight and structure of the user. Finally, the participant was randomly assigned to apply one of three types of force settings, where the results acquired by the sensors were later checked to see if they matched the action performed. This procedure was repeated until a total of 20 results per person.

Lastly, once the participant was minimally adapted to the cane movement control, he was instructed to walk freely, and also to simulate walking with an injured leg for a total of 6 minutes, a standard duration widely used in training. of walking [44]. During this time, sensory information was acquired from the haptic detection system and the axial force system related to each participant. At the end of the experimental tests, a small questionnaire was carried out to the participants regarding the operability of the cane. The questions asked to the participants sought to know: (i) if the ARCane is considered lightweight and easy to maneuver; (ii) if the preparation procedures to start the ARCane, were considered an easy procedure; (iii) what is the level of psychological fatigue it was felt after using the system on a scale of 1 to 5; and if (iv) the participants considered that the system has adequate dimensions and that it does not restrict movement during gait.

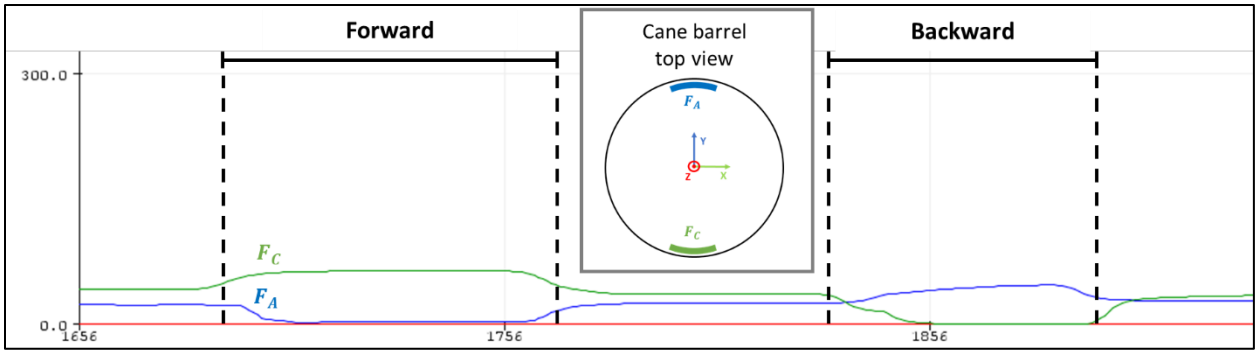

Figure 6.18: Data acquisition by the axial force sensors with force applied in the y-axis direction, when a participant was asked to move in the forward direction and in the backwards direction.

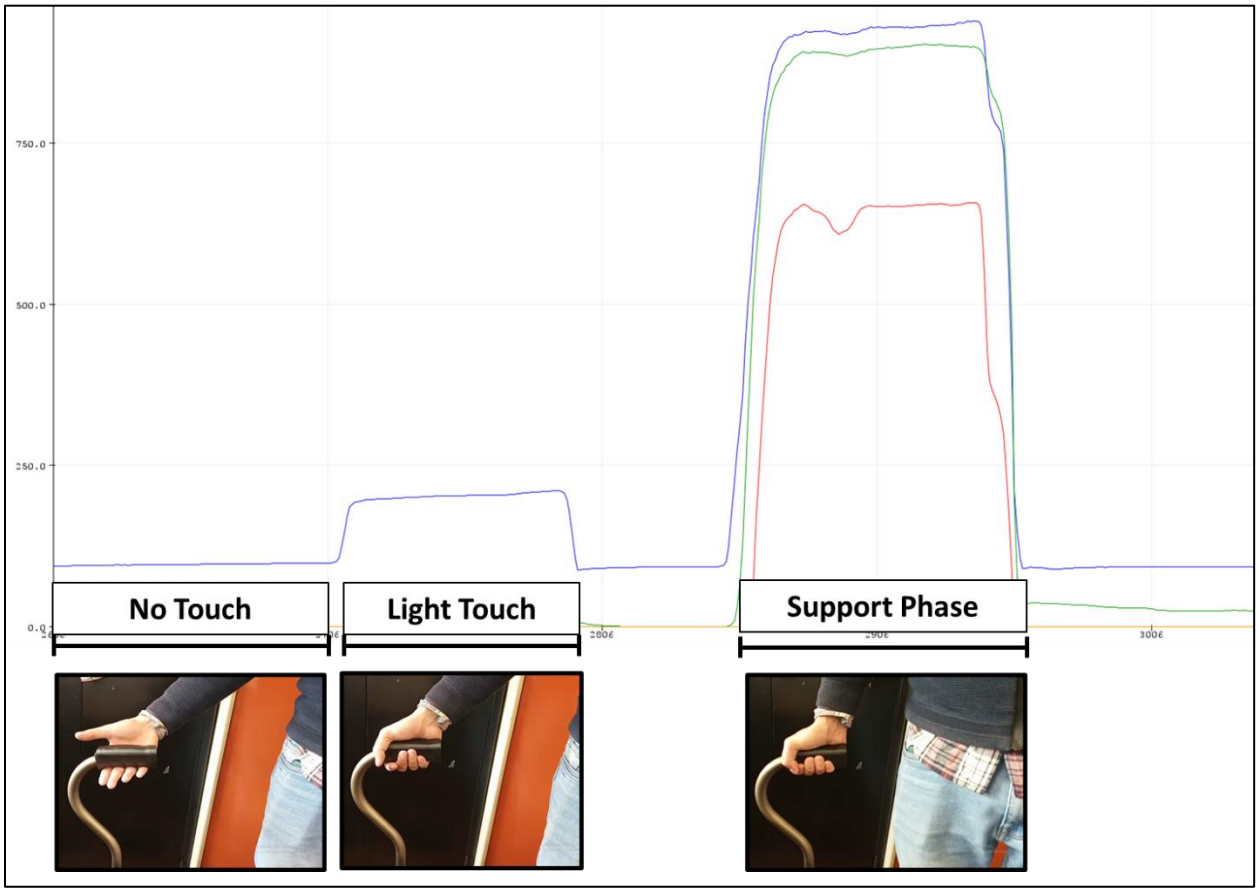

Figure 6.19: Data acquisition by the haptic sensing system with force applied in the z-axis direction, when a participant was asked to: stand still, place his hand on the handle, and to lean its weight on the cane.

6.6.2 Results

It was finally obtained as the results for the detection of the user's motion intention with the implemented axial force system, a total of 58 correct results were obtained in a total of 60 tests performed, achieving an accuracy of 97% for the axial force system. Regarding the user's gait phase recognition with the implemented haptic sensing system, a total of 81 correct results were obtained in a total of 90 tests performed, achieving an accuracy of 90% for the haptic detection system. It is listed below in Table 6.2 the obtained experimental results of the axial force system and the haptic detection system referring to the detection of motion intention and gait phase recognition, respectively.

Table 6.2: Experimental results obtained from the axial force system and haptic detection system

	Axial force system	**Haptic sensing system**		
Participant nº	Forward intention (n/10)	No touch (n/5)	Light touch (n/5)	Support phase (n/5)
1	9	5	5	5
2	10	4	4	5
3	10	3	4	5
4	9	3	5	5
5	10	5	5	5
6	10	4	4	5
Success/Total	58/60	81/90		
Accuracy	0.97	0.9		

The experimental results referring to when the participant was instructed to walk freely, and also to simulate gait with an injured leg, seek to provide the participants a better idea and understanding of how the implemented motion control strategy actually works, with ARCane in motion. It also presents an overview of the ARCane's features and capabilities as well as its use in a real-life context. It is represented in Figure 6.20 the acquisition of data by the sensory components while a participant was asked to move in the forward direction, by simulating the gait with an impaired leg. Additional data related to the results obtained with the experimental validation, are presented in Appendix V.

At the end of the experimental tests, a small questionnaire was carried out to the participants about the operability of the cane, obtaining the following results: (i) all participants consider that the device is lightweight and easy to maneuver; (ii) the preparation procedures, which coincide with pressing the switch button, were considered an easy procedure by all users; (iii) all users rated the level of psychological fatigue they feel after using the system < 2 on a scale of 1 to 5; (iv) all participants considered that the system has

adequate dimensions and that it does not restrict movement during gait. It was also mentioned that the system has good sensitivity and is comfortable in terms of usability.

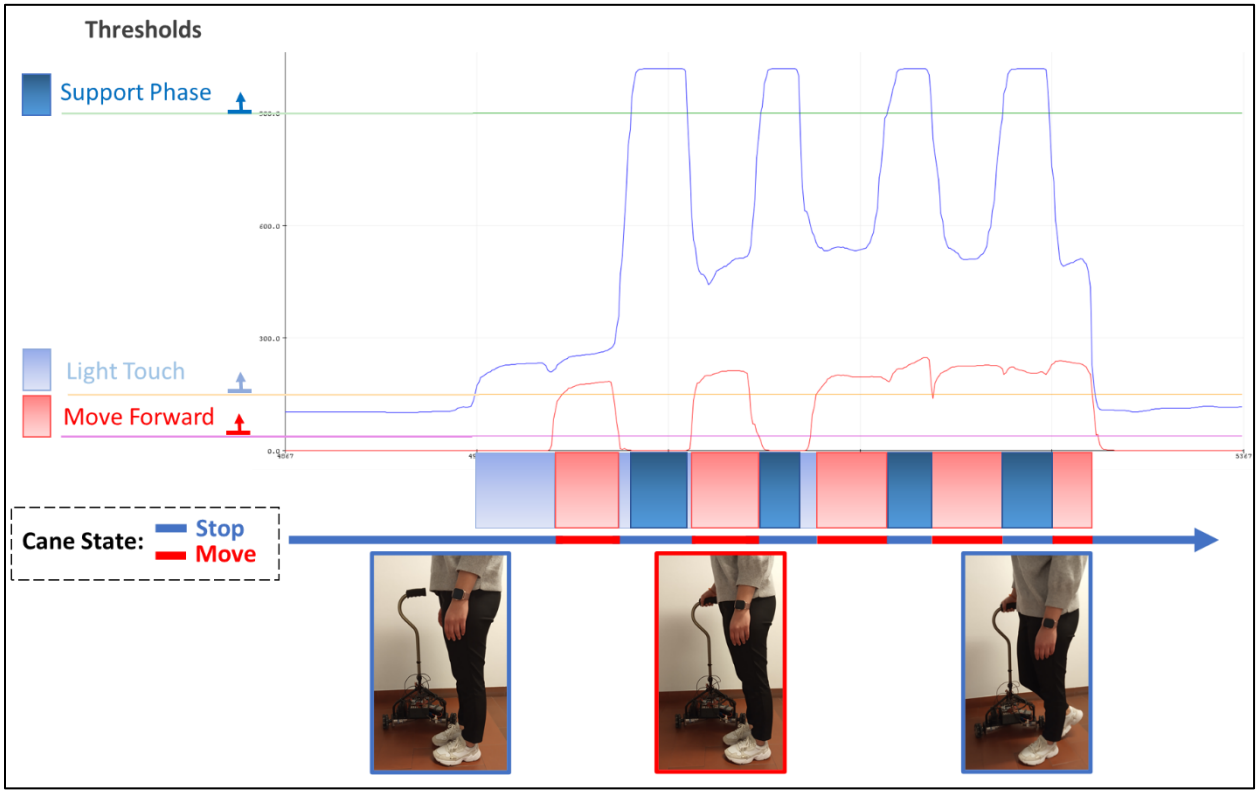

Figure 6.20: Data acquisition by the haptic sensing system and the axial force sensors while a user was asked to move in the forward direction, while simulating a two-point gait with an impaired leg. Detection of the user intended direction and gait phase detection.

During the experimental tests, it was possible to obtain a critical opinion of the ARCane in a real context environment, which made it possible to verify future improvements for the ARCane system, namely: (i) to place the power button in a higher position, located relatively close to the cane handle, for easier and quicker access; (ii) to implement a control strategy on the motors to obtain a smoother and more controlled movement; and finally, (iii) take take into account the person's stride length, in order to adjust the speed of the cane to the user's walking speed.

6.7 Discussion

This chapter started with the identification of the admittance control as the motion control method to be incorporated into the ARCane, from a comparison between the methods applied in the robotic canes review literature, since it proved to be the most compatible considering the structure and the components that make up the developed ARCane. It was then possible to define a strategy for the control of the ARCane that is based on the four gait phases with a cane: standing phase, cane swing phase, healthy leg stance phase, and support phase of the affected leg. The ARCane must then detect the user's intention to move, in order to drive in the desired direction and follow his gait, as well as interpret the user's gait phase, in so that it remains immobile when greater body weight is applied to the cane, providing a stable support to the user.

Afterwards, it was presented a solution to obtain: the user's movement intention, based on force sensors located on the ARCcane rod; and also, the detection of the user's gait phase, based on force sensors located on the ARCane handle. These settings provide detailed detection of user interaction with the ARCane, by detecting forces applied in the x-axis, y-axis, and z-axis. Since piezoresistive force sensors were used, which more adequately detect the pressure, structures in PLA material were developed through 3D printing, in order to obtain a better distribution of the applied load and more reliable force measurements acquired by the FSR sensors.

Finally, operability tests were performed with six healthy participants, in order to obtain a validation of the implemented motion control system, verifying the feasibility of the proposed solutions and analyzing the use and behavior of the ARCane in experimental context to assess the potential for acceptance of this device by future users. The main results obtained from the experimental tests were an accuracy of 97% for user movement intention recognition and 90% accuracy for user gait phase recognition.

7 Towards Fall Detection and Prevention Strategy

In addition to the actual ARCane assistance in the user's gait through the built-in motion control system, that ensures greater user stability, better cane maneuverability, and an effective cane-user interaction, it is also of great importance to achieve a fall detection and prevention system. These systems aim to ensure user safety, with the objective of reducing their rate of falls. All this will be possible through detection and actuation mechanisms, and later calculations and evaluations processed in the high-level CU. Thus, the ARCane will be able to obtain a sufficiently fast response to complement the user's reaction time, guaranteeing a successful fall prevention strategy.

7.1 Fall detection

Falls are among the most damaging events that older people can experience, and they can happen suddenly and without warning in all types of contexts and environments. With the increasing aging of the population, fall detection technology is becoming an invaluable resource that saves lives, leading to an urgent need for the development of fall detection systems. For falls to be detected and predicted, it is necessary to use several sensory devices to obtain information and continuous assessments about the user while walking and using the cane. Then, various parameters are taken into account, being later analyzed and processed by the high-level control system, using computational methods that ultimately allow the user to accurately identify the user's gait state and detect if a fall is occurring.

Fall detection can be generally classified as **pre-impact detection** and **post-fall detection** [145]. Post-fall detection methods are based on sending an emergency alert signal to the emergencies in case a fall is detected, thus reducing the time of arrival of medical assistance. However, this type of fall detection can only detect falls after impact, so all injuries (physical and psychological) caused directly by the impact of the fall cannot be prevented or even diminished. Pre-impact detection uses predictive methods that seek to predict fall incidents before or during their occurrence, allowing immediate prevention actions, as in the case of airbag activation during an automobile accident, in order to prevent physical accidents caused by the impact.

Considering that certain falls can cause damage to health, or even fatalities, it is of great importance that fall detection systems can operate in (almost) real time, with high computational efficiency. Since real time is a key characteristic for fall detection systems, it is necessary to consider the fall detection time,

depending on the computational method and detection instruments used, so that it is fast enough, allowing a time window to activate the fall prevention system.

A **fall event can be divided into four distinct phases** (Figure 7.1): (i) pre-fall phase, when normal activities of the daily living occur; (ii) critical phase, when the fall event happens; (iii) post-fall, when the person has no movement, lying on the ground; and (iv) recovery phase, when the person stands up and shows movement [146], [147]. The **critical phase** is where this section will take his focus since it represents the window time to detect and prevent falls. During the critical phase there is a temporary period of free fall during which the vertical speed increases linearly with time due to gravitational acceleration, and its duration can be estimated to be around 300-500 ms [148] and 900 ms [145].

Lead time and detection time are typically used to assess the efficiency of fall detection. Detection time represents the time difference between the fall initiation and the fall detection, and is used to indicate how quickly the fall detection system responds to a fall. On the other hand, the lead time is defined by the time interval between when the fall is detected and the fall impact, accounting for the time for protective measures to be activated to protect fall victims from the impacts of the fall. In short, the smaller the detection time and the longer the lead time, the better the fall detection performance.

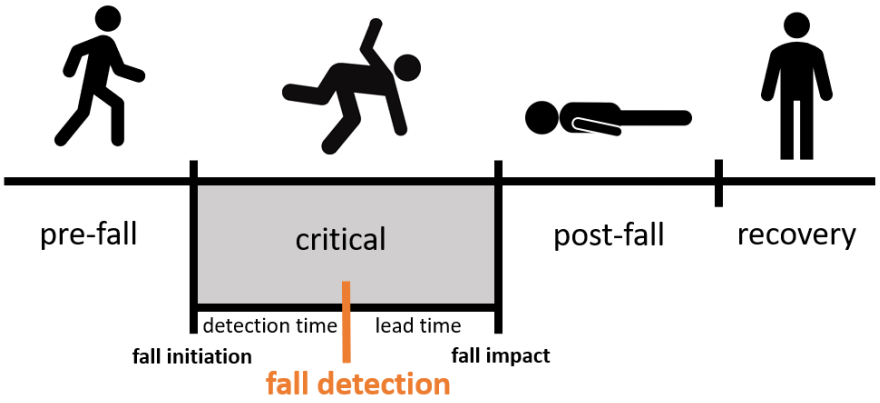

Figure 7.1: The main phases of a fall event.

7.1.1 Fall detection algorithms

Currently, computing power is technologically developed to the point that its processing time scale allows the performance of mathematical and analytical calculations, through computational algorithms, within the time window for detecting and preventing a fall, i.e., the critical phase. According to the literature,

threshold-based and data-driven algorithms, including machine learning and deep learning, have been the two main approaches used for fall detection [110], [145], [147], [148].

With the application of threshold-based algorithms, a fall is considered to be detected if the selected fall detection indicators are beyond pre-defined threshold values established empirically. The algorithms are computationally efficient which allows them to be easily implemented in real-time applications. However, setting an appropriate threshold can be challenging. Typically, with a threshold too low, the system may detect negative events (i.e., false positive), resulting in less misdetection but more false alarms. Whereas with a threshold too high, the system may not detect positive events (i.e., false negative), leading to fewer false alarms but more misdetection of falls [145]. This threshold value is also dependent on the subject-to-subject variability. To overcome this difficulty, a learning period may be used, by asking the user to carry out a series of voluntary movements in order to mark the reference values of execution [148].

The method of predicting falls using a threshold is inconsistent depending on the types of fall situations, age, physical characteristics and so on. To overcome this limitation, machine learning models seek to increase the accuracy of pre-impact fall detection based on various experimental data for training [147]. A training period is required to collect data during non-fall activities to facilitate resource extraction and activity classification. Overall, data-driven algorithms are more computation-intensive compared to threshold-based algorithms and therefore may lead to a longer detection time. On the other hand, data-driven algorithms can achieve greater accuracy in event recognition, leading to fewer false alarms compared to threshold-based algorithms. The evaluation of these results can be defined by the **quality criteria of the fall detectors**, represented by the sensitivity, which measures the rate of correctly detected falls, and the specificity, measures the rate of falls correctly classified situations of non-fall. In short, the higher the sensitivity and the specificity of the system, the optimal the system performance [148], [149].

According to the literature, the **parameters of the fall detection methods applied** vary depending on the framework and application of each detection system. Such variables involve different: (i) s**patial contexts,** whether falls are in an enclosed or open space; (ii) types of users, targeted at a certain age group, physical condition and/or health status; (iii) detection times, detection in real time or not (pre-impact detection or post-fall detection); (iv) types of instrumentation, wearable or context-aware systems; and (v) computational algorithms, like threshold-based algorithms, but also machine learning techniques such as Support Vector Machine (SVM), Hidden Markov Model (HMM), Discriminant Model (DM) and deep learning techniques,

comprising Convolutional Neural Networks (CNN), Long Short-Term Memory (LSTM), Recurrent Neural Networks (RNN), and so on.

As an example, FallDeFi [150] is a non-wearable indoor fall detection system that uses commodity WiFi devices as the physical fall monitoring infrastructure. In practical terms we can evaluate the variables of this detection method as: (i) spatial context destined to a closed space; (ii) proposed use for all types of users; (iii) with post-fall detection, i.e., detection time after impact; (iv) detection tools based on context-aware systems; and (v) machine learning techniques, more specifically a SVM classifier trained to classify the gait state. On the other hand, Tamura et al. [151] designed a system that integrated the fall detection algorithm with an inflatable wearable airbag system to protect falls from body-ground impact. If we evaluate this system considering the parameters described above, we can classify it with: (i) spatial context intended for an open or closed space; (ii) mainly intended for elderly people; (iii) with pre-fall detection, i.e., detection time before impact; (iv) wearable-based detection instruments; and (v) uses thresholding technique as fall detection algorithm.

This comparison served to demonstrate the multiplicity of variables that involve the detection of falls in several studies, applications and commercial devices. Therefore, the present work focused its study, takin as a reference, the fall detection systems presented in subsection 2.2.5, as a way to obtain a more oriented and objective solution for the ARCane's fall detection system. It was shown in Chapter 2 that 50% of the robotic canes under review contained a fall detection system, featuring various fall detection methods used, such as Zero Moment Point (ZMP), Leg-motion-based detection, Human-robot coordination stability (HRCS) and Cane balance-stability. A critical analysis of these methods will be carried out, with the intention of finding a **fall detection system applied to robotic canes** that corresponds to the intended fall detection parameters to be placed in the ARCane.

One of the advantages of the **Zero moment point** (ZMP) method is that it takes into account the cane-user system, allowing a configuration that seeks to maintain the stability of both during the entire time of use. This method also has a fall detection time of 350 ms, which is within the critical phase time window. Although the ZMP presents itself as a viable option for a fall detection method, it has a disadvantage as it requires the mandatory use of wearable sensors, i.e., shoes with built-in force sensors, to measure the forces applied by each lower limb in the ground, in order to obtain the point of center-of-pressure.

The **Human-robot coordination stability** is a method that has similarities with the ZMP method in the way that both robot and user stability are considered, which makes it more reliable and convenient to

measure the stability of the human-robot system. However, as for the ZMP method, in order to obtain the stability constraints for the user, posture measurements are needed, such as the angle between the body and the ground, which are detected by using wearable sensors.

A simpler method is the **Cane balance-stability** method, which is simply based on the forces of interaction between the user and the robotic cane. It is mainly used in 1- or 2-wheel canes, with a design and system based on an inverted pendulum. As already mentioned, this method cannot be applied to robotic canes with three or more fixed legs, as they are always stable in their neutral position, with or without the application of forces in the cane, making the selection of this fall detection method unfeasible for the ARCane.

The fall detection system based on **Leg-motion-based detection**, which is based on the storage and analysis of the user's gait data, allowing later to distinguish the gait, consists of two detection methods. Both methods have the learning ability to adapt to different users, building the possibility and probability distributions of the normal walking status.

First, the **Dubois possibility theory** method, by measuring the distance between the robotic cane and the location of the user's feet, and the relative acceleration of the user's legs, it allows to obtain histogram data for each feature, which are later computed to obtain an experimental training set of data from various gait states. According to Di et. al. [28], this method allows the detection of stumble within 50 ms and does not necessarily require the use of wearable sensors. The limitation of this method is that it can only detect stumbling events, which does not always cause people to fall, but it still poses a high potential risk of falling. This fall detection method can be used as a future reference for tripping detection as it presents a very short detection time, which is ideal for fall detection systems.

Finally, there is the **Gaussian distribution** method, which uses data obtained through normal walking, namely the distance between the user's legs and the robotic cane, and the frequency of the user's legs position in the x-y plane in relation to the robotic cane, in order to obtain a Gaussian distribution, as shown in Figure 7.2. After all the information is acquired and the Gaussian distribution obtained, a threshold probability (e.g., 90%) is then decided to define an interval to distinguish between the walking state and the emergency state. After this procedure has been performed, the detection system is ready, and a fall can then be detected by evaluating the relative position of the user's legs while he is walking, in relation to the Gaussian distribution. When the relative position of the user with respect to the robotic cane is within the mixture Gaussian distribution, the user is evaluated as being in the walking state. On the other hand, when the

relative position of the user is out of the mixture Gaussian distribution, the user state must be transitioned to the emergency state, and therefore prevention methods must be triggered.

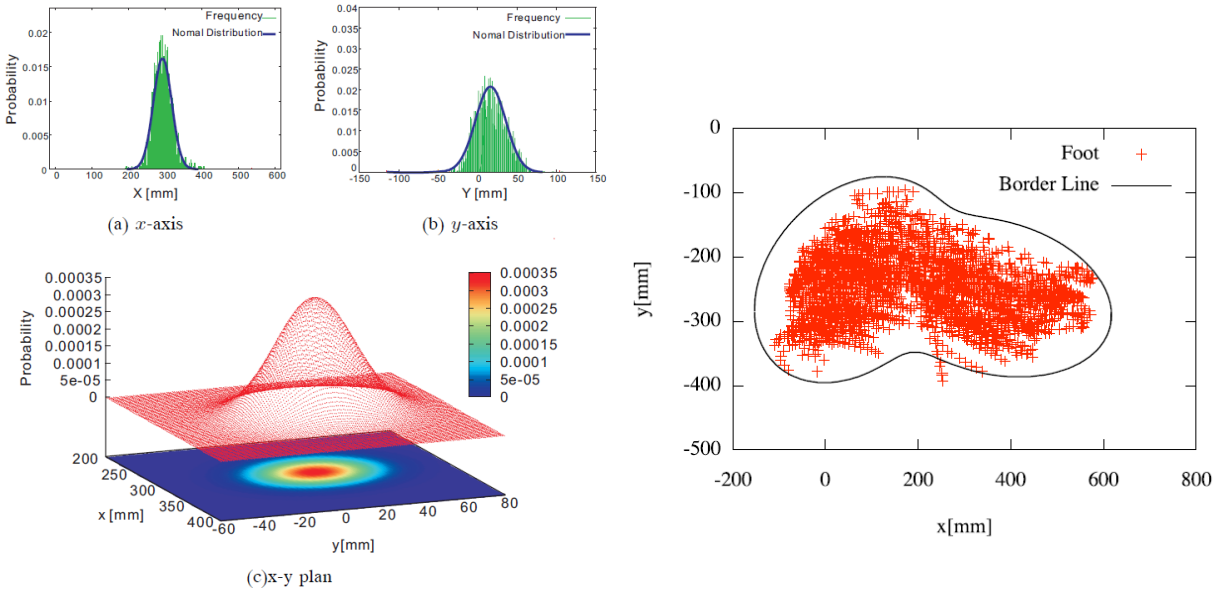

(a) (b)

Figure 7.2: Gaussian distribution obtained by the cane user's legs position during walking (a) Image from [68] (b) Image from [58].

This detection method **does not require the use of wearable sensors**, as information about the position of the user's legs in relation to the cane can be obtained through distance sensors. Furthermore, this method has the learning **ability to adapt to different users** by building the probability distributions of the normal walking status. It also enables the detection of all types of falls, as it analyzes the entire spectrum of information obtained on the state of normal gait, detecting all situations that do not fall into this class, i.e., abnormal gait. For these various reasons, this is the method of fall detection chosen to be incorporated into the ARCane. Although this detection method presents itself as the ideal method, it is necessary to have a critical position to observe and recognize that there are **points to improve** in a way to increase its performance, in order to obtain a more efficient, complete and accurate fall detection system for the ARCane.

One aspect of this method is that it uses a threshold-based algorithm, as it requires deciding a probability threshold to define an interval to distinguish between walking state and emergency state. Although this type of computational algorithm is easy to implement in real-time applications, these threshold values must be established empirically, and defining a suited value to its needs can be challenging. Furthermore, this method is inconsistent for predicting falls as it depends on subject-to-subject variability and does not

adapt to different types of fall situations. To overcome this barrier, the solution would be to **incorporate data-driven algorithms** to achieve greater accuracy in event recognition and pre-impact fall detection, leading to fewer false alarms compared to threshold-based algorithms, as well as a way to make this method more adaptable to different users. A possible proposal to incorporate data-driven algorithms in the evaluation of Gaussian distributions would be to use machine learning, more specifically, Radial Basis Function (RBF) kernel, a class of algorithms used for pattern analysis commonly used in support vector machines (SVM) classification.

Additionally, during walking there are phases in which the user becomes more stable (e.g., mid-stance phase) and less stable (e.g., during heel strike). On this matter, another improvement for this detection method would be to get **information and data analysis channeled to specific gait states**. Currently, the Gaussian distribution method uses a distribution relative to the user's gait, i.e., intended for all gait phases. One way to improve the performance of this method would be, first to distinguish the phase of the user's gait, and later, to attribute a Gaussian distribution of the location of the user's feet in relation to the cane for each phase, thus obtaining more objective results and, consequently, greater chance of detecting possible falls. It is represented below in Figure 7.3 a scheme of the Gaussian distribution fall detection method to be incorporated in the ARCane, and represented in Figure 7.4 the scheme of the respective fall detection method with the added proposed improvements, both in the training phase and in the experimental phase.

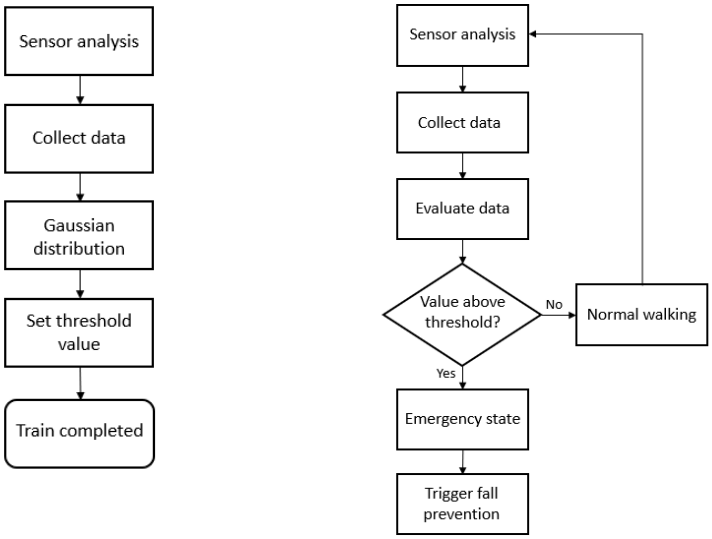

(a) (b)

Figure 7.3: Threshold Gaussian distribution method for fall detection (a) train schematic (b) experimental schematic.

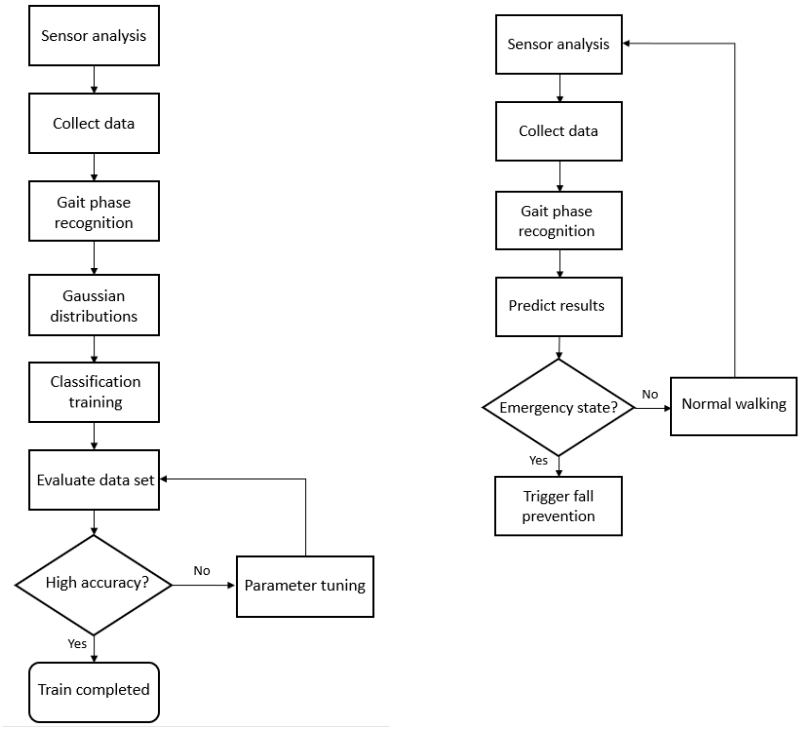

(a) (b)

Figure 7.4: Proposed data-driven Gaussian distribution method for fall detection (a) train schematic (b) experimental schematic.

7.1.2 Fall detection devices

The selection of appropriate **fall detection indicators** is essential to achieving desirable fall detection performance, however, there is not much empirical and theoretical evidence indicating the most appropriate set of fall detection indicators [145]. The fall detection indicator, in relation to the fall detection method to be used, involves monitoring the user's lower limbs, in particular the position of the user's legs in relation to the ARCane. Considering the detection method and the fall detection indicator, it will be necessary to have a detection instrument capable of acquiring the desired data for a fall to be detected. The devices used in the existing pre-impact fall detection can be generally classified into the **context-aware systems** and **wearable sensors** [145], [152].

Wearable sensors can be defined as electronic sensor-based devices that are worn by the bearer under, with or on top of clothing [152]. Due to the advancement of microelectronics and wireless communication technology, wearable MicroElectroMechanical Systems (MEMS) such as accelerometers and

gyroscopes have become small, lightweight, and low-cost. They are able to unobtrusively capture body movement and allow kinematic measurements to be monitored in extended space and time. Additionally, wearable sensors often have wireless communication capabilities that allow them to easily communicate with smartphones or other internet-enabled devices, with the benefit of not requiring additional infrastructure installation. This feature in particular makes them suitable for pre-impact fall detection. Today's smartphones come with a rich set of built-in sensors such as accelerometer, digital compass, gyroscope, GPS, microphone and camera. Several researchers are taking advantage of this fact to develop smartphone-based fall detectors. However, most studies devoted to smartphone-based fall detectors placed them in standardized positions, which allowed for highly stereotyped measurements that helped with accuracy ratings but made the results less applicable to the way people carry their smartphones every day (e.g., in pockets or purses) [152].

There are some limitations related to the use of wearable-sensors for fall detection systems. A major drawback of wearable sensors is that people under fall detection surveillance are required to wear the sensors at all times, adding that some wearable sensors are still bulky and intrusive. This can result in low user compliance because they can be uncomfortable to use, or people can sometimes forget to use them. In addition, data stability is lower compared to context-ware sensors due to insufficient battery power, and because alarm transmission may be affected by data loss due to wireless communications. Lastly, some fall detection indicators cannot be measured directly by wearable sensors and must be obtained based on estimation basis. For instance, body segment velocity variables must be estimated by integrating acceleration signals from accelerometers, which inevitably leads to some errors resulting from such an estimation procedure [145].

Vision-based or **context-aware systems** rely on sensors to acquire information about the surrounding environment, such as: colors, shadows, contrasts, depth, shapes and motion detection. The context-aware systems often have high computational demands as the visual data is much larger compared to the one-dimensional signal coming from non-vision based wearable devices. Furthermore, such systems can be difficult to implement, expensive, and restricted by space [110], [145]. One of the main challenges of vision-based detection is that context-aware systems are much more prone to privacy concerns than other detection devices, due to the levels of detail that cameras can capture, such as personal information, appearance and visuals of the living environment [110], [152]. However, with technological development over the years,

innovative context-aware detection systems have been developed and used, keeping privacy issues to a minimum by not providing information about the user's appearance and the living environment involved.

In terms of sensor placement, vision-based approaches are applicable to a limited field-of-view, or a restricted space defined by the camera position and settings [153]. In the case of the ARCane, this does not necessarily apply, as it is not necessary a high field-of-view for the detection of the fall indicators, and also because the cane accompanies the user's movements while walking, allowing continuous monitoring of the visual-data coming from the visual sensors.The acceptance of elders is also a big problem as they may not be familiar with electronic devices. To overcome this challenge, the way the system operates is essential. Vision systems, like other non-intrusive methods, are very good in this regard, as they can operate automatically, without user intervention. The main advantage of context-aware systems is that the person does not need to use any special devices for falls to be detected. Additionally, one of the benefits of using vision-based approaches for fall detection is that fall detection indicators can be accurately determined, since the biomechanical convention for calculating body kinematic measurements based on the capture system of movement has been well established in several studies [145].

Overall, in correspondence with the literature, sensor acceptance is generally lower if the sensor is carried on the person (i.e., endosensor) rather than installed in their environment (i.e., exosensors) [145], [148], [152]–[154]. Therefore, the use of wearable sensors as fall detection devices for the ARCane system is questioned and, based on the factors discussed above, the final decision lies on the **use of vision-based sensors**, since they are capable of acquire the fall detection indicators that enable the detection of the user's fall, through the proposed computational method. Regarding the decision of the visual sensor to be used by the ARCane detection system, a **comparative analysis** is carried out **between the most used context-aware sensors** in robotic canes and the most used in general applications, based on the literature. Among all fall detection systems, the most used visual sensors are RGB cameras and depth cameras, while for fall detection systems more focused on robotic cane applications, as seen in subsection 2.2.2, the most used visual sensor is the Laser Range Finder.

The working principle of the **Laser Range Finder** is that it uses laser beams to measure distances by detecting the time-of-flight between the transmitted and the reflected laser beam. They are known best for their high precision, fast data rate and long detection range, making them suitable for all types of robotic applications. There are different types of LRF sensors, namely 1D, 2D and 3D Laser Range Finder (Figure 7.5). The 1D-LRF detects in one dimension, i.e., it measures the distance from a single point in space,

making it the cheapest sensor (ranging from €50 to more than €300) and the easiest to program computationally. The 2D-LRF and 3D-LRF, also known as laser scanners, are the most used in autonomous applications for obstacle detection, and have the ability to accurately capture two-dimensional and three-dimensional data, respectively, with the consequence of making them more expensive (ranging from €100 to more than €1500 for the 2D-LRF, and from €750 to more than €5000 for the 3D-LRF) and requiring more processing power. The different types of LRF sensors are intended for different applications, corresponding to the needs of each system. In the case of the ARCane, it would be necessary to implement 3D-LRF sensor in order to acquire the monitoring and sensing of the user's lower limbs, namely the relative position of the user's legs and feet in relation to the cane. In addition to limitations associated with LRF sensors due to ambient light intensity, which can alter the laser beam and result in inaccurate measurements, and also when measuring the distance from reflective surfaces values, a 3D-LRF sensor has a very high cost, which consequently limits the availability of the ARCane in the future market.

(a) (b) (c)

Figure 7.5: Example of laser range finder sensors available in the market (a) 1D-LRF (140.44€). Image from [155]; (b) 2D-LRF (532.85€). Image from [156]; (c) 3D-LRF (910.00€). Image from [168].

Moving on to image capture devices, **RGB cameras** are designed to create images that replicate human vision, capturing light in red, green, and blue (RGB) wavelengths to achieve an accurate representation of colors. In vision-based action recognition, many works have used conventional RGB cameras, which may be associated with being: (i) widely available; (ii) cost-effective; (iii) easy to operate; and (iv) able to provide rich texture information of the scene.

However, there are limitations associated with the utilization of RGB cameras: (i) they require a considerable amount of hardware resources, in order to run computationally intensive image processing and

computer vision algorithms [164]; (ii) the accuracies of RGB camera-based detection systems vary drastically due to environmental conditions, such as illumination changes, which often results in limitations during the night [155], and occlusion problems, where part of the human body is occluded by a certain object [169]; and lastly, (iii) they are prone to privacy concerns, due to the levels of detail that cameras can capture, such as personal information, appearance, and visuals of the living environment.

In the case of **depth cameras**, they are designed to create images based on depth information from the surrounding environment, and have become the most popular vision-based sensor in the field of fall detection, since 2014, taking the place of the traditional RGB cameras [155]. One of the main possible limiting features of depth cameras compared to RGB cameras is that: (i) depth information is sensitive to materials with different refection properties (e.g., transparent materials, and light absorbing materials); (ii) they do not provide color and texture change information of the environment [164].

While depth cameras have certain limitations compared to RGB cameras, these parameters do not have as much impact in the context of fall detection systems. In addition, the advantages arising from the use of depth cameras outweigh its disadvantages, having several parameters that stand out, namely: (i) widely available; (ii) cost-effective; (iii) easy to operate; (iv) provide 3D structure information of the scene; (v) insensitive to lighting conditions and illumination changes, meaning it can work in total darkness; (vi) do not require complicated calibration [155]; (vii) high performance in human action recognition [164]; and (viii) can only capture depth information, which makes it less intrusive of privacy. The last parameter is one of the most important, as it has a high weight on user adherence and acceptance in the application of fall detection systems. Since the advent of affordable depth sensing technology, fall detection with depth cameras has been extensively and thoroughly studied due to its inexpensive price and easy installation. The Microsoft Kinect (Figure 7.6) is a device with depth sensing technology that is highly regarded and cited throughout the literature due to its cost-effectiveness and performance in context-aware systems, and tt can be obtained for around €355. Kinect uses an RGB-D camera, which can capture RGB images like a regular camera and also capture depth images with a depth camera (Figure 7.7(a)). An important key of this device is that the Kinect System Developer Kit (SDK) has skeletal tracking (Figure 7.7(b)), which allows researchers to analyze the main joints of the human body and the recognition of human action for fall detection [169], [170]. In a comparison process, Table 7.1 was created to consider various parameters and their insertion into the context-aware system discussed in this section. The depth camera is finally defined as the choice of visual sensor to be inserted into the cane to obtain the fall detection indicators and to enable a possible fall

prevention, mainly due to its very cost-effectiveness, but also for its ability of skeletal tracking, and because it is not intrusive to users' privacy. A simulation of the depth camera's visibility when inserted into the ARCane is shown in Figure 7.8.

(a) (b)

Figure 7.6: (a) Microsoft Kinect (discontinued manufacturing). Image from [171]; and Microsoft Azure Kinect. Image from [161].

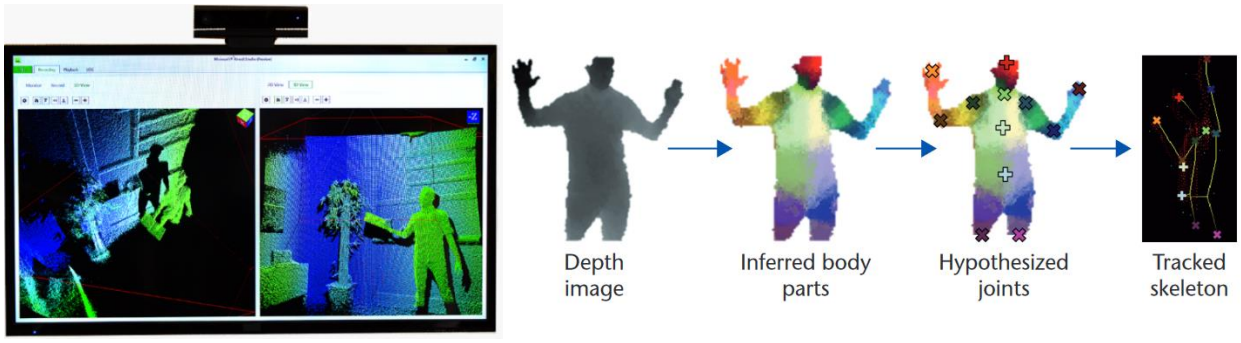

(a) (b)

Figure 7.7: (a) Depth images obtained with Microsoft Kinect. Image from [171]; (b) Microsoft Kinect skeletal tracking pipeline. Image from [173].

Table 7.1: Comparison of potential vision-based devices for the ARCane fall detection, considering different parameters

Parameters	3D-LRF	Depth camera	RGB camera
Widely available		x	x
Cost-effective		x	x
Provides 3D structure information of the scene	x	x	
Easy to calibrate	x	x	
Skeletal tracking		x	

Parameters	3D-LRF	Depth camera	RGB camera
Insensitivity to lighting conditions		x	
Insensitivity to materials with different refection properties			x
Gives color and texture information			x
Not intrusive to privacy	x	x	

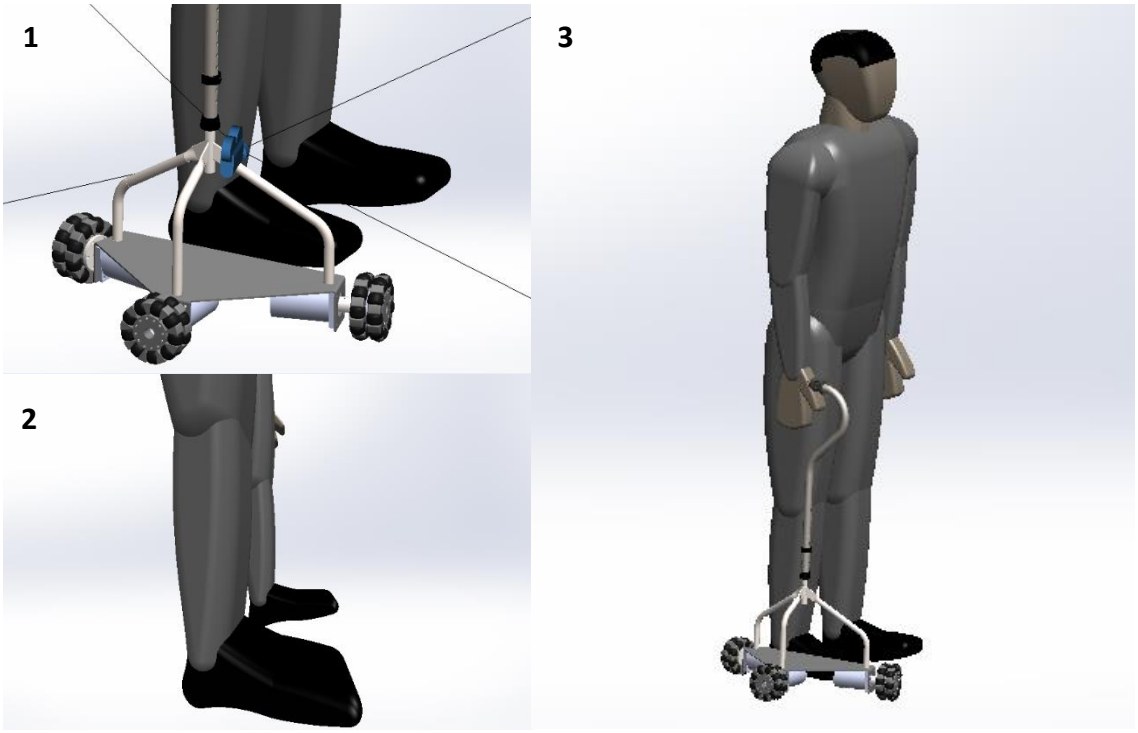

Figure 7.8: Simulation of the depth camera's visibility inserted in the ARCane. 1- SolidWorks camera mode; 2- Simulated camera view; 3- Trimetric view of the simulated human model using the ARCane.

It is also worth noting that vision-based methods are not required to be a standalone fall detection system as they can also be combined with other modules to form an overall system. **Sensor fusion** involves using different signals coming from multiple devices. This is all done to complement the strengths of all the devices and develop a more robust algorithm to monitor the user's gait and detect potential falls. Therefore, the accuracy of the overall ARCane fall detection system can be improved, and additional functionalities can be included. An example of application of a fusion sensor in the cane is the force system present in the cane's handle, which uses multiple force sensitive resistor sensors that can measure the force applied to the cane. With this configuration, it allows to detect when the user is leaning or not on the cane, since falling risk situations are more likely to happen when the user does not exert or exerts little force on the cane.

7.2 Fall prevention

The fall prevention system is the superior attribute that distinguishes the robotic cane from a conventional cane. This system is the complement of the cane fall detection system, as it is based on the way the cane will react to the detection of a user's state of emergency to keep the cane-user system in balance and safety. According to the literature, there are already several devices with fall detection, the vast majority with post-fall detection (i.e., after an impact), but few with fall prevention. The response time of the fall arrest mechanisms of action is crucial, as they must be fast enough so that the body balance of the user who is in the act of falling can be recovered in time to avoid a fall. impact situation with the ground or surroundings. In this sense, it is extremely necessary that the time of detection and prevention of falls be within the critical phase, of gait events, with sufficient lead time for a fall to be effectively prevented.

7.2.1 Prevention mechanism

There are several fall prevention methods already reported from the latest generation of robotic canes. Each method is adapted to the physical structure of each cane, also considering its degrees of freedom, number of wheels, type of movement control, as well as the sensory unit and the unit of action that compose them. In the absence of a specific type, or already pre-defined, of fall prevention method to be used by robotic canes in general, it was then sought to obtain a method more intended for the ARCane of the present study, which corresponds to all its characteristics. and makes it possible to carry out successful fall prevention actions.

7.2.1.1 Vibrotactile feedback

Starting with vibrotactile feedback, this method is based on the context of **direct robot-human communication and interaction**, through vibrational actuation methods integrated into the cane. The vibrating motors integrated into the cane are intended to notify and adjust irregular gaits, through vibrating signals that propagate through the cane handle to the user's hand, in order to enable a controlled and monitored gait. These vibration signals can then be triggered with certain emission rhythms to adjust the pace of the user's stride, which can also be incorporated in rehabilitation centers to adjust the pace and speed of the patient's movement by considering the length of the user's stride while using the cane.

The other application of the vibrating signals is emitting signals of great amplitude, with the purpose of **notifying any type of irregularity or associated danger during the execution of the gait**. This system is interleaved with the high-level control unit that analyzes and processes the signals obtained by the fall detection system, which continuously monitors the relative position of the user's legs in relation to the cane. An example of a dangerous situation when walking is when the user is in a tandem position, i.e. a state where both legs form a line along the direction of walking, which results in a lower base of support of both legs and a smaller stability margin (Figure 7.9(a)). The use of vibrotactile feedback can then behave in a way that prevents the user from being in a tandem position, signaling the possibility of this occurrence when analyzing the angle between each leg, and when it detects that they are below a certain value (Nakagawa et al. [38] used 5 degrees as a threshold value to detect tandem posture), this system acts to alert the user to increase the distance between each foot during gait (Figure 7.9(b)). Although this method of actuation and user interaction may not directly prevent a detected fall, the fact that it informs the user of any irregularities in gait makes it a passive method of fall prevention, which makes it possible to reduce the chances of a fall caused by an irregular gait.

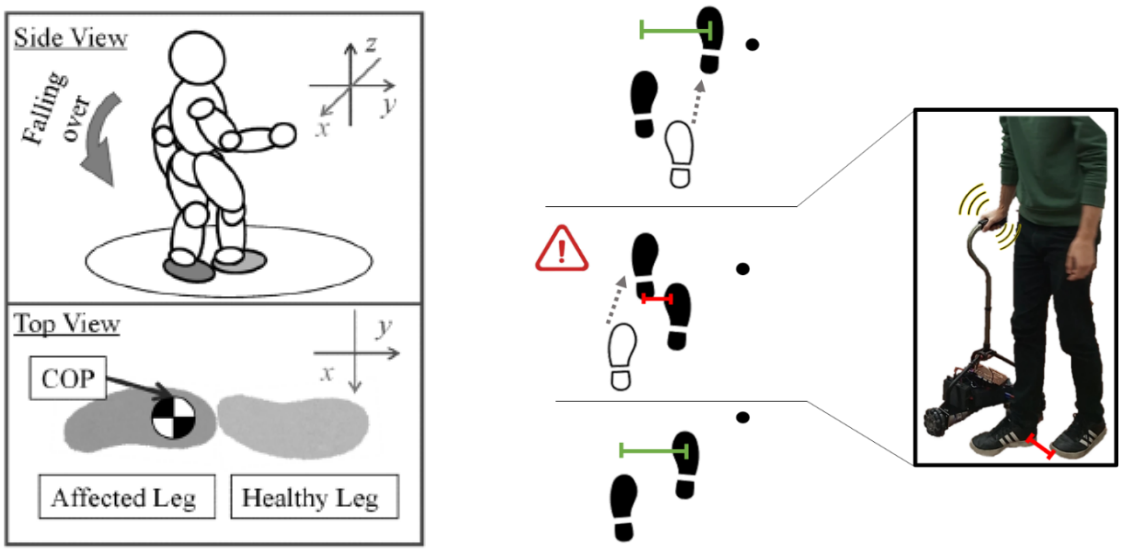

(a) (b)

Figure 7.9: (a) Fall event caused by tandem stance. Image from [38]; (b) Tandem stance prevention through vibrotactile feedback.

7.2.1.2 Cane displacement

Having already incorporated a passive fall prevention system, it is essential to implement an active prevention system that complements the functionalities of the ARCane. Considering the prevention methods presented by the eight robotic canes of the state-of-art which include a fall prevention system, it was decided to implement a prevention system similar to the methods applied in cane no. 1, 4, 5 and 7, which are based on **moving the robotic cane to ensure the stability of the cane-user system**.

Cane methods no. 2, 6, 12 and 13 were excluded because: they were intended for canes with one or two wheels based on the inverted pendulum model (cane nº 2 and 6); they do not use drive motors to move the cane, instead they have wheel brakes to stop the passive movement of the cane (cane nº 12); and because it is intended for canes with legs, i.e., that do not use wheels, in which the height of each leg can be easily adjusted (cane nº 13).

The fall prevention system intends to perform quick actions in situations of high risk of falling, preventing the occurrence of this tragic event that can be fatal for many users. For the **proposed prevention method** to be implemented, when detecting a state of emergency by the fall detection system, the cane robot will be able to **reposition itself strategically and quickly**, by rotating along the user and moving to the direction that the user is falling, in order to provide an effective and preventive support. As soon as the cane moves to the specified position, **all three omnidirectional wheels of the ARCane will stop** and ensure the user's balance. Figure 7.10 demonstrates an example of the fall prevention method to be implemented when a fall event occurs, and Figure 7.11 illustrates the human-in-the-loop control flowchart in the ARCane system circuit.

The fall situation is unpredictable, and there are numerous possibilities for the direction of falls, so it is very important to reconcile the fall detection system with the fall prevention system. As the fall event usually follows a voluntary movement, which is performed mainly in the sagittal plane, most falls occur in the forward or backward direction [155], and **at least 60% of the fall behavior occurs in the forward direction** [46], On this matter, the fall prevention mechanism can be trained initially in these two directions, and later, expand the prevention spectrum for different fall situations.

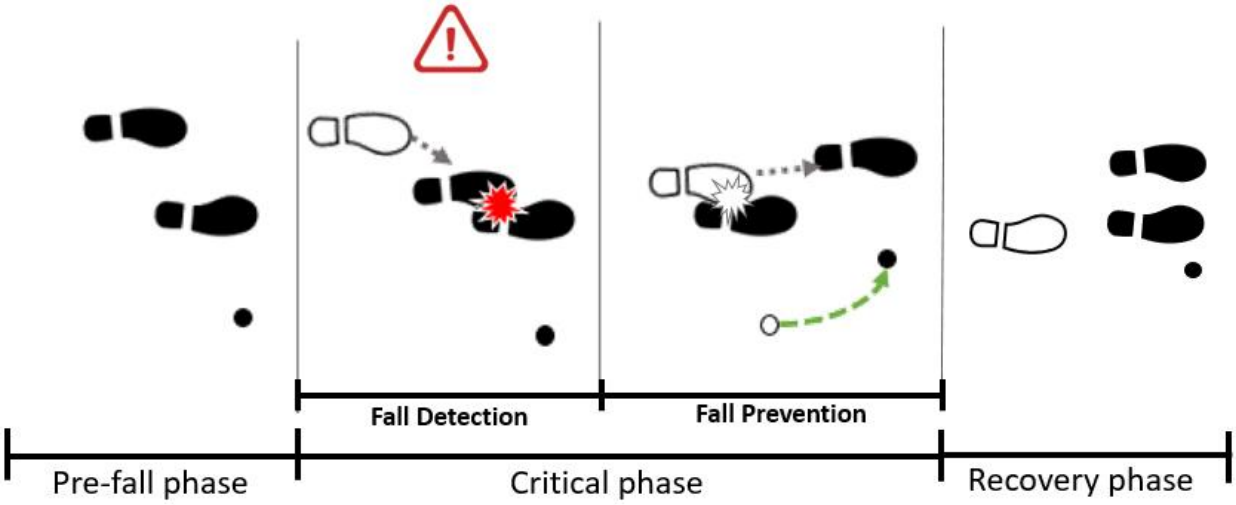

Figure 7.10: Example of a detected fall situation, with the fall detection and prevention mechanism in action.

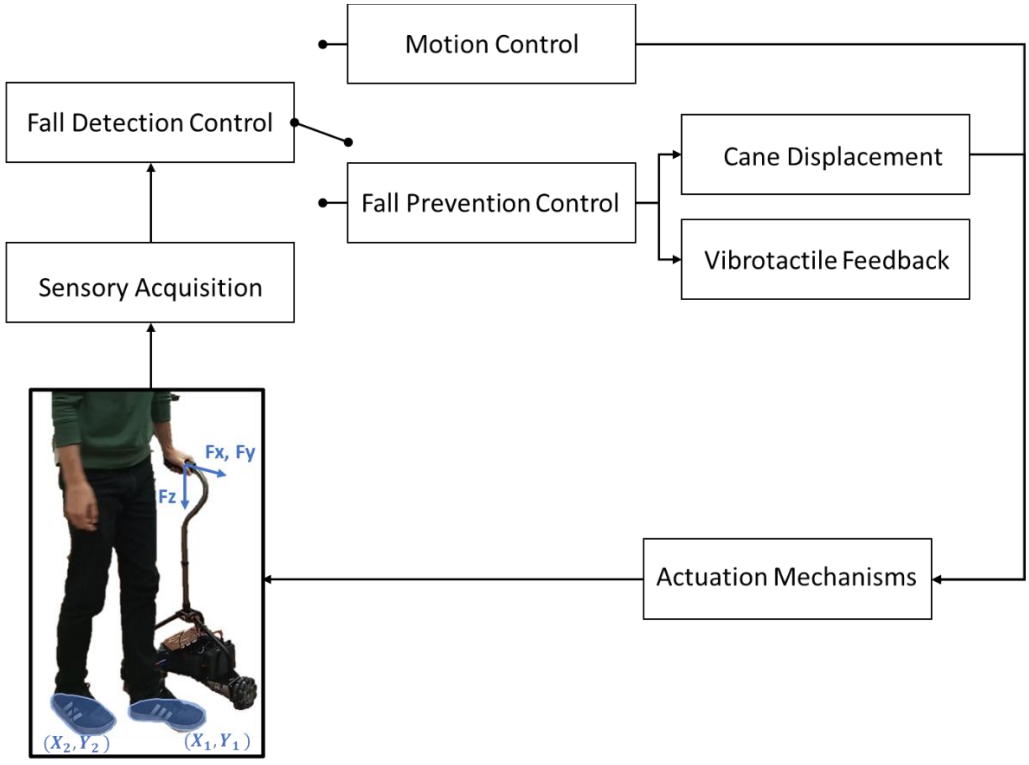

Figure 7.11: Representation of the human-in-the loop control flowchart of the ARCane system.

7.3 Discussion

This chapter aimed to investigate a fall detection and prevention system that can be implemented in the ARCane, with the main objective of obtaining a system that, during the critical phase (i.e., the time interval in which the fall occurs), it occurs the detection and prevention of the fall, through detection and prevention mechanisms. Regarding the fall detection system, it was defined that the goal is to obtain a fall detection system, which seeks to predict fall incidents before or during their occurrence, allowing immediate prevention actions. In a first step, in order for a fall to be detected, it is necessary to have a clear definition of which detection method to use, i.e., to take into account which indicators and parameters of the user's gait and body biomechanics, which can describe whether the user is performing normal or abnormal walking.

Considering the fall detection methods present in the State-of-the-Art, the method based on the Gaussian distribution was chosen as a fall detection method to be integrated in the ARCane. This method takes as a fall detection indicator the relative position of the user's legs and feet, where in an initial training phase it uses this data to create a Gaussian distribution in relation to the user's gait. After the training phase, this method is prepared to evaluate the user's gait event in a real context, distinguishing between normal and abnormal walking depending on whether the relative positions of the fall indicators are inside or outside the Gaussian distribution, allowing the detection of an emergency state, leading to the activation of fall prevention mechanisms.

In order to improve the performance of this detection method, since this method is based on threshold algorithms, it was proposed to incorporate data-driven algorithms to achieve greater accuracy in event recognition and pre-impact fall detection. Thus, it would lead to the acquisition of less false alarms compared to threshold-based algorithms, as well as a way to make this method more adaptable to different users. Additionally, it was pointed out that another way to improve this detection method would be to distinguish the phase of the user's gait and, therefore, assign a Gaussian distribution to each phase, thus obtaining more objective results and, consequently, a greater chance of fall detection.

Having the fall detection method to be incorporated into the cane well defined, and considering which fall detection indicators need to be sensed in order for a fall to be detected, it is required a suitable detection instrument which fits the ARCane system, the consumer needs, and that is also cost-effective. From an analysis between context-aware systems and wearable sensors, a visual-based sensor was defined as a detection instrument to be incorporated. Being one of the main reasons the user compliance, since sensor

acceptance is generally lower if the sensor is carried on the person (i.e., endosensor) rather than installed in their environment (i.e., exosensors). Considering an evaluation carried out between the three most used visual-based devices in fall detection systems, the depth camera was defined as the most suitable instrument to be used for the detection of falls in the ARCane. This decision lies in the fact that the depth camera has few limitations in terms of noise readings from the surrounding environment, being ideal for outdoor use; it has a good cost-benefit ratio; and is not intrusive to the user's privacy as it only captures depth information

Regarding the prevention of falls, two preventive methods were defined for the ARCane, one passive and the other active. As a passive method, it is implemented a vibrotactile feedback that is based on the communication and interaction between the cane and the user, by sending vibrating signals through the cane handle, to alert dangerous situations, signal irregular gait situations, or as a way to adjust the gait speed and stride rhythm. As an active method of fall prevention, and based on the literature research of fall prevention methods applied to robotic canes, it was decided to apply a prevention method based on the displacement of the cane. Therefore, when a fall is detected, the ARCane is repositioned in the direction of the user's fall. After reaching the desired position, the ARCane's omnidirectional wheels will lock to support the user's body weight, ensuring stability and safety for the user.

8 Conclusion

A fall can be defined as an event that results in a person inadvertently coming to rest on the ground, floor or other lower level. **Falls are timeless and unpredictable**, and they can happen anywhere and to anyone. People who fall, even if they are not injured, can become afraid of falling, as the non-fatal injuries associated with falls can range from minor to severe, such as broken bones, soft tissue injuries, bruises, and head trauma. Although falls can happen to anyone, they are mostly related to age and frailty level, as the **elderly are more susceptible to falls with a greater risk of death or serious injury resulting from a fall**. By focusing on this majority, it can also be verified through statistical data that the elderly population in the world finds itself in constant growing. Also, by considering that there is an increase in lack of nursing professionals, it originates in conservative methods with the elderly, in order to avoid possible falls, which results in many consequences such as: loss of motor functions, lack of feeling of independence, monotonous life, many health, mental and physical problems.

This dissertation seeks to respond to these problems caused by falls, by integrating a **robotic gait assist device capable of detecting and preventing falls**, orientated at an early stage to the geriatric community. Initially, a superficial analysis of the robotic assistive devices present in the literature was carried out, where it was identified the pros and cons of each device. The cane was then defined as the device to be integrated, due to: (i) its low cost, which makes it a more accessible product on the market; (ii) their reduced weight, facilitating its use and operation; (iii) its reduced dimensions, which allows its use in external and uncontrolled environments, and (iv) the fact that it also provides greater body activity and more extensive and complete muscular use of the lower limbs. With this moderate support, the user will have a better recovery, greater independence and a more practical use during walking and rehabilitation. A study of the State-of-the-art of robotic canes in the literature was then carried out, in order to obtain a broad and in-depth knowledge on the matter. It was possible to identify a **total of 18 robotic canes**, verifying several different designs and structures, providing each one different degrees of freedom to the system. The electronic components implemented in the robot-user system were also identified, verifying that **50% of the robotic canes** in the literature required the **use of wearable sensors** by the users, and that **100% of the robotic canes** contained **sensors implemented in the structure of the cane**. An analysis on the types of motion control, fall detection and fall prevention strategies implemented in each cane was also carried out, verifying that out of these 18 robotic canes, **100% have movement control**, **50% uses fall detection** and **44% have fall prevention strategies**. Finally, experimental

protocols, main results, limitations and challenges were also evaluated, obtaining as **predominant parameters missing** in the development of robotic canes: **(i)** the lack of clinical gait trials, with the elderly or people with reduced mobility, to test the robotic cane in real conditions with patients that meet the specifications and needs of the cane; **(ii)** the lack of robotic canes with fall prevention strategies that do not require the use of wearable sensors, and **(iii)** the lack of strategies to recognize the user's gait phase, to determine the user's gait state and enable abnormal gait detection.

The next step is related to the product design, where, having already identified an opportunity for the development of a robotic cane, it was possible to improve the product's mission by defining a description of the future product as a robotic cane with an integrated system real-time fall detection and prevention with intuitive motion control. Then, the **main barriers related to the use of the cane** were evaluated, obtaining as main results the fact that the cane device made the users **look old or fragile**. As a solution to this problem, some seniors felt that **fashionable assistive devices** would make them more likely to use them rather than standard medical-looking devices, and ultimately, they believed that **motorized equipment** offered not only **convenience** and **ease of use**, but also, a **youthful appearance**. The list of customer needs metrics was then identified in order to update the target specifications of the ARCane, extended teamwork [13], to obtain a product with market compatible design and engineering that meets the needs and desires of the cane users. Finally, the cane design is presented, along with the **structural modifications** carried out related to the displacement of the cane handle to the position directly above the cane's center of mass. This new modification would ensure a robust and stable structure that can withstand the user's weight during the gait.

The hardware architecture was then defined in chapter 4, where the features that are intended to be incorporated by the ARCane were defined first, as well as the main functionalities to be implemented that differentiate the ARCane from a conventional cane. Subsequently, the control units responsible for processing all the information that encompass the cane electronic system were identified, defining through a benchmark the STM32 F446RE as the control unit responsible for the low-level processing, and the NVIDIA JetsonNano as the device responsible for ARCane's high-level processing, dedicated to fall detection and fall prevention strategies. The components for the sensory, actuation and energy units were also identified and implemented, based on the problem statement and scope defined in Chapter 1, and based on the review analysis carried out in Chapter 2. Resulting from the **acquisition of all the components** necessary for the incorporation of the ARCane, the total purchase price was **€688.97**. Although this value is slightly higher than the €650 mentioned in the target cane specification, it is important to bear in mind that this version of

the ARCane is not the final product, but a prototype of a potential future commercially available product. Thus, all parts were purchased in single quantities, and all hardware components are considered experimental, which later in the design can be either over-engineered, to optimize performance and also change the overall price of the ARCane. Afterwards, the UART and I2C communication modes were discussed, and the operating frequencies were analyzed for each component present in the electronic system of the ARCane. Regarding operating frequencies, a **hierarchical management of sensory data and actuation commands** was chosen, with the respective priority being defined for each component. This configuration aims to maximize the efficiency of the processing time of the control units, by prioritizing the most relevant data, to ensure the safety of the user, as well as the proper functioning of the cane.

After the incorporation of all electronic components into the ARCane, **interoperability tests** were carried out as a way of validating the functioning of the components individually and collectively. It was obtained as **main results** that: **(i)** all communications were carried out successfully and without loss of associated information; **(ii)** the system has an autonomy of 2 hours and 30 minutes, highlighting the possibility of using the **ARCane in rehabilitation sessions**; and **(iii)** the vibrations in the cane handle, arising from the haptic feedback system, could be perceived, as well as distinguish between different amplitudes and frequencies of vibration, which demonstrates the possibility of the **cane interacting with the user** by varying the vibratory stimuli applied.

Regarding the **motion control strategy** to be implemented at the ARCane, it was initially defined that the objective was to obtain a **simple and intuitive and cost-effective system**. This proposition takes into account that most robotic canes often rely on expensive sensors or require major modifications to the cane, which makes them more inaccessible, limiting the number of potential users. Having first developed the intended working **admittance control strategy** for the cane based on the gait of a healthy person and a person with an affected leg, it was identified the admittance control as the movement control method to be implemented. This evaluation was based on the methods outlined in the SoA review, the ARCane design, and the previously identified mission statements. The motion control was then divided into **three categories**: **(i)** movement intention recognition; **(ii)** recognition of the gait phase; and **(iii)** motion control of the holonomic base. For categories (i) and (ii), simulations were initially performed with strain gages implemented in the cane rod, showing that they do not present sufficient sensitivity to detect the user's interaction with the ARCane. It was then decided to implement FSR sensors as the sensory device of the motion control system, as they are durable, thin, flexible, widely available and cost-effective sensors with a wide range of force

sensitivity. It was also proposed a method to improve the acquisition of sensory data from the FSR through a better distribution of the applied forces. The sensors were then placed on the cane rod and arranged on the cane handle, making the motion control an innovative cost-effective system that doesn't require major structural changes to the cane, as mentioned in the problem and scope statement. The holonomic base movement was based on the admittance control method, which allows the transformation of the user's intention forces into the movement of the cane, through forward kinematics and matrix equations, considering the configuration of the wheels and motors arranged in the holonomic base. Finally, **operability tests** were carried out with **six volunteers** in order to validate and obtain a critical analysis of the motion control system implemented in the ARCane. The **main results** of the experimental tests were: **(i) 97% accuracy** for user **movement intention recognition**, and **(ii) 90% accuracy** for **user gait phase recognition**.

Aiming at the future integration of fall detection and prevention systems in the ARCane, it was idealized a **fall detection strategy** with a commercial device capable of obtaining images based on **depth information** of the surrounding environment, in order to complement the fall detection method based on **Gaussian distribution**, through leg-motion-based detection during the gait. Regarding the **fall prevention system**, were addressed strategies and action mechanisms that make it possible to assist the user in a fall situation, based on **vibrotactile feedback** as a passive prevention method and the **locomotion of the cane** as an active prevention method.

Furthermore, with the developed master thesis, the goals that were established in Chapter 1 were all achieved and the RQ can be answered:

- **RQ1:** How are robotic canes in the scientific literature instrumented to provide motion control? This RQ is adressed in Chapter 2. Among the 18 robotic canes present in the literature, it was found that all had sensors implemented in the cane, with the axial force/torque sensor being the predominant component. Regarding the use of wearable sensors, only nine robotic canes required their use, with the IMU being the predominant sensor implemented. These two sensor components have in common the fact that they are intended to assist the motion control of the robotic canes, as they make it possible to obtain and monitor information about the interaction of forces applied by the user to the cane, and the user's gait state. Additionally, LRF sensors were also implemented in some canes to detect the movement of the user's lower limbs during gait, as well as wearable force sensors and wearable inertial sensors were implemented in order to detect the user's gait phase,

and the distance the user is from the cane, respectively. Regarding the movement and design of the robotic canes, it appears that a total of 16 robotic canes use motors as a drive mechanism to carry out their locomotion. After studying the implemented instrumentation, it was found that all robotic canes in the literature have motion control. For this reason, it is then possible to associate movement control as the priority strategy to be implemented in a robotic cane.

- **RQ2:** What are the main fall prevention methods implemented in robotic canes among the scientific literature? This RQ is adressed in Chapter 2. There are a total of seven robotic canes that have fall prevention methods, being that there are three fall prevention methods applied that stand out. The first method is intended for robotic canes with one or two wheels, which are based on the inverted pendulum model so that they are capable of maintaining self-balance. This is mode of operation is intended to counteract the forces applied to the cane by moving in the same direction so that it maintains an upright position. Thus, when forces are applied in the direction of forward movement, as if in a possible falling situation, the cane will move in that direction to maintain balance, while assisting the user from falling, by moving alongside him. The second method is intended for robotic canes with passive motion control, where the cane's movement results directly from forces applied by the user, without any triggering mechanism. This method is based on controlling the braking torques of the wheels in order to control the movement of the robotic cane. The braking system allows to adjust the speed of the mobile base, which consequently, can help and prevent the user from falling, by ensuring the stability of the robotic cane to support the user's body weight. Finally, the third method of fall prevention is applied to robotic canes with actuation mechanisms destined to move the cane. This method is based on moving the robotic cane to a strategic position favorable to the user during a fall situation, so that it can stably support your body weight on the cane. In some cases, polygonal support area is used to assist this method, so that it is considered the distribution of forces to obtain an estimate of where the center of mass of the cane-user system is located.
- **RQ3:** What are the best sensors and the respective location on the ARCane to detect the user's motion intention and gait phase recognition? This RQ is adressed in Chapter 6. Through the study of motion control strategies, it was verified that the detection of the user's

movement intention, as well as the recognition of the user's gait phase, could be detected through the interaction of the forces that the user applies in the ARCane. However, most robotic canes that contained systems to detect the interaction of user forces, were found to either rely on expensive sensors or to require major modifications to the cane structure. Thus, to overcome this problem, an innovative motion control method was implemented, being cost-effective, simple and intuitive. In an initial phase, a comparison was made between cheaper sensors, capable of detecting user interaction forces, without the need for structural modifications in the ARCane. Finally, based on the mechanical study carried out, it was found that the FSR sensors are the most suitable for acquiring information about the forces applied by the user. For the detection of the user's gait phase, three FSR sensors were implemented in the cane handle, as the location is subject to the forces applied directly by the user. Regarding the detection of the user's motion intention, four FSR sensors were implemented in the lower position of the cane axis, due to the obtained results from the mechanical studies. Finally, these motion control methods were validated through experimental tests, obtaining as final results 97% accuracy for user movement intention recognition and 90% accuracy for user gait phase recognition.

RQ4: What is the best fall prevention strategy to be implemented in the ARCane? This RQ is adressed in Chapter 7. The choice of the fall prevention strategy for the ARCane was based on the study of fall prevention methods implemented by robotic canes in the literature, which in turn supported the assessment performed to respond to QR2. It was then verified that the fall prevention strategy compatible with ARCane is based on the displacement of the cane. Thus, when a fall is detected, the ARCane will reposition itself in a strategic position in the direction of the user's fall. After reaching the desired position, the ARCane motors will lock the wheels, so that they do not move, to support the user's body weight, and provide stability and safety to the user. This method is compatible with the ARCane as it has an integrated holonomic base with three omni-directional wheels and three high torque motors, allowing the ARCane to be moved anywhere in order to support the user and prevent him from falling. Additionally, it is important to note that no feedback method is present in robotic canes in the literature, with the intention of the cane interacting with the user. On this matter, vibrating motors were integrated into the ARCane to send vibrating signals through the

Arcane handle to the user's hand. Thus, this method could act as a passive fall prevention mechanism, which could: (i) alert dangerous situations; (ii) to signal that the user is performing an irregular gait, or as a way to (iii) adjust the user's gait speed and stride length.

8.1 Future work

Future work within the scope of this dissertation includes: (1) the implementation of a battery with greater capacity, so that the ARCane has a longer period of use, enabling its applications to domestic use and at hospital areas; (2) the application of the idealized fall detection and prevention strategies; (3) the implementation of a motor control strategy to achieve smoother and more controlled movement of the cane to match the user's changes in speed and acceleration during gait; (4) the implementation of an alert system, triggered when a fall is detected, that contacts the hospital emergency unit and the user's emergency contacts with the location of where the fall occurred; (5) the exploration of a gravity compensation strategy, through the data acquired by the cane's inertial system, to prevent the cane from slipping or falling while moving on inclined planes, using the torque applied by the motors; (6) the conducting of clinical gait trials to obtain results in a real-life context with the elderly or people with reduced mobility, to test the ARCane in real conditions with patients who meet the specifications and needs of the cane.

References

[1] P. D. (2019). United Nations, Department of Economic and Social Affairs, "World Population Prospects 2019: Highlights." [Online]. Available: https://population.un.org/wpp/Publications/Files/WPP2019_Highlights.pdf

[2] P. D. (2019). United Nations, Department of Economic and Social Affairs, "World Population Prospects 2019." [Online]. Available: https://population.un.org/wpp/DataQuery/

[3] M. Marć, A. Bartosiewicz, J. Burzyńska, Z. Chmiel, and P. Januszewicz, "A nursing shortage – a prospect of global and local policies," *International Nursing Review*, vol. 66, no. 1, pp. 9–16, 2019, doi: 10.1111/inr.12473.

[4] Z. C. Y. Chan, W. S. Tam, M. K. Y. Lung, W. Y. Wong, and C. W. Chau, "A systematic literature review of nurse shortage and the intention to leave," *Journal of Nursing Management*, vol. 21, no. 4, pp. 605–613, 2013, doi: 10.1111/j.1365-2834.2012.01437.x.

[5] A. M. Gerolamo and G. F. Roemer, "Workload and the nurse faculty shortage: Implications for policy and research," *Nursing Outlook*, vol. 59, no. 5, pp. 259-265.e1, 2011, doi: 10.1016/j.outlook.2011.01.002.

[6] World Health Organization, "Health workforce: Global Strategic Directions for Nursing and Midwifery Report by the Director-General," vol. 73, no. April, pp. 4–9, 2021, [Online]. Available: https://apps.who.int/iris/handle/10665/336661,

[7] L. M. Haddad, P. Annamaraju, and T. J. Toney-Butler, "Nursing Shortage.," Treasure Island (FL), 2022. [Online]. Available: https://pubmed.ncbi.nlm.nih.gov/29630227/

[8] D. L. Murman, "The Impact of Age on Cognition," *Seminars in Hearing*, vol. 36, no. 3, pp. 111–121, 2015, doi: 10.1055/s-0035-1555115.

[9] M. E. Fischer *et al.*, "Age-Related Sensory Impairments and Risk of Cognitive Impairment," *J Am Geriatr Soc*, vol. 64, no. 10, pp. 1981–1987, 2016, doi: 10.1111/jgs.14308.

[10] W. Zhang, L. F. Low, M. Schwenk, N. Mills, J. D. Gwynn, and L. Clemson, "Review of Gait, Cognition, and Fall Risks with Implications for Fall Prevention in Older Adults with Dementia," *Dementia and Geriatric Cognitive Disorders*, vol. 48, no. 1–2, pp. 17–29, 2019, doi: 10.1159/000504340.

[11] World Health Organization, "Fact sheets - Fall details." [Online]. Available: https://www.who.int/news-room/fact-sheets/detail/falls

[12] B. J. Vellas, S. J. Wayne, L. J. Romero, R. N. Baumgartner, and P. J. Garry, "Fear of falling and restriction of mobility in elderly fallers," *Age and Ageing*, vol. 26, no. 3, pp. 189–193, 1997, doi: 10.1093/ageing/26.3.189.

[13] R. J. L. Durães, "Design and development of an anti-fall cane prototype," 2021.

[14] H. I. Sahin and A. R. Kavsaoglu, "Autonomously Controlled Intelligent Wheelchair System for Indoor Areas," *HORA 2021 - 3rd International Congress on Human-Computer Interaction, Optimization and Robotic Applications, Proceedings*, pp. 5–10, 2021, doi: 10.1109/HORA52670.2021.9461335.

[15] R. S. Rao *et al.*, "Human robot interaction: Application to smart wheelchairs," *Proceedings-IEEE International Conference on Robotics and Automation*, vol. 4, no. May, pp. 3583–3588, 2002, doi: 10.1109/ROBOT.2002.1014265.

[16] Y. Sato *et al.*, "Multiple robotic wheelchair system able to move with a companion using map information," *ACM/IEEE International Conference on Human-Robot Interaction*, pp. 286–287, 2014, doi: 10.1145/2559636.2563694.

[17] K. Han, J. Lee, J. Kim, and W. K. Song, "Design of assessment tool for smart mobile walker," *2013 10th International Conference on Ubiquitous Robots and Ambient Intelligence, URAI 2013*, pp. 548–549, 2013, doi: 10.1109/URAI.2013.6677335.

[18] K. Han, B. Ko, J. Shin, W. Cho, and W. Song, "Usability testing of smart mobile walker: A pilot study," in *2014 11th International Conference on Ubiquitous Robots and Ambient Intelligence (URAI)*, Nov. 2014, pp. 112–115. doi: 10.1109/URAI.2014.7057409.

[19] Y. Han, "Walker robot structural design and performance analysis," *Proceedings of 2019 IEEE 4th Advanced Information Technology, Electronic and Automation Control Conference, IAEAC 2019*, no. Iaeac, pp. 934–937, 2019, doi: 10.1109/IAEAC47372.2019.8997833.

[20] A. Esquenazi, M. Talaty, and A. Jayaraman, "Powered Exoskeletons for Walking Assistance in Persons with Central Nervous System Injuries: A Narrative Review," *PM and R*, vol. 9, no. 1, pp. 46–62, 2017, doi: 10.1016/j.pmrj.2016.07.534.

[21] H. Herr, "Exoskeletons and orthoses: Classification, design challenges and future directions," *Journal of NeuroEngineering and Rehabilitation*, vol. 6, no. 1, pp. 1–9, 2009, doi: 10.1186/1743-0003-6-21.

[22] G. Orekhov, Y. Fang, J. Luque, and Z. F. Lerner, "Ankle Exoskeleton Assistance Can Improve Over-Ground Walking Economy in Individuals With Cerebral Palsy," *IEEE Transactions on Neural Systems and Rehabilitation Engineering*, vol. 28, no. 2, pp. 461–467, Feb. 2020, doi: 10.1109/TNSRE.2020.2965029.

[23] T. Afzal, M. Kern, S. C. Tseng, J. Lincoln, G. Francisco, and S. H. Chang, "Cognitive demands during wearable exoskeleton assisted walking in persons with multiple sclerosis," *2017 International Symposium on Wearable Robotics and Rehabilitation, WeRob 2017*, pp. 1–2, 2018, doi: 10.1109/WEROB.2017.8383853.

[24] D. Moher *et al.*, "Preferred reporting items for systematic reviews and meta-analyses: The PRISMA statement," *PLoS Medicine*, vol. 6, no. 7, 2009, doi: 10.1371/journal.pmed.1000097.

[25] P. Di, J. Huang, K. Sekiyama, and T. Fukuda, "A novel fall prevention scheme for intelligent cane robot by using a motor driven universal joint," in *2011 International Symposium on Micro-NanoMechatronics and Human Science*, Nov. 2011, pp. 391–396. doi: 10.1109/MHS.2011.6102215.

[26] T. Fukuda *et al.*, "Advanced service robotics for human assistance and support," in *2011 International Conference on Advanced Computer Science and Information Systems*, Dec. 2011, pp. 25–30.

[27] S. Nakagawa, P. D, J. Huang, K. Sekiyama, and T. Fukuda, "Control of intelligent cane robot considering usage of ordinary cane," in *2013 IEEE RO-MAN*, Aug. 2013, pp. 762–767. doi: 10.1109/ROMAN.2013.6628405.

[28] P. Di *et al.*, "Fall detection and prevention control using walking-aid cane robot," *IEEE/ASME Transactions on Mechatronics*, vol. 21, no. 2, pp. 625–637, 2016, doi: 10.1109/TMECH.2015.2477996.

[29] P. Di, J. Huang, S. Nakagawa, K. Sekiyama, and T. Fukuda, "Fall detection and prevention in the elderly based on the ZMP stability control," in *2013 IEEE Workshop on Advanced Robotics and its Social Impacts*, Nov. 2013, pp. 82–87. doi: 10.1109/ARSO.2013.6705510.

[30] P. Di, J. Huang, S. Nakagawa, K. Sekiyama, and T. Fukuda, "Fall detection for elderly by using an intelligent cane robot based on center of pressure (COP) stability theory," in *2014 International Symposium on Micro-NanoMechatronics and Human Science (MHS)*, Nov. 2014, pp. 1–4. doi: 10.1109/MHS.2014.7006152.

[31] T. Fukuda, J. Huang, P. Di, and K. Sekiyama, "Motion control and fall detection of intelligent cane robot," *Springer Tracts in Advanced Robotics*, vol. 106, pp. 317–337, 2015, doi: 10.1007/978-3-319-12922-8_12.

[32] P. Di, J. Huang, K. Sekiyama, and T. Fukuda, "Motion control of intelligent cane robot under normal and abnormal walking condition," in *2011 RO-MAN*, Jul. 2011, pp. 497–502. doi: 10.1109/ROMAN.2011.6005201.

[33] J. Huang, P. Di, T. Fukuda, and T. Matsuno, "Motion control of omni-directional type cane robot based on human intention," in *2008 IEEE/RSJ International Conference on Intelligent Robots and Systems*, 2008, pp. 273–278. doi: 10.1109/IROS.2008.4650936.

[34] P. Di *et al.*, "Optimal posture control for stability of intelligent cane robot," in *2012 IEEE RO-MAN: The 21st IEEE International Symposium on Robot and Human Interactive Communication*, 2012, pp. 725–730. doi: 10.1109/ROMAN.2012.6343837.

[35] P. Di, J. Huang, S. Nakagawa, K. Sekiyama, Q. Huang, and T. Fukuda, "Optimized Motion Control of an Intelligent Cane Robot for Easing Muscular Fatigue in the Elderly During Walking," *JOURNAL OF ROBOTICS AND MECHATRONICS*, vol. 25, no. 6, SI, pp. 1070–1077, Dec. 2013, doi: 10.20965/jrm.2013.p1070.

[36] H. Umverslty, "Real-Time Fall and Overturn Prevention Control for Human-Cane Robotic System Pei Di\ Jian Huang2, Shotaro Nakagawa\ Kosuke Sekiyama\ and Toshio Fukuda3,4 2," pp. 2–7.

[37] J. Huang, P. Di, K. Wakita, T. Fukuda, and K. Sekiyama, "Study of fall detection using intelligent cane based on sensor fusion," *2008 International Symposium on Micro-NanoMechatronics and Human Science, MHS 2008*, pp. 495–500, 2008, doi: 10.1109/MHS.2008.4752503.

[38] S. Nakagawa *et al.*, "Tandem Stance Avoidance Using Adaptive and Asymmetric Admittance Control for Fall Prevention," *IEEE Transactions on Neural Systems and Rehabilitation Engineering*, vol. 24, no. 5, pp. 542–550, May 2016, doi: 10.1109/TNSRE.2015.2429315.

[39] S. Nakagawa *et al.*, "Virtual friction model for control of cane robot," in *2015 24th IEEE International Symposium on Robot and Human Interactive Communication (RO-MAN)*, Aug. 2015, pp. 128–133. doi: 10.1109/ROMAN.2015.7333583.

[40] P. van Lam and Y. Fujimoto, "A Robotic Cane for Balance Maintenance Assistance," *IEEE Transactions on Industrial Informatics*, vol. 15, no. 7, pp. 3998–4009, 2019, doi: 10.1109/TII.2019.2903893.

[41] P. van Lam and Y. Fujimoto, "Completed hardware design and controller of the robotic cane using the inverted pendulum for walking assistance," in *2017 IEEE 26th International Symposium on Industrial Electronics (ISIE)*, Jun. 2017, pp. 1935–1940. doi: 10.1109/ISIE.2017.8001547.

[42] K. Shimizu, I. Smadi, and Y. Fujimoto, "Examination of a control method for a walking assistance robotics cane," in *IECON 2014 - 40th Annual Conference of the IEEE Industrial Electronics Society*, Oct. 2014, pp. 2768–2773. doi: 10.1109/IECON.2014.7048899.

[43] S. Itadera, T. Aoyama, Y. Hasegawa, K. Aimoto, K. Kato, and I. Kondo, "A clinical pilot study on posture stabilization via light contact with cane-type companion robot," *ROBOMECH Journal*, vol. 6, no. 1, 2019, doi: 10.1186/s40648-019-0145-y.

[44] S. Itadera, Y. Hasegawa, T. Fukuda, M. Tanimoto, and I. Kondo, "Adaptive walking load control for training physical strength using cane-type robot," in *2017 IEEE/RSJ International Conference on Intelligent Robots and Systems (IROS)*, 2017, pp. 521–526. doi: 10.1109/IROS.2017.8202202.

[45] S. Itadera *et al.*, "Coordinated movement algorithm for accompanying cane robot," in *2016 International Symposium on Micro-NanoMechatronics and Human Science (MHS)*, Nov. 2017, pp. 1–3. doi: 10.1109/MHS.2016.7824241.

[46] Q. Yan, J. Huang, C. Xiong, Z. Yang, and Z. Yang, "Data-Driven Human-Robot Coordination Based Walking State Monitoring With Cane-Type Robot," *IEEE Access*, vol. 6, pp. 8896–8908, 2018, doi: 10.1109/ACCESS.2018.2806563.

[47] Q. Yan, J. Huang, and W. Xu, "Limbs synergies based human motion intention estimation algorithm for using cane-type walking-aid robot," in *2017 2nd International Conference on Advanced Robotics and Mechatronics (ICARM)*, Aug. 2017, pp. 656–661. doi: 10.1109/ICARM.2017.8273240.

[48] C. Tao, Q. Yan, and Y. Li, "Hierarchical Shared Control of Cane-Type Walking-Aid Robot," *JOURNAL OF HEALTHCARE ENGINEERING*, vol. 2017, 2017, doi: 10.1155/2017/8932938.

[49] Q. Yan, J. Huang, and Z. Luo, "Human-robot coordination stability for fall detection and prevention using cane robot," in *2016 International Symposium on Micro-NanoMechatronics and Human Science (MHS)*, Nov. 2016, pp. 1–7. doi: 10.1109/MHS.2016.7824171.

[50] P. van Lam and Y. Fujimoto, "Two-Wheel Cane for Walking Assistance," in *2018 INTERNATIONAL POWER ELECTRONICS CONFERENCE (IPEC-NIIGATA 2018 -ECCE ASIA)*, 2018, pp. 571–574.

[51] P. van Lam, T. Shimono, and Y. Fujimoto, "Using a nonlinear disturbance observer to estimated the human force applied to a two-wheeled cane for walking assistance," *Proceedings: IECON 2018 - 44th Annual Conference of the IEEE Industrial Electronics Society*, vol. 1, pp. 5122–5127, 2018, doi: 10.1109/IECON.2018.8591158.

[52] M. A. Naeem and S. F. M. Assal, "Development of a 4-DOF cane robot to enhance walking activity of elderly," *Proceedings of the Institution of Mechanical Engineers, Part C: Journal of Mechanical Engineering Science*, 2019, doi: 10.1177/0954406219830440.

[53] M. A. Naeem, S. F. M. Assal, and A. A. Abouelsoud, "Modeling and real-time dynamic control of cane robot for fall prevention," in *2016 International Conference on Control, Decision and Information Technologies (CoDIT)*, Apr. 2016, pp. 694–699. doi: 10.1109/CoDIT.2016.7593647.

[54] H. Wang, B. Sun, X. Wu, H. Wang, and Z. Tang, "An intelligent cane walker robot based on force control," in *2015 IEEE International Conference on Cyber Technology in Automation, Control, and Intelligent Systems (CYBER)*, Jun. 2015, pp. 1333–1337. doi: 10.1109/CYBER.2015.7288137.

[55] M. R. Afzal, I. Hussain, Y. Jan, and J. Yoon, "Design of a haptic cane for walking stability and rehabilitation," in *2013 13th International Conference on Control, Automation and Systems (ICCAS 2013)*, Oct. 2013, pp. 1450–1454. doi: 10.1109/ICCAS.2013.6704114.

[56] R. Ady, W. Bachta, and P. Bidaud, "Development and control of a one-wheel telescopic active cane," in *5th IEEE RAS/EMBS International Conference on Biomedical Robotics and Biomechatronics*, Aug. 2014, pp. 461–466. doi: 10.1109/BIOROB.2014.6913820.

[57] S. Pyo, M. Oh, and J. Yoon, "Development of an active haptic cane for gait rehabilitation," in *2015 IEEE International Conference on Robotics and Automation (ICRA)*, May 2015, pp. 4464–4469. doi: 10.1109/ICRA.2015.7139817.

[58] S. Suzuki, Y. Hirata, and K. Kosuge, "Development of Intelligent Passive Cane controlled by servo brakes," in *RO-MAN 2009 - The 18th IEEE International Symposium on Robot and Human Interactive Communication*, 2009, pp. 97–102. doi: 10.1109/ROMAN.2009.5326139.

[59] T. Ito and G. Oshita, "Development of MR fluid-based gait assist cane for elderly people," in *2015 IEEE International Conference on Advanced Intelligent Mechatronics (AIM)*, Jul. 2015, pp. 694–699. doi: 10.1109/AIM.2015.7222618.

[60] Y.-Z. Zhang and S.-S. Yeh, "Motion control design for robotic walking support systems using admittance motion command generator," in *IMECS 2011 - International MultiConference of Engineers and Computer Scientists 2011*, 2011, vol. 2, pp. 781–786. [Online]. Available: https://www.scopus.com/inward/record.uri?eid=2-s2.0-79960583239&partnerID=40&md5=7e8bccee92b9ee738f160c224d1cf946

[61] M. Kojima *et al.*, "Research on walking support method using cooperative cane robots," in *2018 International Symposium on Micro-NanoMechatronics and Human Science (MHS)*, Dec. 2018, pp. 1–3. doi: 10.1109/MHS.2018.8887027.

[62] K. Yamada, K. Ohara, A. Ichikawa, and T. Fukuda, "User intention estimation by grip sensor for cane-type walking support robot," 2017. doi: 10.1109/MHS.2016.7824207.

[63] M. Kato, A. Ichikawa, I. Kondo, and T. Fukuda, "Walking-aid cane robot applying light touch effect," in *2017 International Symposium on Micro-NanoMechatronics and Human Science (MHS)*, Dec. 2017, pp. 1–6. doi: 10.1109/MHS.2017.8305182.

[64] K. Wakita, J. Huang, P. Di, K. Sekiyama, and T. Fukuda, "Human-Walking-Intention-Based Motion Control of an Omnidirectional-Type Cane Robot," *IEEE/ASME Transactions on Mechatronics*, vol. 18, no. 1, pp. 285–296, Feb. 2013, doi: 10.1109/TMECH.2011.2169980.

[65] W. Inc., "Capacitive 6-axis force/torque sensor (500N)." [Online]. Available: https://wacoh-tech.com/en/products/dynpick/500n.html

[66] Forsentek, "Bi-axial load cell force sensor." [Online]. Available: http://www.forsentek.com/prodetail_404.html

[67] Futek, "Biaxial Load Cell MBA400-FSH03934." [Online]. Available: https://www.futek.com/store/multi-axis-sensors/biaxial/biaxial-load-cell-MBA400/FSH03934

[68] Y. Hirata, A. Muraki, and K. Kosuge, “Motion control of intelligent passive-type walker for fall-prevention function based on estimation of user state,” *Proceedings - IEEE International Conference on Robotics and Automation*, vol. 2006, no. May, pp. 3498–3503, 2006, doi: 10.1109/ROBOT.2006.1642236.

[69] L. Resnik, S. Allen, D. Isenstadt, M. Wasserman, and L. Iezzoni, “Perspectives on use of mobility aids in a diverse population of seniors: Implications for intervention,” *Disability and Health Journal*, vol. 2, no. 2, pp. 77–85, 2009, doi: 10.1016/j.dhjo.2008.12.002.

[70] F. I. Care, “How to Encourage a Senior Parent to Use a Cane or Walker.” 2020. [Online]. Available: https://www.firstincare.com/senior-care-advice/how-to-encourage-a-senior-parent-to-use-a-cane-or-walker/

[71] C. Luz, T. Bush, X. Shen, and R. Pruchno, “Do canes or walkers make any difference? nonuse and fall injuries,” *Gerontologist*, vol. 57, no. 2, pp. 211–218, 2017, doi: 10.1093/geront/gnv096.

[72] B. Norman, “Canes, Crutches and Walkers.” Muscular Dystrophy Association, 2007. [Online]. Available: https://www.mda.org/quest/article/canes-crutches-and-walkers

[73] N. Owen, G. Healy, C. Matthews, and D. Dunstan, “Too Much Sitting: The Population Health Science of Sedentary Behavior,” *Exerc Sport Sci Rev*, vol. 38, pp. 105–113, 2010, doi: 10.1097/JES.0b013e3181e373a2.

[74] M. S. W. Yu, C. C. H. Chan, and R. K. M. Tsim, “Usefulness of the Elderly Mobility Scale for classifying residential placements,” *Clinical Rehabilitation*, vol. 21, no. 12, pp. 1114–1120, 2007, doi: 10.1177/0269215507080789.

[75] E. G. Spilg, B. J. Martin, S. L. Mitchell, and T. C. Aitchison, “Falls risk following discharge from a geriatric day hospital,” *Clinical Rehabilitation*, vol. 17, no. 3, pp. 334–340, 2003, doi: 10.1191/0269215503cr615oa.

[76] P. Patil, K. S. Kumar, N. Gaud, and V. B. Semwal, “Clinical Human Gait Classification: Extreme Learning Machine Approach,” *1st International Conference on Advances in Science, Engineering and Robotics Technology 2019, ICASERT 2019*, vol. 2019, no. Icasert, pp. 2–7, 2019, doi: 10.1109/ICASERT.2019.8934463.

[77] N. Abhayasinghe and I. Murray, “Human gait phase recognition based on thigh movement computed using IMUs,” *IEEE ISSNIP 2014 - 2014 IEEE 9th International Conference on Intelligent Sensors, Sensor Networks and Information Processing, Conference Proceedings*, no. April, pp. 21–24, 2014, doi: 10.1109/ISSNIP.2014.6827604.

[78] R. Grasso, L. Bianchi, and F. Lacquaniti, “Motor patterns for human gait: Backward versus forward locomotion,” *Journal of Neurophysiology*, vol. 80, no. 4, pp. 1868–1885, 1998, doi: 10.1152/jn.1998.80.4.1868.

[79] L. Ren, R. K. Jones, and D. Howard, “Predictive modelling of human walking over a complete gait cycle,” *Journal of Biomechanics*, vol. 40, no. 7, pp. 1567–1574, 2007, doi: 10.1016/j.jbiomech.2006.07.017.

[80] L. A. Research, I. Education Institute, R. L. A. N. R. Center, R. L. A. N. R. Center. P. Service, and R. L. A. N. R. Center. P. T. Department, *Observational Gait Analysis*. Los Amigos Research and Education Institute, Rancho Los Amigos National Rehabilitation Center, 2001. [Online]. Available: https://books.google.pt/books?id=sZdMPgAACAAJ

[81] K. Kong and M. Tomizuka, “Smooth and continuous human gait phase detection based on foot pressure patterns,” *Proceedings - IEEE International Conference on Robotics and Automation*, pp. 3678–3683, 2008, doi: 10.1109/ROBOT.2008.4543775.

[82] M. Abid, N. Mezghani, and A. Mitiche, “Knee joint biomechanical gait data classification for knee pathology assessment: A literature review,” *Applied Bionics and Biomechanics*, vol. 2019, 2019, doi: 10.1155/2019/7472039.

[83] H. (Howe) Liu, J. Eaves, W. Wang, J. Womack, and P. Bullock, “Assessment of canes used by older adults in senior living communities,” *Archives of Gerontology and Geriatrics*, vol. 52, no. 3, pp. 299–303, 2011, doi: 10.1016/j.archger.2010.04.003.

[84] S. R. Faruqui and T. Jaeblon, “Ambulatory assistive devices in orthopaedics: Uses and modifications,” *Journal of the American Academy of Orthopaedic Surgeons*, vol. 18, no. 1, pp. 41–50, 2010, doi: 10.5435/00124635-201001000-00006.

[85] C. T. P. Camara, S. M. S. F. de Freitas, C. A. Lima, C. F. Amorim, J. M. Prado-Rico, and M. R. Perracini, “The walking cane length influences the postural sway of community-dwelling older women,” *Physiotherapy Research International*, vol. 25, no. 1, pp. 1–9, 2020, doi: 10.1002/pri.1804.

[86] K. Kim and Y. J. Cha, “Cane length influence on the plantar pressure distribution of adult hemiplegia patients,” *Journal of Physical Therapy Science*, vol. 23, no. 3, pp. 451–454, 2011, doi: 10.1589/jpts.23.451.

[87] SeniorSupported, “What is the proper height for a cane?” [Online]. Available: https://seniorsupported.com/importance-of-length-of-walking-canes/

[88] E. P. Choi, S. J. Yang, A. H. Jung, H. S. Na, Y. O. Kim, and K. H. Cho, “Changes in Lower Limb Muscle Activation and Degree of Weight Support according to Types of Cane-Supported Gait in Hemiparetic Stroke Patients,” *BioMed Research International*, vol. 2020, 2020, doi: 10.1155/2020/9127610.

[89] A. H. Maslow, “A theory of human motivation.,” *Psychological Review*, vol. 50, no. 4, pp. 370–396, 1943, doi: 10.1037/h0054346.

[90] O. A. Atoyebi *et al.*, “Mobility Challenges Among Older Adult Mobility Device Users,” *Current Geriatrics Reports*, vol. 8, no. 3, pp. 223–231, 2019, doi: 10.1007/s13670-019-00295-5.

[91] Dring, “Dring: the connected rod.” [Online]. Available: https://dring.io/

[92] HIP’GUARD, “Hip’Safe.” [Online]. Available: https://hipguard.eu/en/

[93] A. I. Batavia and G. S. Hammer, “Toward the development of consumer-based criteria for the evaluation of assistive devices,” *Journal of Rehabilitation Research and Development*, vol. 27, no. 4, pp. 425–436, 1990, doi: 10.1682/jrrd.1990.10.0425.

[94] ISO, “ISO 11334-4:1999 - Walking aids manipulated by one arm — Requirements and test methods — Part 4: Walking sticks with three or more legs.” [Online]. Available: https://www.iso.org/standard/24915.html

[95] ISO, “ISO 10993-1:2018 - Biological evaluation of medical devices — Part 1: Evaluation and testing within a risk management process.” [Online]. Available: https://www.iso.org/standard/68936.html

[96] ISO, “ISO 24415-1:2009 - Tips for assistive products for walking — Requirements and test methods — Part 1: Friction of tips.” [Online]. Available: https://www.iso.org/standard/42202.html

[97] J. A. Lenker, F. Harris, M. Taugher, and R. O. Smith, “Consumer perspectives on assistive technology outcomes,” *Disability and Rehabilitation: Assistive Technology*, vol. 8, no. 5, pp. 373–380, 2013, doi: 10.3109/17483107.2012.749429.

[98] L. J. Cohen and R. Perling, “Barriers to mobility device access: Implications for policies and practices of assistive technology reutilization programs,” *Topics in Geriatric Rehabilitation*, vol. 31, no. 1, pp. 19–25, 2015, doi: 10.1097/TGR.0000000000000047.

[99] P. H. Chen, Y. H. Li, C. W. Chiou, C. Y. Lee, and J. M. Lin, “A smart safety cane for human fall detection,” *International Journal of Ad Hoc and Ubiquitous Computing*, vol. 20, no. 1, pp. 49–65, 2015, doi: 10.1504/IJAHUC.2015.071662.

[100] ISO, “ISO 24415-2:2011 - Tips for assistive products for walking — Requirements and test methods — Part 2: Durability of tips for crutches.” [Online]. Available: https://www.iso.org/standard/42273.html

[101] J. D. Evans, *Statistics for the behavioural sciences 7th edition*. 1996.

[102] P. Sedgwick, “Pearson’s correlation coefficient,” *BMJ (Online)*, vol. 345, no. 7864, pp. 1–2, 2012, doi: 10.1136/bmj.e4483.

[103] S. M. Bradley and C. R. Hernandez, “Geriatric assistive devices,” *American Family Physician*, vol. 84, no. 4, pp. 405–411, 2011.

[104] “ORTHOS XII, P1 Tripod.” [Online]. Available: https://www.orthosxxi.com/pt/product/piramide-tripe-cab-crv-p1-anz-chpbase-prt

[105] W. R. de Silva and R. Munasinghe, “Development of a holonomic mobile robot for field applications,” *ICIIS 2009 - 4th International Conference on Industrial and Information Systems 2009, Conference Proceedings*, no. December, pp. 499–504, 2009, doi: 10.1109/ICIINFS.2009.5429809.

[106] F. Tajti, G. Szayer, B. Kovács, and P. Korondi, *Robot base with holonomic drive*, vol. 19, no. 3. IFAC, 2014. doi: 10.3182/20140824-6-za-1003.00785.

[107] “100mm Double Plastic OmniWheel w/ Central Bearing - RobotShop.” [Online]. Available: https://www.robotshop.com/eu/en/100mm-double-plastic-omni-wheel-central-bearing.html

[108] M. Goodrich and A. Schultz, “Human-Robot Interaction: A Survey,” *Foundations and Trends in Human-Computer Interaction*, vol. 1, pp. 203–275, 2007, doi: 10.1561/1100000005.

[109] STM32CubeIDE installation guide Introduction, “STM32 Nucleo-64 User Manual,” vol. 3304, no. January, pp. 1–148, 2012.

[110] X. Wang, J. Ellul, and G. Azzopardi, “Elderly Fall Detection Systems: A Literature Survey,” *Frontiers in Robotics and AI*, vol. 7, no. June, 2020, doi: 10.3389/frobt.2020.00071.

[111] "Jetson Nano 2GB Developer Kit User Guide." NVIDIA. [Online]. Available: https://developer.nvidia.com/embedded/learn/jetson-nano-2gb-devkit-user-guide

[112] "FSR 101 Force Sensing Resistor Theory and Applications." Sensitronics, pp. 1–15, 2017. [Online]. Available: https://www.sensitronics.com/fsr101.htm

[113] C. Lebossé, B. Bayle, M. de Mathelin, and P. Renaud, "Nonlinear modeling of low cost force sensors," *Proceedings - IEEE International Conference on Robotics and Automation*, pp. 3437–3442, 2008, doi: 10.1109/ROBOT.2008.4543736.

[114] InterlinkElectronics, "FSR (Force Sensing Resistors)," no. 94, 2015, [Online]. Available: https://www.generationrobots.com/media/FSR400-Series-Integration-Guide.pdf

[115] "FSR ® 400 Series Data Sheet Human - Machine Interface Solutions for a Connected World FSR ® 400 Series Data Sheet." Interlink Electronics, 2015. [Online]. Available: https://cdn2.hubspot.net/hubfs/3899023/Interlinkelectronics November2017/Docs/Datasheet_FSR.pdf

[116] "Force Sensing Resistor Integration Guide and Evaluation Parts Catalog." Interlink Electronics, p. 26. [Online]. Available: https://www.sparkfun.com/datasheets/Sensors/Pressure/fsrguide.pdf

[117] "Voltage Converter TL7660CDR." Texas Instruments. [Online]. Available: https://www.digikey.pt/product-detail/en/texas-instruments/TL7660CDR/296-21856-1-ND/1629226

[118] M. Çelebi, "Digital Filter Design Based on ARDUINO and Its Applications," *TIPTEKNO 2020 - Tip Teknolojileri Kongresi - 2020 Medical Technologies Congress, TIPTEKNO 2020*, pp. 263–266, 2020, doi: 10.1109/TIPTEKNO50054.2020.9299311.

[119] M. J. Brown and D. E. Jacobs, "Residential light and risk for Depression and falls: Results from the LARES study of eight European cities," *Public Health Reports*, vol. 126, no. SUPPL. 1, pp. 131–141, 2011, doi: 10.1177/00333549111260s117.

[120] C. Todd and D. Skelton, "What are the main risk factors for falls amongst older people and what are the most effective interventions to prevent these falls ?," *World Health*, no. March, p. 28, 2004, [Online]. Available: http://scholar.google.com/scholar?hl=en&btnG=Search&q=intitle:What+are+the+main+risk+factors+for+falls+amongst+older+people+and+what+are+the+most+effective+interventions+to+prevent+these+falls+?#0

[121] "LSM6DSOX + LIS3MDL 9 DOF IMU." Adafruit Industries LLC. [Online]. Available: https://www.digikey.pt/product-detail/pt/adafruit-industries-llc/4517/1528-4517-ND/11684812

[122] R. Velik, "Effect of On-Demand Cueing on Freezing of Gait in Parkinson' s Patients," *International Journal of Medical, Pharmaceutical Science and Engineering*, vol. 6, no. 6, pp. 10–15, 2012, [Online]. Available: http://www.researchgate.net/publication/257846272_Effect_of_On-Demand_Cueing_on_Freezing_of_Gait_in_Parkinsons_Patients%0Ahttp://xueshu.baidu.com/s?wd=paperuri%3A%28c244e5319d871615c55319fdddc5827b%29&filter=sc_long_sign&sc_ks_para=q%3DEffect of On-Demand

[123] E. van Wegen *et al.*, "The effect of rhythmic somatosensory cueing on gait in patients with Parkinson's disease," *Journal of the Neurological Sciences*, vol. 248, no. 1–2, pp. 210–214, 2006, doi: 10.1016/j.jns.2006.05.034.

[124] “Albert - Haptic Feedback Cane.” miio-studio. [Online]. Available: https://www.miio-studio.com/albert

[125] V. S. Chib, K. M. Lynch, J. L. Patton, F. A. Mussa-Ivaldi, K. Myles, and M. S. Binseel, “The Tactile Modality: A Review of Tactile Sensitivity and Human Tactile Interfaces,” *Proceedings - 12th International Symposium on Haptic Interfaces for Virtual Environment and Teleoperator Systems, HAPTICS*, no. May, pp. 375–382, 2004, [Online]. Available: http://oai.dtic.mil/oai/oai?verb=getRecord&metadataPrefix=html&identifier=ADA468389

[126] “Model No. 310-103.005 10mm Vibration Motor - 3mm Type.” Precision Microdrives. [Online]. Available: https://catalogue.precisionmicrodrives.com/product/310-103-005-10mm-vibration-motor-3mm-type

[127] “Haptic Motor Driver - DRV2605L.” SparkFun. [Online]. Available: https://www.sparkfun.com/products/14538

[128] “Driving Vibration Motors With Pulse Width Modulation.” Precision Microdrives. [Online]. Available: https://www.precisionmicrodrives.com/ab-012

[129] “3W LED - Keyestudio.” [Online]. Available: https://abcescolar.pt/products/modulo-led-de-3w-para-arduino-keyestudio?_pos=1&_sid=576fc4bed&_ss=r

[130] “NEMA23 High Torque DC Servo Motor 300RPM With Step/Dir Drive.” Active-Robots. [Online]. Available: https://www.active-robots.com/high-torque-dc-servo-motor-300rpm-with-step-dir-drive.html

[131] “Gens ace 8000mAh 14.8V 80C 4S2P Lipo Battery Pack with EC5 Plug.” Gens Ace. [Online]. Available: http://www.gabahobby.com/v2/lipo2-lithium-polymer-/349369-gens-ace-8000mah-14-8v-80c-4s2p-lipo-battery-pack-with-ec5-plug.html

[132] “Step-Down DC-DC Converter with current regulation 8A.” [Online]. Available: https://www.botnroll.com/pt/conversores-dcdc/3675-conversor-dc-dc-step-down-12a-c-regula-o-de-corrente.html?fbclid=IwAR1pVrMKV2yySMezPY6S-8SoDnJipkpKF_lk9gXTmXiUO_qXmGf007iwYzs

[133] “Step-Down DC-DC Converter 300W up to 20A.” [Online]. Available: https://www.botnroll.com/pt/conversores-dcdc/4003-conversor-dc-dc-step-down-300w-at-20a.html

[134] “FUSE GLASS 7A 250VAC 3AB 3AG.” Littlefuse Inc. [Online]. Available: https://www.digikey.pt/product-detail/pt/littelfuse-inc/0312007-MXP/F4785-ND/778273

[135] “Rocking Push Button with 230 VAC with Illumination - Red.” [Online]. Available: https://www.botnroll.com/pt/interruptores-botoes/2652-bot-o-de-press-o-basculante-com-ilumina-o-230vac-vermelho.html

[136] S. Campbell, “Basic of the I2C communication protocol.” Circuit Basics. [Online]. Available: https://www.circuitbasics.com/basics-of-the-i2c-communication-protocol/

[137] A. Corporation, “Data Sheet ATmega328P,” pp. 1–294, 2015, [Online]. Available: http://ww1.microchip.com/downloads/en/DeviceDoc/Atmel-7810-Automotive-Microcontrollers-ATmega328P_Datasheet.pdf

[138] U. S. B. Otg and H. S. Fs, “STM32 F446RE Datasheet,” no. January. 2021. [Online]. Available: https://www.st.com/resource/en/datasheet/stm32f446re.pdf

[139] N. M. Peel, S. S. Kuys, and K. Klein, “Gait speed as a measure in geriatric assessment in clinical settings: A systematic review,” *Journals of Gerontology - Series A Biological Sciences and Medical Sciences*, vol. 68, no. 1, pp. 39–46, 2013, doi: 10.1093/gerona/gls174.

[140] J. Ballesteros, A. Tudela, J. R. Caro-Romero, and C. Urdiales, “Weight-bearing estimation for cane users by using onboard sensors,” *Sensors (Switzerland)*, vol. 19, no. 3, pp. 1–13, 2019, doi: 10.3390/s19030509.

[141] J. W. Youdas, B. J. Kotajarvi, D. J. Padgett, and K. R. Kaufman, “Partial weight-bearing gait using conventional assistive devices,” *Archives of Physical Medicine and Rehabilitation*, vol. 86, no. 3, pp. 394–398, 2005, doi: 10.1016/j.apmr.2004.03.026.

[142] “Strain Gage Technical Data.” Omega. [Online]. Available: https://www.omega.co.uk/techref/pdf/STRAIN_GAGE_TECHNICAL_DATA.pdf

[143] “Strain sensor with mV/V-output (strain gauge measuring bridge).” XSensors. [Online]. Available: http://www.swsensors.com/admin/uploadpic/201806/20180604133455529.pdf

[144] “Measuring Strain with Strain Gages.” NI - Engineer Ambitiously. [Online]. Available: https://www.ni.com/pt-pt/innovations/white-papers/07/measuring-strain-with-strain-gages.html

[145] X. Hu and X. Qu, “Pre-impact fall detection,” *BioMedical Engineering Online*, vol. 15, no. 1, pp. 1–16, 2016, doi: 10.1186/s12938-016-0194-x.

[146] N. A. Mohamed, M. A. Zulkifley, A. A. Ibrahim, and M. Aouache, “Optimal training configurations of a CNN-LSTM-based tracker for a fall frame detection system,” *Sensors*, vol. 21, no. 19, pp. 1–34, 2021, doi: 10.3390/s21196485.

[147] T. H. Kim, A. Choi, H. M. Heo, H. Kim, and J. H. Mun, “Acceleration magnitude at impact following loss of balance can be estimated using deep learning model,” *Sensors (Switzerland)*, vol. 20, no. 21, pp. 1–17, 2020, doi: 10.3390/s20216126.

[148] N. Noury, P. Rumeau, A. K. Bourke, G. ÓLaighin, and J. E. Lundy, “A proposal for the classification and evaluation of fall detectors,” *Irbm*, vol. 29, no. 6, pp. 340–349, 2008, doi: 10.1016/j.irbm.2008.08.002.

[149] S. Fudickar, A. Lindemann, and B. Schnor, “Threshold-based fall detection on smart phones,” *HEALTHINF 2014 - 7th International Conference on Health Informatics, Proceedings; Part of 7th International Joint Conference on Biomedical Engineering Systems and Technologies, BIOSTEC 2014*, no. March, pp. 303–309, 2014, doi: 10.5220/0004795803030309.

[150] S. Palipana, D. Rojas, P. Agrawal, and D. Pesch, “FallDeFi,” *Proceedings of the ACM on Interactive, Mobile, Wearable and Ubiquitous Technologies*, vol. 1, no. 4, pp. 1–25, 2018, doi: 10.1145/3161183.

[151] T. Tamura, T. Yoshimura, M. Sekine, M. Uchida, and O. Tanaka, “A wearable airbag to prevent fall injuries,” *IEEE Transactions on Information Technology in Biomedicine*, vol. 13, no. 6, pp. 910–914, 2009, doi: 10.1109/TITB.2009.2033673.

[152] R. Igual, C. Medrano, and I. Plaza, “Challenges, issues and trends in fall detection systems,” *BioMedical Engineering Online*, vol. 12, no. 1, 2013, doi: 10.1186/1475-925X-12-66.

[153] C. Chen, R. Jafari, and N. Kehtarnavaz, “A survey of depth and inertial sensor fusion for human action recognition,” *Multimedia Tools and Applications*, vol. 76, no. 3, pp. 4405–4425, 2017, doi: 10.1007/s11042-015-3177-1.

[154] N. Otanasap and P. Boonbrahm, “Falling Pattern Analysis Based on 3D Euclidean Distance of Human Skeleton Joints,” *The International Conference on Information and Communication Technology for Embedded Systems (ICICTES2014)*, no. June, pp. 3–8, 2014, [Online]. Available: https://saki.siit.tu.ac.th/icictes2014/

[155] “LIDAR-Lite 3 Laser Rangefinder.” Garmin. [Online]. Available: https://www.robotshop.com/eu/en/lidar-lite-3-laser-rangefinder.html

[156] “YDLIDAR TG30 360° Laser Scanner (30 m).” YDLIDAR. [Online]. Available: https://www.robotshop.com/eu/en/ydlidar-tg30-360-laser-scanner-30-m.html

[157] “Yujin YRL Series 3d LiDAR - 5m range - 270° horizontal & 90° vertical f.o.v.” Yujin Robot. [Online]. Available: https://www.robotshop.com/eu/en/yujin-yrl-series-3d-lidar-5m-range-270-horizontal-90-vertical-fov-exceptional-performance-price.html

[158] Z. Zhang, C. Conly, and V. Athitsos, “A survey on vision-based fall detection,” *8th ACM International Conference on PErvasive Technologies Related to Assistive Environments, PETRA 2015 - Proceedings*, 2015, doi: 10.1145/2769493.2769540.

[159] O. S. Seredin, A. v. Kopylov, S. C. Huang, and D. S. Rodionov, “A skeleton features-based fall detection using Microsoft Kinect v2 with one class-classifier outlier removal,” *International Archives of the Photogrammetry, Remote Sensing and Spatial Information Sciences - ISPRS Archives*, vol. 42, no. 2/W12, pp. 189–195, 2019, doi: 10.5194/isprs-archives-XLII-2-W12-189-2019.

[160] “Microsoft Kinect.” [Online]. Available: https://developer.microsoft.com/pt-pt/windows/kinect/

[161] “Microsoft Azure Kinect.” 2019. [Online]. Available: https://azure.microsoft.com/zh-cn/services/kinect-dk/

[162] Z. Zhang, “Microsoft kinect sensor and its effect,” *IEEE Multimedia*, vol. 19, no. 2, pp. 4–10, 2012, doi: 10.1109/MMUL.2012.24.

[163] U. S. B. Otg and H. S. Fs, “STM32 F446RE Datasheet,” no. January, 2021, [Online]. Available: https://www.st.com/resource/en/datasheet/stm32f446re.pdf

[164] “STM32 F446RE Board Pinouts.” [Online]. Available: https://os.mbed.com/platforms/ST-Nucleo-F446RE/

[165] “Jetson Nano 2GB Developer Kit.” NVIDIA. [Online]. Available: https://developer.nvidia.com/embedded/jetson-nano-2gb-developer-kit

[166] “Cmos Voltage Converter Description / Ordering Information Cmos Voltage Converter,” no. June, 2006, [Online]. Available: https://www.ti.com/lit/ds/symlink/tl7660.pdf?ts=1647445785176&ref_url=https%253A%252F%252Fwww.ti.com%252Fproduct%252FTL7660

[167] “MUX50x 36-V , Low-Capacitance , Low-Leakage-Current , Precision Analog Multiplexers,” 2016, [Online]. Available: https://www.ti.com/lit/ds/symlink/mux506.pdf?ts=1647445822819&ref_url=https%253A%252F%252Fwww.ti.com%252Fproduct%252FMUX506%253Fqgpn%253Dmux506

[168] “Vibrating Mini Motor Disc.” PT Robotics. [Online]. Available: https://www.ptrobotics.com/motor-dc/2951-vibrating-mini-motor-disc.html?gclid=CjwKCAiAhreNBhAYEiwAFGGKPOmLwtuwrgiLNIbP0hGAQWW6ibQRFq6doO4c5GaK8WMilrEVU-gVbhoCkAsQAvD_BwE

[169] P. H. Appliance, “Installation Manual and Datasheet,” no. 847, pp. 1–6, 2000.

[170] “NVIDIA Jetson Nano 2GB Developer Kit.” Sparkfun. [Online]. Available: https://www.sparkfun.com/products/17244

[171] “FAN - TUBEAXIAL 5V RIB STD 2 WIRES.” NMB Technologies Corporation. [Online]. Available: https://www.digikey.pt/products/pt?keywords=12-04020VA-05Q-AA-00-ND

[172] “Edimax EW-7811Un Wireless N Nano USB 150Mbps.” [Online]. Available: https://www.pccomponentes.pt/edimax-ew-7811un-wireless-n-nano-usb-150mbps?kk=a4c6327-1757416fa1e-2d9ed&gclid=Cj0KCQjws-OEBhCkARIsAPhOkIYt2H_H6wwJvBUVjp9YIGcwea2CcJYmtMFDHoTDo7ANktdnudfx3q8aAsnmEALw_wcB&utm_source=kelkoopt&utm_medium=cpc&utm_campaign=kelko

[173] “SD Memory Card MICROSDXC 64GB CLS10 TLC.” ATP Electronics, Inc. [Online]. Available: https://www.digikey.pt/product-detail/pt/atp-electronics-inc/AF64GUD4-BBBXM/1282-AF64GUD4-BBBXM-ND/12336510

[174] “NUCLEO-64 STM32F446RE.” STMicroelectronics. [Online]. Available: https://www.digikey.pt/products/pt?keywords=NUCLEO-F446RE

[175] “FSR 402 - Force Sensor.” Interlink Electronics. [Online]. Available: https://www.digikey.pt/product-detail/pt/interlink-electronics/34-00015/1027-1018-ND/5416350

[176] “FSR 402 - Force Sensor.” Interlink Electronics. [Online]. Available: https://www.digikey.pt/product-detail/pt/interlink-electronics/34-00004/1027-1014-ND/2798665

[177] “Multiplexer - MUX506IPWR.” Texas Instruments. [Online]. Available: https://www.digikey.pt/product-detail/en/texas-instruments/MUX506IPWR/296-48620-1-ND/8567664

[178] “OpAmp - MIC7300YM5-TR.” Microchip Technology. [Online]. Available: https://www.digikey.pt/product-detail/en/microchip-technology/MIC7300YM5-TR/576-1319-1-ND/771923

[179] “Capacitor 10uF.” KEMET. [Online]. Available: https://www.digikey.pt/product-detail/en/kemet/C0805X106J9RAC7800/399-15703-6-ND/7427633

[180] “PHOTOCELL 16-33KOHM.” Advanced Photonix.

[181] “USB type-C cable.” Tripp Lite. [Online]. Available: https://www.digikey.pt/product-detail/pt/tripp-lite/U040-006-C-5A/TL2261-ND/7696257

[182] “USB type-A to Mini-B cable.” CUI Devices. [Online]. Available: https://www.digikey.pt/product-detail/pt/cui-devices/CBLT-UA-MB-1/102-5948-ND/9838600

[183] “EC5 Cable - Male.” AMASS. [Online]. Available: https://mauser.pt/catalog/product_info.php?cPath=1874_640_2465&products_id=011-2276

[184] “JST Connector.” SparkFun Electronics. [Online]. Available: https://www.digikey.pt/product-detail/en/sparkfun-electronics/PRT-09914/1568-1568-ND/6833927

[185] “6-PinHeader 2.5mm.” Molex. [Online]. Available: https://www.digikey.pt/product-detail/en/0353120660/WM14768-ND/3185044?itemSeq=368356647

[186] “2-Pin Terminal Block.” Weidmüller. [Online]. Available: https://www.digikey.pt/product-detail/pt/1716020000/281-1435-ND/269780?itemSeq=368359496

[187] “Fuse Support Clip 250V 15A.” Littelfuse Inc. [Online]. Available: https://www.digikey.pt/product-detail/pt/littelfuse-inc/01020071Z/F3781-ND/2498889

Appendices

Appendix I

This appendix contains an example of the Elderly Mobility Scale (EMS), a mobility assessment tool explored during the third chapter.

Table A.1: Elderly Mobility Scale (EMS) [88]

Task	Scores	Date
Lying to Sitting	2 Independent 1 Needs help of 1 person 0 Needs help of 2+ people	
Sitting to Lying	2 Independent 1 Needs help of 1 person 0 Needs help of 2+ people	
Sitting to Standing	3 Independent in under 3 seconds 2 Independent in over 3 seconds 1 Needs help of 1 person 0 Needs help of 2+ people	
Standing	3 Stands without support and able to reach 2 Stands without support but needs support to reach 1 Stands but needs support 0 Stands only with physical support of another person	
Gait	3 Independent (+ / - stick) 2 Independent with frame 1 Mobile with walking aid but erratic/unsafe 0 Needs physical help to walk or constant supervision	
Timed Walk (6 meters)	3 Under 15 seconds 2 16-30 seconds 1 Over 30 seconds 0 Unable to cover 6 meters (Recorded time in seconds)	
Functional Reach	4 Over 20 cm 2 10-20 cm 0 Under 10 cm (Actual reach in centimeters)	
	Score	/20

Appendix II

This appendix is related to all the electronic components instrumented in the ACRane, being represented their technical specifications along with the respective electronic circuits and connections.

- **Low-level control unit**

Table A.2: STM32 F446RE technical specifications [163][90]

STM32 F446RE Technical Specifications	
CPU	Arm® Cortex®-M4 32-bit
Clock Speed	180 MHz
CPU Flash Memory	512 Kbytes
SRAM	128 Kbytes
Voltage Supply (USB)	5V
Voltage Supply (External)	3.3V; 5V; 7 - 12V
GPIO Pins	50
PWM pins	30
Analog Pins	16
UART ports	4
SPI ports	4
I2C ports	4

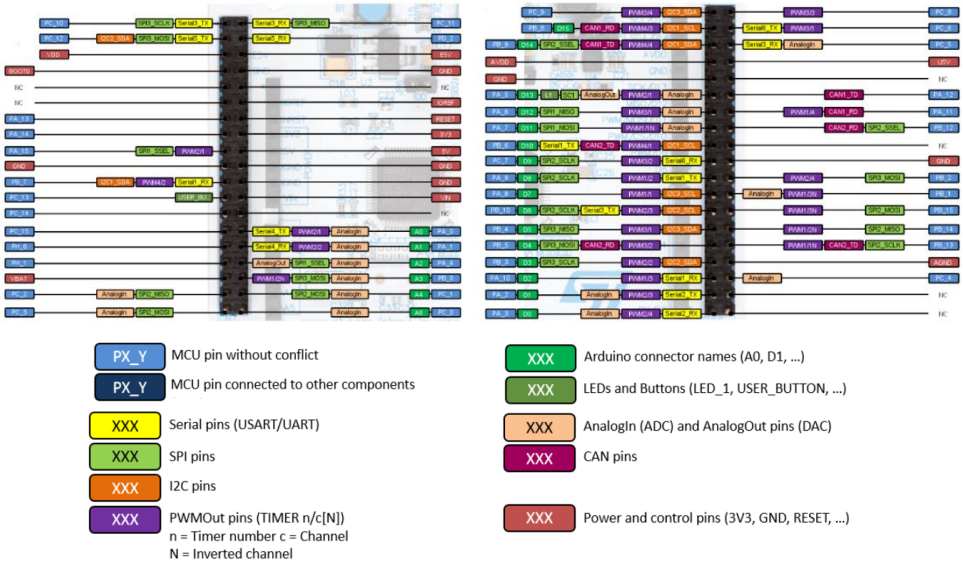

Figure A.1: STM32 F446RE board pinout and pins legend [155][151].

Table A.3: Pin functions and connections of the STM32 F446RE board pins used in the cane system

STM32F446RE Pins	Pin Function	Pin Connection
PA_0	Analog Input	Photoresistor
PA_7	Digital Output	LED
PC_2	Analog Input	FSR (Handle)
PA_13	Digital Output	Mux EN (Handle)
PA_14	Digital Output	Mux A0 (Handle)
PA_15	Digital Output	Mux A1 (Handle)
PH_1	Digital Output	Mux A2 (Handle)
PC_3	Analog Input	FSR (Axial)
PA_11	Digital Output	Mux EN (Axial)
PA_12	Digital Output	Mux A0 (Axial)
PC_6	Digital Output	Mux A1 (Axial)
PC_8	Digital Output	Mux A2 (Axial)
PB_8	I2C SCL (Channel 1)	IMU SCL
PB_9	I2C SDA (Channel 1)	IMU SDA
PB_5	Digital Output	Motor 1 Pulse/Steps
PA_10	Digital Output	Motor 1 Direction
PA_6	Digital Output	Motor 2 Pulse/Steps
PC_5	Digital Output	Motor 2 Direction
PB_1	Digital Output	Motor 3 Pulse/Steps
PB_2	Digital Output	Motor 3 Direction
PA_8	I2C SCL (Channel 3)	Vibrotactile Motors SCL
PB_4	I2C SDA (Channel 3)	Vibrotactile Motors SDA
PC_7	PWM Output	Vibrotactile Motors IN
PA_9	Digital Output	Vibrotactile Motor 1 EN
PB_6	Digital Output	Vibrotactile Motor 2 EN

- **High-level control unit**

Table A.4: NVIDIA® Jetson Nano™ 2GB Developer Kit technical specifications [165]

NVIDIA® Jetson Nano™ 2GB Developer Kit Technical Specifications	
CPU	Quad-core ARM® A57 @ 1.43 GHz
GPU	128-core NVIDIA Maxwell™
Memory	2 GB 64-bit LPDDR4 25.6 GB/s
USB	1x USB 3.0 Type A,2x USB 2.0 Type A, USB 2.0 Micro-B
Pin Connections	40-pin header (GPIO, I2C, I2S, SPI, UART) 12-pin header (Power and related signals, UART) 4-pin Fan header
Dimensions	100 mm x 80 mm x 29 mm

- **Interlink FSR® sensor**

Table A.5: Technical specifications of Interlink FSR® sensor [114], [116]

Interlink FSR® sensor Technical Specifications	
Actuation Force	~0.2N min
Force Sensitivity Range	~0.2N to >100N
Force Resolution	Continuous (analog)
Force Repeatability	+/- 2% of initial reading
Non-Actuated Resistance	>10 Mohms
Hysteresis	+10% Average
Device Rise Time	<3 Microseconds
Long Term Drift **1kg load, 35 days**	<5% per log10(time)
Operating Temperature Performance **Cold: -40°C after 1 hour** **Hot: +85°C after 1 hour** **Hot Humid: +85°C 95RH after 1 hour**	 -5% average resistance change -15% average resistance change +10% average resistance change
Tap Durability **Tested to 10 million actuations, 1kg, 4Hz**	10% average resistance change
Standing Load Durability	-5% average resistance change

Interlink FSR® sensor Technical Specifications	
2.5kg for 24 hours	
EMI (Electromagnetic Interference)	Generates no EMI
ESD (Electrostatic Discharge)	Not ESD sensitive

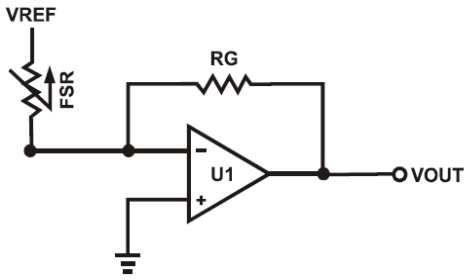

Figure A.2: FSR current-to-voltage converter reading circuit. Image from [116].

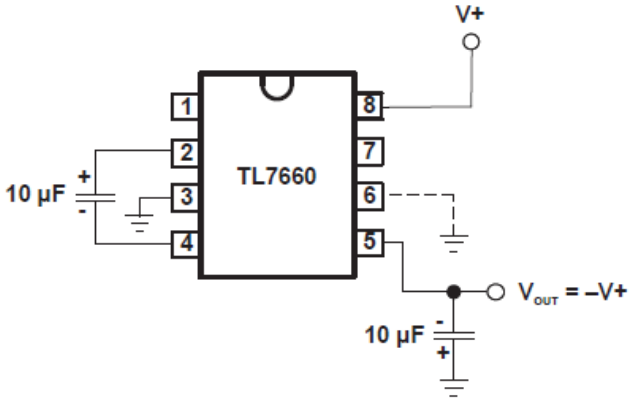

Figure A.3: Voltage conversion circuit with TL7660. Image from [166].

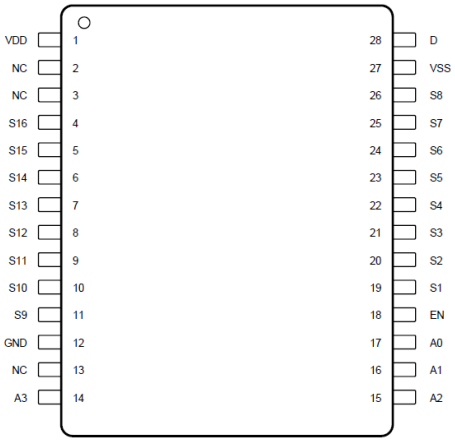

Figure A.4: Pin configuration of the multiplexer MUX506IPWR. Image from [167].

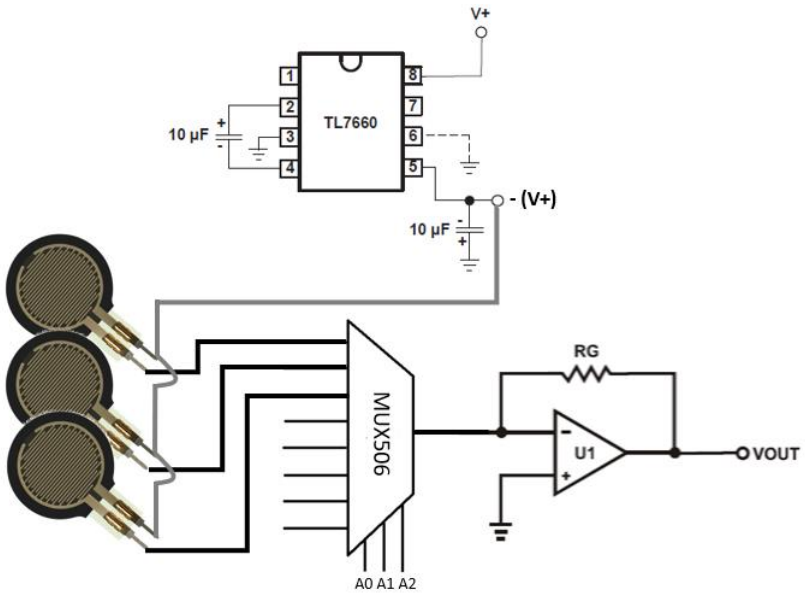

Figure A.5: Schematic of the handle force sensors reading circuit.

- **Light sensor**

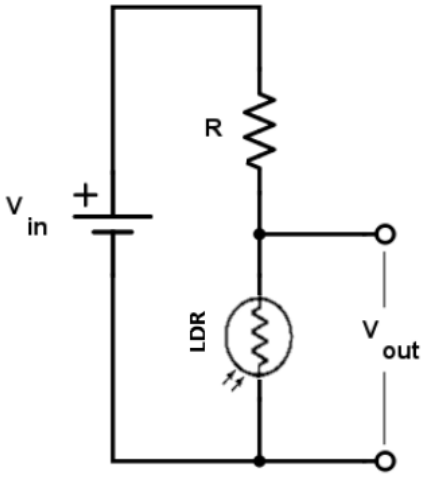

Figure A.6: Schematic of the photoresistor reading circuit.

- **Vibrating motors**

Table A.6: Vibrating motors technical specifications [126], [168]

Precision Microdrivers Vibrating Motors Technical Specifications	
Body diameter	10 mm
Body length	2.7 mm
Operating voltage	2 - 5 V
Vibration speed	12,200 rpm [+/- 3000]

Precision Microdrivers Vibrating Motors Technical Specifications	
Operating Current	100 mA

- LED

Table A.7: LED technical specifications.[129]

LED Technical Specifications	
Color temperature	6000~7000K
Luminous flux	180~210lm
Supply voltage	3.3V to 5V
Power	3W
Connection type	Digital
Field-of-view	140°
Dimensions	40 mm x 28 mm
Weight	6g

- Wheel motors

Table A.8: DC Servo motor NEMA23 (RMCS-2255) technical specifications [169]

NEMA23 Motor Technical Specifications	
Operating Voltage	12V
Maximum Speed	300 rpm
Weight	0.18Kg
No-load current	0.8A
Maximum load current	7.5A
Torque (Kg/cm) (N/m)	 30 Kg/cm 2.94 N/m
Encoder resolution	0.2° per step
Steps per rotation	1800 steps

- **Battery**

Table A.9: Battery technical specifications [131]

Gens Ace Lithium-polymer Battery Technical specifications	
Voltage	14.8V
Capacity	8000mAh
Discharge Rate (C)	80C
Connector Type	EC5
Weight	0.740 Kg
Dimmensions	157 mm x 53 mm x 43 mm

- **ARCane components**

Table A.10: Summary of all components that make up the robotic cane

	Component	Quan-tity	Weight (Kg)	Average Current Drawn (A)	Voltage (V)	Price (Per unit)	Reference
Physical Structure	P1 Tripod Main Body	1	0.729	–	–	3.52 €	[104]
	Holonomic Base	1	0.327	–	–	4.61 €	–
	Omnidirectional wheel	3	0.350	–	–	22.86 €	[107]
	Set Screw Hub	3	0.178	–	–	3.27 €	–
Control Unit	Jetson Nano	1	0.249	3.0	5.0	52.31 €	[170]
	Jetson Nano Fan	1	–	–	3.0	8.67 €	[171]
	Wi-fi Adaptor	1	–	–	5.0	11.68 €	[172]
	Memory Card SD	1	–	–	–	25.92 €	[173]
	STM32 F446RE	1	0.198	0.3	5.0	12.32 €	[174]
Sensory Unit	Force Sensitive Resistor 402 (Handle)	3	–	–	-3.3	8.08 €	[175]
	Force Sensitive Resistor 400 (Rod)	4	–	–	-3.3	7.07 €	[176]
	Multiplexer	1	–	–	±3.3	3.03 €	[177]
	AmpOp	1	–	–	±3.3	0.26 €	[178]
	Capacitor (10uF)	2	–	–	±3.3	0.76 €	[179]
	Voltage Converter	1	–	–	±3.3	1.31 €	[117]
	Photoresistor	1	–	–	5.0	0.74 €	[180]
	IMU	1	0.002	–	5.0	12.37 €	[121]

	Component	Quantity	Weight (Kg)	Average Current Drawn (A)	Voltage (V)	Price (Per unit)	Reference
Actuation Unit	Vibrotactile motors	2	0.001	0.1	5.0	3.08 €	[168]
	Haptic Drivers	2	--	--	5.0	7.54 €	[127]
	LED	1	0.006	0.7	5.0	1.95 €	[129]
	DC motor	3	0.180	3.6	12.0	76.75 €	[130]
Power Unit	Battery	1	0.733	--	14.8	106.35 €	[131]
	DC Voltage Regulator (5V)	1	0.063	--	5.0	12.80 €	[132]
	DC Voltage Regulator (12V)	1	0.100	--	12.0	12.50 €	[133]
	Fuses	4	--	--	--	0.42 €	[134]
	Power Button	1	0.005	--	--	1.90 €	[135]
Cables and Connectors	USB type-C (male)	1		---	5.0	11.90 €	[181]
	USB type-A to Mini-B (male)	1	--	--	5.0	3.19 €	[182]
	EC5 Cable (male)	1	--	--	--	2.05 €	[183]
	JST Connector (male)	12	--	--	--	0.78 €	[184]
	6-Pin Connector (male)	6	--	--	--	0.22 €	[185]
	2-Pin Terminal Block	3	--	--	--	0.81 €	[186]
	Fuse Support	4	--	--	--	0.22 €	[187]
	Total	71	5.5 Kg	7.8 A	--	688.97€ (All units)	--

Appendix III

This appendix contains some of the steps performed to obtain the low-pass filter, as well as a comparison with the Kalman filter implemented for signal processing of the acquired data by the FSR sensors.

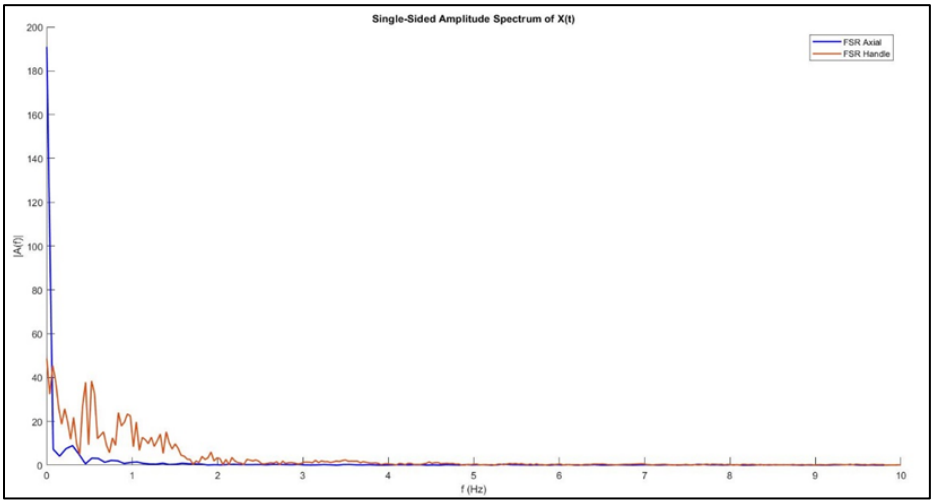

Figure A.0.7: Plot of the single-sided amplitude spectrum of the FSR sensor acquired signal, to find its frequency domain.

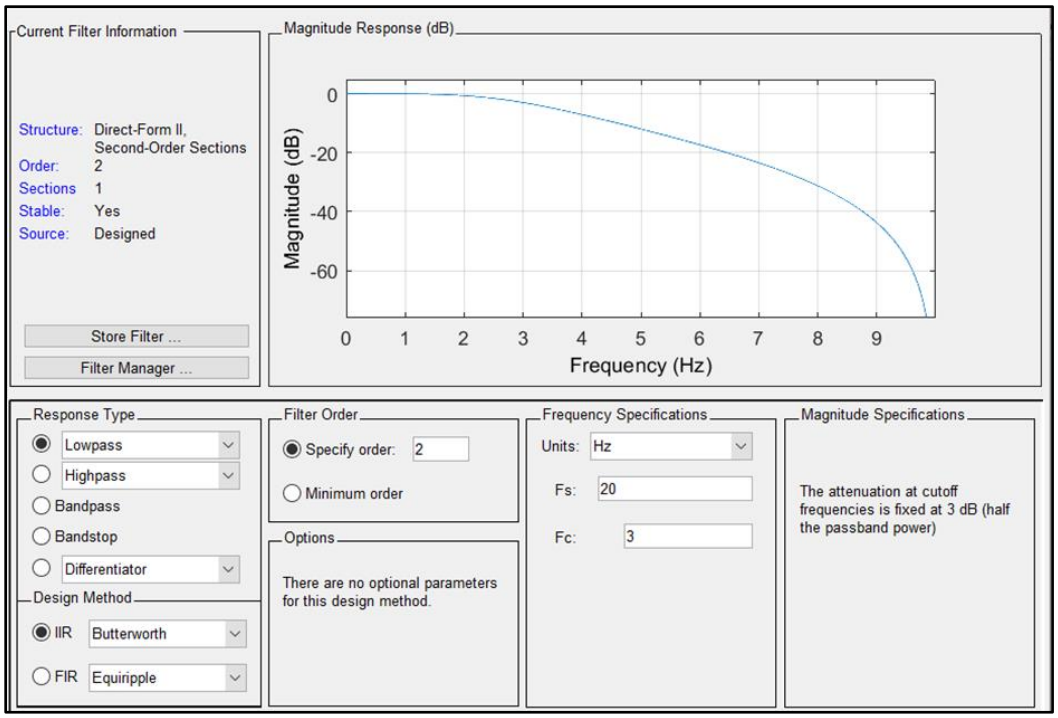

Figure A.8: Development of the low-pass filter, through the Filter design application, using MATLAB.

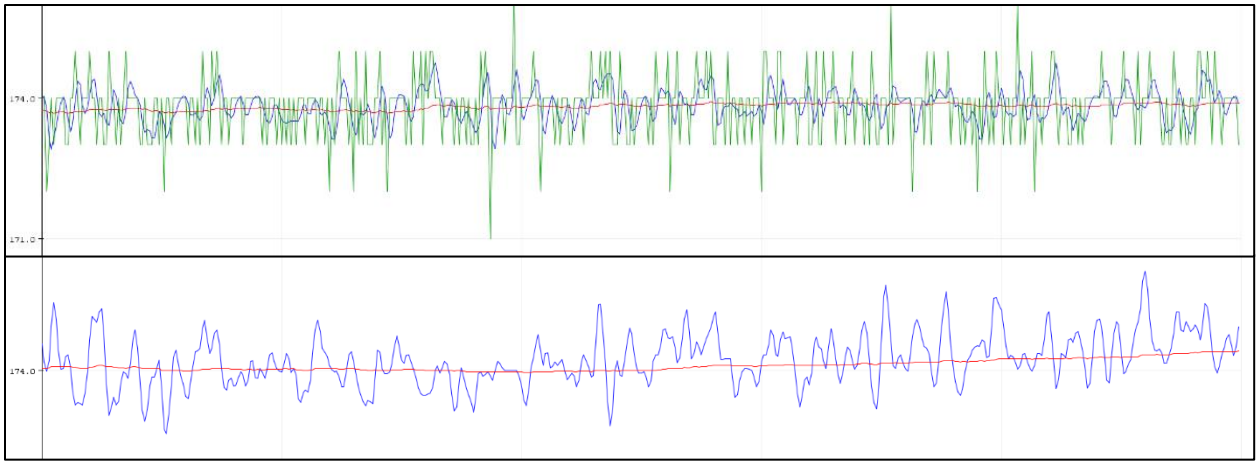

Figure A.9: Comparison between the acquired and processed FSR signals. Green: real signal; Blue: low-pass filter; Red: Kalman filter.

Appendix IV

This appendix contains the set of requirements and eligibility criteria performed in the interoperability tests, as well as some information and visual context of how some of the results were obtained.

Table A.11: Interoperability tests requirements and eligibility criteria

Requirement	Req. ID	Eligibility criteria	Test ID	Select if achieved
1 - Battery				
Battery powered system	R1_001	The system has an autonomy of 1 hour.	1	☒
		Power can be turned on and off.	1	☒
		The system can be recharged.	2	☒
		Battery charging connector is easily accessible.	2	☒
Continuous usage time	R1_002	The system displays all functions for 1 continuous hour.	1	☒
Increase autonomy	R1_003	It is possible to replace the existing battery with a higher capacity without hardware and software modifications.	5	☒
Safety when interacting with the battery	R1_004	It is safe to connect and disconnect the battery from the circuit.	2	☒
2 – Motors and wheels				
Average consumption of motors	R2_001	Check that each motor consumes up to 0.5A without the weight of the cane.	10	☒
		Check that each motor draws up to 3A when inserted into the cane.	11	☒
Motor velocity	R2_002	Check that the motor reaches the maximum angular speed of 300 rpm.	10	☐
3 – Axial force system				
Cane movement direction	R3_001	The cane moves in the direction desired by the user in the x-axis (transverse axis) direction.	15	☒
Cane accompanies the user	R3_002	Check if the cane accompanies the user during the gait.	15	☒
4 – Haptic sensing system				
Detection of user contact with the cane	R4_001	Verify that the FSR sensors on the handle can detect user contact on the handle while the cane is at rest.	16	☒
		Verify that the FSR sensors on the handle can detect user contact on the handle while the cane is moving	16	☒
Gait phase detection	R4_002	Check if it is possible to detect when the user exerts greater support force on the cane, referring to the support phase	16	☒

5 – Light sensor				
Luminosity detection	R5_001	Check if the photoresistor can detect low-luminosity conditions	12	☒
6 – Luminosity device				
Average consumption of LED	R6_001	Check if the LED consumes up to 1A	12	☒
Luminosity provided by the LED	R6_002	Check if the LED can light up a low luminosity environment.	12	☒
7 – Inertial system				
Inertial measurements	R7_001	Verify if the IMU is taking the correct accelerometer, gyroscope and magnetometer readings	13	☒
8 – Haptic feedback system				
Vibrating motors functioning	R8_001	Drivers can be successfully calibrated	14	☒
		Check if different stimuli are perceptible and distinguishable by the user	14	☒
Vibration perception	R8_002	All users were able to perceive the vibration	14	☒
		All users were able to perceive the vibration	14	☒
Vibration interference	R8_003	Verify that the IMU and force sensor readings are maintained due to vibration propagation from vibrating motors	14	☒
9 - Data processing and storage				
Data storage during cane usage	R9_001	There is data recorded on the memory card	4	☒
		The memory card connector is easily accessible	4	☒
		All predefined data are being monitored	3	☒
		All predefined data are being recorded	4	☒
		The pre-defined data organization structure is verified	4	☒
		The pre-set reading frequency is checked	3	☒
Data protection	R9_002	There is no logical relationship between the data and the people who gave rise to it	9	☒
Increase data storage	R9_003	It is possible to change the existing memory card to one with more storage without hardware and software modifications	5	☒
10 – Usage of the ARCane				
Cognitive effort	R10_001	All users rated the level of psychological fatigue they feel after using the system < 3 on a scale of 1 to 5	8	☒
Cane setup	R10_002	Preparation procedures coincide with pressing the switch	8	☒
		Preparation procedures are considered easy by all users	8	☒

Weight	R10_003	Cane weight < 6000g	7	☒
		All users considered the system lightweight	8	☒
Dimmensions	R10_004	No user considers that the system has large dimensions	8	☒
Freedom of move-ment	R10_005	No user considers that the cane system restricts the movement of the arms	8	☒
Electric circuits	R10_007	Electrical circuits are physically isolated from the user	6	☒

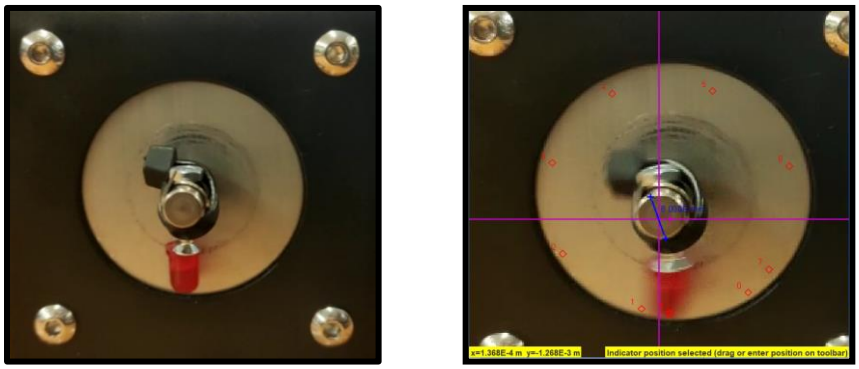

(a) (b)

Figure A.10: Method to acquire the velocity speed of the motor using Tracker, a video analysis and modeling tool software. (a) Placed a reference indicator on the motor shaft (red LED) (b) position of the indicator over time;

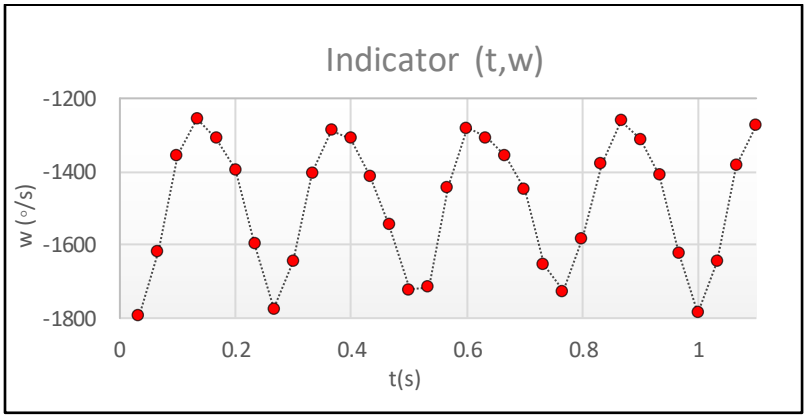

Figure A.11: Measurements acquired of the indicator angular speed over time, representing the motor shaft angular speed over time.

Table A.12: Motor max velocity results in accordance with the measurements achieved, presented in Figure A.11

Theoretical value	Experimental value		Efficiency
300 rpm	Min. value: 209 rpm	Avg. value: 248 rpm	82.51%
	Max. value: 299 rpm		

Appendix V

This appendix contains relevant information regarding the studies carried out in SolidWorks simulation software, to obtain an analytical validation with the objective of a possible implementation of strain gauge sensors in the ARCane. These simulations were performed for applied forces of 100N in the direction of the x- axis and y-axis, and for applied forces of 300N applied in the direction of the z-axis, on the ARCane handle.

Table A.13: Mesh information and details

Mesher type	Solid mesh
Mesher used	Standar mesh
Element size	5.04 mm
Tolerance	0.25 mm
Mesh quality	High
Total nodes	25309
Total elements	12537

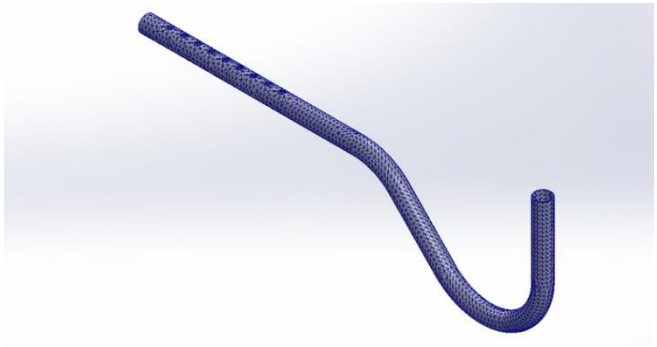

Figure A.12: Mesh results of the ARCane main body.

Table A.14: 3003 aluminium alloy properties, information retrieved from the SolidWorks material library

Yield strength	4.13613e+07 N/m^2
Tensile strength	1.10297e+08 N/m^2
Elastic modulus	6.9e+10 N/m^2
Poisson's ratio	0.33
Mass density	2,700 kg/m^3
Shear modulus	2.7e+10 N/m^2
Thermal expansion coefficient	2.3e-05 /Kelvin

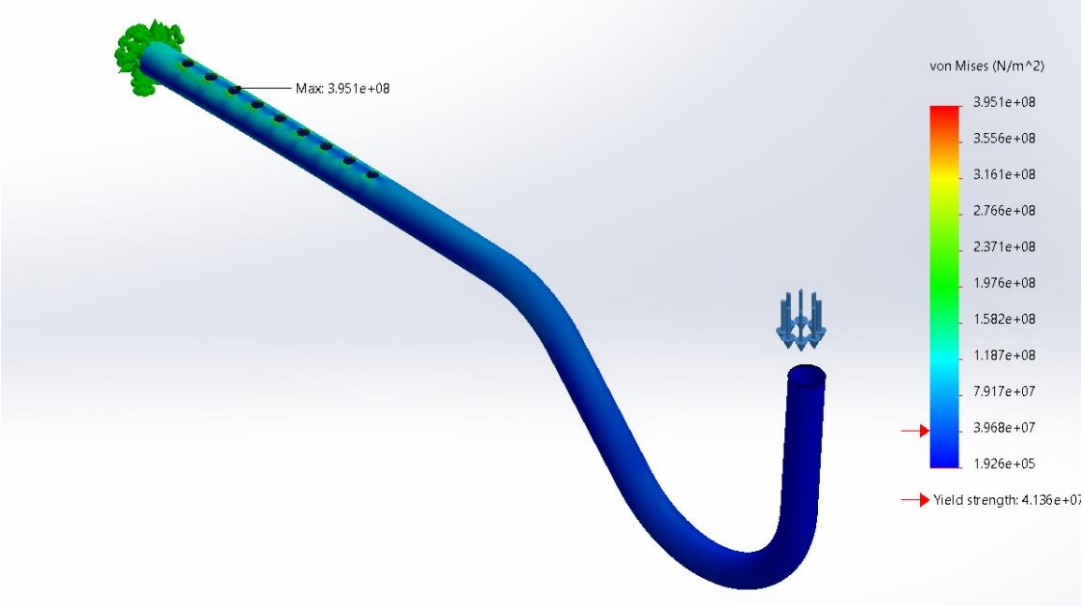

Figure A.13: Von Mises Stress obtained in the static load test simulation, for applied forces of 100N in the y-axis direction at the handle, where the maximum strain is equal to 3.951e+08 N/m^2.

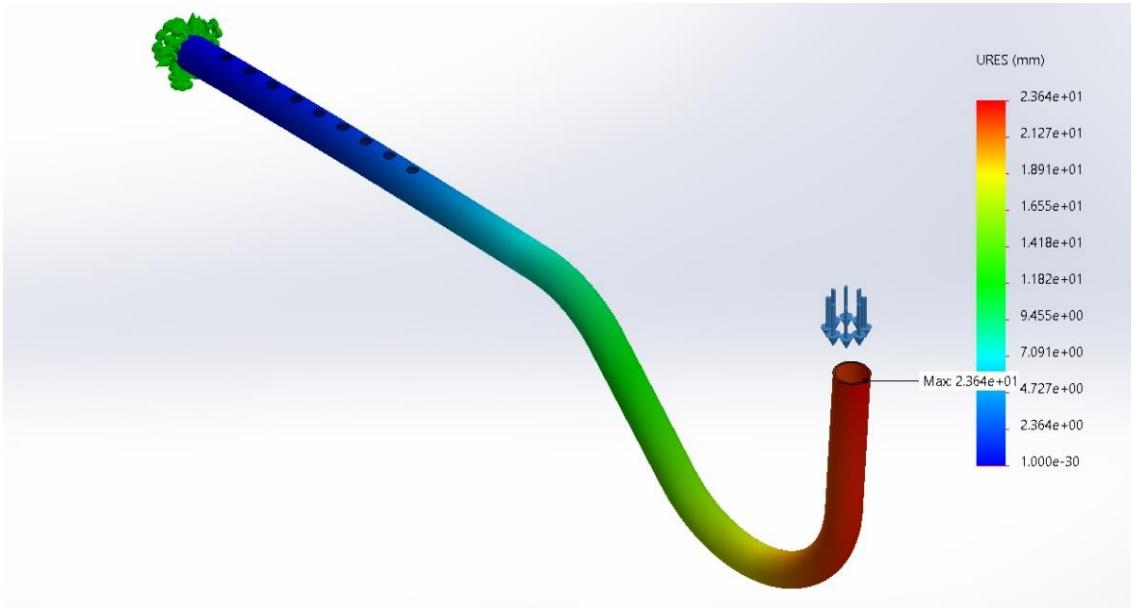

Figure A.14: Resultant displacement plot obtained in the static load test simulation, for applied forces of 100N in the y-axis direction at the handle, where the maximum displacement is equal to 2.364e+01mm.

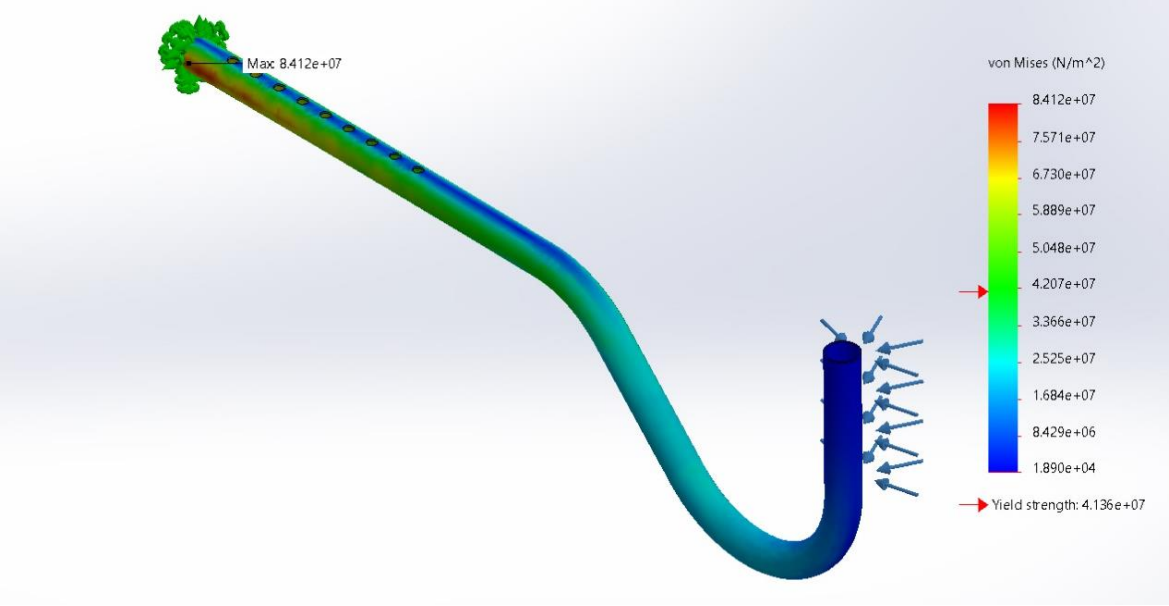

Figure A.15: Von Mises Stress obtained in the static load test simulation, for applied forces of 100N in the x-axis direction at the handle, where the maximum strain is equal to 8.412e+07 N/m^2.

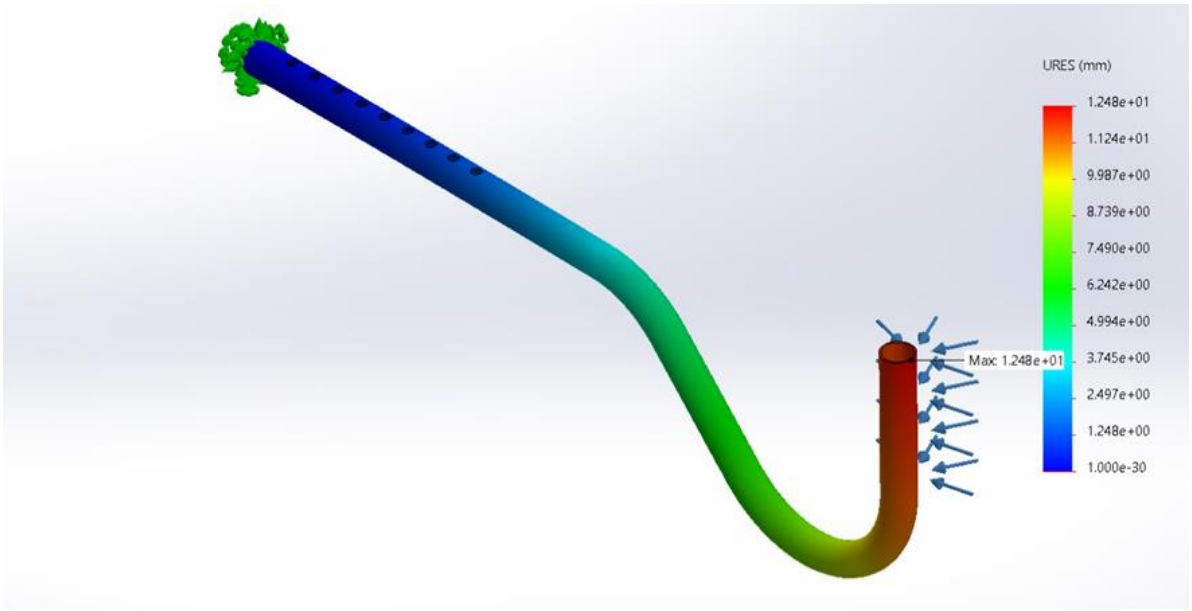

Figure A.16: Resultant displacement plot obtained in the static load test simulation, for applied forces of 100N in the x-axis direction at the handle, where the maximum displacement is equal to 1.248e+01mm.

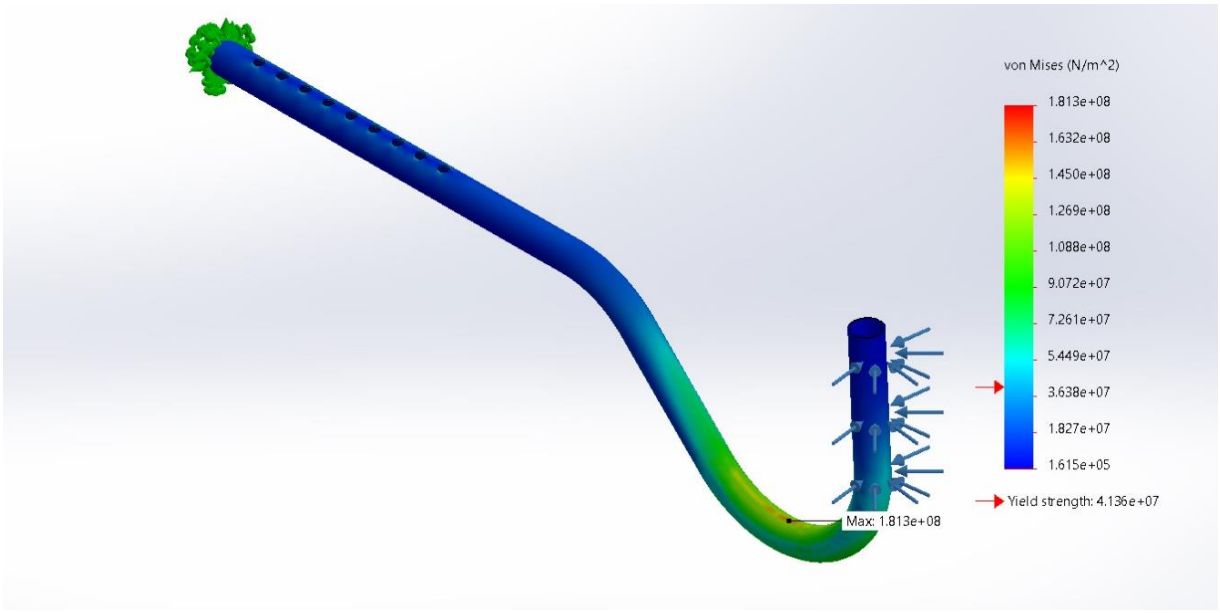

Figure A.17: Von Mises Stress obtained in the static load test simulation, for applied forces of 300N in the z-axis direction at the handle, where the maximum strain is equal to1.813e+08 N/m^2.

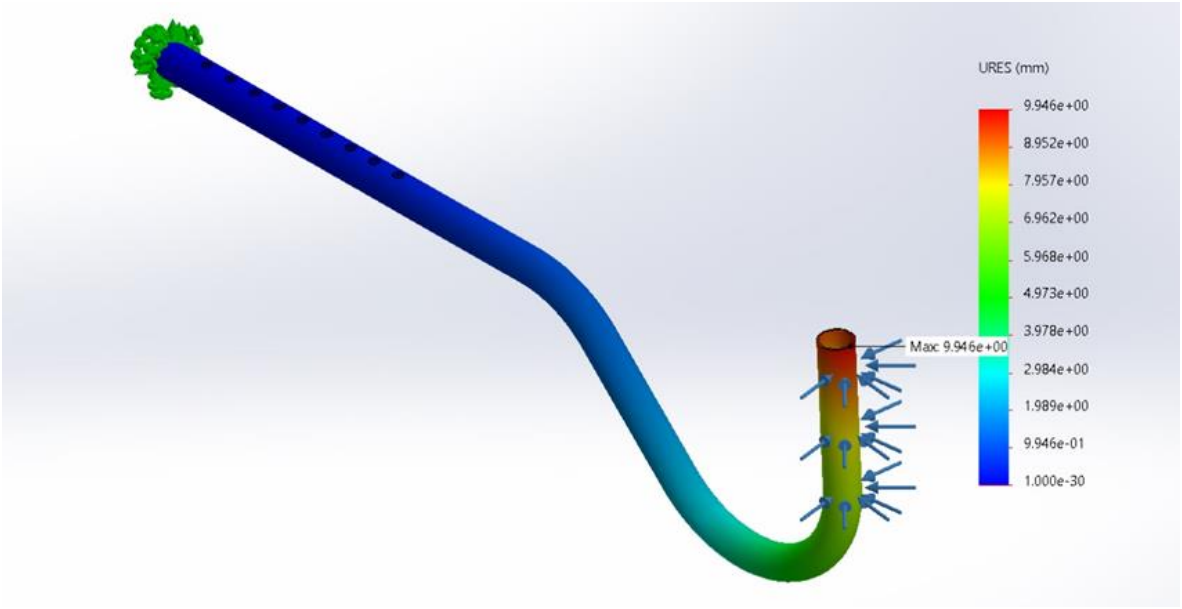

Figure A.18: Resultant displacement plot obtained in the static load test simulation, for applied forces of 300N in the z-axis direction at the handle, where the maximum displacement is equal to 9.946 mm.

Appendix VI

This appendix contains relevant information on the motion control methods implemented, and on the data and procedures performed in the experimental tests.

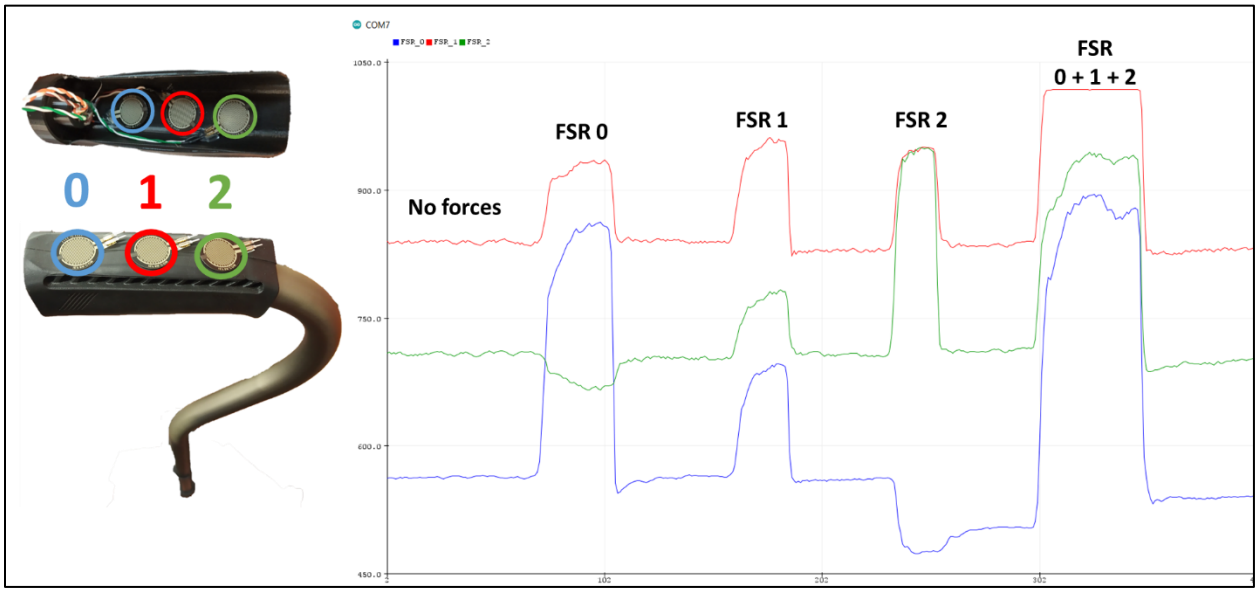

Figure A.19: Data acquisition by the haptic sensing system with force applied in the z-axis direction at different locations of the cane handle.

Figure A.20: Representation of the place where the experimental tests were carried out, along with the movement trajectory of the participants.